

Copyright is owned by the Author of the thesis. Permission is given for a copy to be downloaded by an individual for the purpose of research and private study only. The thesis may not be reproduced elsewhere without the permission of the Author.



MASSEY
UNIVERSITY

Starch retrogradation *in tuber*: mechanisms
and its implications on microstructure and
glycaemic features of potatoes

A thesis presented in partial fulfilment of
the requirements for the degree of

Doctor of Philosophy

in

School of Food and Advanced Technology

at Massey University, Palmerston North, Manawatū, New Zealand

Yu-Fan Nicole Chen

2020



Thesis committee

Chief supervisor: Dr. Jaspreet Singh, Associate Professor, Massey University.

Co-supervisor: Dr. Joceyln Midgely, Agri-Food Science & Technology Manager, Simplot Australia Pty. Ltd.

Co-supervisor: Prof. Richard Archer, Logan Campbell Professor of Food Technology, Massey University.

Examiners

Mr. Allan Hardacre, Senior Research Officer, Massey University.

Mr. Marco Morgenstern, Team Leader Food Structure Engineering, Plant & Food Research.

Dr. Qiang Liu, Research Scientist, Agriculture and Agri-Food Canada.

Dedicated to my loving parents and my partner.

Abstract

An increase in the occurrence of diabetes mellitus, cardiovascular disease and obesity in recent years led to the project “Starch retrogradation *in tuber*: mechanisms and its implications on microstructure and glycaemic features of potatoes”. Potato products can play a role in mitigating these hyperglycaemic events, if starch in these processed products is slowly digested and/or starch-derived glucose is released into the circulation in a slower and more attenuated manner. Three stages were envisaged for the project with an aim to create slowly digestible starch in whole potato tuber (*in tuber*) through starch retrogradation.

Plant-based whole food systems, such as potato tubers encompass different cell compartments, (e.g. cell wall, vacuole, cytoplasm and intracellular spaces) within which starch gelatinisation and retrogradation occur, subject to local interactions of other cell components and water availability. Structural changes of potato starch during retrogradation *in tuber* and its resulting digestibility were studied. Different water pools in a cooked whole tuber were discerned by the low-field NMR (LF-NMR), having relaxation times T_{20} at <1 ms, T_{21} at 10-15 ms, T_{22} at 70–200ms, and T_{23} at > 400 ms. A significant reduction in *eGI* was observed after cooling and storage compared to freshly cooked tubers. Reheating of retrograded tuber restored some of the susceptibility to enzymatic hydrolysis and internal water mobility. Longer chilled storage (7 days) yet improved the stability of retrograded tuber against reheating effects (at 90 °C). Realignment of the gelatinised amylose and amylopectin changed the distribution of crystalline and amorphous regions during refrigerated storage and subsequent reheating, resulting in starch digestibility varying with treatment combination. Several, but not all, of time-temperature cycle processes were observed to induce stepwise nucleation and propagation, facilitating starch retrogradation *in tuber* more than did storage fixed at 4 °C. *Sous vide* processing (at 55 and 65°C), akin to annealing, combined with starch retrogradation *in tuber*, resulted in potatoes with intermediate *eGI* (40-72). After reheating at 60°C, the *eGI* of *sous vide* cooked-chill potatoes increased moderately, displaying a mixture of partially gelatinised starch and swollen granules. Food processing, i.e. optimum TTC process or *sous vide* process might facilitate the formation of retrograded starch *in tuber*, resulting in a reduced *eGI* (than freshly cooked tubers). To retain the resistance to digestive enzymes in retrograded starch *in tuber*, reheating at low temperatures (50-60°C) were needed.

Acknowledgements

My PhD journey resembles a one-way road, leading to an ultimate goal of graduation. It has been enjoyable yet accompanied with ups and downs which would not have been possible without many people's help.

I would like to, first of all, thank my supervisors, Dr. Jaspreet Singh, Dr. Jocelyn Midgley, and Prof. Richard Archer for their help and encouragements. Jaspreet was an amazing mentor of guiding me in conducting my research. Jocelyn's insightful advice always helped me in fine-tuning the research direction. Richard's excellence in food engineering was instrumental and I learned a lot from his reader-friendly and precise wordings in writing research articles. It was a great pleasure to work in a team with diverse expertise.

My sincere thanks go to few scientists at School of Fundamental Science and Institute of Agriculture and Environment. I cannot begin to express my appreciation to Dr. Rob Ward, who helped me setting up LF-NMR and optimising parameters. I valued constructive discussions on DSC results and X-ray diffraction patterns with Prof. Geoff Jameson, and the training of using FTIR apparatus from Assoc. Prof. Mark Waterland, and the help of running the X-ray from Assoc. Prof. Bob Stewart (at IAE) and a PhD student David Perl. Finally, yet importantly, thank you, Graham, for giving me some LF-NMR glass tubes.

Thank you, Riddet management and administration team, John, Ansley, Terri, Hannah, Meg, Fliss, Sarah, Angela, and Rebecca, for taking care of administration and finance and organising all the events, including student colloquiums, conferences, and researcher development workshops.

None of the experimental works would have been able to be carried out without the help from Janiene, Chris, Maggie, Warwick, Garry, Steve, Michelle, John, and Byron (for the customised corker borer), thank you all. I appreciated Matt and Tim's help on IT related issues, they're always efficient.

Some indispensable people were Dr. Lovedeep Kaur, thank you for the generous tips on writing and publishing articles, as well as all visiting scientists, Assist. Prof. Masa Tamura, Kanyanat (App), Praw, Jorge, and Yudy, I enjoyed the inspiring discussion with you. Geeshani, Thomas, Nina, Alice, Grupreet, Edward, Akashdeep, and Abhilasha never wavered in their support and accompany. Involving in Rina's 4th-year honour project was a great mutual learning process.

I had a precious experience working with Sarah, Feng Ming and Sewuese on "Nutri Sprinky". We pushed as far as we could and achieved to the "Innovate, 2018" final. Thanks for the efforts and contributions, Nutri Sprinky team.

I would also like to acknowledge the support from the RISS community and other PhDs, which helped me maintain my sanity through the journey. Having Taiwanese food with Chih-Chieh and Che really soothed my soul. Thanks to my flatmates, Giovanna, Jackie, Martina, and Hilary for tolerating my fussy temper.

Last but not least, a shout-out to fantastic humans, Sha, Christian, Grace, Emily, Flo, Doreen, William, Ben, Erica, Luke, Jayne, David, Lulu, Paige, Ivalya, Matthew, Kristina, Johannes, Daniel, Marcela, and Clayton. Thank you all for great climbing adventures and humorous banter, definitely the most unforgettable memories during this period.

List of publications and presentations

Research outputs:

- A review article in Comprehensive Reviews in Food Science and Food Safety- Starch retrogradation: An old tool to design new low glycaemic foods (Chen, Kaur, Singh, Midgley, & Archer, submitted).
- A journal article in LWT- Reheating stability of retrograded starch in processed potato tubers (Chen, Singh, Midgley, & Archer, in preparation).
- A journal article in International Journal of Biological Macromolecules- *In tuber* starch retrogradation of *sous vide* processed potato: physico-chemical and microstructural characteristics and oral-gastric-small intestinal starch digestion *in vitro* (Chen, Singh, Midgley, & Archer, submitted).
- A journal article in Food Hydrocolloids, Vol. 98, Jan. 2020, 105240- Influence of time-temperature cycles on potato starch retrogradation *in tuber* and starch digestion *in vitro* (Chen, Singh, Midgley & Archer, 2019).
- A journal article in Food Hydrocolloids, Vol. 84, Nov. 2018, P.552-560- Potato starch retrogradation *in tuber*: Structural changes and gastro-small intestinal digestion *in vitro* (Chen, Singh, & Archer, 2018).
- A book chapter in “Starch in Food: Structure, Function and Applications 2nd Ed.”, 2018, P.283-321-Chemical Modification of Starch (Chen, Kaur, & Singh, 2017).

Oral presentations:

- Simplot Mentone head office, 2017- Potato starch retrogradation *in tuber*: mechanisms and its implications on starch digestibility.
- NZIFST Annual Conference, 2017- Retrogradation of potato *in tuber* and starch digestion *in vitro*.

Poster presentations:

- Food Structures, Digestion and Health International Conference, 2019- Potato starch retrogradation of *sous vide* processed potato tubers and oral-gastric-small intestinal starch digestion *in vitro*.
- Riddet Student Colloquium, 2018-Influences of time-temperature cycles process on potato starch retrogradation *in tuber* and its digestibility *in vitro*.
- Best poster award “Retrogradation of potato starch *in tuber* and its digestibility “in 1st ICC Asia-Pacific Grain Conference, 2017.

Report

- Physico-chemical properties of commercial potato starches and MSPrebiotic®.

Other achievements:

- Finalist of “Innovate, 2018” by The Factory.

Table of Contents

I	Introduction and thesis outline.....	1
	I.1 Preface.....	1
	I.2 Potato tubers.....	2
	I.3 Potato starch <i>in tuber</i>	3
	I.3.1 Starch granule architecture.....	5
	I.3.2 Starch molecular structure.....	6
	I.4 Potato microstructure and starch digestion.....	8
	I.5 Potato tuber consumption and human health.....	9
	I.5.1 Resistant starch content in potato tubers.....	10
	I.5.2 Cooking methods and the effects on starch digestion.....	11
	I.6 Research aim and thesis outline.....	11
II	Review of literature.....	13
	II.1 Introduction.....	13
	II.2 Mechanism of starch retrogradation.....	15
	II.2.1 Kinetics of starch retrogradation.....	16
	II.2.2 Fine structure of amylopectin during retrogradation.....	17
	II.2.3 Methods to depict starch retrogradation.....	18
	II.2.4 Starch retrogradation in food matrix.....	24
	II.2.5 Starch retrogradation: formulated vs natural systems.....	30
	II.3 Starch retrogradation as influenced by type of food processing.....	33
	II.4 Starch nutritional fractions as delivered by various food processing.....	38
	II.4.1 Kinetics of glucose release and starch digestibility.....	38
	II.4.2 Formation of slowly digestible/resistant starches in processed foods.....	40
	II.5 Designing foods with low GI via enhancing starch retrogradation.....	45
	II.6 Conclusion.....	47
	II.7 Research gaps.....	48
	II.8 Objective.....	50
III	Methodology and methods development.....	52
	III.1 Methods development.....	52
	III.1.1 Molecular chains mobility measured by relaxation times via LF-NMR.....	52
	III.1.2 Starch digestibility <i>in tuber</i> by oral-gastro-small intestinal digestion <i>in vitro</i>	60

III.2	General methods	68
III.2.1	Microscopy	69
III.2.2	ATR-FTIR.....	72
IV	Potato starch retrogradation <i>in tuber</i>: structural changes and gastro-small intestinal digestion <i>in vitro</i>.....	76
IV.1	Introduction.....	76
IV.2	Materials and methods	77
IV.2.1	Materials and sample preparation	77
IV.2.2	Pasting properties.....	77
IV.2.3	Thermal characteristics	78
IV.2.4	Relative crystallinity	78
IV.2.5	Water mobility	78
IV.2.6	Starch digestion <i>in vitro</i> and its kinetics	79
IV.2.7	Microstructural characteristics of digesta	79
IV.2.8	Statistical analysis.....	79
IV.3	Results and discussion	80
IV.3.1	Pasting profile	80
IV.3.2	Thermal characteristics	81
IV.3.3	Relative crystallinity (%).....	82
IV.3.4	Water mobility in potato tuber cells.....	83
IV.3.5	Starch hydrolysis (%) and its kinetics.....	86
IV.3.6	Microstructure before and during small intestinal enzymatic digestion	88
IV.4	Conclusion	90
V	Influence of time-temperature cycles on potato starch retrogradation <i>in tuber</i> and starch digestion <i>in vitro</i>.....	92
V.1	Introduction	92
V.2	Materials and methods.....	93
V.2.1	Materials and sample preparations.....	93
V.2.2	Total starch content, amylose content, dry matter, and the blue value	94
V.2.3	Thermal characteristics	95
V.2.4	Water mobility	95
V.2.5	Texture analysis	95
V.2.6	Starch digestion <i>in vitro</i>	96
V.2.7	Statistical analysis.....	97

V.3	Results and discussion.....	97
V.3.1	Total starch content, dry matter and blue value (BV).....	97
V.3.2	Thermal characteristics of TTC-processed potato tuber.....	98
V.3.3	Water mobility of TTC processed potato tubers.....	100
V.3.4	Texture profile analysis.....	101
V.3.5	Starch hydrolysis (%) and estimated glycaemic index.....	102
V.4	Conclusion.....	108
VI	Starch retrogradation of <i>sous vide</i> processed potato tubers and oral-gastric-small intestinal starch digestion <i>in vitro</i>	110
VI.1	Introduction.....	110
VI.2	Materials and methods.....	111
VI.2.1	Materials and sample preparation.....	111
VI.2.2	Dry matter, total starch content, and amylose content.....	112
VI.2.3	Potato microstructure.....	112
VI.2.4	Pasting properties.....	112
VI.2.5	X-ray diffraction.....	113
VI.2.6	Thermal characteristics.....	113
VI.2.7	Water mobility by LF-NMR.....	113
VI.2.8	Oral-gastric-small intestinal digestion <i>in vitro</i>	114
VI.2.9	Statistical analysis.....	115
VI.3	Results and discussion.....	115
VI.3.1	Dry matter, total starch content, amylose content.....	115
VI.3.2	Microstructure of <i>sous vide</i> cooked potatoes.....	115
VI.3.3	Pasting properties.....	118
VI.3.4	Relative crystallinity.....	119
VI.3.5	Thermal characteristics of <i>sous vide</i> cooked potato tubers.....	121
VI.3.6	Water mobility of <i>sous vide</i> cooked potatoes.....	124
VI.3.7	Oral-gastric-small intestinal digestion <i>in vitro</i> of <i>sous vide</i> cooked potatoes.....	127
VI.4	Conclusion.....	129
VII	Stability of retrograded starch <i>in tuber</i> during reheating.....	131
VII.1	Introduction.....	131
VII.2	Materials and methods.....	132
VII.2.1	Materials and sample preparations.....	132
VII.2.2	Water mobility.....	133

VII.2.3	ATR-FTIR measurement	133
VII.2.4	X-ray	134
VII.2.5	Starch digestion <i>in vitro</i>	134
VII.2.6	Statistical analysis	134
VII.3	Results and discussion	135
VII.3.1	Structural stability of TTC-retrograded+reheated starch <i>in tuber</i> and its digestibility	135
VII.3.2	Structural changes of <i>sous vide</i> cooked potato tubers during reheating.....	137
VII.3.3	Digestibility of <i>sous vide</i> cooked-chill+reheated potatoes.....	139
VII.4	Conclusion	140
VIII	Industrial relevance	142
VIII.1	Introduction.....	142
VIII.1.1	Retrograded+reheated potato tubers	143
VIII.1.2	Time-temperature cycles process.....	145
VIII.1.3	<i>Sous vide</i> cooked-chill/cooked-frozen then reheated potato wedges	147
IX	General discussion and conclusion	155
IX.1	Introduction.....	155
IX.2	Main findings and discussions	155
IX.3	Concluding remarks	158
	Bibliography	160
	Appendix A.....	211

List of figures

Figure I.1 Potato tuber crosscut section (left) and the micrographs of pith (up right) and cortex (bottom right). Different crosscut sections contain various amount of starch granules and protein.....	4
Figure I.2 Preharvest and postharvest conditions affect qualities of potato tubers.....	4
Figure I.3 The hierarchical structure of starch granule. (a) Under polarised light microscope, starch granules showed “Maltese cross”, a radial organisation of starch granules. (b) A hypothetical granule (in this case polyhedral) with growth rings extending from the hilum. (c) Blocklets in semi-crystalline (black) and amorphous (grey) rings. (d) Crystalline and amorphous lamella formed by double helices (cylinders) and branched segments of amylopectin (black lines), respectively. Amylose molecules (red lines) are interspersed among the amylopectin molecules. (e) Three double-helices of amylopectin. Each double-helix consists of two polyglucosyl chains, in which the glucosyl residues are symbolised by white and black circles, respectively. The double helices form either A- or B-polymorphic crystals (A and B, respectively, in which the circles symbolises the double helices seen from the edge). (f) Glucosyl units showing α -(1,4)- and α -(1,6)-linkages at the base of the double-helix. The bar scale (in nm) is only approximate to give an impression of the size dimensions.	6
Figure II.1 Model of retrograded gel network based on the amylopectin “building block backbone model”. Short chains (thin lines) show weaker gels with short double-helices, poor intra-molecular alignment, and short inter-molecular double-helical junctions (left), whereas long chains (bold lines) form intra-molecular, inter-molecular, and junction zone (right).....	18
Figure II.2 Model of starch retrogradation <i>in tuber</i> and its relaxation time distribution curve (Chen et al., 2018).....	33
Figure III.1 (a) The spin of a proton (brown curve) under a constant magnetic field (B_0), and (b) the corresponding changes of magnetisation (M_{xy} and M_y). The recovery at 63% of magnetisation (dark blue line) represents the proton longitudinal (spin–lattice) relaxation time (T_1), while the decay at 37% of magnetisation (light blue line) indicates transverse (spin–spin) relaxation time (T_2).	53
Figure III.2 Four water pools with relaxation times (T_{20} , T_{21} , T_{22} , and T_{23}) in raw potato cells.	54
Figure III.3 Changes in relaxation times T_{21} and T_{22} during starch gelatinisation <i>in tuber</i>	55
Figure III.4 (a) Sampling of a raw potato cylinder and (b) the raw potato cylinder in a LF-NMR glass tube.	56
Figure III.5 Raw data of relaxation time of distilled water, the sample of 10% H_2O +90% D_2O , and potato flour.....	57
Figure III.6 Raw data of relaxation time of distilled water, raw potato tuber, and raw flour-water suspension (potato flour: water=1:3).....	58
Figure III.7 Relaxation time distribution curves of raw potato flour-water suspension (potato flour: water=1:3), raw potato tuber, and pure water.	59
Figure III.8 Raw data of relaxation time of raw potato <i>cv.</i> Agria (A) and <i>cv.</i> Nadine (N).	59
Figure III.9 Relaxation time distribution curves of raw potato <i>cv.</i> Agria (A,—) and <i>cv.</i> Nadine (N, ---)....	60
Figure III.10 Diagram of oral-gastric-small intestinal digestion <i>in vitro</i>	61

Figure III.11 (a) The 3-day retrograded potato chips before reheating; (b) the 3-day retrograded+reheated (at 90°C) potato chips; (c) the increase in core temperature of a retrograded potato cube (2*2*2cm ³) by time during reheating.	62
Figure III.12 Cooked potato boluses formed by (a) myself chewing 20 times and by (b) Minifood processor blended for 1min, or (c) for 2min.	63
Figure III.13 Bolus particle size analysis by ImageJ.	63
Figure III.14 Particle size distribution of boluses formed by Minifood processor blending and by 20 times of chewing measured by Mastersizer.	64
Figure III.15 Starch digestion <i>in vitro</i> with digesta placed inside polyethylene mesh.	65
Figure III.16 Elements of human gastric simulator.....	67
Figure III.17 Starch hydrolysis curves of freshly cooked potato tuber carried out in a jacketed glass reactor (●) in gradient blue areas or in the human gastric simulator (■) in grey areas.	68
Figure III.18 Schematics of (a) transmission FTIR and (b) attenuated total reflectance (ATR)-FTIR.....	73
Figure III.19 FTIR spectra of raw potato <i>cv.</i> Agria.	73
Figure III.20 FTIR spectra of freeze-dried and powdered raw potato <i>cv.</i> Agria and <i>cv.</i> Nadine over wavenumber 4000-400 cm ⁻¹	74
Figure III.21 Deconvoluted FTIR curves of freeze-dried and powdered raw potato <i>cv.</i> Agria, A _{raw} and <i>cv.</i> Nadine, N _{raw} . The values represented the 1047/1022 of each sample and different superscripts indicated significant differences (n=3, p<0.05).	75
Figure IV.1 The pasting profiles of (a) the 1, 3, and 7-day retrograded samples (FCR1, FCR3, and FCR7) and (b) the retrograded+ reheated samples (FCR1-r90, FCR3-r90, and FCR7-r90) (n=3).	81
Figure IV.2 The endothermal profile of the raw potato tuber, freshly cooked (FC), the 3-day retrograded (FCR3), and the retrograded+ reheated (FCR3-r90) samples.	82
Figure IV.3 The X-ray diffraction patterns of the freshly cooked (FC), the retrograded (FCR) and the retrograded+reheated (FCRr) samples. FC, freshly cooked sample; FCR1, the 1-day retrograded sample; FCR3, the 3-day retrograded sample; FCR7, the 7-day retrograded sample; FCR1-r90, the 1-day retrograded+reheated sample; FCR3-r90, the 3-day retrograded+reheated sample; FCR7-r90, the 7-day retrograded+reheated sample.	83
Figure IV.4 Different water pools, T ₂₃ , T ₂₂ , T ₂₁ , and T ₂₀ , in potato tubers, including raw, freshly cooked (FC), 3-day retrograded (FCR3), and retrograded+ reheated (FCR3-r90) tubers.	85
Figure IV.5 The development of relaxation time T ₂₃ , T ₂₂ and T ₂₁ under different cold storage times for 1, 3, and 7 days (FCR1, FCR3, and FCR7) and reheating temperatures at 50°C, 70°C, and 90°C (FCR1-r50, FCR1-r70, FCR1-r90, FCR3-r50, FCR3-r70, FCR3-r90, FCR7-r50, FCR7-r70, and FCR7-r90). Error bars represent standard deviation (n=3).....	86
Figure IV.6 Starch hydrolysis (%) of freshly cooked (FC), retrograded (FCR1, FCR3, FCR7) and retrograded+reheated (FCR1-r90, FCR3-r90, FCR7-r90) tuber. Error bars represent standard deviation (n=3).....	87
Figure IV.7 The CLSM time-lapse images of FC in SIF at T ₀ (a), T ₅ (b), T ₁₀ (c) and T ₃₀ (d); FCR3 incubating in SIF at T ₀ (e), T ₅ (f), T ₁₀ (g), and T ₃₀ (h); and FCR3-r90 incubating in SIF at T ₀ (i), T ₅ (j), T ₁₀ (k), and T ₃₀ (l).	89

Figure V.1 Definitions of the parameters of texture profile analysis.	96
Figure V.2 Endotherm curve of potato tuber and its derivative curve.	98
Figure V.3 Endothermal curves of 3-day retrograded tuber and TTC processed potato tubers.	99
Figure V.4 Water pool profiles of (a) freshly cooked potato tubers, FC, and 3-day retrograded potato tubers, FCR3, and (b) TTC1-processed potato tubers, (c) TTC2-processed potato tubers, and (d) TTC-4/25 and 4/65 potato tubers.	101
Figure V.5 Starch hydrolysis (%) of 3-day retrograded tubers, TTC1-processed tubers, and TTC2-processed tubers. Error bars represent standard deviation (n=3).....	103
Figure V.6(a) Particle size distribution curves of bolus (O ₂ , ---) and digesta (I ₁₂₀ , -) of freshly cooked potato tubers, and (b) the volume changes of small particles and (c) the large particles of different samples during and after digestion. *The particle size distribution of the digesta I ₁₂₀ of FCR3-t(4/65/4) was a unimodal curve with a shoulder at 43µm. And error bars indicate the standard deviation of triplicate results.	105
Figure V.7 SEM images of freshly cooked potato tubers digesta at O ₂ (a), I ₅ (b), and I ₁₂₀ (c); and 3-day retrograded tubers digesta at O ₂ (d), I ₅ (e), and I ₁₂₀ (f); and FCR3-t(-20/4/4) digesta at O ₂ (g), I ₅ (h), and I ₁₂₀ (i); and FCR3-t(4/65/4) digesta at O ₂ (j), I ₅ (k), and I ₁₂₀ (l).	107
Figure VI.1 Appearance of <i>sous vide</i> cooked <i>cv. Agria</i> (a) at 55°C and <i>cv. Nadine</i> (b) at 55°C and (c) at 65°C.....	114
Figure VI.2 LM and SEM micrographs of (a) raw <i>cv. Agria</i> , <i>sous vide</i> cooked (b) at 55°C and (c) at 65°C <i>cv. Agria</i> ; and for (d) raw <i>cv. Nadine</i> , and <i>sous vide</i> cooked at (e) 55°C and (f) 65°C <i>cv. Nadine</i>	117
Figure VI.3 Particle size distribution of (a) A _{raw} and N _{raw} , for (b) A ₅₅ and N ₅₅ , and for (c) A ₆₅ and N ₆₅	118
Figure VI.4 Pasting profile of freeze-dried and powered (a) raw potato <i>cv. Agria</i> and <i>cv. Nadine</i> and (b) <i>sous vide</i> cooked (at 55°C and 65°C) potatoes.....	119
Figure VI.5 X-ray diffraction patterns and relative crystallinity of freeze-dried and powered raw and <i>sous vide</i> cooked (a) <i>cv. Agria</i> and (b) <i>cv. Nadine</i>	121
Figure VI.6 Endothermal curves of <i>sous vide</i> cooked-chill then reheated potato <i>cv. Agria</i> and <i>cv. Nadine</i>	122
Figure VI.7 Endothermal curves of <i>sous vide</i> cooked-chill then reheated potato <i>cv. Agria</i> and <i>cv. Nadine</i>	123
Figure VI.8 Relaxation time distribution curves of (a) raw <i>cv. Agria</i> and <i>cv. Nadine</i> and A ₅₅ , and (b) cooked <i>cv. Agria</i> and A ₆₅	125
Figure VI.9 Development of relaxation time T ₂₀ (from 0.6 to 0.8ms, ■□), T ₂₁ (from 5 to 10ms, ●○), T ₂₂ (from 50 to 120ms, ◆◇), and T ₂₃ (from 250 to 1000ms, ▲△) during <i>sous vide</i> cooking at 55°C. Filled symbols represent <i>cv. Agria</i> and empty symbols represent <i>cv. Nadine</i> (mean ±SD, n=3).	126
Figure VI.10 Development of relaxation time T ₂₀ (from 0.6 to 0.8ms, ■□), T ₂₁ (from 5 to 30ms, ●○), T ₂₂ (from 50 to 240ms, ◆◇), and T ₂₃ (from 250 to 2000ms, ▲△) during <i>sous vide</i> cooking at 65°C. Filled symbols represent <i>cv. Agria</i> and empty symbols represent <i>cv. Nadine</i> (mean ±SD, n=3).	127

Figure VI.11 Starch hydrolysis (%) of (a) <i>sous vide</i> cooked potato wedges, (b) <i>sous vide</i> cooked-chill potato wedges, and (c) <i>sous vide</i> cooked-chill+reheated potato wedges. Error bars represent standard deviation (n=3).....	128
Figure VII.1 Relaxation time distribution curves of (a) traditionally cooked retrograded+reheated potato tubers and (b)-(e) TTC retrograded+reheated potato tubers.	136
Figure VII.2 Starch hydrolysis (%) of (a) traditionally cooked retrograded+reheated, (b) the TTC1 retrograded+reheated, and (c) the TTC2 retrograded +reheated potato tubers.	137
Figure VII.3(a) Deconvoluted FTIR curves of freeze-dried powder of <i>cv. Agria</i> , A and <i>cv. Nadine</i> , N. The values represented the 1047/1022 of each sample and different superscripts indicated significant differences ($p<0.05$) (n=3). (b) X-ray diffraction patterns and relative crystallinity of freeze-dried powder of <i>cv. Agria</i> and <i>cv. Nadine</i>	139
Figure VII.4 Starch hydrolysis (%) of retrograded +reheated <i>cv. Agria</i> potato tubers and <i>sous vide</i> cooked+reheated <i>cv. Agria</i> and <i>cv. Nadine</i> potato.	140
Figure VIII.1 Characteristics of different uses of potatoes (TOMRA Food, 2019).....	142
Figure VIII.2 Starch nutritional fractions (%) in boiled-chill+reheated potato tubers. Values on the bars indicate the relative amount of starch nutritional fractions (%). And error bars indicate the standard deviation of triplicate results.....	144
Figure VIII.3 Starch nutritional fractions (%) in TTC processed and TTC processed+reheated potato tubers. Values on the bars indicate the relative amount of starch nutritional fractions (%). And error bars indicate the standard deviation of triplicate results.	146
Figure VIII.6 Appearance of <i>sous vide</i> cooked wedges from <i>cv. Agria</i> (a) at 55°C and (c) at 65°C and from <i>cv. Nadine</i> (b) at 55°C and (d) at 65°C.	149
Figure VIII.7 Changes in hardness of potato <i>cv. Agria</i> and <i>cv. Nadine</i> during <i>sous vide</i> cooking at (a) 55°C and (b) 65°C.....	150
Figure VIII.8 Comparison of the hardness between the traditionally cooked-chill then reheated and the <i>sous vide</i> (at 65°C) cooked-chill then reheated potato <i>cv. Agria</i>	151
Figure VIII.9 Appearances and micrographs of <i>sous vide</i> cooked-frozen then reheated <i>cv. Agria</i> by (a) a microwave or (b) a water bath.....	152
Figure VIII.10 Relaxation time of (a) freshly cooked and <i>sous vide</i> cooked (at 65°C) <i>cv. Agria</i> , and for (b) cooked-frozen and <i>sous vide</i> cooked-frozen <i>cv. Agria</i> , and for (c) cooked-frozen then reheated and <i>sous vide</i> cooked-frozen then reheated <i>cv. Agria</i>	153

List of tables

Table I.1 Nutrition Facts of potatoes.	2
Table I.2 Some of the common potato cultivars in Australia and New Zealand.	3
Table I.3 Physicochemical properties of amylose and amylopectin.	7
Table I.4 Subtypes of resistant starch.	10
Table II.1 Techniques to study starch retrogradation.....	21
Table II.2 Interactions of starches and the other food components during starch retrogradation.	28
Table II.3 Effects of food processing technologies or treatments on starch retrogradation	37
Table II.4 The comparison of kinetics constant κ estimation by different model.....	39
Table II.5 Food processing and starch nutritional fractions	44
Table III.1 Microstructure of raw potato tuber observed by (a) light microscope (LM), (b) confocal laser scanning microscope (CLSM) and (c) scanning electron microscopy (SEM) with a comparison of selected features of each microscope technique.....	71
Table IV.1 Thermal characteristics of freshly cooked (FC), retrograded (FCR) and retrograded+reheated (FCRr) potato tubers.	82
Table IV.2 Optimised parameters (left) and the raw data of raw, cooked and cooled (1h, 24h, and 1wk) potato cylinders (right).	84
Table IV.3 Kinetics of starch hydrolysis percentage, hydrolysis index (HI) and estimated glycaemic index (<i>eGI</i>) of freshly cooked (FC), retrograded (FCR) and retrograded+reheated (FCRr) potato tubers.....	88
Table IV.4 Pearson correlation	91
Table V.1 Summary of all time-temperature cycle processes (left) and the test method that was performed (right).	93
Table V.2 Blue values of different time-temperature cycle processed potato samples.	98
Table V.3 Thermal characteristics of time-temperature cycle treated potato starch <i>in tuber</i>	100
Table V.4 Texture profile analysis of 3-days retrograded potato tubers under different time-temperature cycles process.....	102
Table V.5 Starch hydrolysis (C_{∞} experimental), hydrolysis index (HI), and estimated glycaemic index (<i>eGI</i>) of TTC-processed potato tubers.....	104
Table V.6 Retrogradation enthalpies of the TTC digesta samples (J/g d.b.) at different digestion time and stages.	108
Table V.7 Summary of all time-temperature cycle processes (left) and the relative level of starch crystalline structure implied by the test method was indicated by the number of stars (right).	109
Table VI.1 Dry matter, total starch content and amylose content of potato <i>cv. Agria</i> and <i>cv. Nadine</i>	115
Table VI.2 Cold-water solubility of <i>sous vide</i> cooked samples.....	118
Table VI.3 Thermal characteristics of <i>sous vide</i> cooked potato tubers.....	123
Table VI.4 Starch hydrolysis (C_{∞} experimental), hydrolysis index (HI), and estimated glycaemic index (<i>eGI</i>) of <i>sous vide</i> cooked-chill then reheated potato wedges.....	129
Table VI.5 Observations and interpretations of <i>sous vide</i> cooked potatoes.	130
Table VII.1 Processing conditions of retrograded+reheated potato starch <i>in tuber</i> (left) and the structural stability refers to the parameters from the test methods (right).....	132

Table VII.2 Starch hydrolysis (C_{∞} experimental), hydrolysis index (HI), and estimated glycaemic index (eGI) of TTC-retrograded+reheated potato tubers.....	137
Table VII.3 Starch hydrolysis (C_{∞} experimental), hydrolysis index (HI), and estimated glycaemic index (eGI) of <i>sous vide</i> cooked potato tubers.....	140
Table VII.4 Structural stability refers to the parameters from the test methods.	141
Table VIII.1 Processing flow charts of some common frozen potato products	142
Table VIII.2 Enzyme activities of potato <i>cv.</i> Russet Burbank after a certain level of blanching.	148
Table VIII.3 Processing steps and critical control points (CCPs) of <i>sous vide</i> cooked-chill/ cooked-frozen potato.	153
Table VIII.4 Examples of hurdles.	154

Table of glossary

Terms	Definition
Crystalline perfection	It describes the optimisation of crystalline order in excess (60% w/w) or intermediate (40–55% w/w) water contents below gelatinisation temperature, profoundly used in starch annealing. Hydration of the starch granule increases the α -glucan mobility of both amorphous and crystalline domains. This dynamic nature allows limited side by side movement of the double helices. With the progress of annealing, starch molecules are aligned in a distinct series of layers, with their axes lying perpendicular to the plane of the layers, thereby 'perfecting' starch crystallites. The initially weaker or imperfect crystallites become organised gradually due to fusion or re-crystallisation.
Gelatinisation <i>in tuber</i>	Gelatinisation is the transition of starch molecules from order to disorder. Gelatinisation <i>in tuber</i> depicts the structural changes of starch in potato tuber cells during processing. Swelling of starch granules in a potato cell initiates under heating. Simultaneously, water molecules in the cells penetrate amorphous growth rings of the starch granule, leading to the leaching of amylose. As a significant amount of water enters the amorphous regions, providing sufficient stress on the connectivity between the amorphous growth rings and the semi-crystalline lamellae, crystalline regions are irreversibly disrupted; double helices unwind and the loss of birefringence. Starch gelatinisation and the rounding-off of cells by internal turgor pressure soften the texture of potatoes. Thermal β -eliminative degradation of pectin in the middle lamella causes cell separation and permits cells to distend spontaneously. Cells retain the cell wall outline and are filled with gelatinised starchy matrix.
<i>In tuber</i>	It is referred to a whole potato tuber as a unit.
<i>In vitro</i>	It means "in the glass" in which studies of biology and its subdisciplines are conducted.
Retrogradation <i>in tuber</i>	Retrogradation is the re-association of disrupted amylose and amylopectin during cooling/storage conditions. Retrogradation <i>in tuber</i> subjects to the water availability in potato tuber cells and the interaction of starch with other cellular materials.
Starch nutritional fractions	The starch in food can be classified as RDS, SDS, and RS, suggested by Englyst, Kingman, & Cummings (1992), using controlled enzymic hydrolysis with pancreatin and amyloglucosidase and measuring the glucose release at 20min and 20 to 120min and the remaining after 120min.

Acronyms and abbreviations

AM	Amylose
AP	Amylopectin
AUC	Area under the curve
CLSM	Confocal laser scanning microscope
CPMG	Carr-Furcell-Meiboom-Gill
DSC	Differential scanning calorimetry
DP	Degree of polymerisation
<i>e</i> GI	Expected glycaemic index
FC	Freshly cooked
FCR	Freshly cooked retrograded
FCRR	Freshly cooked retrograded+reheated
FID	Free induction decay
ATR-FTIR	Attenuated total reflectance-Fourier transform infrared spectroscopy
FSANZ	Food Standards Australia New Zealand
Fv	Final viscosity
GI	Glycaemic index
GL	Glycaemic load
HI	Hydrolysis index
HPAEC	Performance anion-exchange chromatography
HPv	Hot-paste viscosity
LF NMR	Low field nuclear magnetic resonance
LM	Light microscope
LOS	Logarithm of slope
PHI	Peak height index
PT	Pasting temperature
Pv	Peak viscosity
RC	Relative crystallinity
RDS	Rapidly digestible starch
RS	Resistant starch
SAXS	Small-angle X-ray scattering
SDS	Slowly digestible starch
SEC	Size exclusion chromatography
SEM	Scanning electron microscope
SSF	Simulated saliva fluid
SGF	Simulated gastric fluid

SH	Starch hydrolysis
SIF	Simulated intestinal fluid
TS	Total starch
WAXD	Wide-angle X-ray scattering
XDR	X-ray diffraction

Chapter I Introduction and thesis outline

I.1 Preface

Due to an increase in the occurrence of diabetes mellitus, cardiovascular disease and obesity in recent years, there has been significantly more research and development on plant-based whole foods such as rice (Tian et al., 2018), wheat (Wu, Qiu, Wang, & Li, 2019) and potatoes (Singh & Kaur, 2016a). The functionality and the overall quality of potatoes have been related to the physicochemical attributes of their carbohydrates (starch), which mostly depend on the botanical origin (Singh & Singh, 2001). The physicochemical characteristics of starches, microstructure of cell and cell wall, complexation of starch with lipids and proteins (Do, Singh, Oey, & Singh, 2018), processing and post-processing storage alter starch digestibility pattern along with sensory attributes (Singh, Dartois, & Kaur, 2010). Cooked or gelatinised starch is hydrolysed to glucose, maltose and malto-oligosaccharides by amylase and other related digestive enzymes (Englyst, Kingman, & Cummings, 1992). These enzymes are active in the gastro-intestinal tract of humans and are responsible for the converting starch completely to glucose, which is later absorbed in the blood (Foster-Powell, Holt, & Brand-Miller, 2002). After gelatinisation or thermal processing and upon cooling of starch and starchy foods, the starch re-associates into an ordered structure. These structural transformations are termed as retrogradation, during which, the starch fractions becomes more resistant to amylolytic enzymes (resistant starch) (Lynch et al., 2007). Starch retrogradation initiate the aggregation of amylose fraction and then later to the linear fraction of amylopectin. Depending on the resistance of starch towards enzymatic digestibility, starches can be classified as rapidly digestible starch (RDS), slowly digestible starch (SDS), or resistant starch (RS) (Goñi, Garcia-Alonso, & Saura-Calixto, 1997). Resistant or slowly digestible starches have physiological functions similar to those of dietary fibres along with some additional benefits (Haugabrooks, 2013). Several studies have indicated that starch retrogradation and type of processing change the amount of the slowly digestible and resistant starches of foods (Goñi et al., 1997; Singh et al., 2010).

The project will be helpful in gaining insight into how potato starch structural changes *in tuber*, during processing and post-processing, affect digestibility. In addition, how it can be tailored to gain desirable functionalities. Starch digestion *in vitro* techniques involve imitation of the physiological conditions within the human body and generally show a very good agreement with starch digestibility calculated *in vivo* (using both animal and human subjects). Knowledge about digestion kinetics is a powerful tool to design processed potato products with low and slow digestibility. Therefore, we studied the digestibility of retrograded potato starch *in tuber* by oral-gastric-small intestinal digestion *in vitro*.

I.2 Potato tubers

The annual world production of potato (*Solanum tuberosum* L.) exceeded 388 million metric tonnes in 2017, of which China is the top producer (FAOSTAT, 2019). The high yield per unit area and the abundant nutrients (Table I.1) have led to an increase in potato production over past years compared with other tuber crops. The potato plant, a perennial herb belonging to the family Solanaceae, bears white to purple flowers with yellow stamens, and some cultivars bear small green fruits, each containing up to 300 seeds. Potato tuber is an underground stem bearing auxiliary buds and scars of scale leaves and is rich in starch and storage proteins. Potatoes can be grown from the botanical seeds or tuber propagation i.e. seed potatoes with optimum sprouting. A sprouted potato, however, is not acceptable for consumption and processing due to the formation of glycoalkaloids (Furrer, Chegeni, & Ferruzzi, 2018; Laus, Klip, & Giuseppin, 2017).

Potato possesses a high economic yield and nearly 80% of the harvested tuber is processed to a wide range of applications (Singh & Kaur, 2016b). Based on the composition of different potato cultivars (Table I.2), they are suited to various culinary uses. Potato tubers can be consumed either freshly cooked or as processed potato products. The compositional attributes such as specific gravity, total solids, and starch content are found to be correlated with some sensory perception, and thus, leading to different culinary uses (Bordoloi, Kaur, & Singh, 2012; Kirkpatrick, Heinze, Craft, Mountjoy, & Falatko., 1956; Sterling & Bettelheim, 1955). Most commonly processed potatoes are French fries ("chips" in British and Commonwealth English) that the production processes simply include peeling/cutting, blanching, frying, freezing and packaging. Another similar processed product is potato crisp ("chips" in the US) which is made from thin slices of deep-fried or baked potato or made from a dough of dehydrated potato flakes. Dehydrated potato flakes and granules are made by drying cooked potatoes to a moisture level of 5 to 8 percent. Potato flakes can be used to make mashed potato products, or as ingredients in snacks, or even as food aid. Other dehydrated product, such as potato flour, is ground from whole and cooked potatoes, which retain a distinct potato taste. Potato flour, a good source of starch and is gluten-free. It is often used by the food industry to make and bind meat mixtures or to thicken gravy and soup. Further purified potato starch features a fine, tasteless and excellent mouthfeel, along with providing higher viscosity than wheat and corn starches. So potato starch is commonly used as a thickener for sauces and stews, or as a binding agent in cake mixes, dough, biscuits and ice cream (Luallen, 2017; Wurzburg,

Table I.1 Nutrition Facts of potatoes.

Nutrients	Amount (/100g)
Calories	77 kcal
Protein	2 g
Total lipid (fat)	0.0 g
Cholesterol	0.0 mg
Total carbohydrate	17 g
Fibre, total dietary	2.2 g
Sugars, total	0.8 g
Minerals	
Calcium, Ca	14 mg
Iron, Fe	0.73 mg
Potassium, K	419 mg
Sodium, Na	0 mg
Vitamins	
Vit C, total ascorbic acid	18.2 mg

USDA Food Composition Databases.
<https://ndb.nal.usda.gov/ndb/>

1972). Beside general food application, potatoes are processed and fermented in eastern Europe and Scandinavia to make Vodka and Akvavit. Crushed potatoes are heated to convert their starch to fermentable sugars that are used in the distillation of alcoholic beverages (Survase, Singh, & Singhal, 2016). Potato starch is widely used by the pharmaceutical, textile, wood and paper industries as an adhesive, texture agent and filler, etc. It is a 100% biodegradable plant-based material and a good substitute for polystyrene and other plastics uses such as disposable plates, dishes and knives (Kaur & Singh, 2016). Potato peel and other wastes from potato processing often still contain a high amount of starch, for example potato pulp contain 30% of starch, that can be liquefied and fermented to produce fuel-grade ethanol (Arapoglou, Varzakas, Vlyssides, & Israilides, 2010; Srichuwong et al., 2009).

Table I.2 Some of the common potato cultivars in Australia and New Zealand.

Cultivars	Flesh colour	Dry matter	Starch content	Culinary uses
Russet Burbank	White	High	Medium to high	Fairly firm (multi-purpose) to Mealy (floury type)
Desiree	Light yellow	Medium to high	Medium to high	Fairly firm (multi-purpose) to Mealy (floury type)
Bintje	Light yellow	Medium to high	Medium to high	Fairly firm (multi-purpose) to Mealy (floury type)
Agria	Yellow	Low to high	Low to medium	Fairly firm (multi-purpose) to Mealy (floury type)
Moonlight	White	Low to medium	Medium	Fairly firm (multi-purpose type)
Nadine	Cream	Very low to low	Low	Fairly firm (multi-purpose type)

I.3 Potato starch *in tuber*

“Tuber” originates from Latin, meaning lump and swelling. Potato tuber is a swollen stem, a stolon that thickens to develop into a storage organ. In the crosscut section, there are four distinguishable areas including skin or a periderm, parenchyma tissue, the ring of vascular bundles, and the pith (Figure I.1). **Skin or periderm** is a ring of six to ten suberized cell layers (Reeve, Hautala, & Weaver, 1969). The skin thickness depends on the variety and growing conditions. The skin of immature tubers can be removed easily but not for fully mature tubers. Potato eyes, bud and stem ends are present on the skin/periderm surface. **Parenchyma tissue** is composed of cells of the cortex and the perimedullary zone. It represents the major part of the tuber and contains starch granules as reserve material (Figure I.1). A ring of **vascular bundles** is observed when the tuber is cut lengthwise, also known as the xylem. The medullar rays and medulla are known as the **pith**.

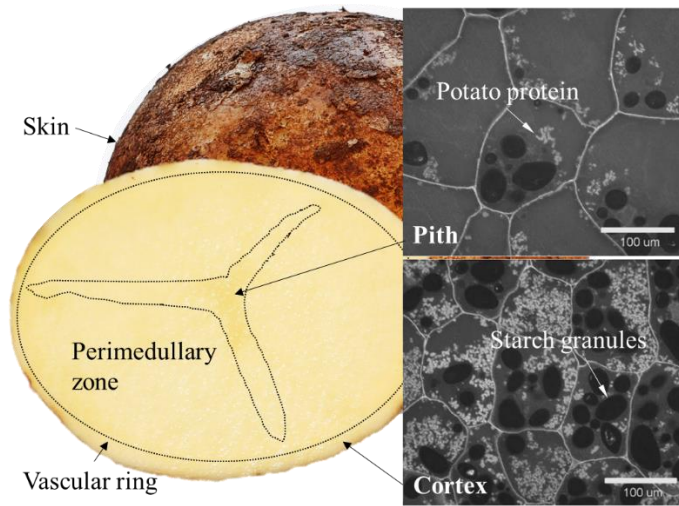


Figure I.1 Potato tuber crosscut section (left) and the micrographs of pith (up right) and cortex (bottom right). Different crosscut sections contain various amount of starch granules and protein.

The conditions of pre-harvest and post-harvest affect the chemical composition of potato tubers (Figure I.2). For example, when potato tubers are exposed to light ($> 3\text{--}11 \text{ W/m}^2$) during storage, the green colour will develop in the periderm or the outer parenchyma cells of the cortex, i.e. greening effect (Salunkhe, Desai, & Chavan, 1989). Greening effect is due to the formation of solanidine by the synthesis of chlorophyll. Solanidine can cause off-flavours upon cooking at concentrations of 15–20mg/100g (McKenzie & Corrigan, 2016; Morris, Shepherd, Verrall, McNicol, & Taylor, 2010). Glycoalkaloids impart a bitter taste and can be toxic above threshold levels (200 mg/kg) (Friedman, McDonald, & Filadelfi-Keszi, 1997). Tuber handling and storage is another important stage for different proposed uses. Low-temperature storage ($<4 \text{ }^\circ\text{C}$) is an effective method of hindering sprouting and control fungal and bacterial growth for table stock and seed potatoes (Burton, van Es, & Hartmans, 1992). Conditioning below 9 or 10°C for tubers destined for processing can, however, result in accumulation of reducing sugars, e.g. glucose and fructose called LTS (low-temperature sweetening). Reducing sugars cause Maillard browning reaction with free amino acids during frying, resulting in dark brown fries and chips (Burton, 1978).

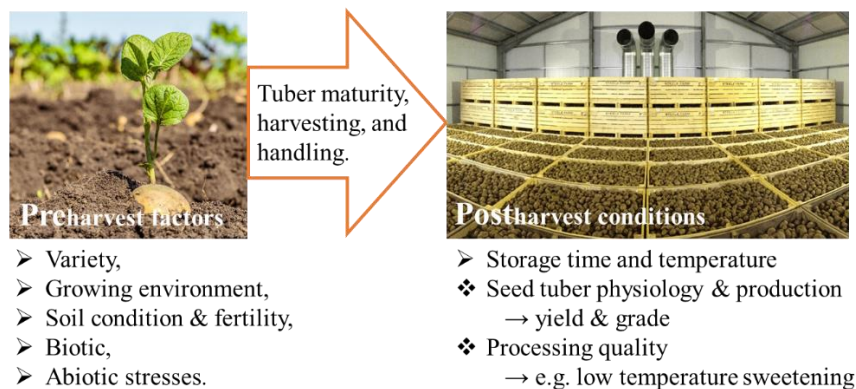


Figure I.2 Preharvest and postharvest conditions affect qualities of potato tubers.

Starch, the main nutrient of the potatoes, is synthesised and stored in plant organs by amyloplasts. Large numbers of amyloplasts can be found in fruit and in underground storage tissues of some plants, such as in potato tubers. Starch synthesis and storage also take place in chloroplasts, a type of pigmented plastid involved in photosynthesis. Amyloplasts and chloroplasts are closely related, and amyloplasts can turn into chloroplasts; this is, for instance, observed when potato tubers are exposed to light and turn green. The composition of the dry matter in potatoes can vary substantially according to variety, conditions during growth i.e. type of soil, fertilizer application, temperature, moisture supply and light and degree of maturity (Pinhero & Yada, 2016). Moreover, the dry matter within the tuber varies between each cross-cut section (Mohr, 1972) where the amount of starch in pith tissue is found to be lower and cortex possess the higher content of starch and proteins (Figure I.1) (Karlsson & Eliasson, 2003b; Matsuura-Endo, Ohara-Takada, Yamauchi, Mori, & Fujikawa, 2002; Reeve, Weaver, & Timm, 1971).

I.3.1 Starch granule architecture

Starch granules, in the form of spherical granules with a range of 10 to 110 μm are the product of starch biosynthesis (Guilbot & Mercier, 1985). Unlike the natural morphology of starch granules, starch composition such as the amylose to amylopectin ratio can be modulated genetically by crossbreeding. Starches from different botanical resources show varied polymorphic types and degrees of crystallinity (Buléon, Gérard, Riekkel, Vuong, & Chanzy, 1998; Frost, Kaminski, Kirwan, Lascaris, & Shanks, 2009; Pérez & Bertoft, 2010; Van Soest, Tournois, de Wit, & Vliegthart, 1995). Structure of starch in the whole tuber is laid down in different length scale from micrometres of granules to few nanometres composed of glucose molecule (Figure I.3). Distinct refractive indices i.e. maltase-cross birefringence with a unique pattern of potato starch granules are observed by a polarized light microscope (Figure I.3a). The alternating amorphous and semi-crystalline growth rings are widely recognised in native starch granule (Figure I.3b). The semi-crystalline growth ring consists of the repeats of alternating amorphous and crystalline lamellae (Figure I.3c). The amorphous lamellae are related to branch points of the less ordered amylopectin side chains and linear amylose molecules. Whilst the crystalline lamellae are formed by the short-chain fractions of amylopectin arranged as double helices and packed in small crystallites (Figure I.3d) (Pérez & Bertoft, 2010; Witt, Douth, Gilbert, & Gilbert, 2012). Amylopectin is widely accepted to support the framework of the semi-crystalline regions of the starch granule and forms double helices (Figure I.3e) (Buléon & Tran, 1990; Imberty & Pérez, 1988). The double helical structure of A-type crystallites are in a monoclinic unit cell with 8 water molecules per unit cell (Figure I.3A), whilst the double-helical structure of the B-type crystallites are in a hexagonal unit cell with 36 water molecules per unit cell (Figure I.3B). All starches contain two anhydroglucose polymers, which are amylose and amylopectin (Figure I.3f).

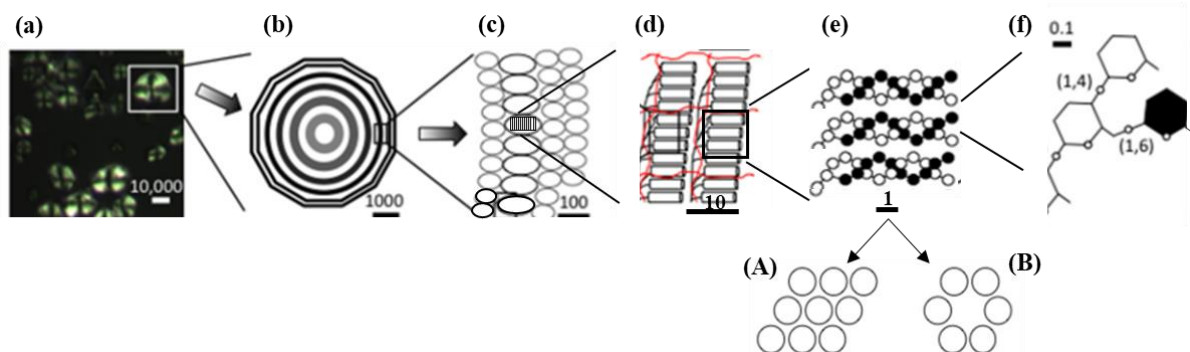


Figure I.3 The hierarchical structure of starch granule (Bertoft, 2017). (a) Under polarised light microscope, starch granules showed “Maltese cross”, a radial organisation of starch granules. (b) A hypothetical granule (in this case polyhedral) with growth rings extending from the hilum. (c) Blocklets in semi-crystalline (black) and amorphous (grey) rings. (d) Crystalline and amorphous lamella formed by double helices (cylinders) and branched segments of amylopectin (black lines), respectively. Amylose molecules (red lines) are interspersed among the amylopectin molecules. (e) Three double-helices of amylopectin. Each double-helix consists of two polyglucosyl chains, in which the glucosyl residues are symbolised by white and black circles, respectively. The double helices form either A- or B-polymorphic crystals (A and B, respectively, in which the circles symbolises the double helices seen from the edge). (f) Glucosyl units showing α -(1,4)- and α -(1,6)-linkages at the base of the double-helix. The bar scale (in nm) is only approximate to give an impression of the size dimensions. Modified and reproduced from an open access journal- Agronomy “Understanding Starch Structure: Recent Progress”, Vol 7, P56, Bertoft, 2017.

I.3.2 Starch molecular structure

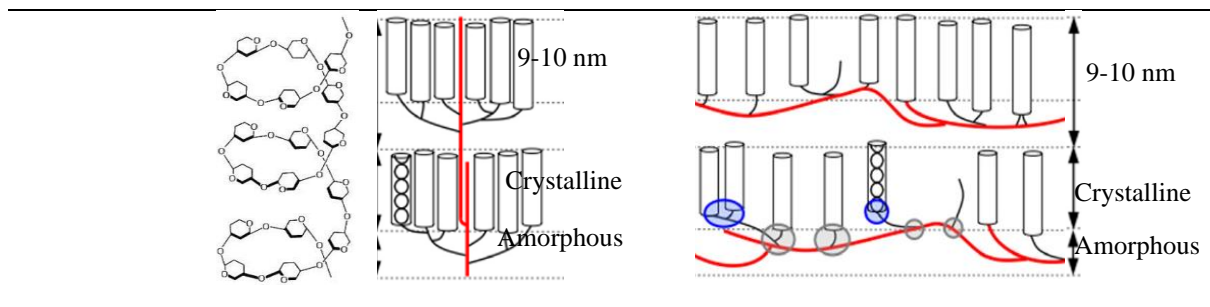
Amylose, primarily a linear macromolecule, is linked by α -1,4 bonds. Amylose predominately forms the single-chain helix with less than 1% long-chain branches in a disordered amorphous conformation. Amylose can bind with itself in a 6-fold left-handed double helix as a A or B amylose structures with a pitch height of 2.08–2.38 nm (Imberty, Buléon, Tran, & Péerez, 1991; Imberty, Chanzy, & Perez, 1988). The interior of the helix is hydrophobic/lipophilic due to a predominance of hydrogen atoms, while the hydroxyl groups are positioned on the exterior of the coil. Amylose helix is, therefore, known to form V-type crystalline inclusion complexes with small molecules such as lipids, alcohols, or flavours during thermal treatments (Buléon, Colonna, Planchot, & Ball, 1998; Buléon, Véronèse, & Putaux, 2007) (Table I.3).

Amylopectin is linked by α -1,4 bonds in linear segments and by α -1,6 bonds at branching points that contains many short branches of 4-5% of branching points. Amylopectin is present in all common starches and consists of 70–80% (weight basis) of those starch varieties. Some starches containing predominately amylopectin are called waxy or amylopectin starches. The relative molecular weight of highly branched amylopectin is 10^7 - 10^9 Da (Imberty et al., 1991, 1988). The size-distribution of amylopectin chains was analysed after debranching by either SEC (Hizukuri, 1985, 1986), high-performance anion-exchange chromatography (HPAEC) or fluorophore-assisted carbohydrate electrophoresis (Jane et al., 1999). The chains of amylopectin are divided into two major groups, short (S) and long (L) chains based on the degree of polymerisation. The complexity of amylopectin in the form of unit chains, internal chains, and diverse branched units with their composition of chains was

assembled in two main models, the “cluster model” and the “building block backbone model” (Figure I.3d). A cluster-type of molecule model of amylopectin is widely accepted nowadays (Haworth, Hirst, & Isherwood, 1937; Meyer, Gurtler, & Bernfeld, 1947; Staudinger & Husemann, 1937). In this model, the short chains in amylopectin form clusters and the long chains interconnect the clusters (Table I.3). But some researchers found a periodicity among the amylopectin short chains, not among the amylopectin long chains. This appears that the periodicity of amylopectin short chains may interconnect building blocks in the isolated α -dextrins (Hanashiro, Abe, & Hizukuri, 1996). In addition, a molecular model showed that the amorphous chain segments involved in interconnecting double-helices in the crystalline lamellae came into parallel alignment and almost perpendicular to the directions of the helices (O’Sullivan & Perez, 1999) (Table I.3). Another model suggests that the double-helices are linked to the amorphous “backbone” of clusters through flexible spacer arms instead of compact groups branches in “cluster model” (Perry & Donald, 2000c; Waigh, Gidley, Komanshek, & Donald, 2000a; Waigh, Kato, et al., 2000). The backbone model can better explain the granule structural changes during the process of annealing and gelatinisation. Initially swollen granules remain intact because the backbones of the amylopectin molecules stretch in all directions. The backbones of the amylopectin molecules only breakdown once the temperature exceeds transition peak temperature. The building block backbone model is compatible with the former data in favour of the cluster model indicating it also explains satisfactorily many of the properties of starch granules. Building block backbone model perhaps implies new ways to interpret the biosynthesis of starch and the structure-function relation after processing (Bertoft, 2017).

Table I.3 Physicochemical properties of amylose and amylopectin.

Physico-chemical properties	Amylose	Amylopectin
Molecular structure/branches	Mainly linear/ primarily α -1,4	Highly branched/ α -1,4 and α -1,6
Molecular weight	10^5 - 10^6 Da	10^7 - 10^9 Da
Iodine bonds/ colour	20%/ blue-black	<1%/ red-purple
Molecular diagram*	Amylose helix	Cluster model Building block backbone model



* Molecular diagrams were modified and reproduced from an open access journal- Agronomy “Understanding Starch Structure: Recent Progress”, Vol 7, P56, Bertoft, 2017.

I.4 Potato microstructure and starch digestion

The granular architecture of the native starch provides a physical barrier to the diffusion of digestive enzymes resulting in a lower digestion rate. Enzyme-catalysed digestion of starches exhibits differently depending on the type of starches (Gallant, Bouchet, Buléon, & Pérez, 1992). The A-type starches have surface pores connected to interior cavities through channels (Fannon, Hauber, & Bemiller, 1992), whereas the surface of B type starch granules is rather smooth. The digestive enzymes enter the A-type starches from pores and channels and eventually digest the granules from inside out. While the enzymatic digestion of the B-type starch granules occurs on the pit on the granular surface due to no surface pores or interior cavities (Hamaker, Zhang, & Venkatachalam, 2007; Jiang et al., 2015; Zhang, Ao, & Hamaker, 2006). Native A-type starches have therefore been shown to have a higher amount of slowly digestible starch (SDS), whereas native B-type starches have been observed to contain more resistant starch (RS) (Ferguson, Tasman-Jones, Englyst, & Harris, 2000).

The majority of starches in cooked/processed foods are rapidly digested producing high postprandial glycaemia (Fernandes, Velangi, & Wolever, 2005; Foster-Powell et al., 2002; Goñi et al., 1997; Tahvonen, Hietanen, Sihvonen, & Salminen, 2006). Cooked/processed starches undergo gelatinisation that starch granules swell and rupture losing the ordered structure. Swelling of starch granules initiates during heating in excess water. Simultaneously, water molecules penetrate amorphous growth rings of the starch granule leading to the leaching of amylose (Donovan, 1979). As a significant amount of water enters the amorphous regions, providing sufficient stress on the connectivity between the amorphous growth rings and the semi-crystalline lamellae, crystalline regions are irreversibly disrupted; double helices unwind and the loss of birefringence (Jenkins & Donald, 1997; Waigh, Gidley, Komanshek, & Donald, 2000). This molecular order-to-disorder transition is known as gelatinisation.

Raw parenchyma cells generally contain starch granules with a wide range of shapes and sizes. After cooking, cells retain the cell wall outline and are filled with gelatinised starch matrix as shown by the micrographs (Bordoloi, Singh, & Kaur, 2012). Cooking is known to soften the texture of potatoes because of starch gelatinisation and the rounding-off of cells by internal turgor pressure (Shomer, 1995). Thermal β -eliminative degradation of pectin in the middle lamella causes cell separation and permits cells to distend spontaneously (Matsuura-Endo, Ohara-Takada, Yamauchi, Mukasa, et al., 2002). Starch

hydrolysis by simulated small intestinal fluid (SIF)-containing pancreatic amylases led to the digestion of gelatinised starch and its remnants progressively, as evidenced by the homogeneous background of empty cells and empty cavities of SEM micrographs. Cell walls stayed intact during and after the digestion indicating SIF had no effect on the cooked potato tuber cell walls, which are generally made up of cellulose and hemicellulose materials (Bordoloi, Singh, et al., 2012).

Disrupted amylose and amylopectin retrograde differently owing to the distinct molecular structure. Amylose aggregation and crystallisation take place within the first few hours while amylopectin retrogradation occurs at a later stage of cooling and storage. Amylose linear chains facilitate cross-linkages by hydrogen bonding, and hence amylose is proposed to act as a nucleus for amylopectin crystallisation or amylose-amylopectin co-crystallisation (Lian, Cheng, Wang, Zhu, & Wang, 2018; Smits, 2001). Amylopectin retrogradation is generally linked to the ability of the external glucan chains to form double helices (Gudmundsson & Eliasson, 1990; Singh, Lin, Huang, & Chang, 2012). The manner in which the re-association of amylose and amylopectin during cooling/storage conditions to form a relatively ordered network largely determines the subsequent resistance of the starch to enzymatic digestion (which was comprehensively surveyed in Chapter II). Additionally, based on the food processing conditions such as temperature, water content, shear strength, and pressure, changes in starch physicochemical properties lead to various glycaemic responses.

I.5 Potato tuber consumption and human health

Potatoes (*Solanum tuberosum*) are an important food crop worldwide and contribute key nutrients to the diet, including vitamin C, potassium, and dietary fibre (Camire, Kubow, & Donnelly, 2009). Potatoes have been shown to have favourable impacts on several measures of cardiometabolic health in animals and humans, including lowering blood pressure, improving lipid profiles, and decreasing markers of inflammation (McGill, Kurilich, & Davignon, 2013). But potatoes are generally considered as a high GI food due to the blood glucose spike after consumption. The glycaemic index (GI) is defined by the increase in postprandial blood glucose during the first 2 hours after the consumption of carbohydrate foods. Foods with a high GI produce a higher peak in postprandial blood glucose and a greater overall blood glucose response than foods with a low GI. In the context of the pandemic of obesity and glucose intolerance in the modern world, ways to manipulate the rate and extent of starch digestibility are vital, as for the purpose of this project especially. Rate of starch digestion is important because the degree to which blood glucose loading exceeds blood glucose clearance determines the acuteness of the net increase in blood glucose concentrations, and consequently, the intensity of the insulin response required to remove the glucose overload and restore normal blood glucose concentrations. Rate of digestion determines the sustainability of glucose supply during the continued digestion in the gut, and therefore, delay the urge to eat again contributing to satiation during a meal

(Diaz-Toledo, Kurilich, Re, Wickham, & Chambers, 2016; Erdmann, Hebeisen, Lippl, Wagenpfeil, & Schusdziarra, 2007).

A committee of experts brought together by the Food and Agriculture Organization (FAO) of the United Nations and the World Health Organization (WHO) reviewed the available research evidence and endorsed the use of the GI method for classifying carbohydrate-rich foods (Foster-Powell et al., 2002). It is, thus, recommended that the GI values of foods be used in conjunction with information about food composition to guide food choices. To promote good health, the committee also advocated the consumption of a high-carbohydrate diet ($\geq 55\%$ of energy from carbohydrate), with the foods rich in non-starch polysaccharides. For instances, when consuming baked potato topped with cheese (Henry, Lightowler, Kendall, & Storey, 2006), or mashed potato with meat, oil, and salad (Hätönen et al., 2011), or broccoli with mashed potatoes (Ballance et al., 2018), the glycaemic responses were reduced compared to eating potatoes alone. In Australia, official dietary guidelines for healthy elderly people recommend the consumption of low-GI cereal foods for good health (Jenkins et al., 1981), and a GI trademark certification program is in place to put GI values on food labels as a means of helping consumers to select low-GI foods (Krezowski, Nuttall, Gannon, Billington, & Parker, 1987).

I.5.1 Resistant starch content in potato tubers

Starch is the main form of carbohydrate in the diet. It is conveniently divided into three categories, depending on its propensity to be hydrolysed by digestive enzymes during intestinal transit. The three categories of starch are rapidly digestible starch (RDS- hydrolysed within 20 min), slowly digestible starch (SDS- hydrolysed between 20 and 120 min), and resistant starch (RS- not hydrolysed within 120 min) (Englyst et al., 1992). Resistant starch is the fraction of starch that is not digested when it passes through the small intestine (Fuentes-Zaragoza, Riquelme-Navarrete, Sánchez-Zapata, & Pérez-Álvarez, 2010; Nugent, 2005; Sajilata, Singhal, & Kulkarni, 2006). It is at least partially fermented in the large intestine. Five resistant starch (RS) subtypes have been defined and were shown in Table I.4 (Englyst et al., 1992; Gelders, Duyck, Goesaert, & Delcour, 2005). RS1 is physically inaccessible to digestion and is found in whole or partially milled grains. RS2 is granular native starch that is protected from digestion due to the conformational structure of the granule. RS3 refers to non-granular starch that is formed during retrogradation in food processing. Retrogradation occurs when starch granules are disrupted by cooking above their gelatinisation temperature. Upon cooling, the starch granules re-associate into crystalline structures that resist hydrolysis by amylase. RS4 is chemically modified starch (i.e. semi-synthetic) that resists digestion. RS5 refers to amylose-lipid complex. Amylose can form helical complexes with lipids in native and processed starches, thereby enhancing resistance to digestion.

Table I.4 Subtypes of resistant starch.

RS subtype	Description
1	Physically inaccessible to digestion.

2	Native starch granules protected from digestion due to the conformational structure of the granule.
3	Non-granular starch formed during retrogradation of starch granules in food processing.
4	Chemically modified starch to decrease digestibility.
5	Amylose-lipid complex found in native starch granules and processed starch.

I.5.2 Cooking methods and the effects on starch digestion

Uncooked potatoes have 75% of resistant starch; however, potatoes are rarely consumed in the raw form. Once cooked, amount of resistant starch has been observed to decrease to 1.5% (Englyst et al., 1992; García-Alonso & Goñi, 2000). Besides the intrinsic factors of starch such as botanical source, amylose content and other cell components, the extrinsic factors such as different cooking methods have also been shown to affect the starch digestibility (Dupuis, Lu, Yada, & Liu, 2016; Mishra, Monro, & Hedderley, 2008). Some resistant starch or slowly digestible starch may be restored during cooling periods (i.e. boiling potatoes followed by refrigeration) attributed to retrogradation (Colussi, Singh, et al., 2017), resulting in a reduced glycaemic index (Fernandes et al., 2005). Details of food processing and starch retrogradation and its effect on starch digestion are surveyed in Chapter II.

I.6 Research aim and thesis outline

The object of this project is to tailor the digestion characteristics of potato starch *in tuber* through retrogradation in order to achieve functional processed potato product with low glycaemic features. Three stages are envisaged for the project with an aim to design slowly digestible whole processed potato tubers. The first stage is to understand the mechanism and kinetics of starch retrogradation, followed by the second stage of the development of processing technologies or treatments. Then in the third stage, the stability of slowly digestible/ resistant starch during processing and post-processing, i.e. storage and reheating will be discussed. The knowledge gained through these three stages will be used to formulate slowly digestible/ resistant starch-based low GI processed potato products, and the feasibility of scale-up will be discussed. The thesis outline is described per chapter below.

Chapter II Review of literature This chapter provides the current understanding of starch retrogradation including the structure of retrograded starch and its mechanisms as published in the scientific literature. How food processing influences the formation of retrograded starch and interaction with other food components thus leading to a lower or slower rate of starch digestion, is surveyed. This is a basis for investigating how potato starch retrogradation *in tuber*, i.e. in a natural whole food, can be tailored to develop nutritionally processed potato products.

Chapter III Methodology and methods development. This chapter details the developed analytical techniques including experimental setups and method validations for studying potato starch retrogradation *in tuber* and its digestion using an oral-gastric-small intestinal *in vitro* model. Other general methods to study potato starch retrogradation are provided in individual chapters accordingly.

Based on the review of literature in chapter II, research gaps and research questions were identified and thus three main studies were carried out and described in the following chapters. Cooking disrupts starch granular structure from ordered to disordered state, and with subsequent cooling the disordered structure tangles up. This on-going process of starch structural changes i.e. gelatinisation and retrogradation was studied in whole tuber in **chapters IV, V and VI**.

Chapter IV Potato starch retrogradation *in tuber*: structural changes and gastro-small intestinal digestion *in vitro*. This chapter reported study of the mechanisms of potato starch retrogradation *in tuber* by LF-NMR. A gastro small-intestinal *in vitro* model was used to study the starch hydrolysis in the cooked and retrograded tubers. After various storage periods (1, 3, and 7 days) at 4°C in the refrigerator, the estimated glycaemic index (*eGI*) of retrograded tubers decreased, especially the 7-day retrograded tuber which exhibited the lowest *eGI*.

Chapter V Influence of time-temperature cycles on potato starch retrogradation *in tuber* and starch digestion *in vitro*. Time-temperature cycles (TTC) were designed to induce stepwise nucleation and propagation to promote the growth of crystalline regions and the perfection of starch crystallites, and thus presents a piece of new information on the acceleration of starch retrogradation *in tuber*. TTC processed potatoes were studied by *in vitro* oral-gastro-small intestinal digestion.

Chapter VI Starch retrogradation of *sous vide* cooked potato and starch digestion *in vitro*. This study investigated potato starch retrogradation *in tuber* when potatoes were cooked at low temperatures for a long time by following French-style *sous vide* cooking. *Sous vide* cook-chill potato tubers storing at 4°C in a refrigerator were to simulate the catering processing. Structural characteristics of all length scales such as microstructure, pasting properties, relative crystallinity, thermal characteristics, and water mobility were analysed. The effect on digestibility was studied by *in vitro* oral-gastric-small intestinal digestion.

Chapter VII Stability of retrograded potato starch *in tuber* during reheating. This chapter discusses reversible structural changes of the retrograded starch *in tuber* during reheating. The retrograded starches *in tuber* were taken from the three main studies: the constant 4°C retrograded, the TTC retrograded, and the *sous vide* cooked-chill starches *in tuber*.

Chapter VIII Industrial relevance. It is a projection from the main three studies and industrial implications have been presented and discussed.

Chapter IX General discussion and conclusion.

Chapter II Review of literature

This review presents current knowledge on the mechanism of starch retrogradation and explores its health implications, with a focus on the utilization of existing and new technologies to create tailor-made structures with low glycaemic features.

II.1 Introduction

Plants produce starch to store energy for cell metabolism. Humans eat starchy plants for growth and energy and pleasure. Cooking enhances the palatability and digestibility of the starch-based foods, yet incurs loss of nutrients, such as vitamins and minerals at elevated cooking temperatures (Camire et al., 2009). The increase in metabolic response e.g. the glycaemic index after consuming cooked starchy foods is attributed to the disruption of starch (Singh, Dartois, & Kaur, 2010). Increasing occurrence of diabetes mellitus, cardiovascular disease and obesity in recent years has prompted this survey of how starch-based products can play a role in mitigating these hyperglycaemic events.

Raw starch granules range from 1 to 100 μm in size. They are insoluble but disperse in cold water due to starch's well-organized and compact structure (Guilbot & Mercier, 1985). Starch granules show layers of growth-ring structure when observed under microscopy (Jane, Kasemsuwan, Leas, Zobel, & Robyt, 1994). The growth-ring structure is composed of alternating semi-crystalline and amorphous shells developed concentrically from the hilum (Pérez & Bertoft, 2010). The semi-crystalline rings are mainly clusters of highly branched-chain amylopectin, while the amorphous rings consist of long linear-chain amylose (AM) and low-molecular-mass amylopectin (AP) (Witt et al., 2012). Each semi-crystalline ring consists of alternating crystalline and amorphous lamellae, with a lamellar spacing (d) of 9.8 nm. The crystallinity of native starches range from 15 to 45%. Based on the packing of double-helical crystallites, crystal structure is monoclinic (known as A-type starch), or hexagonal (B-type starch), or a mix of both polymorphs (C-type starch) (Zobel, 1992). Amylopectin is widely accepted to support the framework of the semi-crystalline regions of the starch granule and forms double helices. Amylose predominately forms a single chain helix with less than 1% long-chain branches in a disordered amorphous conformation (Buléon & Tran, 1990; Imberty & Pérez, 1988).

The granular architecture of native starch acts as a physical barrier delaying diffusion of digestive enzymes, thus resulting in a low digestion rate. Digestive enzymes act on A-type starches (e.g. cereals) and B-type starches (e.g. tubers) differently due to their different granular architecture (Gallant et al., 1992). Granular dimensions and internal channels and pores more than starch fine structure (e.g. amylopectin branch length profiles, crystallinity, and lamellar periodicity) have been found to be the predominant factors during α -amylase hydrolysis (Shrestha et al., 2015; Warren, Royall, Gaisford, Butterworth, & Ellis, 2011). The A-type starches have surface pores connected to interior cavities through channels (Fannon et al., 1992) whereas the surface of B-type starch granules is rather smooth.

Digestive enzymes enter the A-type starches through the pores and channels, digesting a granule from its core to surface. In contrast, as the B-type starch granules have no surface pores or interior cavities, the enzymatic digestion occurs on the pit of the granular surface (Hamaker et al., 2007; Jiang et al., 2015). Native A-type starches have a higher amount of slowly digestible starch (SDS), whereas the native B-type starches contain more resistant starch (Ferguson et al., 2000).

The blood glucose response after consuming carbohydrate food is measured as glycaemic index (Jenkins, Wolever, & Taylor, 1981; Ludwig, 2002). It is tested by comparing the incremental area under the glucose response curve (AUC) of a test food (with a standard amount of carbohydrate) in relative to a control food (either white bread or glucose) (Jenkins et al., 2002). According to the postprandial glucose responses, starchy food and starch-based products are classified into high ($GI > 70$), medium ($56 < GI < 69$), and low ($GI < 55$) foods (Foster-Powell et al., 2002). Some starches that escape the digestion in oral-gastric-small intestinal process and pass into the large intestine are known as “resistant starch”. Starchy foods with a low level of resistant starch such as white bread increase blood glucose levels rapidly and may increase the risk of type 2 diabetes over time (Collier, Wolever, Wong, & Josse, 1986; Granfeldt, Bjorck, & Hagander, 1991). Other starchy foods with high levels of resistant starch are considered to be beneficial for health because of the stable effect on blood glucose levels (Bird, Lopez-Rubio, Shrestha, & Gidley, 2009). Additionally, the resistant starch can promote a healthy bacterial flora in the large intestine (McCleary & Monaghan, 2002; McCleary & Rossiter, 2004).

Digestibility of starches in formulated starch-water systems have been found to be different than in whole foods (Alsaffar, 2010; Dhital, Bhattarai, Gorham, & Gidley, 2016; Singh, Berg, Hardacre, & Boland, 2014). The other cell components in whole foods may act as extra physical barriers. Surface proteins and lipids may hinder the enzymatic diffusion during digestion (BeMiller & Whistler, 2009). During heating, tissue of starchy whole food (i.e. potato tuber) becomes soft and more susceptible to fracture. This is mainly due to pectin degradation through β -elimination, leading to loss of turgor pressure. Simultaneously, water molecules penetrate amorphous growth rings leading to leaching of amylose and semi-crystalline rings undergo swelling (Donovan, 1979). Gradually, crystalline regions are irreversibly disrupted and the birefringence is lost as double helices unwind, in a process known as gelatinisation (Jenkins & Donald, 1997; Waigh, Gidley, Komanshek, & Donald, 2000). With subsequent cooling, disrupted amylose and amylopectin can re-associate and form a relatively ordered structure; the process is termed as starch retrogradation (Siljestrom et al., 1988). The structure of retrograded starch may create steric hindrance and subsequent mass transfer resistance, limiting enzyme binding during hydrolysis, therefore lower glycaemic index (Fernandes, Velangi, & Wolever, 2005; Kinnear & Wolever, 2010; Singh, Dartois, et al., 2010). Sufficient recrystallisation or dense amorphous packing have been found to either prevent/limit binding and/or slow down catalysis (Zhang, Dhital, & Gidley, 2015).

Our review highlights current knowledge of starch retrogradation tailoring the relationship of starch structure-digestion to explore potential health benefits. It covers and compares most recent information

on mechanisms of starch retrogradation in pure starch-water and in whole food systems. A particular focus of this review is the influence of food processing and post-processing in relation to structures of retrograded starch-digestion.

II.2 Mechanism of starch retrogradation

Starches from different botanical sources show different retrogradation tendencies (Jacobson, Obanni, & BeMiller, 1997) because of the intrinsic characteristics such as the amylose content (Yao, Zhang, & Ding, 2002), the ratio of amylose and amylopectin (Fredriksson, Silverio, Andersson, Eliasson, & Åman, 1998), and the distribution of branch chain length of amylopectin (Jane et al., 1999).

During starch retrogradation, amylose crystallises rapidly and creates initial firmness whereas amylopectin crystallises slowly and changes the texture gradually (Ring et al., 1987). Retrogradation consists of two separable processes: (1) a short term gelation and re-crystallisation of amylose (Miles, Morris, & Ring, 1984) and (2) a long term re-crystallisation of amylopectin (Miles, Morris, Orford, & Ring, 1985). The quicker association of amylose is attributed to its degree of polymerization (DP), generally 40–70 glucose units (Jane & Robyt, 1984). Retrogradation of amylose can be observed as soon as the gelatinisation is completed and cooling commenced (Silverio, Svensson, Eliasson, & Olofsson, 1996). Amylose gelation has been described as arising from the cooling of entangled molecules in solutions during storage causing phase-separation, i.e. formation of a polymer-rich phase and a polymer-poor phase. Amylose gelation has been observed to be irreversible when amylose crystallites were heated above the melting temperature (150°C) (Miles et al., 1985). Amylopectin retrogrades at a slower rate because of its higher water holding capacity, more highly branched structure, and shorter branch chains (Srichuwong & Jane, 2007). Gidley (1989) found that the minimum chain length required for starch retrogradation was 8 or 9 glucose units, however an optimum chain length is essential for the stability of retrograded starch. For both amylose and amylopectin, long chains between DP 13–24 can form long double helices, strengthening hydrogen bonds between chains. These can span the entire length of crystalline regions during retrogradation in cereal, potato, pea and rice starches (Silverio, Fredriksson, Andersson, Eliasson, & Åman, 2000; Vandeputte, Vermeulen, Geeroms, & Delcour, 2003). Short chains around DP 6–12 interfere with the formation of crystalline structures (Zhang & Jackson, 1992). The amylopectin chain length distribution of canna, potato, arrow root and cassava starches was observed to affect the rate and extent of amylopectin retrogradation (Gidley, 1989; Hizukuri, 1986; Jane et al., 1999). Research on waxy and non-waxy rice starches also prompted a similar conclusion, the authors stating that the ratio of short-to-long amylopectin chains affect starch retrogradation (Singh, Lin, Huang, & Chang, 2012). Shin, Kim, Ha, Lee, & Moon (2005) reported the C-type structure of sweet potato starch resolved to A-type during retrogradation. Similarly, retrograded corn starch has been reported to be independent of its native counterpart (A-type) in which the B-type pattern was observed (Eerlingen, Jacobs, & Delcour, 1994).

II.2.1 Kinetics of starch retrogradation

The re-association of gelatinised amylose and amylopectin is a non-equilibrium, thermally reversible crystallisation process governed by a consecutive three-step mechanism of nucleation, propagation, and maturation (Slade & Levine, 1987). Nucleation is the formation of critical nuclei, while propagation is the growth of crystals from the nuclei formed, and maturation is the crystal perfection or continuing slow growth (Silverio et al., 2000). Overall crystallisation rate (i.e. maturation) depends mainly on nucleation and propagation rate (Eerlingen, Crombez, & Delcour, 1993). Nucleation has been observed to be faster at 4°C than at room temperature for potato starch (Nakazawa, Noguchi, Takahashi, & Takada, 1985) and wheat grains (Jankowski & Rha, 1986). Propagation, the development from nuclei to crystallite, has been found to be faster at higher temperatures (25-60°C) (Eerlingen et al., 1994; Shi & Gao, 2016; Silverio et al., 2000; Xie, Hu, Jin, Xu, & Chen, 2014; Zhou, Baik, Wang, & Lim, 2010). Structure of retrograded starches collapsed into disordered form at/above the melting temperature (>120°C for amylose (Botham et al., 1994) and >55-70°C for amylopectin (Eerlingen & Delcour, 1995)). A stepwise nucleation and propagation of retrograded starch has been observed under temperature cycles between glass transition temperature and melting temperature, forming more homogenous and temperature stable crystallites (Hu, Xie, Jin, Xu, & Chen, 2014; Park, Baik, & Lim, 2009; Tian et al., 2012; Xie, Hu, Jin, Xu, & Chen, 2014; Zhou et al., 2010; Zhou & Lim, 2012).

The kinetics of starch retrogradation can be modelled by the Avrami equation,

$$N(t) = \bar{N}e^{-nt}[1 - V(t)]$$

where $N(t)$ reflects the amount of crystallised starch, \bar{N} represents the value of N after a certain storage time, $V(t)$ is the rate of retrogradation, and n is an Avrami exponent (Avrami, 1940; McIver, Axford, Colwell, & Elton, 1968; Roos & Drusch, 2016). The amount of crystallised material present at a given time is a combined function of crystal growth rate and the density of nucleation. Physical characteristics of cooked/gelatinised starches during cooling and storage are measured to estimate the rate of retrogradation. Physical characteristics that can reflect the amount of the crystallite in retrograded starch are starch retrogradation enthalpy (Arik Kibar, Gönenç, & Us, 2011; Doona, Feeherry, & Baik, 2006; Hsu & Heldman, 2005; Lin, Yeh, & Lii, 2001; Shi & Gao, 2016; Siswoyo & Morita, 2010; Zhang et al., 2014), relative crystallinity (Fu, Wang, Li, Zhou, & Adhikari, 2013; Jouppila, Kansikas, & Roos, 1998), firmness/hardness (of bread) (Ronda, Caballero, Quilez, & Roos, 2011), relaxation time of starch molecules determined by NMR (Farhat, 2000; Teo & Seow, 1992), and ratio of the absorbance at certain wavenumbers (1047/1022 represents crystalline to amorphous and 1053/1035 depicts retrograded amylose or amylopectin) from infrared spectroscopy (Van Soest, de Wit, Tournois, & Vliegthart, 1994; Wilson et al., 1991). The Avrami equation has been used to estimate the rate constant and the type of nucleation and growth under the assumption of a thermodynamic equilibrium reaction (Arik Kibar et al., 2011; Hsu & Heldman, 2005; McIver et al., 1968; Miles, Morris, Orford, & Ring, 1985; Vandeputte, Vermeylen, Geeroms, & Delcour, 2003). Parameters obtained from the Avrami model

exhibit only a relative theoretical utilization since starch during retrogradation is in a non-equilibrium state (Levine & Slade, 1988), involving time-dependent changes at above and below the glass transition temperature. Various conditions may be used for obtaining retrogradation rate constants and the type of the nucleation. Extensions have been added to the model to take account of the effects of storage temperature, water content, and possible interactions with other molecules in attempt to model the kinetics of starch retrogradation (Blanshard & Farhat, 2000).

II.2.2 Fine structure of amylopectin during retrogradation

Intrinsic characteristics, i.e. molecular structure of starches affect retrogradation during cooling. For instance, nonwaxy wheat starch, containing higher amylose content or amylopectin with less branched and longer glucan chains, have been found to be more prone to retrogradation than for waxy wheat starch (Sasaki, Yasui, & Matsuki, 2000). Linear chains of amylose facilitate the cross-linkages by hydrogen bonding, and hence amylose is proposed to act as a nucleus for amylopectin crystallisation or amylose-amylopectin co-crystallisation (Lian et al., 2018; Smits, 2001). During retrogradation, the AM-AM interaction of long chain segments resulted in high retrogradation enthalpy (ΔH_R) in high-amylose corn starch (Boltz & Thompson, 1999). But neither the amount of long chain nor short chain amylose have been observed to be correlated with the retrogradation thermal characteristics (i.e. T_o , T_p , T_c , and ΔH_R) of amylopectin in cereal, legume root, and tuber starches (Vamadevan & Bertoft, 2018). This could be that AM-AP interaction were too weak to be observed, compared to AM-AM interaction during retrogradation (Vamadevan & Bertoft, 2018). The external glucan chains of branched amylopectin may form double-helices potentially during retrogradation (Klucinec & Thompson, 1999; Vamadevan & Bertoft, 2015; Würsch & Gumy, 1994). Some literature discussion has focused on the fine structure of amylopectin. A structural model of retrograded starch (Figure II.1) has been proposed based on Pearson's correlation analysis between different branched-chain-length categories (i.e. external-chain segments and inter-block segments (IB-CL)) and the thermal characteristics of re-crystallised amylopectin (Vamadevan & Bertoft, 2018). According to the concept of the backbone model (Bertoft, 2013), amylopectin long chains were suggested to connect all the short-branched chains of amylopectin in retrograded starch (Figure II.1). The model described the existence of both long- and short-chain segments of amylopectin in retrograded starch as evidenced by a broad retrogradation temperature range. The long inter-block segments (IB-CL) are more flexible than short segments to bring individual long chains to form loops or helical structures (Figure II.1) (Vamadevan & Bertoft, 2018). The formation of longer (inter-block) segments and intra-molecular double helices have been shown by the increase in ΔH_R (Figure II.1) (Vamadevan & Bertoft, 2018). Short external chain length and short IB-CL leads to short helices and poor alignment resulting in low ΔH_R (Figure II.1) (Vamadevan & Bertoft, 2018).

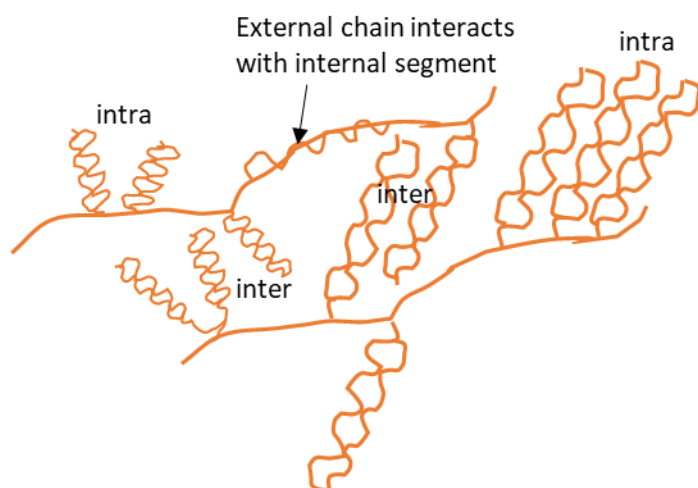


Figure II.1 Model of retrograded gel network based on the amylopectin “building block backbone model” (Vamadevan & Bertoft, 2018). Short chains (thin lines) show weaker gels with short double-helices, poor intra-molecular alignment, and short inter-molecular double-helical junctions (left), whereas long chains (bold lines) form intra-molecular, inter-molecular, and junction zone (right). Reprinted from “Impact of different structural types of amylopectin on retrogradation”, Vol 80, P88-96, Vamadevan & Bertoft, 2018, with permission from Elsevier.

II.2.3 Methods to depict starch retrogradation

Owing to the broad range of physico-chemical change during starch retrogradation, comprehensive and informative studies in different techniques have been presented by various authors (Karim, 2000; Wang, Li, Copeland, Niu, & Wang, 2015). The process of retrogradation is influenced by many factors. A full picture requires starch retrogradation to be studied from the macroscopic scale down to molecular level. Techniques used include rheological analysis, thermal analysis (e.g. DSC), x-ray diffraction, spectroscopic analysis (e.g. NMR, FTIR, and Raman), and microscopy. Each of these methods and techniques have different sample preparations, advantages, and limitations (Table II.1).

Techniques such as blue value and syneresis can be used to quantify the physical properties of retrograded starches by the formation of amylose-iodine complex and the amount of water release from the matrix, respectively (Table II.1). The recrystallisation process during starch retrogradation can be monitored by the rheometry in the starch-water system (Shogren, 1992) or by the mechanical testing (e.g. texture analyser) for the solid food e.g. firmness of bread crumb (Xu, Chung, & Ponte, 1992) (Table II.1). Simple rheological properties such as setback viscosity measured by Barbender or a Rapid Visco Analyser can be used to reflect degree of retrogradation (Singh, Kaur, McCarthy, Moughan, & Singh, 2008) (Table II.1).

The mechanical techniques such as dynamic mechanical analysis (DMA)/ or dynamic mechanical thermal analyser (DMTA) measure the stress-relaxation response (Kalichevsky, Jaroszkiwicz, Ablett, Blanshard, & Lillford, 1992). Degree of crystallisation reflected by the final value of the modulus of DMA has been found to be a strong function of the storage temperature in retrograded wheat starch gel (Roulet, MacInnes, Würsch, Sanchez, & Raemy, 1988). Thermal changes such as the enthalpy

differences and the shifting of transition temperature after various hydrothermal treatments can be observed by differential scanning calorimetry (DSC) (Table II.1). The extent or tendency of retrogradation is indicated by the enthalpy required to disrupt ordered structures formed during storage (Hsu & Heldman, 2005).

Vibrational spectroscopy studies the effect of hydrothermal treatment on internal chemical bonds, skeleton types, connecting forms, and bonding energy. FTIR, Raman and NMR have been used to characterize the crystallinity by the vibration of different chemical groups as well as the skeletal vibration of the glycosidic linkage in gelatinised and retrograded starch (Table II.1). Wilson et al. (1991) used molecular spectroscopy techniques to study starch retrogradation in bread and related starch-based foods. FTIR spectroscopy reveals the skeletal vibration of α -1,4 glycosidic linkages while Raman spectroscopy measures the light scattering of different chemical groups (Table II.1). Infrared (IR) spectroscopy detects chemical groups containing highly polar bonds or bonds whose dipole moment changes during vibration. A stronger vibration of chemical groups results in sharper changes in dipole moment, which in turn leads to stronger IR absorption and a higher peak height in spectra. Raman spectroscopy is suitable for detecting vibrations of less polar molecular bonds such as C–C bonds and pyranoid rings. The chemical shift of the same chemical group observed by Raman and FTIR are similar, but the intensity and peak numbers of the same chemical group are different between spectra. Due to the different signal receiving modes, IR and Raman spectroscopic techniques are regarded as complementary. Distribution of chemical shifts in terms of the effect of the degree of molecular order can be measured by nuclear magnetic resonance (NMR). From the NMR spectrum, a clear decrease in molecular mobility is recorded as molecules undergo ordering transitions during cooling and storage.

X-ray diffraction detects and monitors the helices and semi-crystalline arrays in retrograded starch (Table II.1). The technique reveals the diffraction pattern of different types of crystalline packing such as A, B and C type starch. Cooke & Gidley (1992b) emphasised the difference between degree of molecular order (amount of polysaccharide in the helical conformation) and the degree of crystallinity by wide-angle X-ray diffraction (WAXD) (Table II.1). The nanostructure of amylose gels and gelatinised starches have been studied by scattering techniques owing to the electron density contrast between the crystalline lamellae and the amorphous lamellae (I'Anson, Miles, Morris, Ring, & Nave, 1988; Müller et al., 1995). During starch gelatinisation, alternated layers of crystalline and amorphous lamellae are lost as evidenced by the loss of the lamellar scattering peak of small-angle X-ray scattering (SAXS) (Kuang et al., 2017) (Table II.1). Consistently, the wide-angle X-ray scattering (WAXS) profiles of gelatinised tapioca starch revealed no obvious crystalline structure. More recently, synchrotron X-ray micro beams have been used to study molecular orientation and crystallinity maps by analysing local diffraction patterns of starch granules (Buléon, Gérard, Riekkel, Vuong, & Chanzy, 1998; Cai, Bai, & Shi, 2012) (Table II.1).

Scanning electron microscope (SEM) provides the 3D image of surface morphology of retrograded starch in potato tubers (Table II.1). Other techniques such as light microscope or confocal laser scanning

microscopy (CLSM) can visualise retrograded starch in potato tubers cell structure by suitable dye, such as Acridine orange for cell wall and starch or Acid Fuchsin for protein (Table II.1). Combined techniques such as Raman microscopy with high resolution may be used to visualise the state of starch re-ordering process in formulated starch-water systems or whole foods.

Table II.1 Techniques to study starch retrogradation.

Method types	Techniques	Principles and properties Measured	Sample preparation	Advantages/ Disadvantages	References
Physical properties	Blue value	The formation of the iodine-starch complex in the retrograded starch.	Sample pre-treatments are needed to extract starch for whole foods.	<ul style="list-style-type: none"> √ Colorimetric assay is straightforward and quick. × Retrograded amylose contributed to the most of the iodine-starch binding and thus it is a qualitative method. 	(McIver et al., 1968).
	Syneresis	Water released from the sample after cooling and storage.	Suitable for both formulated systems and whole foods.	<ul style="list-style-type: none"> √ Simple. × Experimental conditions, such as centrifugal forces, freezing temperature and rate, freezing duration and numbers of freeze-thaw cycles can vary in different researches. 	(Zheng & Sosulski, 1998), (Singh, McCarthy, & Singh, 2006).
	Rheology	Viscoelastic behaviour.	Starch gel.	<ul style="list-style-type: none"> √ Alterations in viscoelastic behaviour as manifestations of retrogradation is monitored <i>in situ</i>. × Heterogeneous samples could affect the validity of the results within and between samples obtained. 	(Singh et al., 2008).
	Texture	Texture profile analysis e.g. the fracturability and the hardness.	Solid, semi-solid, and gel-like samples.	<ul style="list-style-type: none"> √ Automatic calculations of texture profile analysis save time and reduce errors. × Destructive measurement. 	(Kaur, Singh, Singh, & Ezekiel, 2007).
Thermal characteristics	DSC	Retrogradation temperature (T_o , T_p , and T_c) and enthalpy (ΔH_R).	Sample can be in starch-water systems or whole foods.	<ul style="list-style-type: none"> √ DSC can simulate cooking and cooling process precisely. It is a quantitative method to determine the amount of retrograded starch and the kinetic of starch retrogradation. × Sampling size is normally less than 20mg. 	(Karlsson & Eliasson, 2003b), (Carlstedt, Wojtasz, Fyhr, & Kocherbitov, 2015).
Spectroscopic analysis	FTIR	Order of crystalline region in relation to amorphous region of the surface/localized retrograded starch.	Solid, semi-solid, and gel-like samples.	<ul style="list-style-type: none"> √ Quick and sensitive method to study the molecular alignment of starch retrogradation by absorbance of 1047 cm^{-1} and 1022 cm^{-1} and their ratio (1047/1022). 	(Van Soest et al., 1995), (H. Jiang et al., 2015).

X-ray diffraction	Raman	Internal and external vibration of molecules.	Suitable for both formulated systems and whole foods.	<p>X Results are limited to the penetration depth, representing only the surface structure of the sample.</p> <p>√ Raman measures molecular covalent character by change in polarisability.</p> <p>X Only detects less/nonpolar molecular bonds, such as C–C bonds and pyranoid rings.</p>	(Huen et al., 2014), (Galvis, Bertinotto, Putaux, Montesanti, & Vuorinen, 2016).
	NMR	¹ H NMR analyses the relaxation time of the starch indicating mobility of starch polymer chains.	Suitable for both formulated systems and whole foods.	<p>√ Relatively large sampling size (10g).</p> <p>XLF-NMR is limited to study sample components in high concentration.</p>	(Straadt, Thybo, & Bertram, 2008), (Zhu, 2017).
	WAXD	Long-range ordered structure.	Starch powders, gels or solutions.	<p>√ Relatively large sampling size (2g).</p> <p>X Hydration is known to influence X-ray patterns, yet a certain amount of water is necessary to reveal structural ordering.</p>	(Chen et al., 2016)
	SAXS	Molecular spacing between repetitive crystalline and amorphous lamellae.	Hydrated samples.	<p>√ Indication of the re-alignment of gelatinised amylose and amylopectin into lamellar layers during starch retrogradation.</p> <p>X Complementary methods (e.g. DSC, WAXD, or SEM) are needed to interpret the high-angle tail patterns of retrograded starch.</p>	(Perry & Donald, 2000b)
	Synchrotron	Crystalline orientation and distribution within fine grid.	Hydrated states or starch suspensions.	<p>√ Similar to DSC, <i>in situ</i> (real time) melting and crystallisation can be monitored. Synchrotron radiation provides higher spectral brilliance with continuous energy tunability, small source size, small beam divergence and high beam flux.</p> <p>X Potential radiation damage on the starch structure, though its non-destructive nature during measurement.</p>	(Buléon, Gérard, et al., 1998), (Cai et al., 2012), (Blazek & Gilbert, 2011).

Microscopic	SEM	3D image of surface morphology.	Dried systems and whole foods.	formulated and whole	✓ Good correlation with other method: lacunarity (gaps or holes of starch SEM image) ↑, ΔH_R ↑. ✗ Sample preparation, such as freeze-drying and cutting may cause the loss of starch materials on sample's surface.	(Utrilla-Coello, Bello-Pérez, Vernon-Carter, Rodriguez, & Alvarez-Ramirez, 2013), (Tamura, Singh, Kaur, & Ogawa, 2016).
	CLSM	Structural changes in whole plant tissue, such as starchy matrix fills up cell interspace, the outline of cell walls and protein distribution can be observed during cooking and cooling.	Formulated systems or thin slices of whole foods.		✓ Structural artefacts are minimum during sample preparation in a whole food system. ✗ Observation of cell wall separation and degradation are not as pronounced as SEM in whole food.	(Bordoloi, Kaur, et al., 2012).

DSC, differential scanning calorimetry; T_o , retrogradation onset temperature; T_p , retrogradation peak temperature; T_c , retrogradation conclusion temperature; ΔH_R , retrogradation enthalpy. FTIR, fourier-transform infrared spectroscopy. (LF-)NMR, (Low field-) nuclear magnetic resonance. SAXS, small angle x-ray scattering. WAXD, wide-angle x-ray diffraction. SEM, scanning electron microscopy. CLSM, confocal laser scanning microscopy.

II.2.4 Starch retrogradation in food matrix

Interactions of starches with other components naturally existing in plant tissues such as the phosphorus content in potato starch (Zaidul, Yamauchi, Kim, Hashimoto, & Noda, 2007), the protein content in wheat (Riva, Fessas, & Schiraldi, 2000; Zaidul et al., 2007), and the lipid as lysophospholipids or free fatty acids in cereals (Boltz & Thompson, 1999; Eliasson & Wahlgren, 2004) can influence starch retrogradation. Extrinsic factors such as the presence of non-starch food compounds (Table II.2) and the cooking and cooling regimes (discussed in Section II.3) all play an important role in starch retrogradation. Other food components influence starch retrogradation by competing for available water, owing to the differences in the electrostatic, van der Waals forces, hydrophobic/hydrophilic interactions, or hydrogen bonds between the chemical functional groups (Eliasson, 2006). Interactions may alter swelling behaviour and amylose leaching during gelatinisation and hence the realignment of starch during retrogradation.

II.2.4.1 Starch and salts

Starch gelatinisation in neutral salt solutions has been shown to be controlled by either the hydrogen bonds between water molecules and ions or by electrostatic interactions between starch-water and starch-ions (Frank & Wen, 1957; Luck, 1980). Depending on the salt concentration and charge density of the ions, the cations or anions of a salt can either stabilize or destabilize the starch granular structure, thus affecting starch gelatinisation and subsequent retrogradation (Jane, 1993). Ions with low charge density (e.g. SCN^- & I^-), highly hydrated in water tend to form helical complexes with starch molecules and thus destabilize granular structure during heating. With subsequent cooling, the ion-starch interactions inhibit any rearrangement during retrogradation, leading to a slower rate of retrogradation and higher transparency of potato starch paste (Zhou et al., 2014). When the high charge density ions (e.g. Li^+ , Na^+ , & SO_4^{2-}) are in high concentrations, the ions will form hydrogen bonds with the $-\text{OH}$ groups on starch, destabilizing starch granules and consequently, will result in lower gelatinisation temperature. Upon cooling, rearrangement of gelatinised wheat starch molecules has been reported to be inhibited in concentrated NaCl solution during retrogradation as evidenced by a decrease in retrogradation enthalpy compared to retrograded wheat gel without salt (Russell & Oliver, 1989). Overall, influence of salts on retrogradation has been generally observed to follow the order of the Hofmeister series in which the anions increase the retrogradation rate in the order of $\text{I}^- < \text{Br}^- < \text{Cl}^- < \text{F}^-$ and the cations decrease rate in the order of $\text{K}^+ < \text{Li}^+ < \text{Na}^+$ (Ciacco & Fernandes, 1979) in the corn and waxy corn starch (Wang et al., 2017).

II.2.4.2 Starch and carbohydrates

The term carbohydrate refer to monosaccharides (e.g. glucose, ribose, fructose), oligosaccharides with 2-20 units (e.g., maltose, lactose, sucrose), and polysaccharides (e.g., guar gum, locust bean gum, xanthan gum, carrageenan, alginate, pectin, arabic gum, carboxyl-methyl-cellulose, and methyl-cellulose, hydroxyl-propyl-methylcellulose).

Sugars (monosaccharides and short oligosaccharides) and cold water-soluble maltodextrins have been shown to affect starch retrogradation in different trends. Simple sugars, such as glucose have been reported to increase retrogradation rate by the cross-linking of outer branches of adjacent amylopectin chains (Hoover & Senanayake, 1996). Larger malto-oligosaccharides, i.e. DP>6 may form small helices that co-crystallise with starch enhancing the formation of retrogradation (Gidley & Bulpin, 1987). Other sugars with DP 2-5, however, may form complexes with starch hydroxyl groups hindering the formation of amylose helices and reducing starch retrogradation (Lee, Kim, & Nishinari, 1998; Rojas, Rosell, & de Barber, 2001; Smits, Kruiskamp, Van Soest, & Vliegthart, 2003).

Non-starch polysaccharides are complex polysaccharides other than the starches that contain several hundreds of thousands of monosaccharides units, joining by glycosidic linkages (Kumar, Sinha, Makkar, de Boeck, & Becker, 2012). Due to the structural complexity of starch and non-starch polysaccharides, the interactions between two compounds depends on several factors including the molecular structure, ionic nature, concentration, and ratio of starch to non-starch polysaccharides (Tester & Sommerville, 2003). Various extrinsic factors such as pH, ionic strength, temperature, and presence of other components also affect the interactions between starch and non-starch polysaccharides. Different mechanisms have been proposed to illustrate interactions between starch and hydrocolloids and the effect on starch retrogradation.

Hydrocolloids generally promote short-term starch retrogradation by immobilizing water molecules in the starch-hydrocolloid solution and therefore increasing the aggregation of starch (primarily amylose molecules) (Sikora, Kowalski, & Tomasik, 2008; Yoshimura, Takaya, & Nishinari, 1998). Galactomannans, such as guar gum, tara gum, and locust bean gum, and konjac glucomannan yet have been shown to retard the long-term retrogradation. Interactions among gums and starch during retrogradation depends on the molecular flexibility (i.e. the degree of conformational expansion) of the gums and thus vary with different glycan chains. For instance, the more galactose side chain present the greater delaying effect has been observed on long-term retrogradation, possibly due to inhibition of amylose crystallisation and/or the co-crystallisation between amylose and amylopectin (Funami et al., 2005a, 2005b).

Freeze-thaw stability, an indicator of starch retrogradation has been shown to be improved in the presence of non-starch polysaccharides. Improved freeze-thaw stability has been observed with sweet potato, yam, corn starches and wheat flour in the presence of xanthan gum (Sae-kang & Suphantharika, 2006); or with rice starch in the presence of konjac glucomannan (Charoenrein, Tatirat, Rengsutthi, &

Thongngam, 2011) and β -glucan (Satrapai & Supphantharika, 2007); or with sago or waxy corn starches in the presence of galactomannan, guar gum, and alginate (Ahmad & Williams, 2001).

II.2.4.3 Starch and proteins

Endogenous proteins (such as the spherical membrane-bound protein bodies or proteins in the cytosol of starchy endosperm cell, i.e. cereal grains) may influence starch retrogradation (Sjoo, Karin, & Eliasson, 2009). Gluten, a wheat protein present naturally in wheat grains, interacts with wheat starch through hydrogen bonds, providing anti-firmness characteristics (Erlander & Erlander, 1969). During kneading and baking, gluten molecules have been reported to form complexes with the C-2 and C-3 hydroxyls of a glucose unit and stabilize the starch helices. This complex may then exhibit steric hindrance for the α -1,4-linked chain, inhibiting the aggregation of amylose and amylopectin, and consequently, reduce starch retrogradation in pasta compared to rice (Riva et al., 2000).

Additional proteins can influence physicochemical properties of starch-based food products by starch-protein interaction, leading to structural changes such as aggregation and gel formation (Samant, Singhal, Kulkarni, & Rege, 2007). When additional gluten was added, the increase in bread firmness could be attributed to hydrogen bonding between the glucan chains and gluten fibrils apart from starch retrogradation (Every, Gerrard, Gilpin, Ross, & Newberry, 1998). The kinetics and the extent or polymorphism of amylopectin retrogradation were however not significantly affected in the presence of gluten (Ottenhof & Farhat, 2004).

Starch-protein interaction has been found to form bonding by electrostatic and van der Waals forces, with less contribution from hydrophobic effects and hydrogen bonds (Marshall & Chrastil, 1992). In the softer gel of soybean protein-wheat starch system, soy protein-amylose complex could be formed by non-covalent bonding, exposing the branches of amylopectin and thus weakening the gel matrix. Consequently, the water-retention capacity of soybean protein-wheat starch gel has been found to be lower than starch only gel during starch retrogradation, leading to higher syneresis (Ribotta, Colombo, León, & Añón, 2007). Glutenins have been shown to delay wheat starch retrogradation (Guo, Lian, Kang, Gao, & Li, 2016), while albumins, globulins, and gliadins promote it (Lian, Guo, Wang, Li, & Zhu, 2014). Soybean protein isolate has little effect on the thermal behaviour and retrogradation of corn starch. However, soybean 7S globulin has been found to delay corn starch retrogradation, while soybean 11S globulin promoted it (Lian, Zhu, Wen, Li, & Zhao, 2013; Yu, Jiang, & Koppurapu, 2015).

II.2.4.4 Starch and lipids

Lipids are abundant in some natural starchy foods such as cereals but various lipids are often added in food applications (Eliasson & Wahlgren, 2004). Amylose may complex with either endogenous or exogenous lipids (such as glycerol monostearate). Exogenous lipid has been shown to reduce stickiness, improve freeze-thaw stability, and retard staling as dough conditioners and crumb softeners in baking goods. This was attributed to the formation of amylose-lipid complexes (Kaur & Singh, 2000; Singh,

Singh, Kaur, Sodhi, & Gill, 2003) and amylopectin-lipid complexes (Eliasson & Ljunger, 1988). The amylose-lipid complex (e.g. cetyltrimethylammonium bromide (CTAB)-amylose) was shown to interfere with the crystallisation of gelatinised amylose/amylopectin retarding potato starch retrogradation (Gudmundsson, 1992). Similarly, starch-lipid complex may have restrained helical conformations in crystalline networks between starch molecules and thus delayed starch retrogradation in cooked rice (Hibi, Kitamura, & Kuge, 1990) and baking goods (Hesso et al., 2015; Matignon & Tecante, 2017) during cooling and storage. Or the amylose–lipid complex possibly changed water distribution in bread, and therefore affected the retrogradation (D’Appolonia & Morad, 1981).

Different hypotheses have been proposed to interpret mechanisms of amylose/amylopectin-lipid complexes in delaying starch retrogradation. For wheat flour with lipid contents of 6.6% (dwb), the amylose-lipid complex was reported to hinder retrogradation more than with potato or cassava flour with lipid contents lower than 0.1% (dwb) (Becker, Hill, & Mitchell, 2001). Outer short branches of the amylopectin have been reported to form amylopectin–lipid complex thus retarding retrogradation (Eliasson & Ljunger, 1988; Huang & White, 1993; Nakazawa & Wang, 2004; Putseys, Lamberts, & Delcour, 2010). Co-crystallisation of amylose and amylopectin in amylomaize starch has, however, been suggested to occur to the extent that eliminates the delaying effect of starch retrogradation by amylose-lipid complex (Russell, 1987).

Table II.2 Interactions of starches and the other food components during starch retrogradation.

Food components	Starch botanical sources	Mechanisms	Influences	References
Anions: F ⁻ , Br ⁻ , I ⁻ , SO ₄ ²⁻ , Cl ⁻ , NO ₃ ⁻ , SCN ⁻ Cations: Na ⁺ , Li ⁺ , K ⁺	Potato starch	Ion-starch interaction inhibited the rearrangement during retrogradation, leading to a slower rate of retrogradation and higher transparency in potato paste with ions than potato starch only paste.	Transparency of the potato starch paste mixed with ions decreased in the order of SCN ⁻ > I ⁻ > NO ₃ ⁻ > Br ⁻ > Cl ⁻ ≈ Control > SO ₄ ²⁻ > F ⁻ (for anions); and Li ⁺ > Na ⁺ > Control > K ⁺ (for cations).	(Zhou et al., 2014)
Salts	Corn and waxy corn starch	Salting-out ions (F ⁻ , SO ₄ ²⁻ , K ⁺) increased the syneresis indicating higher level of retrogradation. Salting-in ions (Br ⁻ , NO ₃ ⁻ , I ⁻ , SCN ⁻ , Na ⁺ , Li ⁺) decreased the syneresis delaying retrogradation.	Syneresis (%) of anions: SCN ⁻ < I ⁻ < NO ₃ ⁻ < Br ⁻ < Cl ⁻ < SO ₄ ²⁻ < F ⁻ and for cations Li ⁺ < Na ⁺ < K ⁺ .	(Wang et al., 2017)
Glucose, fructose, and sucrose	Oat starch	Cross-linking between sugars and the hydroxyl groups on the outer branches of adjacent amylopectin chains led to an increase in chain aggregation and thus increased retrogradation enthalpy (ΔH_R).	ΔH_R increased in the presence of sugar in the order of glucose > fructose > sucrose.	(Ratnajothi Hoover & Senanayake, 1996)
Sucrose	Acorn starch (AS)	Sucrose might prevent the rearrangement of amylopectin during cooling/storage and hence retard the retrogradation.	Retrogradation ratio ($\Delta H_R/\Delta H_G$): AS only > 5% sucrose+ AS > 10% sucrose+ AS > 15% sucrose+ AS.	(H. A. Lee et al., 1998)
Maltose	Potato and wheat starch	Sugars with DP2-5 might intrude between the starch chains hindering the helices formation, and thus reduce retrogradation. Shorter branch-chain length of amylopectin in wheat starch might form complex with the additional maltose recrystallizing to a lesser extent than potato starch.	Crystallinity index: maltose-wheat starch < maltose-potato starch.	(Smits et al., 2003)
Locust, tara, and guar gum	Wheat starch	Molecular flexibility of the gums created various accessibilities to react with the crystallites of the retrograded starch; the more the galactose side chain, the greater the effect on delaying long-term retrogradation.	Decrease in rate constant of dynamic rheological test: guar > tara > locust gum.	(Funami et al., 2005a, 2005b)
Konjac glucomannan (KGM)	Rice starch	KGM inhibited the re-association of disrupted starch and thus retarded retrogradation in rice starch gel preserving quality in freeze-thaw rice starch gels.	Syneresis (%): Rice starch > Rice starch + 0.3% KGM > Rice starch + 0.5% KGM.	(Charoenrein et al., 2011)

Protein	Durum wheat spaghetti and rice	Competition between protein and starch over water availability via hydrogen bonding.	Retrogradation ratio ($\Delta H_R/\Delta H_G$): Rice > Spaghetti.	(Riva et al., 2000)
Soy protein isolate	Wheat starch	Soy proteins and amylose may form complex exposing the branches of amylopectin and weakening gel matrix. Consequently, water-retention capacity of soy protein-wheat starch gel has been shown to be lower than for starch only gel.	Syneresis: Starch-soy protein gel > Starch gel.	(Ribotta et al., 2007)
Glutenins, albumins, globulins, and gliadins	Wheat starch	Glutenins-amylose formed double helices by hydrogen bonding between the hydroxyl group of C-6 and the carbonyl group of Tyr, and thus hindered amylose-amylose short-term retrogradation.	Glutenins-wheat starch complex retarded starch retrogradation, while albumins, globulins, and gliadins-wheat starch complex promoted starch retrogradation.	(Guo et al., 2016), (Lian et al., 2014).
Soybean globulin and soybean globulin	7S and 11S Corn starch (CS)	One end of soy protein polypeptide, abundant with glutamic acid (Glu-Na ⁺) interacts with the C6 of corn starch, while the other end of soy protein polypeptide (Lys) reacted with aldehyde group of corn starch. The polypeptide and glycosidic bonds formed hydrogen bonds in alkaline condition during retrogradation.	ΔH_R : Soybean 11S globulin-CS > Soybean 7S globulin-CS.	(Yu et al., 2015), (Lian et al., 2013).
Palmitic, oleic, and linoleic acids	Cooked rice grains and rice starch	Starch-lipid complex restrained helical conformation and thus retarded starch retrogradation.	Intensity of X-ray diffraction pattern: Non-defatted (native) rice paste > Refatted rice paste > Defatted rice paste.	(Hibi et al., 1990), (Chang & Liu, 1991).
Rapeseed oil (70%) + anhydrous milk fat (30%)	Wheat flour in cake crumb	The B-type crystalline pattern formed in cake crumb after 17 days of storage. Polymorphic types of retrograded crumb displayed the intense peaks at 19° (β form) and at 23° (β' form) under different storage conditions. The crystallisation of starch and lipid components with β form was more pronounced at the ambient temperature than at low temperature during retrogradation.	Intensity of X-ray diffraction pattern: Cake in 20 °C storage for 25dy > in 4 °C storage for 25dy > freshly baked cake.	(Hesso et al., 2015)
Cetyltrimethyl ammonium bromide (CTAB)	Amylopectin (AP) and amylose (AM) from potato starch	Adding surfactant to the mixture of AM/AP in either high or low percentage of AP, the formation of the surfactant-AM complex inhibited the co-crystalline between amylose and amylopectin reducing retrogradation enthalpy.	ΔH_R : AM/AP mixture > AM/AP mixture-CTAB	(Gudmundsson, 1992)

II.2.5 Starch retrogradation: formulated vs natural systems

Models used to illustrate the structure of gelatinised and retrograded starch in formulated and natural systems are discussed below.

At 95 °C, the power-law scattering behaviour of SAXS extended to lower scattering angles especially for the amylose-containing starches, indicating that amylose is essential in the development of large, temperature-stable self-similar structures (Vermeulen, Derycke, et al., 2006). Amylose gelation has been observed to create phase separation into a polymer-rich network phase interpenetrated by a polymer-deficient phase (Huang et al., 2014; I'Anson et al., 1988). Disrupted amylose and amylopectin entangle and form the fractal-like aggregate in retrograded starches. The SAXS profile of tapioca starch exhibited successive changes in the low- q regime (0.0025 - 0.02 \AA^{-1}), revealing formation of aggregates during cooling. The fitted parameters of fractal-like aggregates model (for ellipsoidal primary particles, i.e., amylopectin nanoclusters) revealed an increase in the fractal dimension and in the population of the fractal aggregates and a decrease in the free nanoclusters (Chen & Teixeira, 1986; Lin, Lin, Jeng, Huang, & Huang, 2009). This growth behaviour of fractal aggregates represented by the corresponding scattering invariant Q_{agg} and fractal dimension D_f have been found to be highly correlated to the solution viscosity (Huang et al., 2014). The Bragg's peak, an indication of ordered structure has been observed as the realignment of disrupted amylose and amylopectin reached a sufficient level of ordering during cooling and storage (Carlstedt et al., 2015; Suzuki, Chiba, & Yarno, 2002).

II.2.5.1 Retrogradation of starch in food matrix

A food matrix, as eaten, is typically a multi-component formulated system differing from the natural self-assembled whole foods. Dough is a viscoelastic network formed by gluten (Demirkesen, Campanella, Sumnu, Sahin, & Hamaker, 2014). Gluten, the continuous or the discontinuous protein network can keep the fermentation gas in bread dough and restrict water migration during staling (Wilderjans, Luyts, Brijs, & Delcour, 2013). Staling, commonly perceived as a phenomenon of starch retrogradation, occurs as water migrates between components in bread. Staling thus changes the protein-starch networks and influences moisture loss (Matignon & Tecante, 2017). Different models, based on the main components in cereal products, have been developed to study starch retrogradation. Two models and a mix of both are detailed below. One model describes a matrix such as bread or steam bun (Mantou) (Huang & Moss, 1991; Huang & Miskelly, 2019) in which starch matrix embedded in a continuous gluten network (Jekle, Mühlberger, & Becker, 2016), or a bi-continuous structure of accumulated swollen starch granules and a protein network (Hug-Iten, Escher, & Conde-Petit, 2003). As cooking temperature increased above 65 °C, gluten network has been observed to convert from thick aligned and highly branched protein strands to a homogeneous network of small thin protein threads (Verbauwhede et al., 2019). With subsequent cooling, the gelatinised starch spreads in between the

gluten structure, and reorganises as an amylose and amylopectin entangle, forming retrograded crystallites.

The other model depicts the network such as cake that contains sugar, egg proteins, and fat in either high amounts (12-33%) as an emulsion-based batter (batter-type) (Wilderjans, Luyts, Goesaert, Brijs, & Delcour, 2010) or in low or nil quantities as a foam-based batter (foam-type) (Godefroidt, Ooms, Pareyt, Brijs, & Delcour, 2019). Leached amylose may embed in the mixture of protein-lipid (Hesso et al., 2015) and may further form amylose-lipid complex during baking (Goesaert et al., 2005a). In this system, sugar increases the temperatures (80 to 95 °C) at which starch gelatinises (Kim & Walker, 1992a, 1992b) and protein denatures (Deleu et al., 2019) and thus affects caking setting. During cooling and storage, cakes firm over time. Water migration from different fractions (e.g. gluten or amorphous starch) into retrograded crystals possibly lead to cake firmness, like in bread systems (Willhoft, 1973). The loss of softness in cake has also been attributed to the protein network where protein network present was no longer fully plasticised once moisture loss and starch retrogradation occur during storage (Godefroidt et al., 2019).

II.2.5.2 Retrograded starch in whole foods

Starch gelatinisation and retrogradation take place under a wide range of water contents, a prerequisite in starch-water systems (Donovan, 1979). Whole plant food systems, such as rice grains, legumes, and potato tubers (Berg, Singh, Hardacre, & Boland, 2012) encompass different cell compartments, (e.g. cell wall, vacuole, cytoplasm and intracellular spaces) within which starch gelatinisation and starch retrogradation occur, subject to local influences of other cell components and water availability.

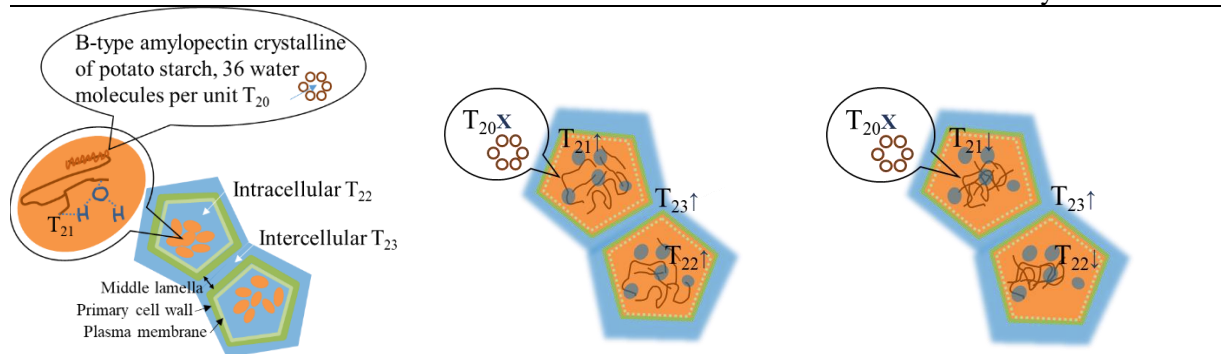
Cooked rice grains (in boiling water, rice to water of 1:1.5 for 30min) exhibit a gelatinised starch and protein mass surrounded by plant cell walls. During cooling, the firmness of cooked rice grains has been found to be linearly related to starch retrogradation and affected by the AM and AP structure (Perdon, Siebenmorgen, Buescher, & Gbur, 1999). Milled, raw rice grains have been observed under SEM microscopy to contain fine cracks throughout the endosperm (Ogawa, Glenn, Orts, & Wood, 2003). The fine cracks in raw grains have been found to serve as channels for water migration into the grain as evidenced by the wider and more defined cracks in cooked rice grains (Horigane et al., 1999; Ogawa et al., 2003). Variable water penetration in cooked rice grains has been attributed to microstructural heterogeneity (e.g. cracks/pores and dense regions) based on observations from magnetic resonance imaging (MRI) and micro-computed tomography (μ -CT) (Mohorič et al., 2009). With subsequent cooling, the cooked rice grain has been observed to develop crevices in the core, becoming prominent over two days of storage (Hsu, Chen, Lu, & Chiang, 2015; Jung, Lee, Lee, & Kim, 2016).

In legumes, starch granules are encapsulated by cellular protein matrices in the cotyledon cells (Daussant, Mosse, & Vaughan, 1983), restricting starch swelling during gelatinisation owing to steric

hindrance and other limiting effects (e.g. water availability) (Do, Singh, Oey, & Singh, 2019; Singh et al., 2014). During cooking, legumes become soft due to gelatinised starch and denatured proteins in cells accompanied by partial solubilisation of the middle lamella leading to separation of individual cotyledon cells (Hultin & Milner, 1978). After cooling, SEM images revealed finely reticulated legumes attributed to shrunk cells and crimples on cell walls during starch retrogradation (Tan, Tan, Tian, Liu, & Shen, 2011).

Starch retrogradation in whole tuber (*in tuber*) has recently been investigated through low field-nuclear magnetic resonance (LF-NMR), a non-invasive technique. Interactions of starch and water, the most abundant component *in tuber* during starch retrogradation were discerned by four relaxation times (Chen, Singh, & Archer, 2018). Effects of cooking, cooling and reheating on the structures formed by gelatinised amylose and amylopectin and the effects on water migration were inferred from the degree of the vibration of hydrogen bonds as indicated by relaxation time. Each relaxation time may indicate the mobility of water within the starch double helices of crystalline regions (T_{20}), in the amorphous region of amylose and amylopectin (T_{21}), loosely associated with the gelatinised starchy matrix (T_{22}), and within potato tuber cell cytoplasm (T_{23}) (Figure II.2b) (Chen et al., 2018; Thybo, Andersen, Karlsson, Dønstrup, & Stødkilde-Jørgensen, 2003). The water population with relaxation time T_{23} was predicted to diffuse into starch granules and interact with the exposed hydroxyl groups of amylose and amylopectin by exchanging hydrogen bonds during heating. As the temperature dropped after heat treatment, progressive aggregation of gelatinised amylose and amylopectin reportedly weakened the interactions between the starchy matrix and water leading to more free water in the T_{23} population; simultaneously the water with T_{21} in the gelatinised amylose and amylopectin network became less mobile (Figure II.2c) (Chen et al., 2018). A cyclic pattern of the relaxation time T_{22} of freshly cooked, retrograded (for 1,3, and 7 days), and retrograded then reheated potato (at 50,70, and 90 °C) was observed (Chen et al., 2018), indicating that longer storage time allowed gelatinised amylose and amylopectin to associate, forming a sufficiently strong structure to maintain integrity despite reheating to 90 °C.

(a) Raw potato parenchyma cells (b) Freshly cooked potato cells- starchy matrix containing leached AM and unwound AP (c) 3-day retrograded potato cells-retrograded AM and AP embedded in starchy matrix



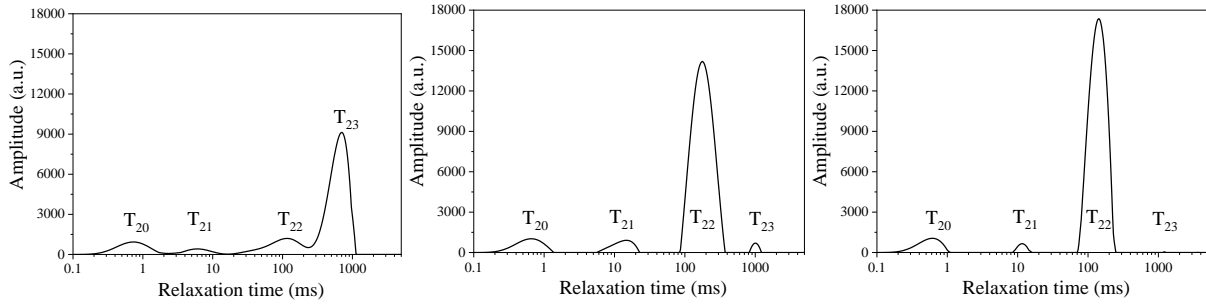


Figure II.2 Model of starch retrogradation in tuber and its relaxation time distribution curve (Chen et al., 2018). *AM represents amylose and AP is amylopectin. Model, not represented to the relative length scale, is only for illustration.

The integrated observations based on interactions of different components in formulated and natural systems in response to a thermal process can provide an overall picture of starch retrogradation leading to better understanding of the mechanisms and exploring the potentials for structural manipulation.

II.3 Starch retrogradation as influenced by type of food processing

Food processing can modify starches physically by inducing changes in the packing of AM and AP and their interactions with other food components which might further affect the formation of retrograded starch. Starch structural changes, particularly the formation of retrograded starch manipulated by existing and new technologies during processing and post-processing are discussed below (Table II.3).

Heat moisture treatment (HMT) is a hydrothermal process applied to starch under low moisture conditions (<35% moisture, w/w) for a length of time (1-24 h). HMT modifies the physico-chemical properties of starches without destroying their granular form. Starch granular form is retained under limited water content, though the mobility of the glycosidic bonds is increased and the helical structure of semi-crystalline lamellae is changed under high temperature (80-130°C) (Zavareze & Dias, 2011). The physico-chemical characteristics such as granule morphology, pasting properties, and gelatinisation temperature and enthalpy of HMT-treated starches has variously been reported to increase, decrease, or not change, depending on the type of starch (Hoover, 2010), moisture content (Lim, Chang, & Chung, 2001), and heating temperature-time (Varatharajan et al., 2011) during HMT.

HMT might disrupt the least stable structures such as the outer branches of amylopectin, resulting in stronger and more rapid lateral association of double helices in retrograded starch during subsequent cooling (Hoover & Vasanthan, 1994a). The relative crystallinity of HMT-treated and retrograded corn and potato starches have been shown to be higher than their native counterparts (Miyoshi, 2002). HMT might also enhance the AM-AP interactions in cereals and legumes starches. For instance, enhanced interactions of AM-AP chains in HMT-treated lentil than wheat starches, owing to the longer AM and AP chains in lentil starch, have less disrupted AM-AP interaction during gelatinisation (Hoover & Vasanthan, 1994b). With subsequent cooling, the increase in retrogradation enthalpy of HMT-treated

starches may be attributed to the enhanced interaction of AM-AP during heat moisture treatment (Hoover & Vasanthan, 1994a). Other results of the ΔH_R of finger millet and mucuna bean starches were, however, shown to be lower than their native counterparts (Adebowale, Afolabi, & Olu-Owolabi, 2005; Adebowale & Lawal, 2003b). This could possibly due to the inherent characteristics of these two starches or to higher storage temperature (at 30 or 40°C) during starch retrogradation- no detailed explanation was provided by the authors.

Extruded starches experience high shear under limited water conditions (< 30%) resulting in the melting of the amylopectin crystallites within swollen granules (Nayak, Berrios, & Tang, 2014). In general, extrusion modifies the pasting behaviour of flour, producing more stable pastes with low retrogradation tendency. Both extruded rice flour (Hagenimana, Ding, & Fang, 2006) and extruded potato and corn flour mixture (Singh, Kaur, McCarthy, Moughan, & Singh, 2009) exhibited lower setback values than their native counterparts during pasting analysis, indicating a decrease of retrogradation tendency. Extrusion under high moisture content (>40%) and low screw speed (<150rpm) has commonly been found to increase retrogradation tendency and thus formation of resistant starch leading to lower starch hydrolysis in extruded sweet potato (Waramboi, Gidley, & Sopade, 2014) and pastry wheat flour (Kim, Tanhehco, & Ng, 2006). An “Improved Extrusion Cooking Technology (IECT)” cooks starches under feed moisture contents of 30 to 70% and has, however, been shown to improve flour solubility and give lower short-term starch retrogradation (Liu et al., 2017). Rice extruded by IECT has been shown to have a lower extent of retrogradation than its native counterpart as evidenced by lower retrogradation enthalpy, lower relative crystallinity and lower ratio of 1047 cm^{-1} to 1022 cm^{-1} (i.e. less ordered structure) in the FTIR spectra, and lower retrogradation rate modelled by Avrami (Zhang et al., 2014).

The low temperature long time process with physical barrier such as *sous vide* processing was invented to avoid overheating surface of foods with low heat transfer coefficient and to minimise surface contamination. *Sous vide* processing usually cooks food at low temperature (50-70°C), akin to annealing, which is known in starch science for treating starches in excess water ($\geq 40\%$, w/w) at temperatures under gelatinisation temperature for specific periods (Tester & Debon, 2000). Annealing enhances chain mobility (owing to plasticization by water), improving the alignment of double helices within the crystalline lattice (Gomand et al., 2012; Kiseleva et al., 2005; Tester & Debon, 2000; Vermeulen, Goderis, & Delcour, 2006) without cleavage of native starch chains (Chung, Liu, & Hoover, 2009; Jayakody & Hoover, 2008; Rocha, Cunha, Jane, & Franco, 2011). The increased molecular rearrangement might prevent the reorganization of amylopectin molecules during storage as evidenced by the lower transition temperature ($T_c - T_o$), which ranged from 50 to 75°C (Siswoyo & Morita, 2010). The retrogradation rate of annealed starch has been found to be less than for the control suggesting that the annealed starch might retard retrogradation (Siswoyo & Morita, 2010).

Ultrasonic processing is another technique to overcome the low thermal diffusivity of foods. Depending on the processing temperature influenced by ultrasound power, time, and intensity, ultrasonication can be either a thermal process or a non-thermal process. Studies have documented morphological (Moza, Mironescu, & Florea, 2012; Sujka & Jamroz, 2013) and physico-chemical (Czechowska-Biskup, Rokita, Lotfy, Ulanski, & Rosiak, 2005; Iida, Tuziuti, Yasui, Towata, & Kozuka, 2008) changes in starches induced by ultrasonic cavitation. Ultrasonication power has been reported to possibly interrupt the branch chains of amylopectin in rice starch resulting in depolymerisation (Sujka & Jamroz, 2013). The decrease in retrogradation enthalpy with increasing ultrasonication power has been thought to be due to the less recrystallized amylopectin molecules (Yu et al., 2013). Syneresis (%) of the sonicated starch gels has been found to be lower than for the untreated starch gel after three freeze-thaw cycles (Sit, Misra, & Deka, 2014). According to Sit et al. (2014), ultrasonic treatment might have broken molecular chains in the amorphous regions leading to extensive reordering of the chain segments. This breakage and reordering of amorphous region may have then allowed a greater number of hydrophilic bonds to be exposed and to hold more water during thawing.

Non-thermal methods are ideal processes without heat deteriorative reactions. Pulsed electric field (PEF) is commonly used in potato industry as a pre-treatment step prior to cutting as the PEF-softened potato tubers have been shown to cut more cleanly (Botero-Urbe, Fitzgerald, Gilbert, & Midgley, 2017; Fauster et al., 2018). PEF treatment has also been reported to disrupt the structure of starch granules as evidenced by the lower gelatinisation enthalpy indicating the potential loss of double helices. In addition, the lamellar spacing (d) in PEF-treated rice starch has been shown to decrease with increasing pulsed electric field strength (Zeng, Gao, Han, Zeng, & Yu, 2016). The morphology, relative crystallinity, and pasting properties of corn (Han, Zeng, Zhang, & Yu, 2009) and potato (Han, Zeng, Yu, Zhang, & Chen, 2009; Li et al., 2019) starches have been observed to be influenced by increasing pulsed electric fields strength. The PEF-treated corn and potato starches might have undergone starch gelatinisation in high pulsed electric fields strength (at 50 kV/cm) as shown by their granular destruction and the molecular rearrangement. Consequently, no significant difference in the final viscosity (the viscosity at the end of cooling) of PEF treated corn and potato starches was observed from their native counterparts. An increase in pasting stability and lower retrogradation tendency (i.e. syneresis) has been observed in PEF-assisted+acetylated potato starch (Hong, Chen, Zeng, & Han, 2016). This might be attributed to the suppression of intermolecular interaction between water and starch molecules due to the presence of phosphate ester at C6/C3 of amylopectin in potato starch (Walter, 1998).

High pressure processing (including ultrahigh (UHP) or high-hydrostatic (HHP) pressure >400MPa and homogenisation by valve homogeniser) is an effective way to keep food product microbiologically safe while maintaining their sensory quality. All UHP-treated starches have been shown to have either a mixture of intact granules and partially gelatinised starch or completely gelatinised starch (Douzals, Perrier Cornet, Gervais, & Coquille, 1998; Kim, Kim, & Baik, 2012). Under UHP, the crystallite dissociation and the unwinding of amylopectin double helices have been reported to be restricted

possibly due to the stabilisation of van der Waals and hydrogen bonds among double helices of amylopectin (Knorr, Heinz, & Buckow, 2006). Consequently, UHP-gelatinised starch has been found to have limited amylose leaching (Stolt, Oinonen, & Autio, 2000), lower swelling power (Douzals et al., 1998), and more resistance to enzymatic digestion (Colussi, Kaur, et al., 2017; Selmi, Marion, Perrier Cornet, Douzals, & Gervais, 2000).

With subsequent cooling, the amount of the retrograded starch has been shown to be proportional to the amount of the gelatinised starch in UHP-treated starch (Kawai, Fukami, & Yamamoto, 2007). Results of Young modulus measurements, calorimetry, and X-ray diffraction have shown a limited level of retrogradation in UHP-treated wheat starch gels. More restricted translational proton mobility in UHP-gelatinised, than for heat-gelatinised wheat starch gels, might have led to less recrystallisation during retrogradation (Douzals et al., 1998). Lower levels of retrogradation, i.e. lower ΔH_R have also been observed in UHP-gelatinised and retrograded wheat starch (Doona et al., 2006). The relative crystallinity of HHP-gelatinised and retrograded sample has been found to be higher for normal corn starch compared to waxy corn starch where higher amylose in corn starch may act as nuclei and co-crystallize with amylopectin chains leading to additional crystallites (Li et al., 2016).

Table II.3 Effects of food processing technologies or treatments on starch retrogradation

Food techniques	Botanical sources	Processing conditions	Storage conditions	Influences	References
HMT	Lentil starch, wheat starch, and oat starch	100°C, 16h, 30% moisture.	25°C, 20day	ΔH_R : Lentil> wheat> oat starches> their native counterparts	(Hoover & Vasanthan, 1994a)
HMT	Corn starch	125°C, 20mins, saturated humidity.	1°C, 7day	Relative crystallinity increased.	(Miyoshi, 2002)
Extrusion	Pastry wheat flour	Co-rotating twin-screw, screw speed 150-250 rpm, constant barrel temperature from feed port to exit die at 40-120°C, feed moisture content 20-60%.	4°C, 0, 7, or 14day	Feed moisture content ↑, setback value by RVA ↑.	(Kim et al., 2006)
Improved Extrusion Cooking Technology	Rice starch	Single screw, screw speed 20-32rpm, barrel temperature 69-120°C mass ratio of sample: water 1:1.5.	4°C, 7day	Lower ΔH_R , lower relative crystallinity, and lower ratio of 1045cm ⁻¹ to 1151cm ⁻¹ in the FTIR spectra.	(Liu et al., 2017; Zhang et al., 2014)
Annealing	Breadfruit starch	10% starch slurry cooked at 45, 50, 55, and 60°C for 24h	22°C, 12day	Lower ΔH_R .	(Siswoyo & Morita, 2010)
Ultrasound	Non waxy rice starch	5% starch slurry, 100, 500, 1000W, operating temperature <60°C.	4°C, 7day	ΔH_R decreased with increasing ultrasonic power.	(Yu et al., 2013)
Ultrasound	Taro starch	50% starch slurry, 30 kHz, 100W, 125 μm amplitude, for 10min keeping slurry temperature at 20±0.5°C.	Repetitive cycle between -20°C 22h and 30°C 2h, for 3day	Improved freeze-thawing stability.	(Sit et al., 2014)
PEF	Corn starch	8% corn starch-water suspension, continuous PEF system operating at electric field strength of 30, 40, and 50 kV/cm.	-	Subtle changes in setback viscosity of PEF treated starch compared with native starch.	(Han, Zeng, Zhang, et al., 2009)
PEF	Acetylated potato starch (DS=0.13)	E = 2 kV/cm, Q = 1.7 × 10 ⁸ J/m ³ , t _p = 40 μs, t _{exp} = 74.5 s, f = 1000 Hz.	25°C, 24h	Lower retrogradation (39.1%), breakdown (155 BU) and setback value (149 BU).	(Hong et al., 2016)
UHP	Wheat starch	30% starch slurry, 600 MPa, 25°C, 15mins.	4°C, 2day	Young compression modulus of heat-gelatinised +retrograded starch> UHP-gelatinised +retrograded starch.	(Douzals et al., 1998)
UHP	Wheat starch	40% starch slurry, 620MPa, 25°C, 30mins.	4°C, 14day	ΔH_R of heat-gelatinised starch> UHP-gelatinised starch.	(Doona et al., 2006)
UHP	Normal/ Waxy corn starch	30% starch slurry, 600 MPa, 15 mins.	Room temperature, 192h	Relative crystallinity of retrograded HHP-gelatinised normal corn starch> retrograded HHP-gelatinised waxy corn starch.	(Li et al., 2016)

HMT, heat moisture treatment; ΔH_R , retrogradation enthalpy; RVA, rapid visco analyser; PEF, pulsed electric field; UHP, ultra-high pressure process.

II.4 Starch nutritional fractions as delivered by various food processing

Healthy people can maintain their plasma glucose concentration within a relatively narrow range, between approximately 3.3 and 8.3 mmol/L. Even within the first hour after the start of the meal, the peak postprandial plasma glucose occurring seldom exceeds 8.3 mmol/L and the increase rarely lasts beyond 120 min (Foster-Powell et al., 2002). Due to the complexity of the human digestion process and the laborious procedure of measuring glycaemic index experiment, starch digestion *in vitro* has been developed as a cost-effective method for screening glycaemic characteristics of foods. Researchers have shown a strong and positive correlation between starch digestion *in vitro* and *in vivo* (Goñi et al., 1997). It is, however, important to consider both physiological and physicochemical events of each step of digestion with realistic transit time, pH, and enzymatic conditions *in vitro* as postprandial glucose response is a reflection of intestinal glucose absorption as well as combined responses of several physiological processes during *in vivo* starch digestion (Guerra et al., 2012).

The *in vitro* starch digestion measures the glucose released at selected time points over 120 min to reflect human starch digestion. Starch nutritional fractions are divided into rapidly digestible starch (RDS), slowly digestible starch (SDS) and resistant starch (RS) fractions (Englyst et al., 1992). The RDS is the fraction that is digested within 20 minutes, SDS is the starch digested between 20 and 120 minutes, and the remaining undigested starch is considered as resistant starch (RS). The relation between the three starch fractions can be illustrated by following equation: $RS=TS-(RDS+SDS)$, where TS is total starch. SDS prolongs the glucose release and places less stress on the blood glucose regulatory system (Lehmann & Robin, 2007b). SDS may prolong satiety which could be incorporated into foodstuffs for weight-loss programs. SDS may also be utilized by athletes as it provides a longer, more consistent source of systemic glucose (Wolf, Bauer, & Fahey, 1999). Retrograded starch is classified as resistant starch type 3 (Haralampu, 2000). RS is the portion of starch that escapes from small intestine and passes to the large intestine. It is digested by colonic microflora enzymes then fermented to produce short-chain fatty acids (acetic, propionic, and butyric) that have been shown to be beneficial to colonic health (Bird et al., 2009).

A low GI starchy food should contain lower amounts of RDS, and a higher proportion of SDS and RS (Gourineni, Stewart, Skorge, & Sekula, 2017; Hamaker et al., 2007; Zhang & Hamaker, 2009). Knowing the influence of food structure and processing on starch nutritional fractions enables the development of starchy products of which the starch-derived glucose evolution is delayed.

II.4.1 Kinetics of glucose release and starch digestibility

Several mathematical models have been proposed to predict and estimate the kinetics of glucose release during starch digestion *in vitro* (Table II.4). The well-known Michaelis–Menten equation depicts the starch digestion *in vitro* by analysing enzyme activity and the relation between substrate and

production. In this reaction of enzyme-substrate binding and production, the enzyme concentration is assumed to be relatively low. The competitive or non-competitive enzyme binding during digestion can lead to either product inhibition or substrate inhibition, and hence, a modified Michaelis–Menten equation has been proposed to consider the impacts (Singh, Dartois, et al., 2010). The modified model successfully describes time courses from various starch samples prepared under different conditions, such as different digestive enzymes (Dona, Pages, Gilbert, Gaborieau, & Kuchel, 2009) (Table II.4).

The first order rate equation $C = C_{\infty}(1 - e^{-kt})$, where C is the concentration of starch hydrolysed at chosen time t, C_{∞} is the equilibrium concentration, k is the kinetic constant (Table II.4). It is proposed by Goñi et al.,(1997) based on assuming the substrates are sufficient throughout digestion process. The area under the hydrolysis curve (AUC) of a specified product divided by the AUC of white bread was defined as hydrolysis index (HI). The estimated glycaemic index (*eGI*) of a wide range of foods, such as spaghetti, rice, biscuit, chickpea etc., were calculated to correlate starch digestion *in vitro* to *in vivo*. It has been shown a positive and significant correlation with the glycaemic index (GI) *in vivo*, where $GI=39.21+0.803 (HI_{90})$ ($r=0.91, p<0.05$) (Goñi et al., 1997). The *eGI* obtained *in vitro* from the same model also has been shown to have a strong and positive correlation to the GI *in vivo* across a variety of cooked potato cultivars (Ek, Wang, Copeland, & Brand-Miller, 2014). Boiled-chill potatoes (8°C, 24h) and the addition of vinegar have been found to reduced glycaemic (GI) and insulinemic (GII) indices in healthy subjects after a potato meal. Cold storage has been found to lower GII with 28%, comparing to the GII of freshly boiled potatoes (Leeman, Östman, & Björck, 2005).

An empirical first order rate equation has been used to model the starch hydrolysis curve by the Log of Slope (LOS) analysis. Instead of defining the starch nutritional fractions by the fixed period, the empirical first order equation reflects the decreasing starch hydrolysis rate as the substrate concentration decreased naturally as the reaction proceeds. The slope of the LOS plot is sensitive to the changes in k during a reaction revealing by discontinuities in the linear plot. A significant correlation between the predictive digestibility curves and experimental data validates the estimation of C_{∞} and k obtained by LOS plots (Butterworth, Warren, Grassby, Patel, & Ellis, 2012; Chen et al., 2016; Edwards, Warren, Milligan, Butterworth, & Ellis, 2014; Kim, Choi, Park, & Moon, 2017; Pinhero et al., 2016). Based on the changes of the slope of the LOS plot, the starch nutritional fractions can be discerned over the digestion time course (Dhital et al., 2016).

Table II.4 The comparison of kinetics constant κ estimation by different model.

Model	Michaelis-Menten	Goñi et al. model	Logarithm of slope (LOS) model
Equation	$v = v_{max}S/(\kappa_m + S)$		$C = C_{\infty}(1 - e^{-kt})$
Parameter	$v = \kappa S$	$\ln \left[\frac{(C_{\infty} - C_t)}{C_{\infty}} \right] = -\kappa t$	$\ln \frac{dC}{dt} = \ln(C_{\infty}\kappa) - \kappa t$
	$\kappa = \frac{\kappa_{cat}E_0}{\kappa_m+S}$	$-\kappa =$ <i>the slope of a linear plot,</i>	$-\kappa$ <i>= the slope of a linear plot,</i>

		$\left(\ln \left[\frac{(C_\infty - C_t)}{C_\infty} \right] \text{ against } t \right)$	$\left(\ln \left[\frac{dC}{dt} \right] \text{ against } t \right)$ $\ln(C_\infty \kappa) = \text{the intercept,}$ $\text{then } \kappa \text{ can be calculated}$
Limits	One-stage reaction exhibit possible substrate inhibition and product inhibition.	All starch fraction inherent same reactivity. A long time digestion is needed to assure an accurate estimation of C_∞ .	Sufficiently spacing between each time interval.

II.4.2 Formation of slowly digestible/resistant starches in processed foods

Knowledge of food processing methods and conditions as well as of the underlying mechanisms that lead to the formation of SDS/RS in foods is of great importance for nutritionists and food companies, since it offers the possibility of increasing the SDS/RS content in processed foods (Table II.5).

Extrusion cooking influences starch digestibility variously depending on the extent of depolymerisation and interactions with other food components such as protein and lipid (Alonso, Aguirre, & Marzo, 2000; Björck, Asp, Birkhed, & Lundquist, 1984; Mahasukhonthachat, Sopade, & Gidley, 2010). The degree of extrusion cooking affects accessibility of starch to digestive enzymes; gelatinised starch in rice flour extrudates has been found to facilitate the amylolytic hydrolysis *in vitro* (Hagenimana et al., 2006). Under high shear conditions, mango starch has been found to be depolymerized, producing unbranched chains that are more likely to retrograde during cooling and storage (Agustiniano-Osornio et al., 2005). This could have contributed to the higher RS in extruded high-amylose barley (Huth, Dongowski, Gebhardt, & Flamme, 2000) and extruded high-amylose corn flour (Zhang et al., 2016). Formation of amylose-lipid complex in corn starches (Asp & Björck, 1989; Bhatnagar & Hanna, 1994) or starch-protein interaction in extruded rice flour (Guha, Ali, & Bhattacharya, 1997) have been linked to a decrease in starch digestibility *in vitro*. Different results of starch digestibility *in vitro* may be due to variable interaction between starch molecules and other components during and after extrusion.

When starch is cooked at high temperature (>140°C) such as in a jet cooker in the presence of a complexing agent, e.g. fatty acids, it may experience a different crystallisation during cooling at 75–95°C. The term “high temperature retrogradation” has been coined to describe re-crystallisation of the amylose with the native lipid material present in corn starch (Davies, Miller, & Procter, 1980). The crystallisation can either form a complex with radial symmetry and birefringence (called starch spherulites) (Singh, Lelane, Stewart, & Singh, 2010) or self-assemble into a starch complex with non-spherical morphology (Conde-Petit, Handschin, Heinemann, & Escher, 2007; Foucault, Singh, Stewart, & Singh, 2016). The starch-lipid complex formed by corn or potato starches with palmitic acid at 140°C, then followed by retrogradation at 70°C, showed a low digestibility. The high retrogradation temperature may have contributed to higher resistance towards enzyme action in the simulated gastro-small intestinal environment (Foucault et al., 2016).

Heat moisture treatment (HMT) processed starches have been observed to exhibit increased (Ambigaipalan, Hoover, Donner, & Liu, 2014; Varatharajan et al., 2011), decreased (Ambigaipalan et al., 2014; Chung, Liu, et al., 2009), or unchanged susceptibility to enzymatic degradation, depending on the starch botanical source and treatment conditions. Different HMT conditions determine the extent of disruption of granular structure, the formation of resulting ordered structures leading to varied amounts of the resistant starch (Hoover, 2010). In some instances, HMT treatment might have disrupted native granular structure at the expense of RS, with the result that either slowly digestible starch or rapidly digestible starch, or both, increased (Jiranuntakul, Puttanlek, Rungsardthong, Pancha-arnon, & Uttapap, 2011; Kim & Huber, 2013). Waxy potato starch has been observed to display visible cracks on the granular surface with a hollow centre owing to the molecular rearrangement during HMT (Lee & Moon, 2015). HMT processed rice and corn starches have been shown to induce moderate increases in thermostable RS and SDS contents that can withstand subsequent thermal processing/cooking conditions, illustrating its practical significance of HMT (da Rosa Zavareze et al., 2012; Kim & Huber, 2013). After cooling and storage, the increase in RS of HMT-treated starch (Pratiwi, Faridah, & Lioe, 2018) has been found to be related to starch retrogradation contributing to an increase in relative crystallinity of HMT-treated potato, corn (Miyoshi, 2002), and lentil starches (Hoover & Vasanthan, 1994b) (section II.3).

Granule porosity of annealed starches has been related to an increase in enzyme susceptibility, negating the effect of crystalline perfection and leading to the conversion of RS to SDS or RDS (O'Brien & Wang, 2008). Annealed pea, lentil and navy bean starches have been shown slight increases (1.6–5%) in SDS and RS levels compared with untreated native counterparts during subsequent heating (Chung, Liu, & Hoover, 2010; Chung, Liu, et al., 2009). Swollen granules in annealed starch have been found to rupture more easily than for native starch once heated (Alvani, Tester, Lin, & Qi, 2014). The ΔH_R of annealed wheat starch has been reported to be lower than for native counterparts during storage (Yu, Wang, Xu, Guo, & Du, 2016). The ΔH_R of annealed starch in *sous vide* cooked potatoes (at 55°C and 4°C 3-day refrigeration) were similar to the ΔH_G of raw potatoes (Chen, Singh, Midgley, & Archer, 2019). Lower *eGI* of *sous vide* cooked-chill potatoes than for boiled-chill potatoes may have attributed to better crystalline/amorphous alignment and less heat disruption of cell microstructure during *sous vide* cooking (Chen, Singh, Midgley, & Archer, 2019).

Microwave heating with no shear involved is an alternative to conventional heating for the preparation of starch slurries. Microwave heating induces starch gelatinisation leading to increased starch digestibility, similar to conduction heating (Emami, Perera, Meda, & Tyler, 2012; Hagiwara, Esaki, Nishiyama, Kitamura, & Kuge, 1986; Kingman & Englyst, 1994). Different heating modes of microwave than conduction heating have been found to result in cooked starch gel with different physicochemical characteristics. Microwave-heated wheat starch gel has been found to result in less amylose leaching into the inter-granular matrix due to the rapid heating rate, forming a weaker amylose

network upon subsequent cooling and storage (at 25°C) (Palav & Seetharaman, 2007). Consequently, re-association of microwave-heated starch has been found to be reduced compared to autoclaved starch in lotus seed during cooling, leading to less RS in the former (Zeng et al., 2015). Other factors such as the microwave irradiation and furnace dimensions and dielectric properties of the starch slurries have also been extensively studied (Braşoveanu & Nemţanu, 2014). Microwave irradiation could lead to the generation of free radicals (Yang et al., 2017), affecting glycosidic bonds of starch molecules at crystalline/amorphous lamella level (Fan et al., 2014) and thus promote the fragmentation of large starch molecules into smaller ones (Kim, Park, & Lim, 2015). In this case, it could possibly result in microwave-heated starch being more ready to aggregate during cooling, leading to a higher RS. Since microwave irradiation is able to remove water efficiently to produce a starch paste with low moisture content, microwave-assisted HMT was developed to shorten processing times (Zhang, Wang, & Shi, 2009). The microwave-assisted HMT induced subtle granular structure changes to minimise the RDS in waxy and non-waxy rice starches (Anderson & Guraya, 2006a; Anderson, Guraya, James, & Salvaggio, 2002) and in *Canna edulis* ker starch (Zhang, Chen, Liu, & Wang, 2010).

HHP process has been found to alter the water distribution within the cellular components in waxy rice (Tian, Li, Zhao, Xu, & Jin, 2014) and waxy wheat (Hu, Zhang, Jin, Xu, & Chen, 2017) starches, leading to the formation of imperfect crystallites (Li, Bai, Mousaa, Zhang, & Shen, 2012). The HHP-treated starch granules were thus more susceptible to amylase hydrolysis (Liu, Hu, & Qun, 2010) resulting in lower RS (Mu, Zhang, Raad, Sun, & Wang, 2015) but higher SDS (Tian et al., 2014). The HHP-gelatinised rice starch had higher amounts of SDS (17.1 %) than heat-gelatinised rice did (4 %), though the gelatinisation enthalpy and the relative crystallinity of both samples were the same. With subsequent cooling, an increase in the amount of SDS in HHP-gelatinised and retrograded rice starch has been reported (Tian et al., 2014). This may have contributed to the greater extent of retrogradation in HHP treated rice starch (as discussed in section II.3). Similar phenomena have also been observed in HHP-gelatinised and retrograded potato starch where the increase in relative crystallinity during retrogradation led to lower starch digestibility (Colussi, Kaur, et al., 2017). HHP may yet promote the formation of amylose-lipid complex resulting in the increase in SDS in HHP-modified buckwheat starch (Liu, Wang, Cao, Fan, & Wang, 2016).

PEF disrupts starch granules in waxy rice as evidenced by lower relative crystallinity and lower gelatinisation temperature (Zeng et al., 2016), resulting in increased accessibility of digestive enzymes to starch granules by exposing α -1-4 and α -1-6 linkages (Han, Zeng, Yu, et al., 2009; Han, Zeng, Zhang, et al., 2009). Consistently, PEF has been reported to increase RDS and decrease SDS in rice starch with increasing electric field intensity (EFI). This may have attributed to the reorganization of starch structures (at short-range order, i.e. disordered amorphous and crystalline lamella alignment) and dents on the surface of PEF-treated rice starch, facilitating hydrolysis by digestive enzymes (Wu et al., 2019). For wheat (an A-type starch) and potato (a B-type starch) starches, the RDS has been found to increase with EFI, while a decrease in SDS and increase in RS have only be observed at some EFI. As for pea

starch (a C-type starch), the increase in RDS and the decrease in SDS with increasing EFI have been reported, but not for RS. This may imply a pronounced effect of PEF on the scatter structure and fractal dimension of self-similar structures in wheat and potato starches than for pea starch (Li et al., 2019). As discussed previously, PEF only displays subtle effects on starch retrogradation as evidenced by the pasting profile, therefore more research on the effects of post-processing of PEF-treated starch is necessary to determine the influence in SDS and RS content.

The effects of ultrasound treatment on the structural and physico-chemical characteristics of starch have been extensively studied (Zhu, 2015) but few reports illustrated an effect on digestibility. Ultrasound treatment has been observed to enhance the crystalline regions in corn starch (Luo et al., 2008). This more compact arrangement of the double-helical structures in starch granules might limit the amylase hydrolysis rate. The RS of ultrasound treated corn starch slurry (6.2%) has been found to be higher than in native corn starch (4.7%). Ultrasonic cavitation may have prompted the formation of short-chain amylose causing granules to rupture easily during gelatinisation. Consequently, gelatinised corn starch pre-treated with ultrasound has been observed to have higher RDS and yet higher RS (4.0%) than for heat-gelatinised corn starch (RS, 2.1%) (Flores-Silva et al., 2017). The short-chain molecules prompted by ultrasound cavitation might have facilitated recrystallisation during retrogradation. The resistant starch level in ultrasound treated and retrograded pea starch has also been shown increase (You et al., 2019).

Table II.5 Food processing and starch nutritional fractions

Food techniques	Botanical sources	Processing conditions	Starch Nutritional fractions	References
Extrusion	Rice starch	Double screw, screw speed 200–300 rpm, barrel temperature 100–160°C, and feed moisture content 16–22%.	RDS↑, SDS↑, RS↓.	(Hagenimana et al., 2006)
ANN	Pea starch, lentil starch, and navy bean	70% moisture at 50°C for 24 h.	RDS↑, SDS↑, RS↓.	(Chung, Liu, et al., 2009)
HMT	Pulse starches: faba bean, black bean and pinto bean	23% moisture at 80, 100, 120°C for 12 h.	SDS↓ at all temperatures of HMT; RS↑ at HMT80 and HMT100, but RS↓ at HMT120.	(Ambigaipalan et al., 2014)
HMT	Corn starch	30% moisture at 120°C for 24 h.	RDS↑, SDS↓, RS↓.	(Chung, Hoover, & Liu, 2009)
HMT	Rice starch	15, 20 and 25% moisture at 110°C for 1 h.	RS↑.	(da Rosa Zavareze et al., 2012)
Microwave	Potato starch	8-25% moisture at 150°C, 2450 MHz, 10min.	Moisture↑, RDS↑.	(Hagiwara et al., 1986)
Microwave-assisted HMT	Waxy and non-waxy rice starch	20% moisture at 140°C for 1 h.	SDS↑, RS↑.	(Anderson & Guraya, 2006b)
HHP	Waxy and non-waxy rice starch	25% starch slurry, 600 MPa, 30°C, 30 min.	SDS↑.	(Tian et al., 2014)
HHP	Buckwheat starch	20% starch slurry, 120, 240, 360, 480, and 600 MPa, 20 min.	RDS↓, SDS↑, RS↑.	(Liu et al., 2016)
HHP	Waxy wheat starch	10% starch slurry, 600 MPa, 20°C, 30 min.	RDS↑, SDS↑, RS↓.	(Hu et al., 2017)
PEF	Waxy rice starch	Continuous system E = 50 kV/cm, t _{exp} = 40 s, 40-45 °C.	RDS↑, SDS↓.	(Zeng et al., 2016)
PEF	Japonica rice starch	60% starch slurry, E= 2.86, 5.71, and 8.57 kV/cm.	RDS↑, SDS↓.	(Wu et al., 2019)
PEF	Wheat, potato, and pea starches	60% starch slurry, E= 2.86, 4.29, 5.71, 7.14, and 8.57 kV/ cm.	Wheat: RDS↑, RS↑ at 2.86 and 4.29 kV/cm. Potato: RDS↑, RS↑ at 2.86 and 5.71 kV/cm. Pea: RDS↑, SDS↓.	(Li et al., 2019)
Ultrasound	Corn starch	30% starch slurry, 24 kHz, 20°C, 1-16 min.	Ultrasound treated starch: RS↑. Ultrasound +gelatinised starch: RDS↑, SDS↓, RS↑.	(Flores-Silva et al., 2017)

RDS, rapidly digestible starch; SDS, slowly digestible starch; RS, resistant starch; ANN, annealing; HMT, heat moisture treatment; HHP, hydrostatic high pressure process; PEF, pulsed electric field.

II.5 Designing foods with low GI via enhancing starch retrogradation

Lowering postprandial glucose and insulin responses to starch-based foods may have significant beneficial implications for prevention and treatment of metabolic disorders. It has long been established that post-prandial glucose response to carbohydrate meals is not only determined by the amount of available carbohydrate but also the proportions of different nutrients, particularly protein and fat, as well as food microstructure (Birt et al., 2013). Processing and post-processing (cooling and storage) affect the starch nutritional fractions in food products, regardless of naturally existing RS or RS-enriched products. Starch retrogradation can be facilitated either by incorporating commercial resistant starch type 3 in starch-based products or via various processing and post-processing in formulated or natural systems, lowering GI potentially, as detailed below.

Incorporating resistant starch type 3 (such as commercial ingredient NOVELOSE 330 (Ingredient Incorporated, Westchester, IL) derived from high amylose corn) in starch-based products is limited because of adverse effects on bread quality, such as texture (Korus, Witczak, Ziobro, & Juszcak, 2009), gas cell size (Sanz, Salvador, Baixauli, & Fiszman, 2009), and gluten network formation (Wang, Rosell, & Benedito de Barber, 2002). However, this retrograded amylose exhibits high melting temperatures, up to 170°C, and thus cannot be dissociated by cooking (Jacobasch, Dongowski, Schmiedl, & Müller-Schmehl, 2006; Jane & Robyt, 1984). Additionally, amylose molecules and long-branch chains of amylopectin form double helices during retrogradation creating steric hindrance of enzymatic binding and lowering starch hydrolysis (Sievert & Pomeranz, 1990). Considerable research is still needed to identify the effectiveness of these type of resistant starches and to investigate mechanisms underpinning their actions.

Effects of different bread making processes, such as different leavening techniques, cooking methods (Jenkins et al., 1986; Lau, Soong, Zhou, & Henry, 2015), proofing period (Pat Burton & Lightowler, 2006), and partial baking freezing technology (Borcak, Sikora, Sikora, Rosell, & Collar, 2012) on postprandial glucose and insulin response to bread has been reviewed comprehensively (Stamataki, Yanni, & Karathanos, 2017). Sourdough bread has been found to be a low GI food possibly due to the slower gastric empty rate (Darwiche et al., 2001; Najjar et al., 2008), or the formation of RS content via starch retrogradation (Novotni et al., 2011), or the interaction between starch and gluten proteins creating physical barrier to enzymatic digestion (Östman, Nilsson, Liljeberg Elmståhl, Molin, & Björck, 2002). The mechanism behind these pronounced effects are still to be fully elucidated. Bread staling, as a result of starch retrogradation after storage, may limit the application to reduce GI due to the increase in hardness. Partial-baking freezing technology has also been reported to facilitate the formation of retrograded starch due to the heating-cooling cycles involved from manufacture to consumer (Ronda et al., 2011). For both homemade and commercial white breads, the glucose response of frozen-defrosted then toasted breads have been found to be significantly lower than for freshly toasted bread in a randomised cross-over design trial of 10 healthy volunteers (Burton & Lightowler, 2008).

Extruded noodles made from high amylose rice starch has been shown to reduce the GI in seven healthy Canadians by 36%, and in diabetics from Canada and Philippines by 24%, suggesting that extruded rice may provide health benefits to both normal and diabetic individuals (Panlasigui et al., 1992). Starch retrogradation and starch packing in extruded rice during cooling and drying steps have been found to be crucial in decreasing the glycaemic response of rice noodles substantially (Lok et al., 2010; Srikaeo & Sangkhiaw, 2014). Unlike extruded noodles, extruded breakfast cereals experience severe processing that involves in high heat, high pressure, and severe shear forces, leading to a porous structure and thus higher GI (Faraj, Vasanthan, & Hoover, 2004; Guha et al., 1997; Zhang et al., 2015). Similarly, adding extruded chickpea flour rather than native chickpea flour to white bread has been shown no significant effect on the reduction of postprandial glucose and insulin response in twelve healthy subjects (Johnson, Thomas, & Hall, 2005).

Cooling appears to be a simple and effective intervention to reduce the GI of cooked rice (Sonia, Witjaksono, & Ridwan, 2015) and cooked potatoes (Beals, 2019). Three main factors have been summarized to explain the variation in glycaemic and insulinaemic responses to rice: (1) inherent starch characteristics (such as ratio of AM: AP in different rice cultivars), (2) processing (particularly parboiling), and (3) at-home preparation (e.g. cooking, storage and reheating) (Boers, Seijen Ten Hoorn, & Mela, 2015). GI of processed rice depends on varieties and the severity of processing, associated with changes of physico-chemical properties. Parboiling consists of soaking in water, heating, drying and milling of paddy rice. Crystalline structure of rice has been found to be transformed to amorphous in parboiled rice (Manful, Grimm, Gayin, & Coker, 2008). However, the glycaemic response of pressure-parboiled rice, in which amylopectin retrogradation was observed, has been reported to be significantly lower than for non-parboiled rice (Larsen et al., 2000). Parboiled rice is generally reheated before consumption leading to disintegration of retrograded amylopectin due to the low melting point (46-65°C) of these retrograded crystallites (Asp, van Amelsvoort, & Hautvast, 1996). As a consequence, little significant difference in postprandial glycaemic response has been observed between freshly cooked parboiled and reheated parboiled rice (at 65°C) (Lu, Venn, Lu, Monroe, & Rush, 2017).

Boiled potato *cv.* Sava showed an significant increase in resistant starch (RS) content from 3.3 to 5.2% (starch basis) after refrigeration at 8°C for 24 h, owing to starch retrogradation (Leeman et al., 2005). Addition of vinegar to cold potatoes have been reported to reduce acute glycaemia (from 168, the GI of freshly boiled potatoes to 96, the GI of cold vinegar potatoes) in 13 healthy subjects (Leeman et al., 2005). Similarly, cooling and cold storage (at 5 °C, 3 days) of potato products made from *cv.* Nicola has been reported to, despite reheating at 70–80 °C, lower GIs of potato products by about 25% in 22 healthy volunteers. Regardless of cooking methods, once starch is fully gelatinised (at >100°C, >30min) in steam boiled potatoes (GI, 104), oven-baked casserole (GI, 95) and mashed potatoes (GI, 106), no significant differences in GIs were observed (Tahvonen et al., 2006). Beyond the composition differences in potato varieties, no significant differences have been found in the RS content of potato *cv.* Dark Red Norland, *cv.* Russet Burbank, and *cv.* Yukon Gold. Post-processing experience plays an

influential role on the RS content in all these cultivars; the RS content has been found to be the highest in cold tubers followed by reheated tubers with the lowest for hot potatoes (Raatz, Idso, Johnson, Jackson, & Combs, 2016). Cooked-cold potato *cv.* Russet (at 4°C for 5days) had a higher concentration of RS, and thus, less available carbohydrate, reducing postprandial glucose and insulin effectively when compared to boiled potatoes, consumed hot, in females with elevated fasting glucose and insulin (Patterson et al., 2019).

With growing consumer preference for convenient but healthy, natural, and high-quality food products, achieving starchy food with low glycaemic features through retrogradation offers great opportunity. Food Standards Australia New Zealand (FSANZ) approved the amendment to the measurement of resistant starch separated from dietary fibre (Food Standards Australia New Zealand, 2018), ahead of the U.S. Food and Drug Administration (FDA) and the European Food Safety Authority (EFSA). The previous method of ‘total dietary fibre’ measured some, but not all, resistant starch in a food. It did not distinguish the resistant starch from other forms of dietary fibre present in the food. The amendment, however, is able to determine the quantity of the resistant starch apart from dietary fibre in the food. Additionally, the amendment adds the declaration of the quantity of resistant starch as a sub-group nutrient of dietary fibre in the nutrition information panel. The addition of resistant starch on the nutrition information panel shines a light on a broader application of resistant starch in the food industry. The change also introduces the possible benefit of resistant starch RS3, the retrograded starch more directly to the public.

II.6 Conclusion

Processing, and then retrogradation post-processing, both influence starch structure greatly. Cooked/processed starch can be partially gelatinised, or de-branched, or fully gelatinised during various food processing/treatments. Consequently, the resulting packing of helices upon cooling and storage leads to different extents and tendency of retrogradation. Enhanced interaction of AM-AP during HMT contributes to an increase in retrogradation enthalpy with subsequent cooling. HHP may induce amylose to act as nuclei and facilitate AM-AP co-crystallisation leading to higher SDS. Short-chain starch molecules prompted by ultrasound cavitation may facilitate re-crystallisation during retrogradation and thus higher RS. Many factors, such as high temperature retrogradation in presence of lipids, lead to the creation of the slowly digestible starch, in which the cooperative interactions give rise to an ordered chain structure, and increase density of these processed then retrograded starches. Reheating tends to negate the effect of starch retrogradation resulting in the increase in GI, though cooling and cold storage seems promising to limit this effect. This could perhaps be improved by enhanced starch retrogradation under optimum time-temperature cycles or combined with existing or new technologies.

II.7 Research gaps

Research Gap I. Starch retrogradation in tuber and its influence during gastro small-intestinal digestion

Retrogradation leads to structural and physical changes in starch, which affects its functional properties. Starch retrogradation in cooked/ gelatinised starch has been reported to depend on the botanical source, morphology and granule size distribution (Singh & Kaur, 2004). Inherent characteristics of starch granules such as amylose/amylopectin ratio (Miles et al., 1985), amylopectin branched-chain-length distribution (Srichuwong, Sunarti, Mishima, Isono, & Hisamatsu, 2005) and crystalline/amorphous alignment (Frost et al., 2009) have been considered as important factors. Processing or cooking disrupts the ordered structure of granular starch, resulting in the increased susceptibility of starch to enzymatic digestion. Subsequent cooling and storage lead to retrogradation, in which starch forms compact and dense starchy matrix leading to resistance to digestive enzymes. Starch retrogradation and starch digestion in whole potato tuber (Bordoloi, Kaur, et al., 2012; Tian et al., 2016) may, however occur in a different manner compared to pure potato starch (Ek, Wang, Brand-Miller, & Copeland, 2014; Noda et al., 2008) or pastes/gels (Suzuki & Hizukuri, 1979).

Potato tubers encompass different cell compartments (e.g. cell wall, vacuole, cytoplasm and intercellular spaces) within which starch gelatinisation and starch retrogradation occur, subject to local influences of other cell components and water availability. *We hypothesise that starch retrogradation in tuber may be different from a retrogradation in a starch-water system. We consider that during cooking, starch in tuber is different from in a starch-water system where excess free water is available, therefore mechanisms and resulting functionalities including retrogradation and starch digestion will be different.*

Research Gap II. Accelerated starch retrogradation in tuber and formation of slowly digestible starch

Chill and freeze temperatures facilitate disrupted amylose and amylopectin to aggregate and re-crystallise during retrogradation. A stable microstructure withstanding freeze-thawing cycles is crucial to maintain the textural quality of frozen products. At storage temperature below ice melting temperature, ice crystals embed in the gelatinised starch network, giving a sponge-like structure. Ice crystals coexist in the gelatinised starch network under a metastable status. Freeze-thawing cycles thus generate alternating the starch-rich and the starch-deplete (once ice) regions (Capron, Robert, Colonna, Brogly, & Planchot, 2007; Levine & Slade, 1988). Retrogradation rate has been found to be faster at temperatures close to 0°C than at room temperature, suggesting the occurrence of the nucleation of retrograded starch (White, Abbas, & Johnson, 1989). Retrograded waxy potato starch, formed under temperature cycle between 4°C and 25°C has been found to have higher onset temperature, relative crystallinity, and 1047/1022 ratio compared to samples stored at constant 4°C (Xie et al., 2014). Retrogradation is a non-equilibrium polymer crystallisation process and proceeding rate is determined by temperature. Crystallisation of amylose and amylopectin is thermally reversible above the melting

temperature. While the temperature is above glass transition temperature, amylopectin crystallisation is referred as a nucleation-limited growth process in a mobile, viscoelastic, fringed-micelle network. Simultaneously, amorphous materials display a thermodynamically metastable equilibrium, driving toward the crystalline state. Low temperature (4°C) thus prompts the nucleation of crystalline and increases the formation of SDS. While high temperatures (25-40°C) induce the propagation and maturation, resulting in less digestible materials (Hu, Huang, et al., 2014; Shi & Gao, 2016). The study suggested that temperature-cycled retrogradation in waxy potato starch is a favourable for preparing the slowly digestible starch (Xie et al., 2014).

We hypothesise the thermodynamics of crystal formation in gelatinised starch in tuber govern the tendency of starch towards retrogradation. The rate of starch retrogradation and recrystallisation of the gelatinised starch in tuber can, therefore, be enhanced by time-temperature cycle treatments which may lead to the formation of a compact and dense microstructure, resulting in the lower and the slower digestibility.

Research Gap III. Stability of retrograded starch in tuber during reheating

After food processing, structures of starch *in tuber* influence the kinetics of glucose release markedly during gastro small-intestinal digestion *in vitro*. For instance, the percentage of starch hydrolysis in freshly cooked tubers has been found to be higher than cooled potato tubers (Tahvonon et al., 2006). An optimum heating process is necessary to create the unique organoleptic properties of potato product. During cooling and storage, disrupted starch molecules regain relatively ordered structure that is generally more resistant to enzymatic digestion (Zhou & Lim, 2012). Retrograded starch gels generally show an extensive aggregation of the gelatinised starch fragments, leading to a more compact structure with less porosity. This aggregation is the effect of retrogradation, during which disrupted amylose and amylopectin chains gradually try to re-associate into a different ordered structure. Reheating renders retrograded starch more susceptible to enzymatic hydrolysis, resulting in higher hydrolysis values almost close to the ones obtained for freshly cooked starch. Results of X-ray diffraction spectra and DSC analysis indicate that the crystalline component in fresh, retrograded and reheated pastes differed considerably between each other and the microstructure of retrograded starch pastes have a more compact network than freshly cooked and reheated pastes (Zhou & Lim, 2012).

We hypothesise that a controlled heating process can retain the microstructure and crystallites of retrograded starch in tuber. We expect that more rigid and compact microstructures in tuber created through accelerated retrogradation by various processing and post-processing will have a higher crystalline perfection and stability during reheating and oral-gastro-small intestinal digestion.

II.8 Objective

The main objective of my PhD project is to understand mechanisms and kinetics of starch retrogradation *in tuber* and its influences on the starch digestion *in vitro*. This knowledge is further used to manipulate the storage conditions to enhance the process of retrogradation, and finally studying the stability of retrograded starch *in tuber* during reheating.

Research Objective I. Starch retrogradation *in tuber* and its influence during gastro small-intestinal digestion *in vitro*

Physicochemical properties (such as moisture content, amylose content and total starch content) of a common New Zealand potato cultivar *Agria* were measured. Different cooking temperatures and refrigerated storage durations were selected to study the mechanism and kinetics of starch retrogradation *in tuber*. Freshly cooked (90°C for 25 minutes) *cv. Agria* potato tubers were refrigerated stored for 1, 3 and 7 days. After storage, samples were reheated at 50, 70 and 90°C, respectively. The thermal characteristics (DSC) of all samples were measured by DSC while the relative crystallinity was determined by X-ray GBC® eMMA X-ray Diffractometer (GBC, VIC, Australia) (Foucault et al., 2016). Starch hydrolysis by digestive enzymes was investigated by an *in vitro* starch digestion model (Bordoloi, Singh, et al., 2012).

Relation between the microstructure of retrograded starch *in tuber* and starch digestibility were investigated. Relaxation time distribution curves (mobility of different water pools) of raw, freshly cooked, retrograded and retrograded+reheated tubers were studied by LF-NMR. Other structural characterisations of samples such as relative crystallinity by X-ray were investigated.

Research Objective II. Accelerated starch retrogradation in tuber and formation of slowly digestible starch

Experiments were carried out in an attempt to accelerate retrogradation *in tuber* by using time-temperature-cycle treatments during post-processing, i.e. storage of cooked tubers. Different combinations of cooking and storage temperatures, processing methods (annealing, par-cooking) were investigated. Physicochemical characteristics of processed starch *in tuber* were studied by blue value, TPA, RVA, DSC, FTIR, and LF-NMR. Samples were then tested for kinetics of glucose release during starch digestion *in vitro*.

Research Objective III. Stability of retrograded starch in tuber during reheating

Stability of retrograded starch *in tuber* after thermal processing was determined by applying different reheating temperatures and heating methods such as microwaving, low-temperature long time cooking. Physicochemical characteristics of retrograded+reheated samples were compared with fresh and

retrograded only samples. Starch digestibility by a simulated oral-gastric-small intestinal model of these samples was analysed.

Following these three stages, we hope the knowledge created can assist in formulating potato products with a high quantity of slowly digestible starch and a lower GI.

Chapter III Methodology and methods development

III.1 Methods development

Methods were developed to satisfy the various objectives of this research, to help investigate starch retrogradation in the whole tuber (*in tuber*), with the view to identify factors of the relationship of starch structure-digestibility. Interactions between starch molecules and other cellular components *in tuber* were studied by relaxation times measured by LF-NMR. Starch digestibility by enzymatic hydrolysis was developed and assessed by *in vitro* oral-gastric-small intestinal digestion models.

III.1.1 Molecular chains mobility measured by relaxation times via LF-NMR

Low field nuclear magnetic resonance, LF-NMR is a non-destructive measurement that can monitor changes in molecular chains mobility of the exact same sample over storage time. Relatively larger sampling size (1 to 10g) is the other advantage of LF-NMR over other methods such as DSC (which the sampling size is 5 to 20mg) to study starch retrogradation *in tuber*. This aspect is particularly beneficial when the heterogeneity of a sample is inherent to its nature, such as starch contents vary in different sections of a potato tuber. LF-NMR measures the molecular order by the chemical bonds shifting and records as the distribution spectrum. Relationship between the degree of (both rotational or translational) molecular mobility and physical or mechanical properties in food systems is well established (Micklander, Peshlov, Purslow, & Engelsens, 2002).

III.1.1.1 Theoretical background

Relaxation describes the status of nuclei from excited to neutral state in an applied magnetic field (B_0) (Marcone et al., 2013). It is analysed in terms of two separate processes, each with its own time constant. One process, associated with T_1 , is responsible for the loss of signal intensity where the nuclear spin magnetization vector M_z is parallel to the external magnetic field, B_0 (Figure III.1). The other process, associated with T_2 , affects the components of M_{xy} , which is perpendicular to B_0 (Figure III.1). The longitudinal (T_1) and transverse (T_2) components occur simultaneously in a relaxation process. The time of the excited nuclei needed to return to equilibrium is called “relaxation time T_2 ” (Figure III.1). Relaxation time can be used to describe the mobility of molecules in a complex system. The mobility of chemical bonds changes due to the interaction between one molecule and another, altering the time for excited nuclei to return to the neutral state. Interactions between starch, water, and other compounds in food products affect the proton longitudinal (spin–lattice) relaxation time (T_1) and transverse (spin–spin) relaxation time (T_2).

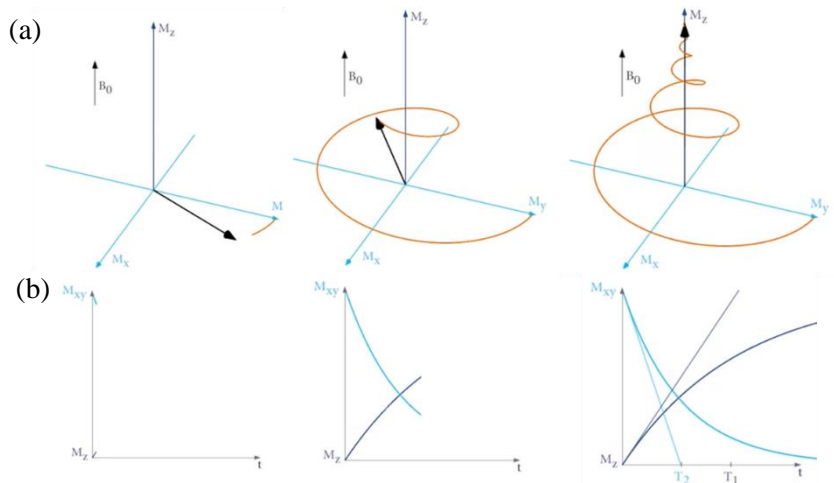


Figure III.1 (a) The spin of a proton (brown curve) under a constant magnetic field (B_0), and (b) the corresponding changes of magnetisation (M_{xy} and M_y). The recovery at 63% of magnetisation (dark blue line) represents the proton longitudinal (spin–lattice) relaxation time (T_1), while the decay at 37% of magnetisation (light blue line) indicates transverse (spin–spin) relaxation time (T_2).

III.1.1.2 Starch gelatinisation/retrogradation and relaxation time

Starch gelatinisation is a transition process involving water diffusion into starch granules, granules hydration and swelling in excess water under heat. Gelatinised starch loses its structural organisation and crystallinity (Biliaderis & Galloway, 1989; Wesaigh, Gidley, Komanshek, & Donald, 2000). Simultaneously, water molecules interact with the exposed hydroxyl groups on amylose and amylopectin by hydrogen bonds. This interaction is not uniform within a starch granule due to the heterogeneous water diffusion contributed to the semi-crystalline nature of starch. Gelatinisation process occurs initially in amorphous regions weakening hydrogen bonding in these areas. When the temperature reaches above gelatinisation peak temperature (T_G), starch granules become increasingly susceptible to shear disintegration as they swell and release materials, such as amylose and unwound amylopectin. Water molecules in both amorphous and crystalline regions become more mobile. During cooling and storage, disrupted amylose and amylopectin molecules re-associate by hydrogen bonding. This re-association forms hydrogen bonding within OH groups of intra- and inter- starch molecules, making the proton exchange between starch molecules and water molecules less likely. Gelatinisation and retrogradation alter water mobility in starch-based systems.

III.1.1.3 Water pools with different relaxation times in starch-water systems and starch-based foods

A number of LF-NMR studies have dealt with changes of relaxation times in starch model systems such as starch pastes/gels, dough, and bread during thermal treatments (Assifaoui, Champion, Chiotelli, & Verel, 2006; Bosmans et al., 2012; Farhat, Belton, & Webb, 2007). Different water pools can be discerned because the water in different cellular compartments is associated differently leading to different relaxation times T_2 (Povlsen, Rinnan, van den Berg, Andersen, & Thybo, 2003; Thybo et al.,

2003; Thybo, Bechmann, Martens, & Engelsen, 2000). Tang, Godward, & Hills (2000) studied the water distribution in potato starch gels (water content 55%) by using the CPMG pulse sequences. They identified four water pools with different relaxation times T_2 and assigned these water pools to cell locations such as extra-granular spaces, amorphous growth rings, semi-crystalline lamellae and hexagonal channels, which exist in B-type amylopectin crystals. Hills & Le Floch (1994) also reported the presence of four water pools in raw potato tissue and tentatively assigned to the corresponding cell compartments. A water pool with the relaxation time T_{20} ranged from 2 to 4ms and T_{21} at about 10ms indicated the water inside starch granules (Figure III.2). The relaxation time T_{22} and T_{23} ranged from 100 to 500ms were possibly the water in the cytoplasm and intercellular regions (Figure III.2). Water pools with longer relaxation time are more mobile owing to less restriction on proton vibration. This allows excited molecules to recover slowly to their neutral state.

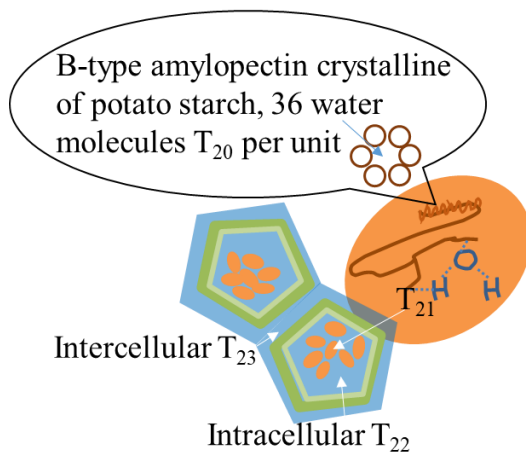


Figure III.2 Four water pools with relaxation times (T_{20} , T_{21} , T_{22} , and T_{23}) in raw potato cells.

When the temperature increased, relaxation times changed due to granules swelling, amylose leaching, and water diffusion. Similar results have been reported for cassava (Chatakanonda et al., 2003), corn (Tananuwong & Reid, 2004), and rice starches (Ritota, Gianferri, Bucci, & Brosio, 2008). Mortensen et al. (2005) found two major water pools with different relaxation times T_{21} at 50ms and T_{22} at 500ms in freshly cooked potato tissues (Figure III.3b). The water pool with relaxation time T_{22} has been assigned to relatively free bulk water in the intercellular cavities and cytoplasm. Relaxation time T_{21} has been shown to represent the water directly associated with starch molecules. During heating, water pool with relaxation time T_{20} which is less than microseconds has been found to be vanished owing to disrupted cells and gelatinised amylose and unwound amylopectin. Structural changes of potato starch *in tuber* has been observed in two stages by the development of relaxation times T_{21} and T_{22} with increasing temperature. When the temperature increased from 25 to 55°C, relaxation times T_{22} and T_{21} have been shown to decrease because chemical exchanges were dominant before starch granules rupture (Figure III.3b). Relaxation time T_{22} has been reported to increase with increasing temperature (above gelatinisation temperature $T_G > 60$ °C) due to cell disruption leading to larger diffusion volumes (Figure III.3c). Relaxation time T_{21} has been observed to be nearly steady

because the increase in the proton exchange rate and the increase in mobility were even out (Figure III.3c). Microstructures of cooked starch re-arranged during cooling and, thus retrograded starch and water interact differently. Free water has been observed during cooling and storage, possibly owing to starch syneresis (Micklander, Thybo, & van den Berg, 2008).

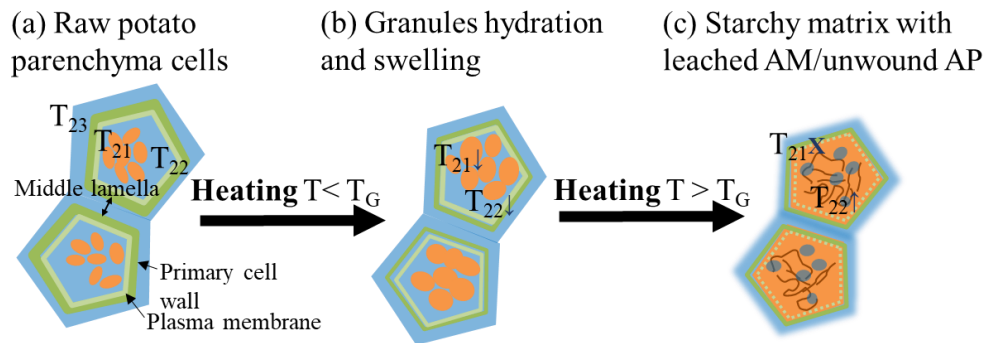


Figure III.3 Changes in relaxation times T_{21} and T_{22} during starch gelatinisation *in tuber*.

*Gelatinisation temperature, T_G is normally around 60°C *in tuber*, AM represents amylose, and AP is amylopectin.

III.1.1.4 Experimental set-up and parameters optimisation

Parenchyma tissue of potato *cv. Agria* was sampled longitudinally (weight 0.5 g) by cork borer (with an internal diameter of $\varnothing 3.4$ mm and 80 mm long) and these samples were inserted into glass tubes of 5 mm outside diameter (Wilmad-LabGlass) and sealed to prevent moisture loss (Figure III.4). The LF-NMR proton relaxation time measurements were performed by a Spinsolve 1.5 LF-NMR spectrometer (Magritek Ltd.) with operating resonance frequency at 42.5 MHz. The apparatus is located in Science tower A and the operational procedures are attached in Appendix A. Transverse relaxation time T_2 was acquired by the Spinsolve®Carbon apparatus' built-in “ T_2 bulk” function using the Carr-Purcell-Meiboom-Gill sequence (CPMG) (Carr & Purcell, 1954; Meiboom & Gill, 1958). The CPMG sequence had a one-millisecond pulse separation and was fitted logarithmically in the relaxation time distribution from 0.1 to 5000 milliseconds with 5000 data points collected (Assifaoui et al., 2006; Rondeau-Mouro et al., 2015). The recycle delay time was 7 seconds. The exponential decay curve of each relaxation time measurement was the result of the accumulation of 4 scans to increase the signal-to-noise ratio (Ward, 2011).

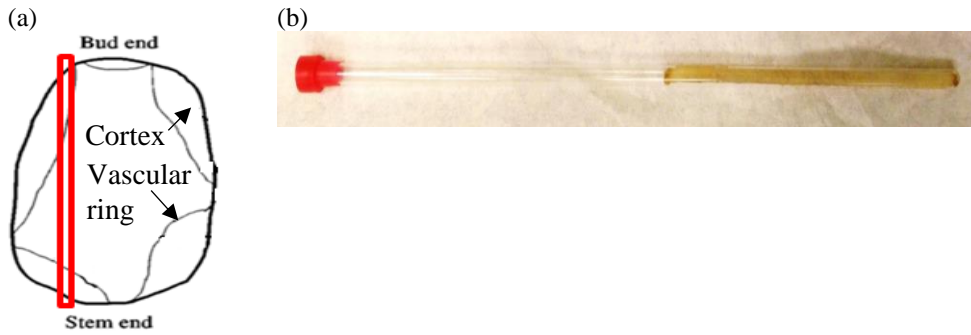


Figure III.4 (a) Sampling of a raw potato cylinder and (b) the raw potato cylinder in a LF-NMR glass tube.

III.1.1.5 Data processing and transformation

Relaxation time can be estimated by the average lifetime of an exponential decay curve of the raw data (Figure III.5). If the decaying quantity, $N(t)$ is the number of different protons with different vibrations in a potato tuber, the average length of time (τ) that an element remains in the set can be estimated by following equation, $N(t) = N_0 e^{-\frac{t}{\tau}}$, with the decay rate (λ) and average length ($\tau = \frac{1}{\lambda}$). The average lifetime can be viewed as a "scaling time" because we can write the exponential decay equation in terms of the average lifetime, τ , instead of the decay constant, λ . The τ is the time that the population assembly reduced to $1/e = 0.368$ times of its initial value. The relaxation time is then retrieved from the exponential decay curve after 37% decay.

The initial amplitude of the raw data is generally proportional to the water content of the samples, i.e. the higher amount of the water content, the higher initial amplitude. The initial amplitude of distilled water, the sample of "10% water +90% D₂O", and potato flour (8% moisture content) were $4.4 \cdot 10^5$ a.u., $1.6 \cdot 10^4$ a.u., and $7.5 \cdot 10^3$ a.u., respectively (Figure III.5), in which the initial amplitude decreased in the order of high to low water content. Proton relaxation time measurement by LF-NMR is, however, limited to detect sample with a relatively high water content to overcome the signal-to-noise. In this case, the two samples with low water content (e.g. the sample of "10% H₂O+ 90% D₂O" and potato flour) were not able to transform the raw data to continuous relaxation time distribution curve due to high signal-to-noise.

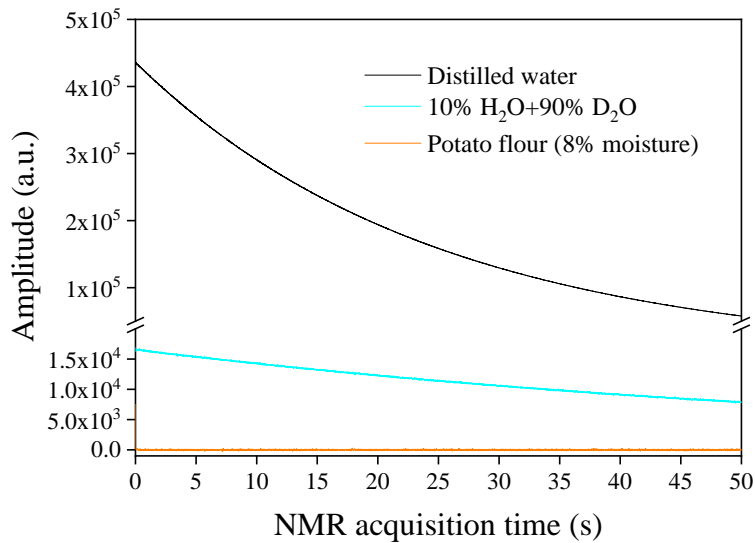


Figure III.5 Raw data of relaxation time of distilled water, the sample of 10% H₂O +90% D₂O, and potato flour.

III.1.1.6 Characterisation of water pools *in tuber*

To identify different water pools *in tuber*, sample sets A and B were carried out:

- sample A. a single component sample of 100% distilled water (W), a raw tuber (T), and the flour-water suspension in the ratio of flour to water at 1:3 and
- sample B. two different potato cultivars with low and high dry matter contents.

Sample A. Whole potato tuber vs potato flour-water system

Exponential decay curves of the raw data (Figure III.6) of the sample set A were transformed to continuous relaxation time distribution curves (Figure III.7) by inverse Laplace transformation. The Lawson and Hanson NNLS analysis method in Prospa©v3.1 (Magritek, 2016) was then used to calculate relaxation time T_2 . Sample set A included distilled water (W), raw potato tuber (dry matter content 23.5%) (T), and potato flour dispersed in water (25%, w/w) (F). The initial amplitude of distilled water, raw potato tuber, and the sample of potato flour dispersed in water were $4.4 \cdot 10^5$ a.u., $3.8 \cdot 10^4$ a.u., and $3.6 \cdot 10^4$ a.u., respectively (Figure III.6). Among these three samples, the initial amplitude of raw data of raw tuber, $3.8 \cdot 10^4$ a.u. and the sample of potato flour dispersed in water, $3.6 \cdot 10^4$ a.u. were very close due to the similar water content.

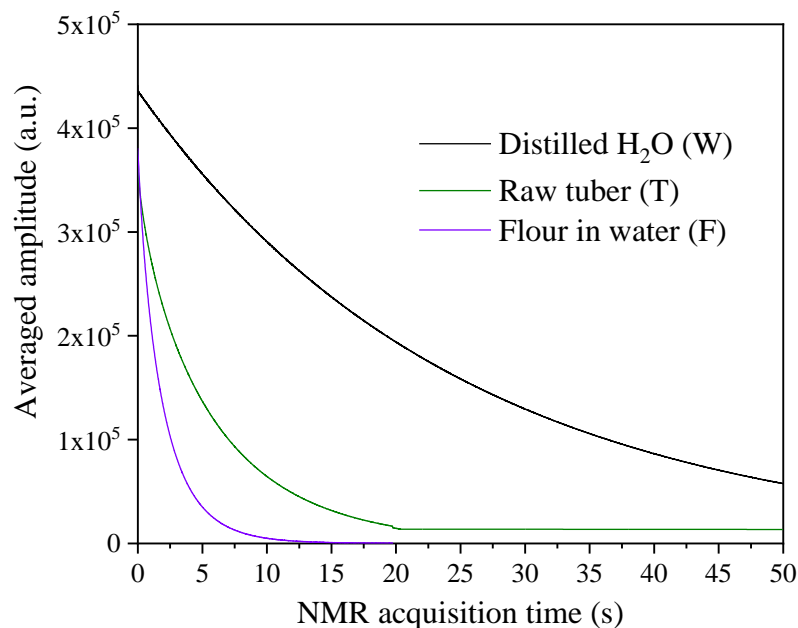


Figure III.6 Raw data of relaxation time of distilled water, raw potato tuber, and raw flour-water suspension (potato flour: water=1:3).

After data transformation, different water pools can be discerned. In distilled water, one sharp peak at relaxation time 2.5s was observed representing the water that can move freely in the glass test tube without any restrictions (Figure III.7). There were four different water pools in raw potato *cv. Agria* (Figure III.7) reflecting different water pools exist various cell compartments. Water pool with relaxation time T_{20} represented the water within starch double helices, while water in amorphous region of amylose and amylopectin were indicated by relaxation time T_{21} . Other water pools at relaxation times T_{22} and T_{23} were the water loosely associated with the starch granule, and the water freely flows within potato tuber cell cytoplasm, respectively (Figure III.7). Different from raw *cv. Agria*, the relaxation time distribution curve of the sample of “raw potato flour dispersed in water” showed only three water pools. This suggested that the water distribution in potato cellular compartments cannot be replicated simply by dispersing raw flour in water with similar water content. Relaxation times T_{20} and T_{21} in potato flour-water system were close to the T_{20} and T_{21} in raw potato tuber (Figure III.7). These tightly bound waters in double helices and amorphous/crystalline regions may not be affected by drying and rehydrating process. The relaxation time T_{22} in the flour-water system was, however, higher than the T_{22} of a raw tuber, exhibiting free movement of water beyond the boundary of the cell wall (Figure III.7). There was thus no relaxation time T_{23} observed in potato flour-water system.

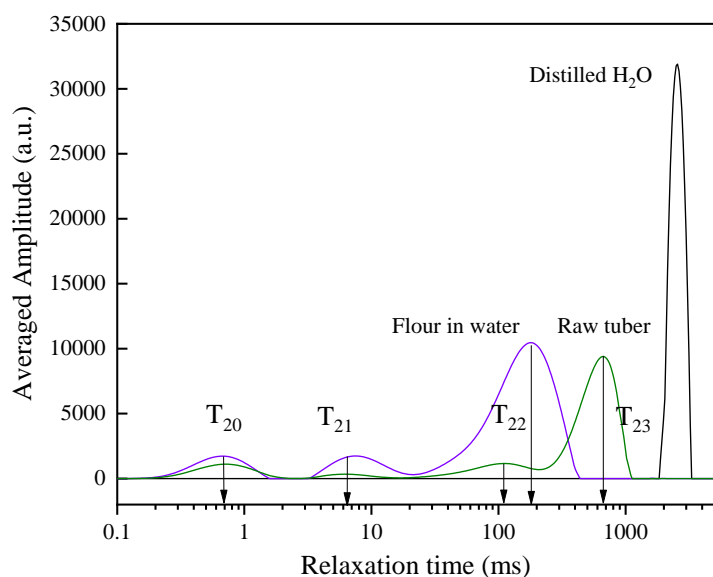


Figure III.7 Relaxation time distribution curves of raw potato flour-water suspension (potato flour: water=1:3), raw potato tuber, and pure water.

Sample B. Potato *cv.* Agria (high dry matter) vs potato *cv.* Nadine (low dry matter)

Dry matter of potato cultivars was negatively correlated to the initial amplitude of relaxation time of the raw data (Hansen et al., 2010). Consistently, the average initial amplitude (M_0) of *cv.* Agria ($3.7 \cdot 10^5$ a.u., $n=3$) was lower than *cv.* Nadine ($3.9 \cdot 10^5$ a.u., $n=3$) attributed to the higher dry matter of *cv.* Agria (22.1 ± 1.4 %) than for *cv.* Nadine (15.7 ± 0.7 %) (Figure III.8). This could be that the higher dry matter of potato *cv.* Agria restrains water mobility resulting in a lower initial amplitude of the raw data (Hansen et al., 2010).

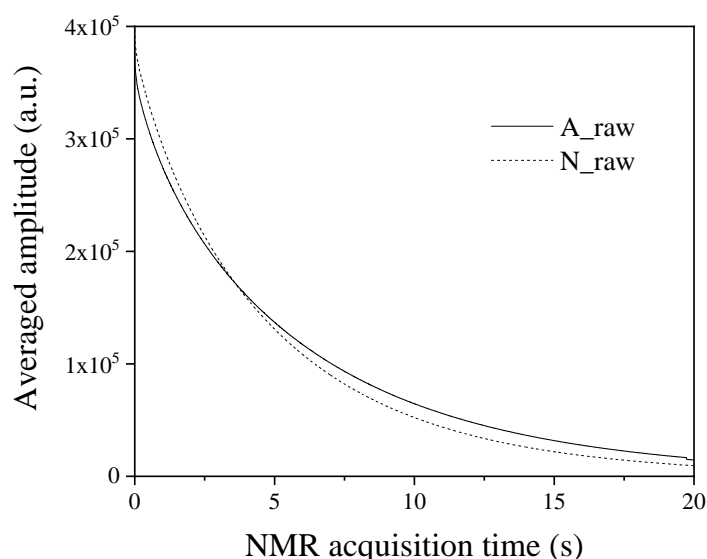


Figure III.8 Raw data of relaxation time of raw potato *cv.* Agria (A) and *cv.* Nadine (N).

Relaxation time T_{20} of raw *cv.* Agria and raw *cv.* Nadine was the same because potato starch is categorised as the B-type crystalline (Figure III.9). The relaxation time T_{21} of raw *cv.* Nadine (8.6 ± 1.2

ms) was significantly higher than for potato *cv. Agria* (6.1 ± 0 ms) ($n=3, p<0.05$). The higher water mobility in crystalline/ amorphous lamella of raw *cv. Nadine* might be due to its higher ratio of amylose to amylopectin ($r= 0.785, p=0.064$) (Figure III.9). The higher amount of amylose in amorphous regions can potentially keep more water in crystalline/amorphous lamella resulting in higher water mobility. While the relaxation time T_{22} of the raw *cv. Agria* (127.1 ± 4.6 ms) was significantly higher than for *cv. Nadine* (92.3 ± 5.0 ms) ($n=3, p<0.05$). Larger starch granules in raw *cv. Nadine* parenchyma cell ($d_{0,5}$ $162.6 \pm 1.8 \mu\text{m}$ compared to the $d_{0,5}$, $58.9 \pm 0.3 \mu\text{m}$ of potato *cv. Agria*) may restrict water movement more than for *cv. Agria*. A negative correlation between T_{22} (by LF NMR) and median diameter of starch granules $d_{0,5}$ ($r=-0.984, p=0.016$) and average diameter of starch granule sizes $d_{3,2}$ ($r=-0.981, p=0.019$) (by Mastersizer) was measured.

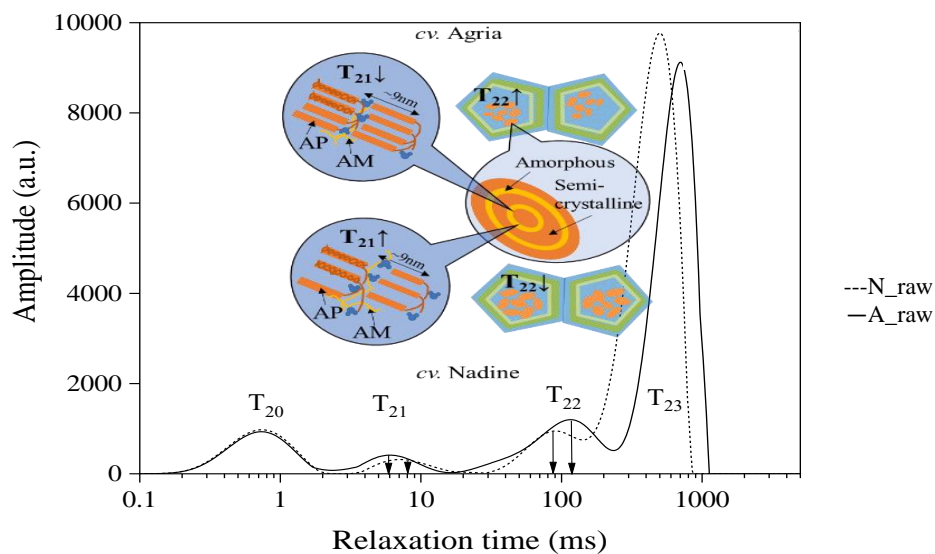


Figure III.9 Relaxation time distribution curves of raw potato *cv. Agria* (A,—) and *cv. Nadine* (N, ---).

III.1.2 Starch digestibility *in tuber* by oral-gastro-small intestinal digestion *in vitro*

Human digestion is a complex process that ingested food is broken into nutrients and used by our body for growth, cell maintenance, and energy source. During human digestion, two main processes occur simultaneously: (i) mechanical size reduction of the food particles; and (ii) enzymatic breakdown of macronutrient into smaller constituents. Food breakdown occurs mostly in the mouth and stomach, whereas enzymatic digestion and absorption of nutrients and water take place mainly in the small and large intestine. Simulated digestion method used in this research consists of oral, gastric and small intestinal phases (Figure III.10) adapted from the previous researches (Bordoloi, Singh, et al., 2012; Tamura et al., 2016) and international consensus (Brodkorb et al., 2019; Minekus et al., 2014).

The purpose is to study the glycaemia responses after consuming starch-based food by mimicking the physiological digestion conditions *in vivo*, taking into account the presence of digestive enzymes and their concentrations, pH, digestion time, and salt concentrations, among other factors. Simulated

digestion methods *in vitro* are less time-consuming, less labour intensive, and no ethical restrictions. This allows a relatively large number of samples to be measured for screening purposes.

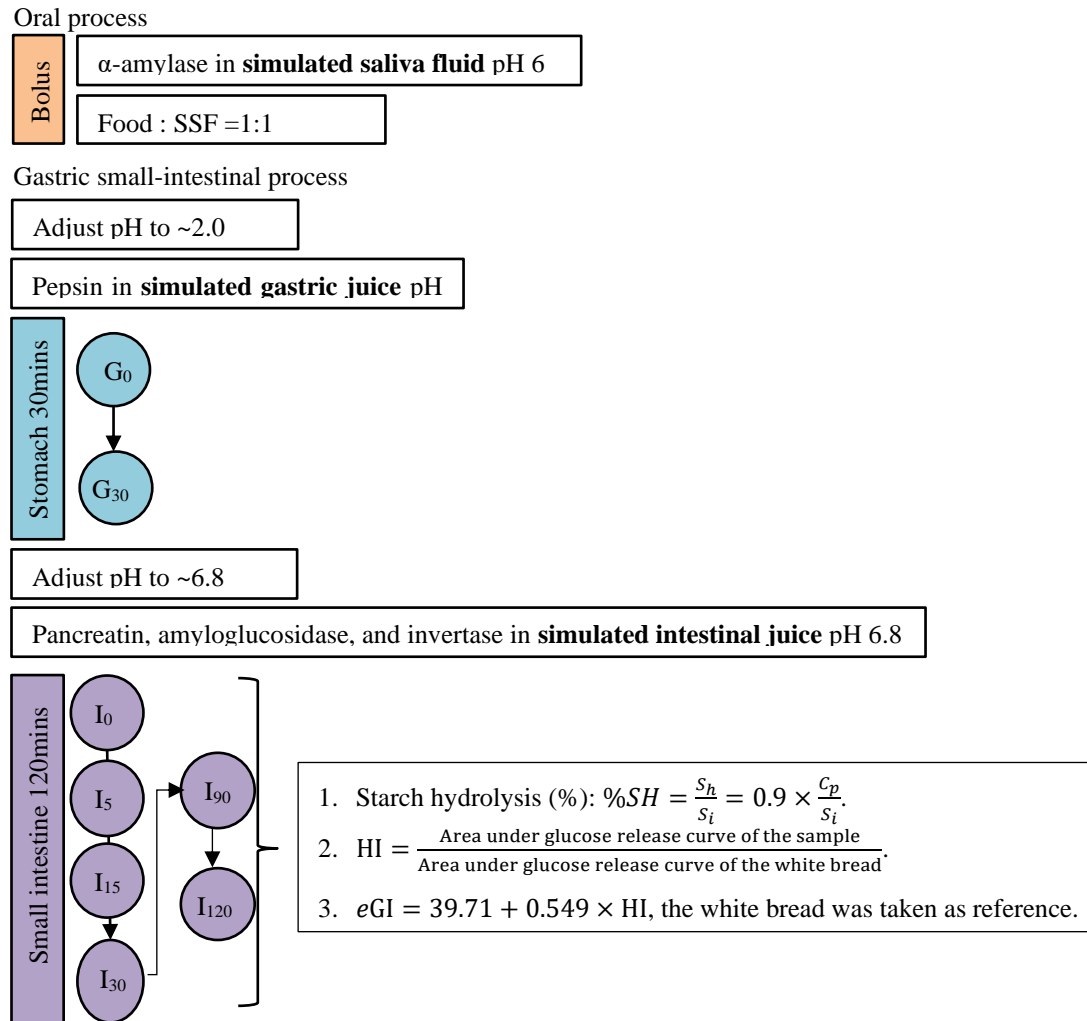


Figure III.10 Diagram of oral-gastric-small intestinal digestion *in vitro*.

III.1.2.1 Sample preparation

Whole fresh tubers (150-200g) were placed individually in a plastic zip bag and cooked at 90°C for 25 minutes. The optimum cooking time was confirmed by a penetration test as described by Bordoloi, Singh, et al. (2012)- an empirical test using skewer to poke through the potatoes. The whole freshly cooked tubers placed singly inside plastic zip were stored in 4°C refrigerator for a certain period of time (depending on the experimental designs of each chapter) to induce starch retrogradation. Following refrigerated storage, the whole tuber was cut into chips of a thickness of 2cm (Figure III.11a). To study the effect of reheating, the samples were reheated at 90°C water bath for 5 minutes (Figure III.11b) based on the time that the core temperature of the potato chip needed to reach 90°C (Figure III.11c).

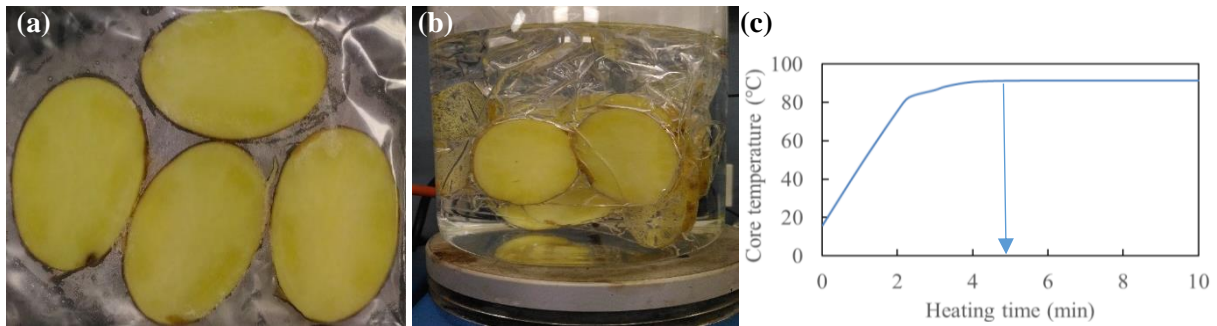


Figure III.11 (a) The 3-day retrograded potato chips before reheating; (b) the 3-day retrograded+reheated (at 90°C) potato chips; (c) the increase in core temperature of a retrograded potato cube (2*2*2cm³) by time during reheating.

III.1.2.2 Simulated oral mastication

Digestion begins with chewing food in the mouth. Mastication reduces particle size and hydrates and lubricates foods by mixing it with saliva. Mouth secretes saliva containing mucus and amylase. Food bolus is formed and travels from the mouth to the oesophagus and to the stomach by peristalsis (Hoebler et al., 2002). Peristalsis describes the contraction of the walls of a flexible conduit, forcing the contents forward (Siddiqui, Provost, & Schwarz, 1991).

Consistency of a food bolus, in terms of both particle size and hydration–lubrication with saliva varies widely depending on the type of food and individuals. Particle size distributions of the ready-to-swallow boluses have been found to be similar within foods of alike physical properties. For instance, particle size distribution curves of boluses of peanuts, almonds, pistachio nuts were similar but differed distinctly from those of foods such as cauliflower, radish, and carrots (Chen, Khandelwal, Liu, & Funami, 2013; Mishellany, Woda, Labas, & Peyron, 2006; Peyron, Mishellany, & Woda, 2004). Interestingly, variations in the particle size distribution of ready-to-swallow boluses between subjects have been regularly reported to be smaller than between foods (Jalabert-Malbos, Mishellany-Dutour, Woda, & Peyron, 2007; Peyron et al., 2004). Within boluses of similar resulting size distribution, they have been discovered to be largely dependent on the different subject with varied chewing time, chewing frequency, vertical and lateral amplitude, jaw velocity and electromyographic activity (Woda, Mishellany, & Peyron, 2006).

To establish a standard procedure of oral digestion for potato tubers, a comparison of chewing by myself and blending by the Minifood processor (Breville, Inc. New Zealand) were conducted (Figure III.12). The 40 grams of potato tuber were chewed by myself till the urge of swallowing and the number of chews were recorded. The ready-to-swallow bolus formed after an average of 20 chews was spat out and was spread on the petri dish for image analysis (Figure III.12a). Similarly, the simulated mastication was carried out by blending the 40g of potato tuber chips with 40g simulated saliva fluid (Minekus et al., 2014), containing α -amylase (*Aspergillus oryzae*, 1.5 U/mg) in the Minifood processor. Different blending times (30s, 1min, and 2min) were tested to test the optimum simulated mastication time (Figure III.12b&c). The boluses from Minifood processor gave a relatively consistent and homogenous

particle size (Figure III.12b&c). Owing to the visual similarity (such as particle size and the form of the boluses) to the human chewing ones, the 2min of blending by Minifood processor with simulated saliva fluid containing α -amylase (Figure III.12c) was, therefore chosen for the oral process.

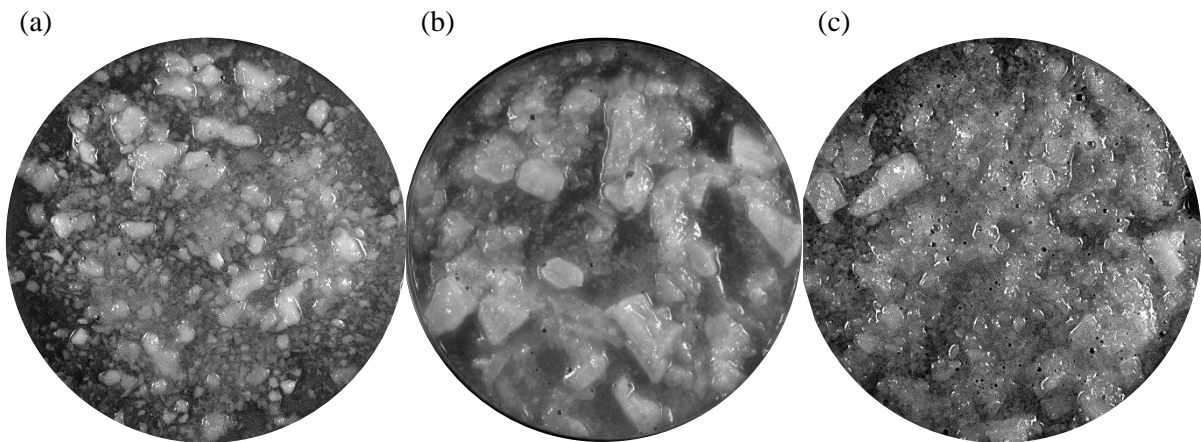


Figure III.12 Cooked potato boluses formed by (a) myself chewing 20 times and by (b) Minifood processor blended for 1min, or (c) for 2min.

Image analysis is a technique where an image of the food bolus is analysed by computer software to evaluate its particle size distribution (Hoebler, Devaux, Karinthi, Belleville, & Barry, 2000; Jalabert-Malbos et al., 2007; Shi, Guan, & Guo, 1990). Food bolus was spread out on a glass petri dish, photographed, digitised and analysed using software ImageJ (Rueden et al., 2017; Schindelin et al., 2012). Irregular shapes can be evaluated by using image analysis, but illuminating particles, such as air bubbles, or the image quality can be troublesome. For instance, the threshold of the background colour can affect how ImageJ defines particles' size, neglecting the overlapped particles or smaller particles (Figure III.13).

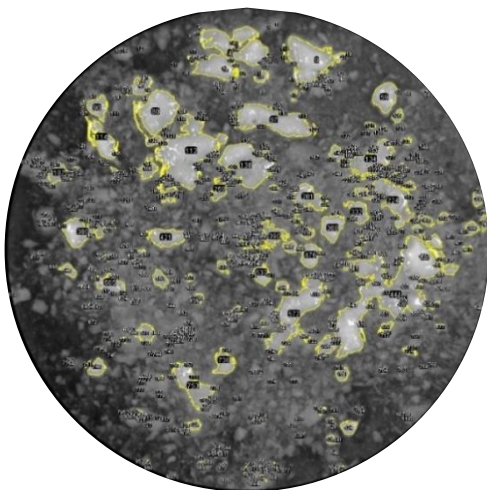


Figure III.13 Bolus particle size analysis by ImageJ.

A Mastersizer uses a laser light diffraction technique to evaluate particle size in a bolus by the diffraction angle as the laser beam interacts with a particle. Particle size distribution curves of boluses formed by chewing and by Minifood processor were shown in Figure III.14. The median diameter ($d_{0,5}$) and the average diameter ($d_{4,3}$ and $d_{3,2}$) of the bolus formed by chewing were 230.7 μm and 243.9 and

55.8 μm , respectively (Figure III.14). While the bolus formed by the Minifood processor had the $d_{0,5}$ at 203.5 μm , the $d_{4,3}$ at 238.8 μm , and the $d_{3,2}$ at 115.2 μm (Figure III.14). The volume of large particles was lower and the volume of small particles was higher in the bolus formed by chewing compared to blending (Figure III.14). Particle size distribution curves of boluses from both chewing and blending showed the bimodal peak (Figure III.14) and were comparable to other mastication results (Hoebler et al., 2000). The Minifood processor has a more consistent mechanical breakdown and, therefore, was chosen to simulate the mastication during the oral process in this research.

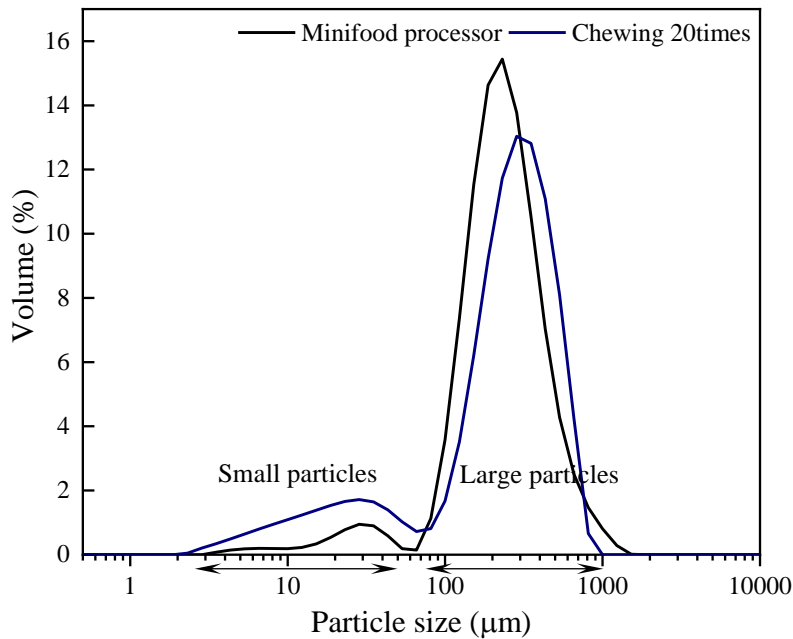


Figure III.14 Particle size distribution of boluses formed by Minifood processor blending and by 20 times of chewing measured by Mastersizer.

III.1.2.3 Gastric-small intestinal starch digestion *in vitro*

A two-stage *in vitro* model was used to represent gastric and small-intestinal digestion. The simulated gastric (SGF) and intestinal (SIF) fluids were prepared in accordance with the US Pharmacopeia (Pharmacopeia U.S, 1995, 2000). After 2min of simulated oral digestion, the bolus mixture was filled up to 170g with distilled water. The 170g of potato digesta samples containing 4% of total starch content was placed in a polyethylene mesh by spatulas to avoid physical damage caused by direct contact with the stirring magnetic bar in the reactor (Figure III.15) (Dhital et al., 2016; Tamura et al., 2016). The jacketed glass reactor was connected to a circulatory water bath to maintain its temperature at $37\pm 1^\circ\text{C}$. The pH was adjusted to 2 and SGF (25 mL) containing pepsin (enzyme/starch (dry weight basis) ratio, 1.765:100, w/w) was added to start the enzymatic hydrolysis. The pH was maintained at 2 ± 0.1 . After 30 min, pepsin was inactivated by increasing pH to 6.8 using 1M NaOH. Small intestine digestion was performed by adding 23ml of SIF containing pancreatin (enzyme/starch (dry weight basis) ratio, 1.3:100, w/w), amyloglucosidase (enzyme/starch (dry weight basis) ratio,

0.26:1, v/w), and invertase (enzyme/ starch (dry weight basis) ratio, 1:1,000, w/w) (Dartois, Singh, Kaur, & Singh, 2010). The pH of mixtures was maintained at 6.8 ± 0.1 .

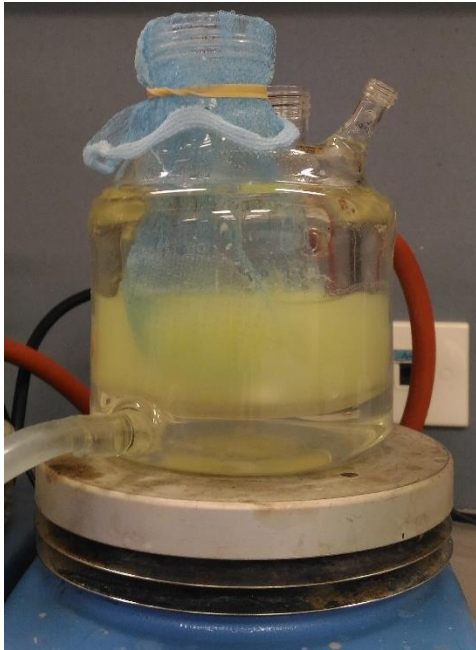


Figure III.15 Starch digestion *in vitro* with digesta placed inside polyethylene mesh.

III.1.2.4 Kinetics of starch hydrolysis, hydrolysis index, and estimated glycaemic index

The 0.5 mL of aliquots were taken at 0 (control) and after 2 minutes of oral step, and then before and after 30 minutes of gastric digestion. During small-intestinal digestion, the 0.5 mL of aliquots were taken at 0 (control) and after 5, 10, 15, 30, 90, and 120 minutes of digestion. All aliquots taken at different digestion stages and times were mixed with 2 mL of 96% ethanol to inactivate enzymatic hydrolysis. All aliquot samples were centrifuge at 1800g for 10 minutes. Afterwards, 0.1 mL of the ethanolic supernatant was transferred to 0.5 mL of amyloglucosidase/invertase in acetate buffer (3.75mg invertase, 0.1 mL amyloglucosidase per 10 mL acetate buffer, pH 5.2) and incubated for 10 min at 37 °C.

The glucose content was analysed by GOPOD (Format K-GLUK 07/11, Megazyme International Ireland Ltd, Ireland). The results were expressed as starch hydrolysis (%) using the following equation:

$$\% SH = \frac{S_h}{S_i} = 0.9 \times \frac{G_p}{S_i}$$

where %SH is starch hydrolysis, S_h is the amount of hydrolysed starch, S_i is the initial amount of starch, and G_p is the amount of glucose produced. A conversion factor of 0.9, calculated from the molecular weight of starch monomer divided by the molecular weight of glucose ($162/180 = 0.9$), was used (Goñi et al., 1997).

A first-order equation model was applied to describe the kinetics of starch hydrolysis:

$$C = C_{\infty}(1 - e^{-kt})$$

where C corresponds to the percentage of hydrolysed starch at time t , C_{∞} is the starch hydrolysis (%) after 2.5 hours of the simulated oral-gastro-small intestinal digestion process, k is the kinetic constant (Goñi et al., 1997). Due to the poor fitting, the kinetics of starch hydrolysis were only assessed in Chapter IV.

The hydrolysis index (HI) of all the samples was calculated as the area under the curves during simulated small-intestinal digestion, using white bread as a reference. And the estimated glycaemic index (eGI) was calculated by the equation $eGI = 39.71 + 0.549HI$ after 120 min of starch hydrolysis (Goñi et al., 1997). The starch hydrolysis (%) was still increasing at 90 min during experimentation so the time point of 120 min was chosen to calculate eGI .

III.1.2.5 Gastric-small intestinal digestion in Human Digestion Simulator

During gastric-small-intestinal digestion in jacketed glass reactor, the digesta placed inside polyethylene mesh is well mixed by a magnetic stirrer. This simplified mechanical force does not reflect the mixing of digesta *in vivo*, so the Human Gastric Simulator (HGS) was trialled to mimic the peristalsis during digestion. In the preliminary experiment, the digesta was exposed to (i) the set pH point of the stomach and small intestine, (ii) the related enzyme activities and concentration, and (iii) the peristaltic forces. Some physiological factors, such as (i) the continuous changes in pH of gastric and small intestinal digestion, (ii) sequential addition of digestive secretions, (iii) gastric and ileal deliveries and transit time, (iv) small-intestinal peristaltic mixing and transport, and (v) passive absorption of water and small molecules were not considered. The complexity of feedback mechanisms, resident microbiota, immune system, or specific hormonal controls involving in human digestion was also simplified in the preliminary experiments.

The Human Gastric Simulator (HGS) (Ferrua & Singh, 2015; Kong & Singh, 2010) used in the preliminary experiment consists of a latex chamber surrounded by a mechanical driving system of four roller sets, effectively emulating the peristaltic movements of human stomach in amplitude, intensity, and frequency. The chamber has a gastric fluid inlet from the top of the latex rubber and a valve at the bottom of the latex rubber to simulate the gastric juice secretion and control gastric empty rate. The temperature of the chamber is controlled at 37°C by a fan (Figure III.16).

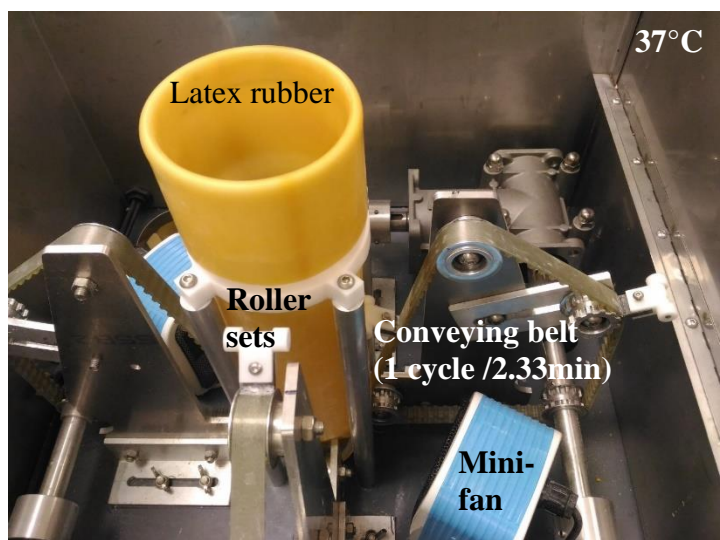


Figure III.16 Elements of human gastric simulator.

In the preliminary experiment of HGS digestion, potato tuber chips (50g) were chewed 20 times by myself. The bolus was spat out and placed inside a net in the latex rubber. The digesta containing 4% of total starch content was then top up to 200ml with distilled water. Due to the capacity of the latex rubber, the total volume of the digesta was increased to 200ml and the ratio of the total starch content to digestive enzymes was kept the same as for jacketed glass reactor. Simulated gastric fluid and simulated small intestinal fluid were adjust proportionally to maintain the same ratio as for the jacketed glass reactor. The temperature of the HGS was maintained at $37\pm 1^\circ\text{C}$. The pH was adjusted and maintained at 2 ± 0.1 . The SGF of 29 mL containing pepsin was added to start the enzymatic hydrolysis. After 60 min of gastric digestion, pepsin was inactivated by increasing pH to 6.8 using 1M NaOH. Small-intestinal digestion was initiated by adding 27ml of SIF and continued for another 180 minutes until the starch hydrolysis (%) reached a plateau (Goebel, Kaur, Colussi, Elias, & Singh, 2019). The pH of mixtures was maintained at 6.8 ± 0.1 . Starch hydrolysis curves of freshly cooked potato tuber conducted in jacketed glass reactor and HGS are shown in Figure III.17. For starch digestion performed in HGS, starch hydrolysis (%) increased gradually and reached 93.8% after 244 minutes of oral-gastric-small intestinal digestion (Figure III.17). The longer period for starch hydrolysis value to reach plateau may be due to the less vigorous mixing in HGS, which provides better mimics of the diffusion of digestive enzymes and hydrolysis of the digesta.

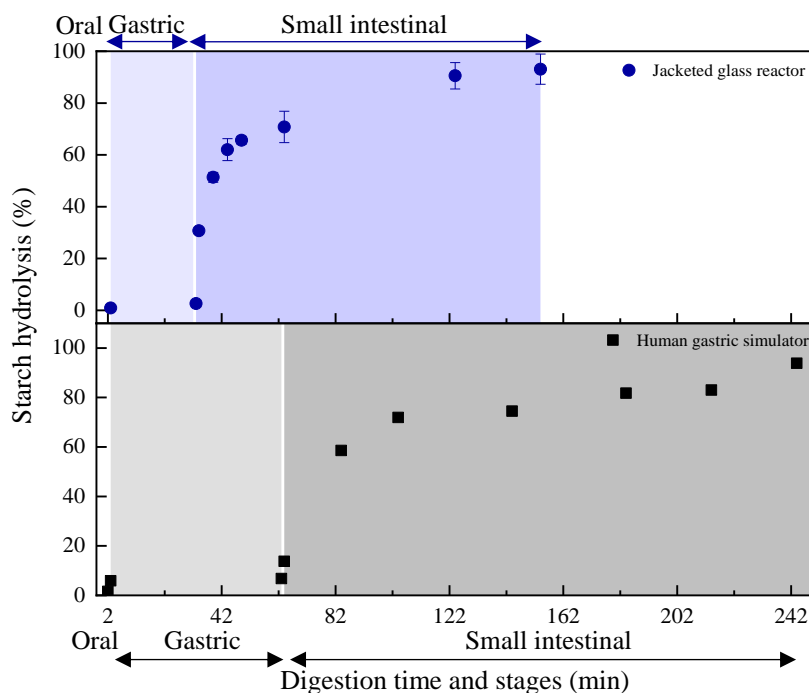


Figure III.17 Starch hydrolysis curves of freshly cooked potato tuber carried out in a jacketed glass reactor (●) in gradient blue areas or in the human gastric simulator (■) in grey areas.

Three-stage oral-gastric-small intestinal digestion *in vitro* was used to analyse starch hydrolysis (%) of retrograded starch *in tuber* in this thesis. The digestion was started with mechanical blending with a food processor to mimic mastication after which further digestion was continued in a “temperature controlled” jacketed glass reactor. Human digestion is rather complex involving peristaltic movement, the physiological factors, and the feedback mechanisms than any *in vitro* static digestion models. This *in vitro* digestion model provides consistent mechanical breakdown force and well-controlled pH during transit, giving repetitive results in triplicate.

III.2 General methods

General methods covered in this section detailed the backgrounds of some analytical methods and preliminary results from microscopy and ATR-FTIR, which were not described elsewhere in the following chapters.

Other methods used commonly to study starch retrogradation in the literature were adapted and are described in the following chapters. Some of these methods, such as Rapid Visco-Analyzer (RVA), X-ray diffraction pattern (X-ray), Fourier transform infrared (FTIR) spectroscopy, and scanning electron microscope (SEM), were limited to the form of samples i.e. dried potato tubers. Freeze-dried and powdered samples were prepared with caution to prevent any possible artefacts. The moisture content of these samples was analysed before every measurement.

III.2.1 Microscopy

Starch microstructure and potato cellular structure in a freshly cooked potato tuber have been evaluated using a number of microscopy techniques (Bordoloi, Kaur, et al., 2012). Microscopic methods involve different sample preparations, which bear advantages and disadvantages. Preliminary experiments were conducted to observe starch granules in a raw tuber under different microscopic methods (Table III.1). The objective of preliminary experiments was to understand and to compare starch granules in the raw potato tissue viewed under different microscopic methods. Sample preparations have mainly been selected to preserve starch granules and cell structure with minimum artefacts. A thin slice, a thickness of 1 μm , of potato parenchyma cell, was taken from the cortex, where starch content has been observed to be more abundant than other crosscut sections (Reeve et al., 1969; Reeve, Hautala, & Weaver, 1970; Reeve et al., 1971).

III.2.1.1 Sample preparation of different microscopic methods

- Light microscope

Thin slices of 1 μm of perimedullary parenchyma of raw potato tuber were mounted onto glass microscope slides, sealed with coverslips, and viewed under an Axiophot light microscope (LM) (Carl Zeiss, Germany). The LM micrographs operating in Differential Interference Contrast (DIC) mode were obtained using the objective of 40x magnification. Representative light micrographs of cell samples were captured using a Leica DFC320 camera equipped with the Leica software application suite LAS V3.8 (Leica Microsystems).

- Confocal laser scanning microscopy

Following the same sampling method as light microscope, thin potato slices were stained with 0.01% acridine orange in 0.1 M phosphate buffer (pH 7) overnight (Adler, Baldwin, & Melia, 1995). The micrographs were collected by confocal laser scanning microscopy (TCS SP5 DM6000B, Leica Microsystems, Wetzlar, Germany). Samples were excited by an Argon laser beam at 488 nm. The emitted lights were then selected by filters to detect starch and cell wall at 530-565 nm. Some other stains that have been used in various studies to observe starch granules and its tissue structures are Safranin O for visualising cell walls and starch (Gray, Kolesik, Hoj, And, & Coombe, 1999; van de Velde, van Riel, & Tromp, 2002) and Acid Fuchsin for protein (Dürrenberger, Handschin, Conde-Petit, & Escher, 2001; Lamberti, 2003).

- Scanning electron microscopy

Scanning electron microscopy (SEM) requires dry samples, and hence samples were frozen by liquid nitrogen then freeze-dried. Freeze-dried samples were coated with a thin layer of conductive silver paint then were deposited with a thin layer of gold by the sputter coating after the silver paint was dried. A thin layer of gold or gold-palladium alloy can prevent charging of the surface promoting the emission

of secondary electrons. It allows the specimen to conduct evenly, providing a homogeneous surface for analysis and imaging.

III.2.1.2 Observation of starch granules in raw potato tubers under different microscopic methods

Three-dimensional structures of potato cells were revealed in CLSM and SEM micrographs, while LM offered two-dimensional images. Informative micrographs displaying different structural aspects of potato tissue were studied by LM, CLSM, and SEM and principles of these microscopic methods are provided in Table III.1. LM provides the image of starch granules in the confined boundary of cell walls in Table III.1a. In CLSM and SEM micrographs, starch granules and cell walls are observed in Table III.1b and c.

Starch granules were unevenly distributed both within and between cells (Table III.1), and not all cells contained starch granules, a result found regardless of the microscopic method used. The presence of starch deficient cells could be artefacts from sample preparations, but was observed almost by all methods, including CLSM where water was not removed and samples were sectioned optically on the on-focus focal plane (Table III.1b). It could be that there are cells in all crosscut sections of the tuber that do not contain any starch granules, although most starch deficient cells have been found in pith tissue (Reeve et al., 1969). Nevertheless, some of these empty cells may be the results of preparation. For instance, sample preparation of LM and CLSM can preserve most of the starch granules within the cell structure, whereas sample preparation of SEM, such as freeze-drying and cutting, may cause the loss of starch granules. Some clusters of starch granules covered by cell walls in raw potato tuber can be observed under CLSM and SEM in Table III.1b and Table III.1c. Starch granules as studied by SEM generally display a smooth surface with some cell components/fragments attached to the cell and surface of starch granules (Table III.1c). These cell components/fragments could be artefacts either from the amyloplast membrane or from ruptured cell walls.

Following chapters focused on structural changes of potato tubers (such as cell separation and starch matrix within cells) during cooking, cooling and storage. In combination with other measurements in each chapter, a better understanding of microstructural changes was obtained. For example, the starchy matrix that filled up the cell space with thinner cell walls shown by CLSM concurred with the decrease in hardness in cooked potato tubers (owing to starch gelatinisation and loss of turgor pressure) (Chapter V).

Table III.1 Microstructure of raw potato tuber observed by (a) light microscope (LM), (b) confocal laser scanning microscope (CLSM) and (c) scanning electron microscopy (SEM) with a comparison of selected features of each microscope technique.

	(a) LM	(b) CLSM	(c) SEM
Principles			
Raw potato cells			
Smallest resolvable size, nm	100	100	10
Overall structure	+	+++	++
Starch distribution	+	+++	++
Starch granules	+++	+++	+++
Cell shape	+	+++	++
Cell walls	+	+	++

*Observation of microstructure analysis of potato tissue samples in relative to each other on a scale from + + + (excellent) to + (normal).

III.2.2 ATR-FTIR

III.2.2.1 Theoretical background

The FTIR equipment located in Science Tower A is equipped with attenuated total reflectance (ATR). For transmission FTIR, the sample embedded in KBr pellet is placed in the path of the IR beam and the resulting transmitted IR signal is recorded by the detector (Figure III.18a). The KBr is used as the background matrix because it is IR transparent. To obtain the resulting peak absorbance between 0.2 to 0.7 units, estimating the optimum sample size in KBr pellet is particularly a challenge. Additionally, the sample must be translucent because the thickness of KBr pellet is limited to 0.5-1 mm to allow sufficient light to pass through and to reach the detector. In ATR-FTIR, unlike transmission FTIR, IR radiation is not transmitted through the sample, and thus the sample does not need to be prepared as a thin pellet (Figure III.18b). The incorporation of the ATR prism improves the signal-to-noise ratios of FTIR spectra (Li, Fredericks, Rintoul, & Ward, 2007).

In ATR mode, an IR beam traverses a prism wherein contact with the sample as it reflects internally in the prism (Figure III.18b). The condition for total internal reflection to occur is when $\sin \theta_i > n_2/n_1$, where θ_i is the angle of incidence on the prism, n_1 is the index of refraction of the prism material, and n_2 is the index of refraction of the sample. Due to its wave, the light is not reflected directly on the boundary surface but by a virtual layer within the optically less dense sample (Goos-Hänchen effect). The fraction of the light wave that reaches into the sample is called the evanescent wave (Figure III.18b). In those spectral regions where the sample absorbs energy, the evanescent wave will be attenuated. After one or several internal reflections, the IR beam exits the ATR prism and is directed to the detector.

The intensity of the absorption depends on the good contact between the sample and the prism, as well as the penetration depth of the evanescent wave. The penetration depth depends on the wavelength, the refractive indices of prism n_1 and sample n_2 , and the angle of the entering light beam θ_i . The depth of penetration (d_p) is, therefore defined as the distance at which the field is reduced by a factor of $1/e$, and is expressed as:

$$d_p = \frac{\lambda}{2\pi n_1 \sqrt{\sin^2 \theta_i - \left(\frac{n_2}{n_1}\right)^2}}$$

where λ is the wavelength of the incident wave, θ_i is the incident angle, n_1 and n_2 are the refractive indices of the ATR prism and the sample (Harrick & Beckmann, 1974). The infrared beam enters the ATR prism at a typical angle θ_i of 45° . Taking $n_1=2.4$ (diamond in this case) for ATR crystal and $n_2 \sim 1.5$ (organic substances generally range from ca. 1.2 to 1.5), the relation can be simplified to: $d_p \sim 0.2 \lambda$.

Penetration depth is directly related to the wavelength; the higher the wavelength, the greater the penetration depth. Polysaccharides, like starches, absorb infrared in the region of $1200 \sim 800 \text{ cm}^{-1}$ (i.e. at wavelength between ~ 8 and $12 \mu\text{m}$). In this region, the average penetration depth is $\sim 2 \mu\text{m}$ (Sevenou, Hill, Farhat, & Mitchell, 2002a). This penetration depth is smaller than the average diameter $d_{3,2}$ of

starch granules, such as it is 13.0 μm for corn starch and 43.0 μm for native potato starch. The ATR-FTIR technique, therefore, measures the overall alignment of growth rings since a unit of the alternative lamellae of semi-crystalline and amorphous (lamellar spacing d) is generally around 0.01 μm (Jane, 2006).

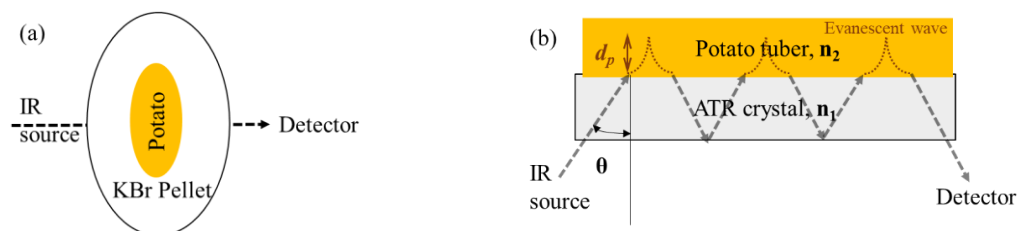


Figure III.18 Schematics of (a) transmission FTIR and (b) attenuated total reflectance (ATR)-FTIR.

III.2.2.2 FTIR spectra of starch in raw potato tuber

FTIR spectra of freeze-dried and powdered raw potato *cv. Agria* were obtained using a Nicolet 5700 spectrometer equipped with a Smart iTR™ Attenuated Total Reflectance (Thermo Electron Scientific Instruments Corp., Madison, WI USA). Samples were scanned from 4000 to 400 cm^{-1} with a spectral resolution of 4 cm^{-1} and 64 co-added scans were made per sample to acquire each spectrum (Figure III.19a). A background spectrum was used as a reference. Spectrum of raw potato tuber was baseline-corrected over the range of 1200 and 800 cm^{-1} (Figure III.19b) and was self-deconvoluted by Happ-Genzel apodization (Bretzlaff & Bahder, 1986; Cameron & Moffatt, 1984; Kauppinen, Moffatt, Mantsch, & Cameron, 1981) with a bandwidth of 38 cm^{-1} and a resolution enhancement factor of 2.1 (Figure III.19c) using Omnic software (Wang, Wang, Wang, & Wang, 2017). IR absorbance values at 1047 and 1022 cm^{-1} were extracted from the spectrum after baseline correction and deconvolution (Figure III.19c).

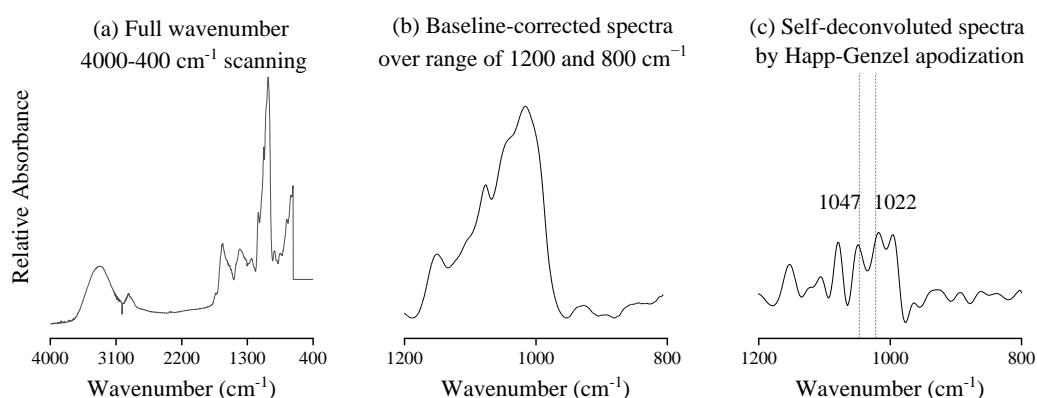


Figure III.19 FTIR spectra of raw potato *cv. Agria*.

The FTIR spectra of the freeze-dried and powdered raw potato *cv. Agria* and *cv. Nadine* ranged from 4000-800 cm^{-1} are shown in (Figure III.20). Both samples showed adsorption bands in three main regions 3700-3000 cm^{-1} , 1700-1200 cm^{-1} , and 1200-1000 cm^{-1} indicating the composition of water, protein and

lipid, and starch, respectively (Figure III.20). The major absorption bands observed in the region of 1200-1000 cm^{-1} was due to the stretching of C-O and C-C bonds and the stretching and bending of C-O-H bond of starch molecules (Cael, Koenig, & Blackwell, 1973; Warren, Gidley, & Flanagan, 2016). The overlapped FTIR spectra of the two cultivars indicated similar chemical compositions, except the amount of starch content and amylose content.

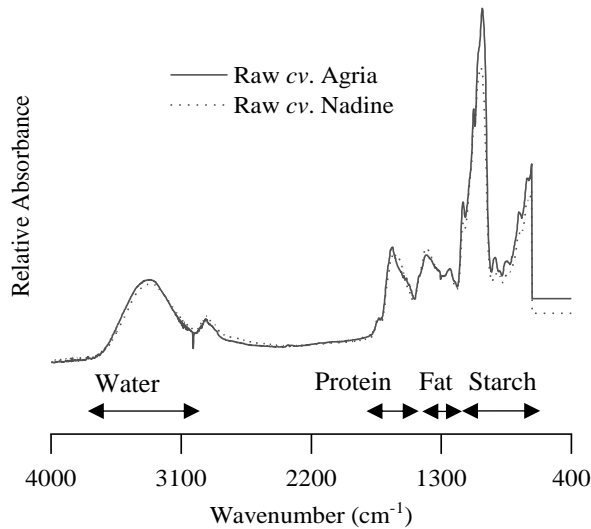


Figure III.20 FTIR spectra of freeze-dried and powdered raw potato *cv. Agria* and *cv. Nadine* over wavenumber 4000-400 cm^{-1} .

FTIR has been shown to be able to detect double-helical order or the so-called short-range order in starches (Goodfellow & Wilson, 1990; Wilson et al., 1991). The IR bands at 1047 and at 1022 cm^{-1} were shown to be associated with the ordered and amorphous structures of starch, respectively (Capron et al., 2007; Sevenou, Hill, Farhat, & Mitchell, 2002b; Van Soest et al., 1995). The ratio of the absorbance at 1047 cm^{-1} to 1022 cm^{-1} from the deconvoluted FTIR spectrum was used to express the amount of ordered crystalline to amorphous domains in starches (Figure III.21). The order of double helices on the surface of starch granules was lower in *cv. Agria* than in *cv. Nadine* as evidenced by the values of 1047/1022. The significantly different in the value of 1047/1022 ($n=3$, $p<0.05$) between raw *cv. Agria* and *cv. Nadine* suggested the different alignments of double helices in these two cultivars. This could be that amylose, distributed primarily close to the surface of the starch granules (Jane & Shen, 1993), disrupts the ordered double-helical amylopectin on the surface of *cv. Agria*. A positive correlation was, however, obtained between the value of 1047/1022 and the ratio of amylose to amylopectin ($r=0.909$, $p=0.033$), this could be that the value of 1047/1022 only represents the local/surface alignment while the value of AM/AP indicates the overall composition.

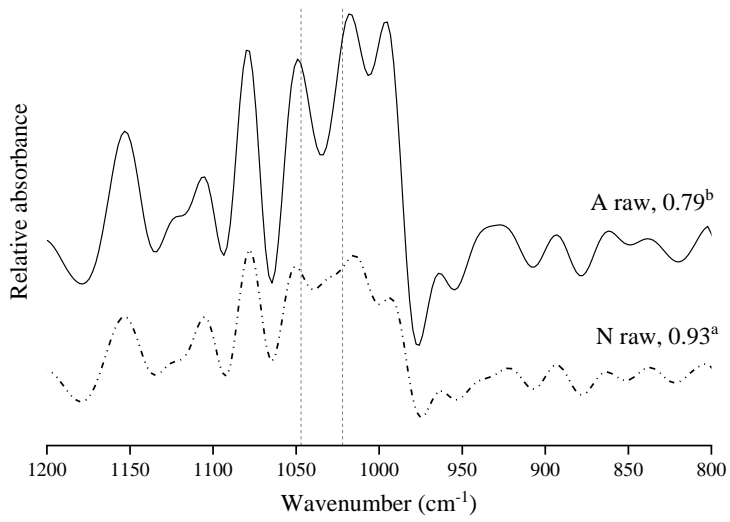


Figure III.21 Deconvoluted FTIR curves of freeze-dried and powdered raw potato *cv.* Agria, A_{raw} and *cv.* Nadine, N_{raw} . The values represented the 1047/1022 of each sample and different superscripts indicated significant differences ($n=3, p<0.05$).

Chapter IV Potato starch retrogradation *in tuber*: structural changes and gastro-small intestinal digestion *in vitro*

IV.1 Introduction

Potato, *Solanum tuberosum*, ranks fourth among world staple crops and contains many nutrients such as starch, proteins, lipids, minerals and vitamins (Hiele, 1959). Most of the starch in potatoes is reserved as a discrete granule in parenchyma cells near the vascular ring. These granules are oval in shape and range from 5 to 100µm long (Fedec, Oraikul, & Hadziyev, 1977). Besides being processed into raw ingredients like flour or isolated starch, potatoes are also made into crisps, mashed potato and frozen potato chips. Heating is an essential unit operation that brings desired sensory attributes to potato products. Hence textural characteristics and microstructural changes after cooking have been well investigated (Bordoloi, Kaur, et al., 2012). Due to increasing occurrence of obesity, the glycaemic index (GI) of starchy foods has gained a lot of attention recently and many groups have studied how different preparation methods affect starch digestibility in foods (Colussi et al., 2017; Foster-Powell, Holt, & Brand-Miller, 2002; Raatz, Idso, Johnson, Jackson, & Combs, 2016; Tian et al., 2016).

Cooking causes potato cell separation because pectic polysaccharides are solubilized or degraded; starch granules lose birefringence and crystallinity as temperature increases above the transition temperatures (Cooke & Gidley, 1992; Goesaert et al., 2005b). The loss of crystallinity in starch granules and the change of water distribution in potato tissue may cause the potato tubers to become less resistant to enzymatic digestion (Bordoloi, Singh, et al., 2012; Farhat et al., 2001). Simultaneously the interaction between the OH groups of starch and the protons in water molecules permit adjustment of the hydrogen bonding networks (Mortensen et al., 2005). With subsequent cooling, the disrupted amylose and amylopectin chains gradually re-associate and aggregate which is called retrogradation. The reorganised structure shows an increased transition temperature and relative crystallinity comparing to freshly gelatinised starch (Karlsson & Eliasson, 2003b; Tian et al., 2016). As a result, the digestibility of retrograded starch decreases because the aggregation of melted amylose and amylopectin upon cooling and storage makes them less accessible to digestive enzymes (Chung et al., 2010; Hu, Xie, et al., 2014).

The glycaemic properties of starch depend strongly on the starch structure set by processing during manufacture (García-Alonso & Goñi, 2000). Based on the kinetics of glucose release during digestion starches are divided into rapidly digestible starch (RDS), slowly digestible starch (SDS) and resistant starch (RS) fractions. Some starches can be modified to slowly digestible starch that can escape digestion and adsorption in the small intestine. Retrogradation of starch paste has been shown to lower the digestibility of the starches within (Colussi, Singh, et al., 2017; Hu, Huang, et al., 2014; Hu, Xie, et

al., 2014; Tian et al., 2016; Xie, Hu, Jin, Xu, & Chen, 2014; Zhou & Lim, 2012). Several studies have been reported on isolated starches but not much information is available on starch retrogradation *in tuber* i.e. within cooked potatoes. Starch retrogradation *in tuber* is rather more complex, hence it is important to form a better understanding of mechanisms of structural change from the starch molecular level to potato tuber cells during cooking, cooling and reheating and their effect on the starch digestibility. We studied the influences of various storage periods and reheating temperatures to investigate how the structural changes associated with changes in physical properties of starch such as pasting profile, thermal characteristics, relative crystallinity, and water mobility within potato tubers and whether these result in different starch digestibility. We have used a gastro small-intestinal digestion model *in vitro* for this purpose.

IV.2 Materials and methods

IV.2.1 Materials and sample preparation

In season *cv.* Agria tubers of uniform size (120-150g) were purchased from a local supermarket. Potato tubers were put in the same zip bag throughout the cooking, cooling and reheating process to prevent moisture loss. The tubers were then cooked in a water bath at 90°C for 25 minutes to yield the freshly cooked tubers, (FC), and cooled in a 4°C refrigerator for 1, 3, and 7 days (giving retrograded tubers, FCR1, FCR3, and FCR7). The whole retrograded tubers, FCR1, FCR3 and FCR7 were cut into chips with 2cm thickness and were reheated for 5 minutes at 50°C (to give retrograded+reheated tubers FCR1-r50, FCR3-r50, and FCR7-r50), or 70°C (FCR1-r70, FCR3-r70, and FCR7-r70), or at 90°C (FCR1-r90, FCR3-r90, and FCR7-r90). The dry matter content of the tubers was determined by the AOAC 934.01 method (AOAC, 1990)- a 2.5g of fresh tuber was placed in 105°C overnight, then was left in the desiccator till constant weight is achieved. Samples were freeze-dried to measure the total starch content, pasting properties, thermal characteristics, and relative crystallinity. The total starch content was determined by a total starch assay kit (K-TSTA 07/11, Megazyme International, Ireland). Pepsin (porcine gastric mucosa, 800–2500 units/mg protein), pancreatin (hog pancreas, 4 × USP), and invertase (Invertase, grade VII from baker's yeast, 401 U/mg solid) were purchased from Sigma–Aldrich Ltd. (St Louis, USA). Amyloglucosidase (3260 U/ml) was purchased from Megazyme International Ireland Ltd. (Ireland).

IV.2.2 Pasting properties

The pasting profiles of ground freeze-dried tuber samples were obtained using a Rapid Visco-Analyzer (RVA, Newport Scientific, Sydney, Australia) with the 7.7 RVATM Potato Starch Method (2.0 g starch and 14% moisture basis) (AACCI Method 76-21.01, 1996; Colussi, Singh, et al., 2017). The sample was equilibrated at 50 °C for 1 minute, heated and held at 95 °C for 3 minutes, and then cooled and held at 50 °C for 2 minutes, with the rotational speed maintained at 160 rpm throughout the

whole process. Parameters including peak viscosity (PV), viscosity at the end of hold time at 95 °C or hot-paste viscosity (HPV), final viscosity (FV) at the end of cooling, breakdown (BD=PV-HPV), setback (SB=FV-HPV) and pasting temperature were recorded. All the measurements were done in triplicate.

IV.2.3 Thermal characteristics

The freeze-dried samples were mixed with distilled water in mass ratio 1:2 and the endothermic curves obtained by scanning from 20°C to 100°C at a rate of 10°C per minute (Tzero Pan and Tzero Hermetic Lid, TA Instruments, New Castle, USA). To determine the dry matter content, the pan was pierced with a hole and placed in an oven at 105°C for 24 hours. The thermal transition temperature (T_c-T_o) and the enthalpy of starch retrogradation (ΔH_R , expressed as J/g dry matter) were determined by TA Universal Analysis 2000 software supplied with the equipment. All measurements were done in triplicate.

IV.2.4 Relative crystallinity

X-ray diffractograms of the freeze-dried samples were obtained using a GBC® eMMA X-ray Diffractometer (GBC, VIC, Australia) (Colussi, Singh, et al., 2017). The scanning region for X-ray diffraction 2θ ranged from 4° to 40° at a target voltage of 35 kV, a current of 28.2 mA, and a scan speed of 1° per minute. The relative crystallinity (RC) was calculated by the equation $RC (\%) = (A_c / (A_c + A_a)) \times 100$, where A_c and A_a represents crystalline and amorphous areas, respectively.

IV.2.5 Water mobility

The freshly cooked (FC), retrograded (FCR), and retrograded+reheated (FCRr) tubers were cut longitudinally by cork borer with caution to minimize incorporating material from the core and stem end. The raw potato cylinder so formed had dimensions of $\varnothing 3.4 \times 80$ mm (approximately 0.5 g) and was inserted into a glass tube (5 mm O.D. WG-5MM-ECONOMY-7 Wilmad-LabGlass) and sealed to prevent moisture loss during cooking, cooling and reheating. The relaxation times of retrograded potato cylinders were measured after cooling and storing at 4°C fridge for an hour (FCR0.04), a day (FCR1), 3 days (FCR3), and 7 days (FCR7). Before every relaxation time measurement, all samples were equilibrated at 25°C.

The LF-NMR proton relaxation time measurements were performed by a Spinsolve 1.5 LF-NMR spectrometer (Magritek Ltd.) with operating resonance frequency at 42.5 MHz. The transverse relaxation time T_2 was acquired by the Spinsolve® Carbon apparatus' built-in T_2 bulk function using the Carr-Purcell-Meiboom-Gill sequence (CPMG) (Carr & Purcell, 1954; Meiboom & Gill, 1958). The CPMG sequence had a one-millisecond pulse separation and was fitted logarithmically in the relaxation time distribution from 0.1 to 5000 milliseconds with 5000 data points collected (Assifaoui et al., 2006; Rondeau-Mouro et al., 2015). The recycle delay time was 7 seconds. The exponential decay curve of

each relaxation time measurement was the result of the accumulation of 4 scans to increase the signal-to-noise ratio (Ward, 2011). An exponential decay curve of the raw data was transformed to a continuous relaxation time distribution curve by inverse Laplace transformation. Then the Lawson and Hanson NNLS analysis method in Prospa©v3.1 (Magritek, 2016) was used to calculate relaxation time T_2 . All measurements were done in triplicate.

IV.2.6 Starch digestion *in vitro* and its kinetics

A two-stage starch gastro-small intestinal digestion *in vitro* model was used to investigate starch hydrolysis (%) (Dartois et al., 2010). The simulated gastric fluids (SGF) and simulated intestinal fluids (SIF) were prepared in accordance with the US Pharmacopeia (Pharmacopeia U.S., 1995, 2000). Samples (170g) of freshly cooked, retrograded and retrograded+ reheated tuber containing 4% of total starch were placed in a polyethylene mesh to avoid physical damage from the magnetic stirring bar in the jacketed glass reactor. The glucose content released during digestion *in vitro* was analysed by GOPOD reagent (Format K-GLUK 07/11, Megazyme International Ireland Ltd, Ireland) and the results were expressed as starch hydrolysis (%) (Tamura et al., 2016).

The hydrolysis index (HI) of the samples was calculated as the area under the curves during simulated small intestinal digestion, using white bread as a reference taken from literature (Goñi et al., 1997). And the estimated glycaemic index (*eGI*) was calculated by the following equation (Goñi et al., 1997): $eGI = 39.71 + 0.549HI$. All measurements were done in triplicate. Parameter estimation was carried out using Origin® 2017.

IV.2.7 Microstructural characteristics of digesta

A thin potato slice (~1mm thickness) was cut from the parenchyma region of freshly cooked (FC), the 3-day retrograded (FCR3), and the retrograded+reheated (FCR3-r90) potato tubers for confocal microscopy (TCS SP5 DM6000B, Leica Microsystems, Wetzlar, Germany), under illumination with the Ar laser ($\lambda = 488$ nm). The sample was stained with 0.01% acridine orange in 0.1M phosphate buffer. Then simulated intestinal fluid (SIF) was added to the curved glass slide and coverslip applied. The concentration of SIF was kept at the same ratio as used during gastro- small intestinal starch digestion *in vitro* experiments. The images were taken before (T_0) and after adding the simulated intestinal fluid and incubating for 5 minutes (T_5), 10 minutes (T_{10}), and 30 minutes (T_{30}). The representative digital images were analysed by Image J software (Rasband, 1997).

IV.2.8 Statistical analysis

The results were calculated as means \pm one standard deviation from three replicates. Subsequently, an analysis of variance (ANOVA) with Tukey's test was used to determine significant differences among the means at a significance level of $p < 0.05$ by Origin® 2017. The data were subjected to

correlation analysis and Pearson correlation coefficients were calculated by Minitab Statistical Software version 13 (Minitab, Inc., State College, PA).

IV.3 Results and discussion

IV.3.1 Pasting profile

The pasting profile of the retrograded samples (FCR1, FCR3, and FCR7) and the retrograded+reheated samples (FCR1-r90, FCR3-r90, and FCR7-r90) are shown in Figure IV.1. The viscosity development of a starchy matrix is dependent on the thermal treatment due to the starch structural changes such as leaching of amylose and the formation of a tightly packed array of melted amylose and amylopectin (BeMiller & Whistler, 2009; Jacobs, Eerlingen, Clauwert, & Delcour, 1995). Prolonging retrogradation significantly increased the pasting temperature of the retrograded samples from $62.78^{\circ}\text{C} \pm 0.03^{\circ}\text{C}$ (FCR1) to $66.13^{\circ}\text{C} \pm 2.18^{\circ}\text{C}$ (FCR7) ($n=3$, $p<0.05$) (Figure IV.1a). This may indicate that the regional crystallinity of melted amylose and amylopectin increased and hence more heat was needed for structural disruption and paste formation (Perdon, Marks, Siebenmorgen, & Reid, 1997; Zhou, Robards, Helliwell, & Blanchard, 2002). The peak viscosity and hot paste viscosity of the retrograded samples (Figure IV.1a), and the retrograded+reheated samples (Figure IV.1b) decreased with increasing retrogradation. This indicated a denser structure of FCR7 which may not imbibe as much water as FCR1. The breakdown viscosity of the retrograded samples (FCR1, 937 cP; FCR3, 582 cP; and FCR7, 709 cP) was higher than for the retrograded+reheated samples (FCR1-r90, 323 cP; FCR3-r90, 351 cP; and FCR7-r90, 63 cP). The viscosity of the retrograded sample decreased more after the maximum viscosity was reached than it did for other samples. The retrograded sample may have been able to absorb more water than the retrograded+reheated samples (Adebowale & Lawal, 2003a). The change in viscosity during cooling of a paste due to re-association of the melted starch molecules is called setback viscosity. The setback viscosities of retrograded+reheated samples (FCR1-r90, 291 cP; FCR3-r90, 223 cP; and FCR7-r90, 103 cP) (Figure IV.1a) were lower than for retrograded samples (FCR1, 487 cP; FCR3, 370 cP; and FCR7, 331 cP) (Figure IV.1a) which indicated less aggregation happened for amylose and amylopectin. This may be due to the reheating process having broken the melted amylose and amylopectin to even smaller fragments ($\text{DP}<14$) that did not favour retrogradation (Shi & Seib, 1992).

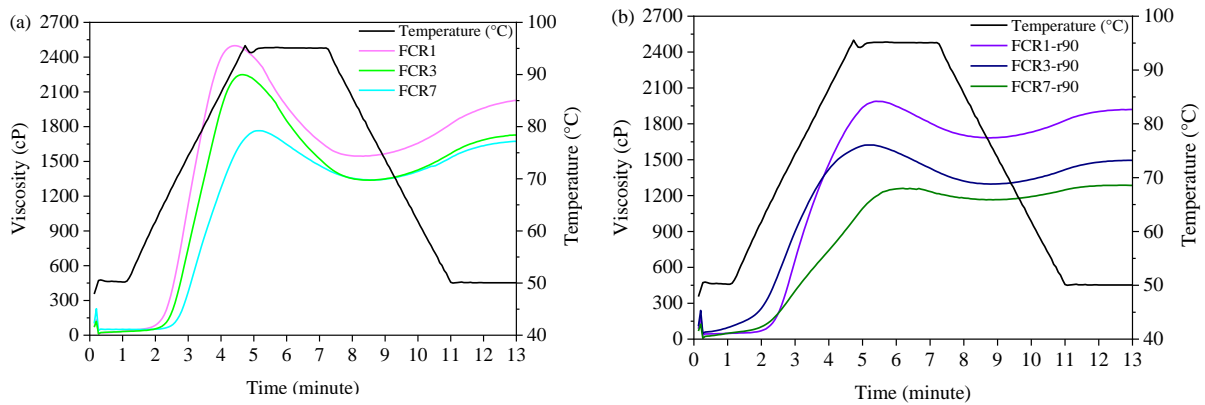


Figure IV.1 The pasting profiles of (a) the 1, 3, and 7-day retrograded samples (FCR1, FCR3, and FCR7) and (b) the retrograded+ reheated samples (FCR1-r90, FCR3-r90, and FCR7-r90) (n=3).

IV.3.2 Thermal characteristics

Cooking, cooling and reheating changed the structure of starch to different degrees resulting in different endothermic profiles (Figure IV.2) and thermal characteristics (Table IV.1). The endothermic peak of raw potato tuber (Raw) diminished after gelatinisation (FC) and slightly reappeared after retrogradation (FCR3) (Figure IV.2). The onset temperature (T_o) of the freshly cooked samples (FC), retrograded samples (FCR1, FCR3 and FCR7) and retrograded+reheated samples (FCR1-r90, FCR3-r90, and FCR7-r90) ranged from 43.5°C to 46.2°C with only FCR1-r90 and FCR7-r90 being significantly different (Table IV.1). The peak temperature (T_p) of the retrograded samples (FCR) showed a higher value than the freshly cooked samples (FC) and the retrograded+reheated samples (FCRr) because of the aggregation of disrupted starch in the retrograded samples (Table IV.1). The conclusion temperature (T_c), as well as the endothermic range (T_c-T_o) of retrograded samples (FCR1, FCR3, and FCR7), were significantly higher than for the freshly cooked samples (FC) or for the retrograded+reheated (FCR1-r90, FCR3-r90, and FCR7-r90) samples. But the T_c and T_c-T_o were not significantly different between the freshly cooked sample (FC) and the retrograded+reheated samples (FCRr) (Table IV.1). Retrogradation properties were studied by analyzing the melting endotherm (ΔH_R) of recrystallized amylose and amylopectin. The enthalpy (ΔH_R) of the 3-day retrograded samples (FCR3) were the highest while the enthalpy (ΔH_R) of the freshly cooked sample (FC) and the retrograded+reheated samples (FCR1-r90, FCR3-r90, and FCR7-r90) were not statistically different from each other (Table IV.1). The higher ΔH of retrograded samples suggested the starch molecules were realigned into more ordered structures (Tian et al., 2016). Therefore, the enthalpy of retrograded+reheated samples (FCR1-r90, FCR3-r90, and FCR7-r90) was lower because the retrograded structure may have melted again during reheating (Table IV.1).

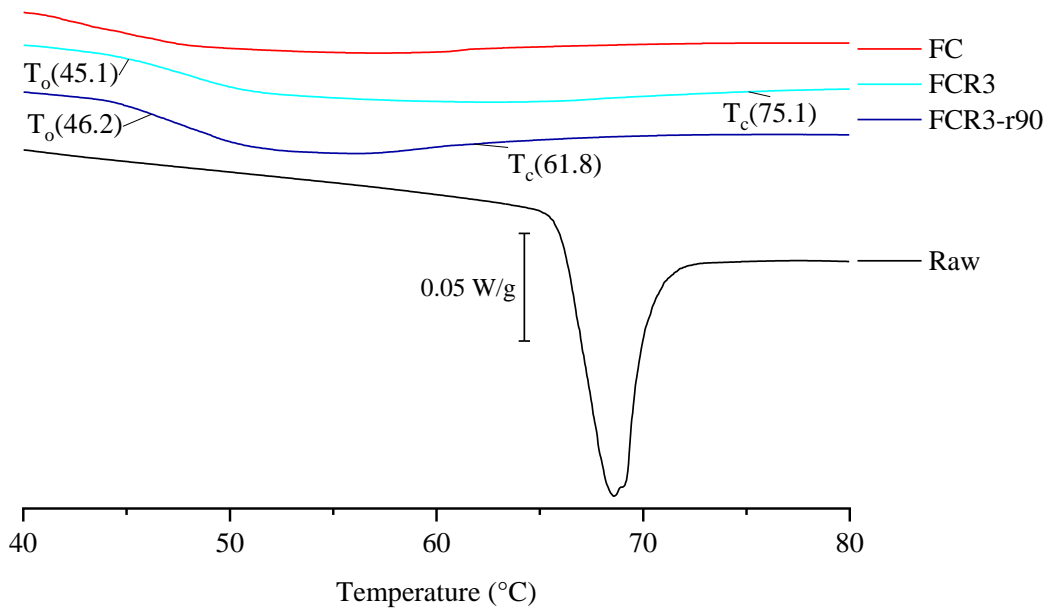


Figure IV.2 The endothermal profile of the raw potato tuber, freshly cooked (FC), the 3-day retrograded (FCR3), and the retrograded+ reheated (FCR3-r90) samples.

Table IV.1 Thermal characteristics of freshly cooked (FC), retrograded (FCR) and retrograded+reheated (FCRr) potato tubers.

Samples	T_o (°C)	T_p (°C)	T_c (°C)	$T_c - T_o$ (°C)	ΔH_R (J/g d.b.)
FC	45.7 ± 1.2 ^{ab}	51.6 ± 1.9 ^b	62.0 ± 0.8 ^c	16.3 ± 0.4 ^c	1.1 ± 0.01 ^b
FCR1	44.8 ± 1.4 ^{ab}	58.7 ± 0.2 ^a	74.0 ± 1.5 ^b	29.1 ± 2.6 ^{ab}	2.6 ± 0.2 ^{abc}
FCR3	45.1 ± 0.1 ^{ab}	55.9 ± 3.4 ^{ab}	75.1 ± 0.1 ^b	30.0 ± 0.2 ^a	5.1 ± 1.4 ^a
FCR7	44.4 ± 1.6 ^{ab}	56.4 ± 4.0 ^{ab}	70.9 ± 0.7 ^a	26.5 ± 1.2 ^b	4.0 ± 0.4 ^{ac}
FCR1-r90	43.5 ± 0.1 ^a	50.5 ± 1.4 ^b	63.3 ± 0.3 ^c	19.7 ± 0.3	2.2 ± 0.3 ^{bc}
FCR3-r90	46.2 ± 0.8 ^{ab}	53.1 ± 0.8 ^{ab}	61.8 ± 0.8 ^c	15.7 ± 0.1 ^c	2.8 ± 0.03 ^{bc}
FCR7-r90	46.3 ± 0.3 ^b	53.1 ± 0.9 ^{ab}	61.3 ± 0.2 ^c	15.1 ± 0.3 ^c	2.5 ± 0.5 ^{bc}

T_o , onset temperature; T_p , peak temperature; T_c , conclusion temperature; and $T_c - T_o$ transition temperature. ΔH_R , starch retrogradation enthalpy. Different superscripts in the same column indicate significant differences ($p < 0.05$) ($n = 3$).

IV.3.3 Relative crystallinity (%)

The structural changes of the starchy matrix in potato cell caused by the realignment of disrupted amylose and amylopectin after cooking (FC), cooling (FCR1, FCR3, and FCR7) and reheating (FCR1-r90, FCR3-r90, and FCR7-r90) were evaluated by the relative crystallinity (Figure IV.3) determined by X-ray diffraction. The relative crystallinity of the FCR3 (22.59%) was the highest, followed by the FCR7 (22.47%) and then by the FCR1 (20.55%) (Hu, Xie, et al., 2014), which accorded with the relative enthalpies of the retrograded samples. This indicated that three days' retrogradation was enough to form the most aggregation. However, reheating at 90°C disrupted the aggregated structure of melted amylose and amylopectin as revealed by the relative crystallinities of FCR1-r90, FCR3-r90 and FCR7-r90

decreasing to 17.92%, 15.41% and 16.15% respectively and becoming close to the crystallinity of freshly cooked samples (18.13%).

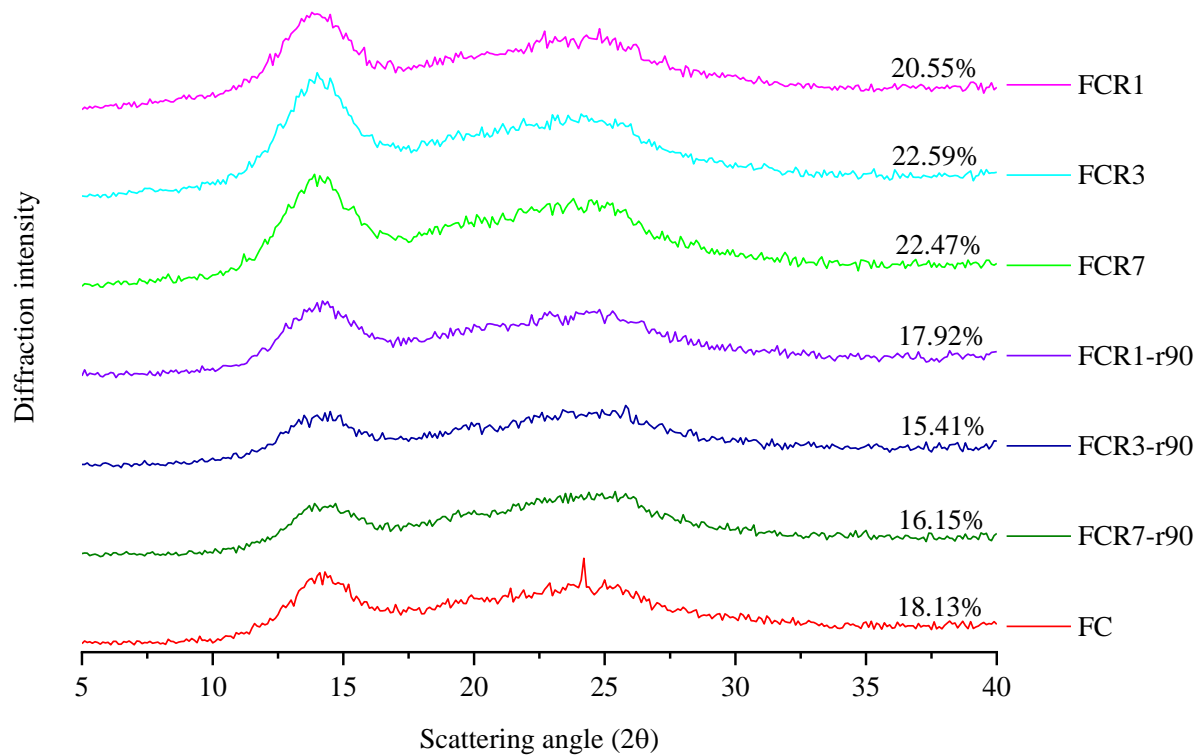


Figure IV.3 The X-ray diffraction patterns of the freshly cooked (FC), the retrograded (FCR) and the retrograded+reheated (FCRr) samples. FC, freshly cooked sample; FCR1, the 1-day retrograded sample; FCR3, the 3-day retrograded sample; FCR7, the 7-day retrograded sample; FCR1-r90, the 1-day retrograded+reheated sample; FCR3-r90, the 3-day retrograded+reheated sample; FCR7-r90, the 7-day retrograded+reheated sample.

IV.3.4 Water mobility in potato tuber cells

If the decaying quantity, $N(t)$ is the number of the different proton with different vibrations in potato tuber, the average length, τ of time that an element remains in the set can be estimated by following equation, $N(t) = N_0 e^{-\frac{t}{\tau}}$, with the decay rate, λ and $\tau = \frac{1}{\lambda}$. The τ is the time that the population assembly reduced to $1/e = 0.368$ times of its initial value. The relaxation time (T_{22}) is thus retrieved from the exponential decay curve after 37% decay (Table IV.2). To analyse water pools with different relaxation times, the exponential decay curve of the raw data was transformed to a continuous relaxation time distribution curve (Figure IV.4) by inverse Laplace transformation. The “Lawson and Hanson NNLS analysis” method in Prospa©v3.1 (Magritek, 2016) was used to calculate relaxation times T_{2i} ($i=0,1,2,3\dots$ etc). Based on the relaxation time T_{2i} of different water pools, the water exists in different cell compartments can then be discerned.

Table IV.2 Optimised parameters (left) and the raw data of raw, cooked and cooled (1h, 24h, and 1wk) potato cylinders (right).

Scan (s)	4	Samples	T_{22} (ms)	
Acquisition time (s)	1.6	Raw	463	
Repetition time (s)	10	Cook (90°C 10min) Cool (25°C 10min)	286	
Number of steps	10	Cook Cool Storage (4°C 1hr)	227	
CPMG echo time (ms)	1	Cook Cool Storage (4°C 24hr)	167	
Final echo time (s)	2	Cook Cool Storage (4°C 1wk)	135	

LF-NMR was used to track changes in mobility of three main water populations found in potato tubers (with the relaxation times T_{23} , T_{22} and T_{21}) which had undergone cooking (FC), cooling (FCR3) or reheating (FCR3-r90) (Figure IV.4). The water population with relaxation time T_{20} may represent the water in the B-type starch structure of potatoes which consists of 36 water molecules per unit cell (Buléon, Colonna, et al., 1998) (Figure IV.4). The T_{20} population's relaxation time and abundance were consistent regardless of tuber treatment. The relaxation time T_{22} of raw tuber showed a bimodal distribution (Figure IV.4) which may have occurred due to the diffusive exchange of water populations between the subcellular compartments (Hills & Le Floc'h, 1994). The water pools with the relaxation time T_{22} and T_{21} of FC, FCR3 and FCR3-r90 (Figure IV.4) were interpreted as the water in the cytoplasm or intra-cellular and the water associated with the starchy matrix, respectively (Mortensen et al., 2005).

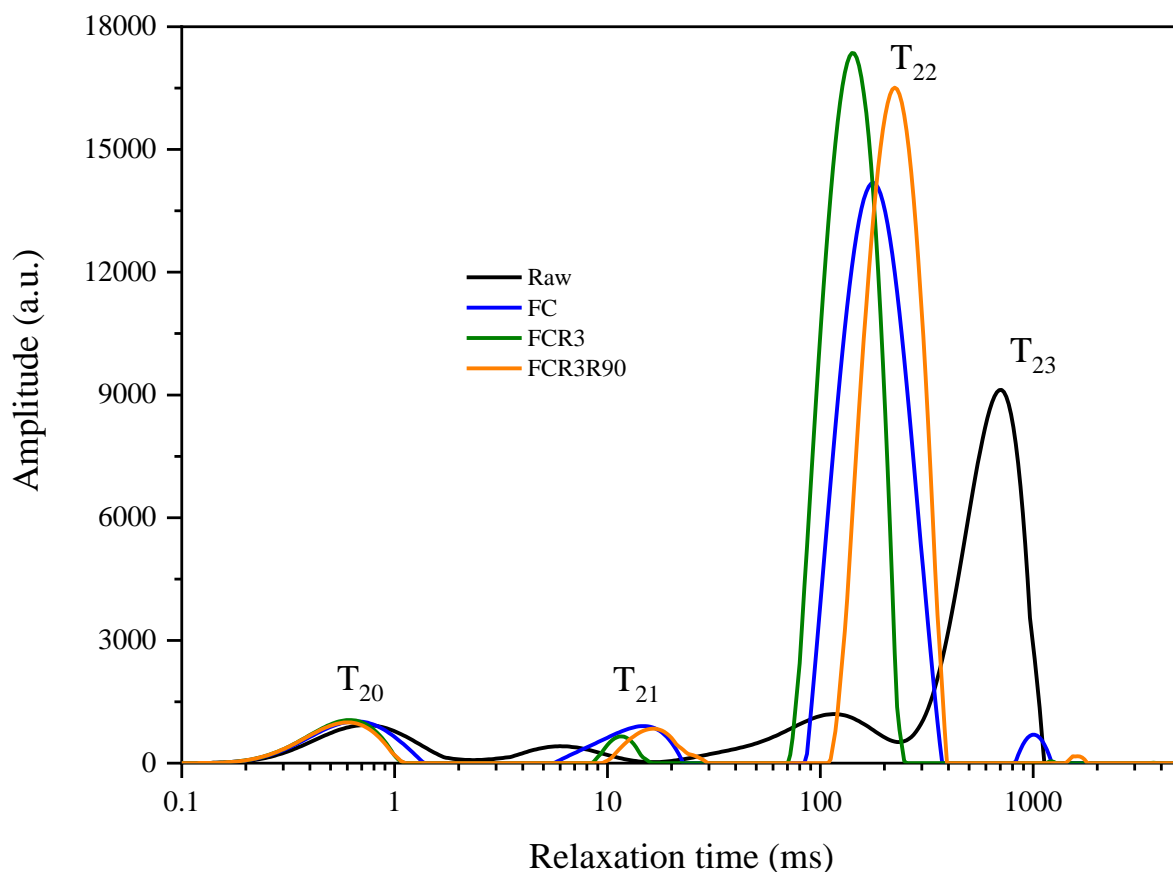


Figure IV.4 Different water pools, T_{23} , T_{22} , T_{21} , and T_{20} , in potato tubers, including raw, freshly cooked (FC), 3-day retrograded (FCR3), and retrograded+ reheated (FCR3-r90) tubers.

The relaxation time T_{22} ranged from 75 to 210 ms (Figure IV.5) and represented the most abundant water population in the tubers which may be the water loosely connected with starch by hydrogen bonding. There was much less water with relaxation times T_{23} and T_{21} than with relaxation time T_{22} . The T_{23} population ranged from 450 to 850 ms (Figure IV.5), and may represent water in inter- and intra-cellular space with no direct connection with starch, whereas the T_{21} population, had relaxation time ranging from 7 to 15 ms (Figure IV.5), and may contain water more tightly bound within the amylose and amylopectin.

The effects of cooking, cooling and reheating on the structures formed by melting amylose and amylopectin and the effects on water migration were inferred from the degree of the vibration of hydrogen bonding as indicated by relaxation time. The water population with relaxation time T_{23} is thought to diffuse into starch granules and interact with the exposed hydroxyl groups of amylose and amylopectin by exchanging hydrogen bonds during heating. As temperature drops after heat treatment, the progressive aggregation of melted amylose and amylopectin should weaken the interactions between the starchy matrix and water leading to more free water in the T_{23} population; simultaneously the water with T_{21} in the melted amylose and amylopectin network would become less mobile. A cyclic pattern of the relaxation time T_{22} of freshly cooked (FC), retrograded (FCR), and retrograded+reheated (FCRr)

is shown in Figure IV.5. The relaxation time T_{22} of FC, FCR0.04, FCR1, FCR3, and FCR7 decreased with prolonged storage and then increased at varied reheating temperatures from 50°C, 70°C to 90°C. However, the pool with relaxation time T_{22} of FCR7-r90 (85.05 ms) was smaller than for FC (212.17 ms) and similar to the level observed for FCR1-r50 (87.52 ms). This may indicate that long storage time allows melted amylose and amylopectin to associate, forming a sufficiently strong structure to maintain rigidity despite reheating to 90°C.

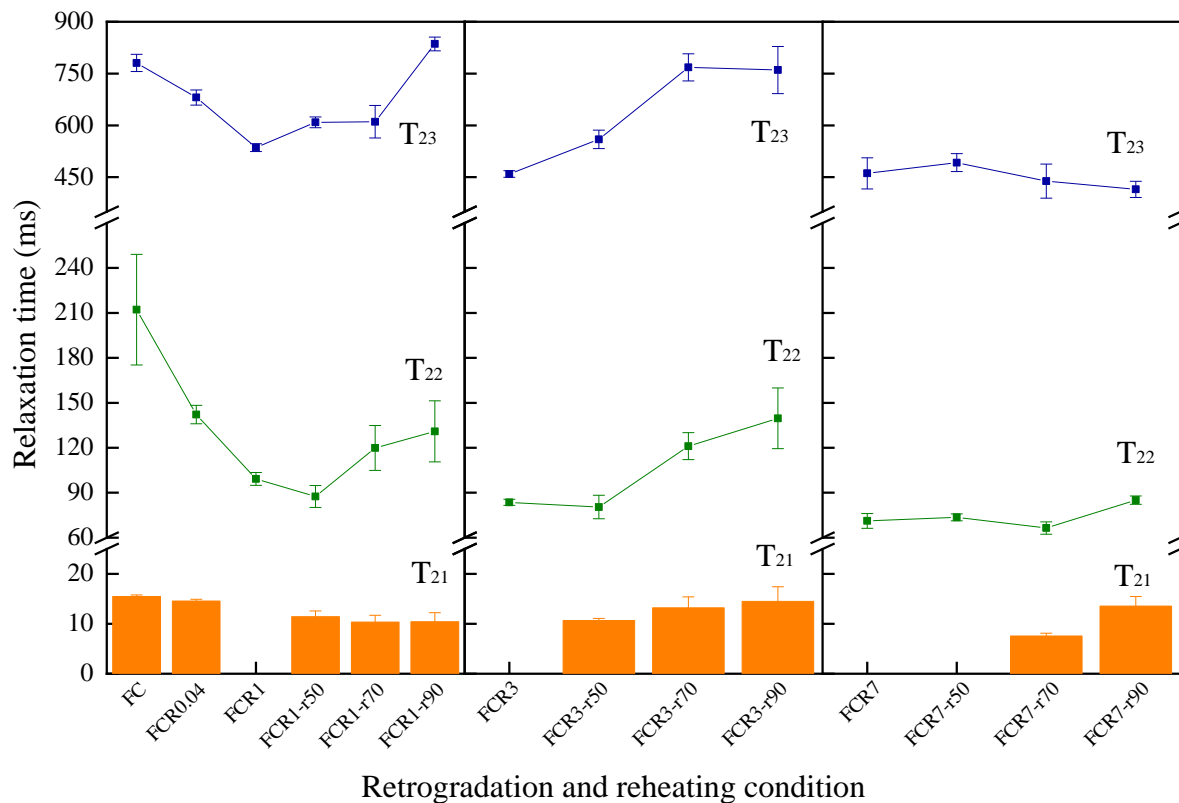


Figure IV.5 The development of relaxation time T_{23} , T_{22} and T_{21} under different cold storage times for 1, 3, and 7 days (FCR1, FCR3, and FCR7) and reheating temperatures at 50°C, 70°C, and 90°C (FCR1-r50, FCR1-r70, FCR1-r90, FCR3-r50, FCR3-r70, FCR3-r90, FCR7-r50, FCR7-r70, and FCR7-r90). Error bars represent standard deviation (n=3).

IV.3.5 Starch hydrolysis (%) and its kinetics

The starch digestibility of all the samples is shown as starch hydrolysis (%) (Figure IV.6). Starch hydrolysis percentage (C_{∞}) and kinetic constant (k) were estimated by fitting a first-order equation model (Table IV.3). During the simulated gastric digestion phase (G_0 and G_{30}), the starch hydrolysis (%) of all samples were similar and ranged from 0.88% to 3.10% indicating most of the starch remained undigested (Figure IV.6). This observation was attributed to the absence of amylases in the gastric juice with the minimal hydrolysis observed being attributed to acid pH. The highest level of hydrolysis was exhibited by the briefly retrograded then severely reheated sample (FCR1-r90, 95.7 ± 4.9), slightly ahead of the freshly cooked sample (FC, 93.1 ± 3.2). Within the starch hydrolysis of all the samples, the least well-hydrolysed samples were those with the longest retrogradation period and lightest

reheating. The relative ease of hydrolysis of starch in freshly cooked potato tubers (FC) was probably because heat disrupted starch granular to the starchy matrix as well as the organized structure of amylose and amylopectin became disordered which facilitated enzyme access to the starchy matrix. Hydrolysis (%) of the 1-day (FCR1), 3-day (FCR3) and 7-day (FCR7) retrograded tubers likely decreased through progressive re-association of the disrupted amylose and amylopectin reducing enzyme access. Amylopectin is thought to be the major component in potato starch governing the retrogradation process in long-term refrigerated storage (Fredriksson et al., 1998; Karlsson & Eliasson, 2003b; Miles et al., 1985; Srichuwong et al., 2005). The retrograded starch structure was differentially unstable as evidenced by the extent of increase in starch hydrolysis (%) after reheating depending on the duration of retrogradation before reheating. The starch hydrolysis (%) of the retrograded+reheated tubers, FCR7-r90 (67.8%), was even lower than the retrograded tubers, FCR3 (75.0%). This indicated that 7-day of retrogradation allowed the melted amylose and amylopectin to form a structure that could partially resist reheating disruption and subsequent enzymatic breakdown.

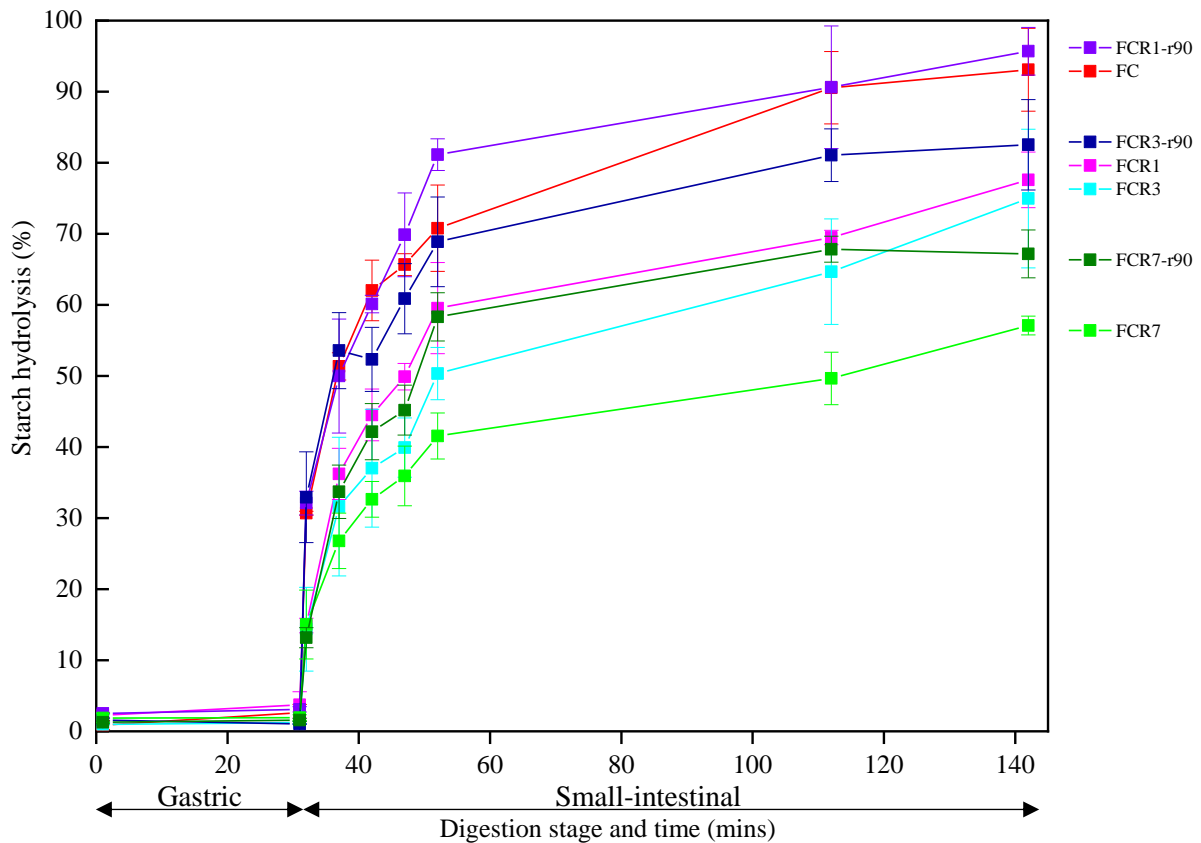


Figure IV.6 Starch hydrolysis (%) of freshly cooked (FC), retrograded (FCR1, FCR3, FCR7) and retrograded+reheated (FCR1-r90, FCR3-r90, FCR7-r90) tuber. Error bars represent standard deviation (n=3).

The concentration of glucose released from each sample was modelled during small intestinal (enzymatic) hydrolysis and expressed in Table IV.3 as starch hydrolysis (%). The kinetic constant ($k \text{ min}^{-1}$, Table IV.3) of each treatment was calculated assuming first-order kinetics for starch hydrolysis. Factors that influence the kinetics of starch digestion are the nature of starch, physical form, protein and

lipids interactions, presence of antinutrients enzyme inhibitors, and food processing (Singh, Dartois, et al., 2010). The kinetic constants of the retrograded tubers (FCR1, FCR3, and FCR7) were significantly lower than the retrograded+reheated tubers (FCR1-r90, FCR3-r90, and FCR7-r90), indicating storage reduced the rate of enzymatic digestion. The hydrolysis index (HI) and the estimated glycaemic index (*eGI*) of all the samples decreased with increasing storage time (Table IV.3). The HI and the *eGI* of the FCR7 were the lowest significantly while the HI and the *eGI* of the FCR7-r90 were similar to the FCR1 and the FCR3 but were significantly lower than FC, FCR1-r90, and FCR3-r90. The *eGI* of the freshly cooked potato (*eGI*, 101.2) and FCR7 (*eGI*, 71.1) were comparable to the GI of boiled potato (GI, 144) (Foster-Powell et al., 2002) and boiled then served cold potato (GI, 79.2) (Fernandes et al., 2005). As the *eGI* were shown to significantly correlated to the glycaemic index (Goñi et al., 1997), the values can be very representative.

Table IV.3 Kinetics of starch hydrolysis percentage, hydrolysis index (HI) and estimated glycaemic index (*eGI*) of freshly cooked (FC), retrograded (FCR) and retrograded+reheated (FCRr) potato tubers.

Sample	C_{∞} experimental (%)	C_{∞} estimated (%)	K ($\times 10^{-2} \text{ min}^{-1}$)	HI	<i>eGI</i>
FC	93.1 ± 7.1 ^a	92.5 ± 1.1 ^a	4.3 ± 1.5 ^a	112.1 ± 0.9 ^a	101.2 ± 0.5 ^a
FCR1	77.6 ± 4.8 ^{abc}	77.6 ± 2.2 ^b	1.7 ± 0.2 ^b	85.7 ± 5.8 ^{bc}	86.8 ± 3.2 ^{bc}
FCR3	75.0 ± 12.0 ^{abc}	75.0 ± 2.8 ^b	1.7 ± 0.2 ^b	75.5 ± 11.2 ^{cd}	81.2 ± 6.1 ^{cd}
FCR7	57.1 ± 1.6 ^c	57.1 ± 1.9 ^c	1.7 ± 0.2 ^b	57.2 ± 4.5 ^d	71.1 ± 2.5 ^d
FCR1-r90	95.7 ± 10.2 ^a	95.1 ± 1.0 ^a	4.3 ± 1.5 ^a	118.3 ± 12.6 ^a	104.6 ± 6.2 ^a
FCR3-r90	82.5 ± 7.8 ^{ab}	82.1 ± 0.2 ^b	4.3 ± 1.5 ^a	102.2 ± 6.0 ^{ab}	95.8 ± 3.3 ^{ab}
FCR7-r90	67.2 ± 4.1 ^{bc}	67.4 ± 0.3 ^c	4.3 ± 1.5 ^a	81.0 ± 4.7 ^c	84.2 ± 2.6 ^c

C_{∞} , experimental starch hydrolysis (%) after 2 hours of simulated small-intestinal digestion; k , kinetic constant; HI, hydrolysis index; *eGI*, estimated glycaemic index. Different superscripts in the same column indicate significant differences ($p < 0.05$) ($n=3$).

IV.3.6 Microstructure before and during small intestinal enzymatic digestion

Confocal laser scanning microscopy (CLSM) was used to capture microstructural changes during small intestine digestion *in vitro*. CLSM allows direct visualisation of the changes in potato tissue microstructure during starch hydrolysis. The images of the freshly cooked tubers (FC), the 3-day retrograded tubers (FCR3) and the 3-day retrograded+reheated tubers (FCR3-r90) were taken before and after adding SIF at the initial time point (T_0), and after 5 (T_5), 10 (T_{10}) and 30 (T_{30}) minutes (Figure IV.7). The homogeneous background of empty cells indicated the effect of enzymatic hydrolysis during the course of digestion. The parenchyma cell walls stayed intact indicated that SIF had little or no effect on the cell wall integrity. All the samples (FC, FCR3, and FCR3-r90) showed the separated cells were filled up by gelled mass after the cooking process. The gelatinised gelled mass in the parenchyma cells of the freshly cooked tuber disappeared quickly after 5 minutes of SIF digestion (Figure IV.7a, b, c, and d). These phenomena could well explain the starch hydrolysis of FC increased rapidly after 5 minutes of SIF digestion. The 3-day retrograded tubers (FCR3) showed greater resistance to digestion as evident from the small amount of gelled mass digested at T_{30} (Figure IV.7e, f, g, and h). This might be the reason that the starch hydrolysis of FCR3 increased steadily throughout the 2 hours intestinal digestion whereas

the starch hydrolysis of the freshly cooked potato tubers and the reheated tubers showed a rapid increase. Although retrogradation facilitates the formation of compact matter from the melted amylose and amylopectin that can withstand reheating, the images of 3-day retrograded reheated tuber (FCR3-r90) disappeared gradually as digestion proceeded (Figure IV.7i, j, k, and l).

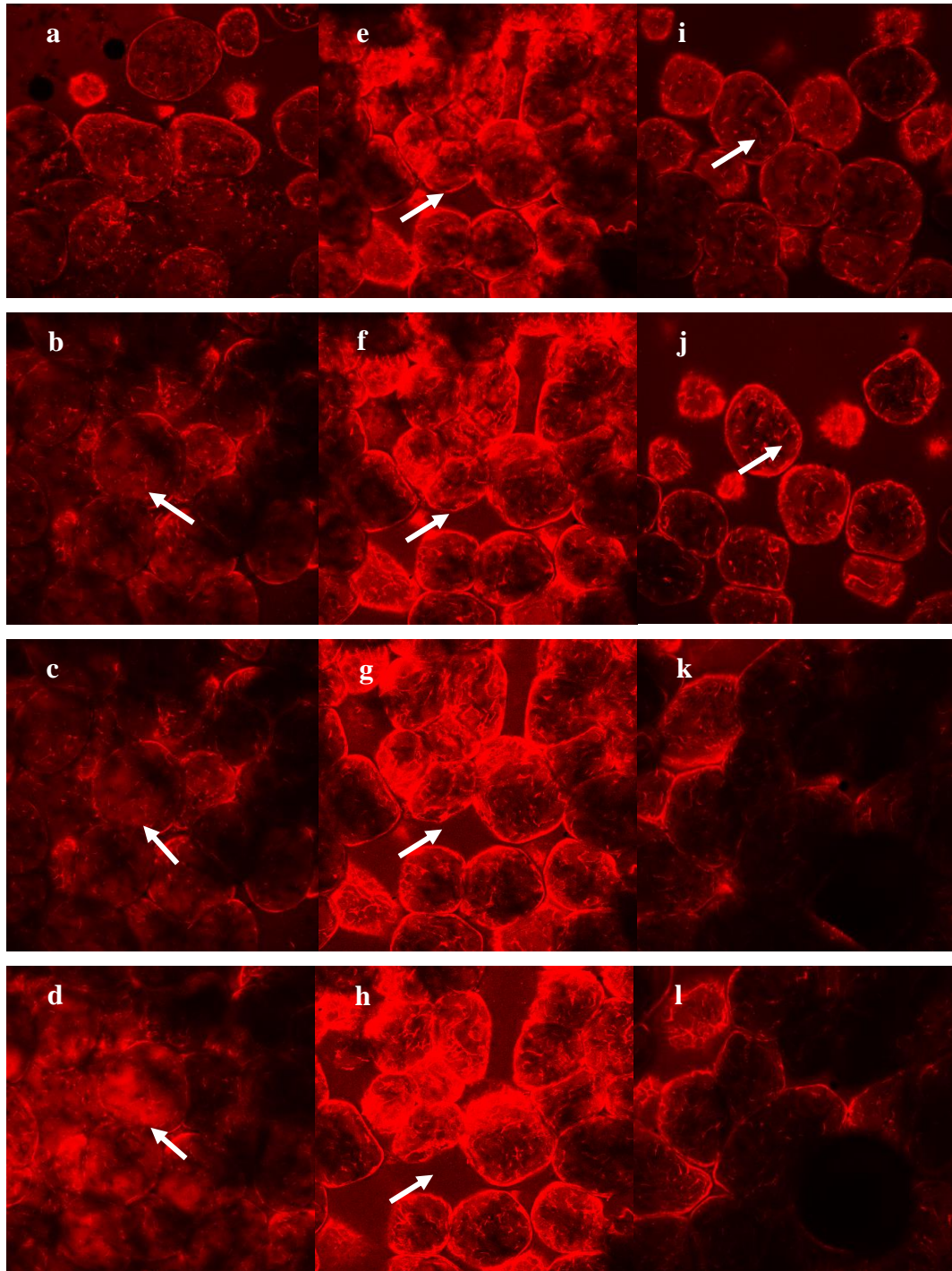


Figure IV.7 The CLSM time-lapse images of FC in SIF at T₀ (a), T₅(b), T₁₀(c) and T₃₀(d); FCR3 incubating in SIF at T₀ (e), T₅(f), T₁₀(g), and T₃₀(h); and FCR3-r90 incubating in SIF at T₀ (i), T₅(j), T₁₀(k), and T₃₀(l).

IV.4 Conclusion

A longer cooling and storage time (4°C, 7days) allowed gelatinised starch to aggregate and realign, as evidenced by a significant increase in the pasting temperature, retrogradation enthalpy and relative crystallinity of retrograded samples of potato tuber when compared to freshly cooked potato samples. In addition, the water mobility represented by relaxation time T_{22} can be an indicator of starch retrogradation; the T_{22} values measured were negatively correlated to both the pasting temperature and the retrogradation enthalpy ($p < 0.05$) (Table IV.4). A significant reduction in the ease of starch hydrolysis (%) by 36% was also measured with longer retrogradation times (7days). Reheating of retrograded tuber restored some of the susceptibility to enzymatic hydrolysis and internal water mobility. The relaxation time of a water population indicates mobility - the water with slow relaxation time is more mobile and less restricted which could facilitate enzyme diffusion leading to greater starch hydrolysis (%): in this study relaxation time T_{22} was positively correlated to greater starch hydrolysis of the treated tubers ($p < 0.05$) (Table IV.4). But longer chilled storage (7days) improved the stability of retrograded tuber against reheating effects (at 90°C). Realignment of the disrupted amylose and amylopectin is thought to have changed the distribution of crystalline and amorphous regions during refrigerated storage and subsequent reheating, resulting in starch digestibility varying with treatment combination.

Table IV.4 Pearson correlation

	Pv	HPv	Breakdown	Fv	Setback	PT	To (°C)	Tp (°C)	Tc (°C)	Tc - To(°C)	ΔH_R (J/g d.b.)	RC	T23	T22	T21	C _∞	K	HI
HPv	0.888																	
Breakdown	0.008	0.801																
Fv	0.000	0.030	0.766															
Setback	0.888	0.945	0.045	0.919														
PT	0.008	0.001	0.003	0.003	-0.595													
To (°C)	-0.754	-0.609	-0.745	-0.591	0.159	-0.249					Cell content:	Correlation coefficient						
Tp (°C)	0.050	0.146	0.054	0.162	0.207	0.590	-0.061				<i>p</i> -value							
Tc (°C)	-0.102	-0.176	0.055	-0.420	0.656	0.455	0.897	0.862										
Tc - To(°C)	0.828	0.705	0.908	0.349	0.207	0.455	0.304	0.390	0.990									
ΔH_R (J/g d.b.)	-0.029	0.237	-0.006	0.042	0.207	0.455	0.240	0.026	0.000	0.695								
RC	0.950	0.609	0.990	0.929	0.656	0.304	0.179	0.564	0.717	0.083								
T23	0.076	0.323	0.045	0.249	0.347	0.426	0.388	0.187	0.070	0.257	0.275							
T22	0.871	0.480	0.924	0.591	0.445	0.297	0.147	0.549	0.300	0.578	0.550							
T21	0.086	0.328	0.033	0.295	0.355	0.468	0.240	0.026	0.000	-0.497	-0.629	-0.118						
C _∞	0.854	0.473	-0.435	0.521	0.435	0.290	0.169	0.692	-0.560	0.257	0.130	0.801	0.807					
K	-0.470	-0.326	0.330	-0.365	-0.249	0.681	-0.179	0.564	0.717	-0.569	-0.766	-0.140	0.807	0.882	0.797	-0.761		
HI	0.288	0.476	0.123	0.421	0.591	0.092	0.700	0.187	0.070	0.182	0.045	0.746	0.028	0.032	0.135			
eGI	0.054	0.144	0.793	-0.039	0.135	-0.110	0.147	0.549	0.300	0.423	0.826	0.634	-0.622	0.380	-0.049	0.282		
	0.908	0.758	0.305	0.934	0.773	0.814	0.753	0.202	0.513	0.478	0.085	0.250	0.262	0.188				
	0.421	0.366	0.507	0.502	0.269	-0.775	-0.169	0.692	-0.560	-0.383	-0.623	-0.442	0.882	0.797	-0.761			
	0.347	0.420	0.698	0.251	0.559	0.041	0.716	0.085	0.191	0.397	0.135	0.320	0.009	0.032	0.135			
	0.719	0.533	0.081	0.568	0.528	-0.967	0.215	0.621	-0.576	0.355	-0.605	-0.235	0.355	0.380	-0.049	0.282		
	0.069	0.210	-0.437	0.184	0.223	0.000	0.643	0.136	0.176	-0.924	0.150	0.612	0.434	0.401	0.938	0.540		
	-0.465	-0.124	0.462	-0.380	-0.314	0.491	0.350	0.814	0.537	0.001	0.085	0.250	0.262	0.188				
	0.431	0.842	0.344	0.528	0.607	0.401	0.563	0.093	0.350	0.001	-0.623	-0.442	0.882	0.797	-0.761			
	0.483	0.494	0.450	0.614	0.367	-0.702	-0.124	-0.640	-0.431	-0.583	-0.623	-0.442	0.882	0.797	-0.761			
	0.272	0.260	-0.249	0.143	0.417	0.079	0.792	0.122	0.335	0.397	0.135	0.320	0.009	0.032	0.135			
	-0.295	-0.423	0.590	-0.444	-0.526	-0.289	0.569	-0.670	-0.924	-0.951	-0.605	-0.235	0.355	0.380	-0.049	0.282		
	0.521	0.344	0.241	0.318	0.225	0.530	0.158	0.100	0.003	0.001	0.150	0.612	0.434	0.401	0.938	0.540		
	0.362	0.339	0.603	0.455	0.197	-0.702	-0.020	-0.746	-0.629	-0.583	-0.737	-0.428	0.911	0.806	-0.792	0.967	0.500	
	0.425	0.457	0.241	0.305	0.672	0.078	0.965	0.054	0.130	0.130	0.059	0.338	0.004	0.028	0.110	0.000	0.254	
	0.362	0.339	0.603	0.455	0.197	-0.702	-0.021	-0.746	-0.629	-0.583	-0.737	-0.428	0.911	0.806	-0.792	0.967	0.500	1.000
	0.425	0.457	0.241	0.305	0.672	0.078	0.965	0.054	0.130	0.130	0.059	0.338	0.004	0.028	0.110	0.000	0.254	0.000

RVA parameters: Pv, peak viscosity; Breakdown, breakdown viscosity; HPv, hot paste viscosity; Fv, final viscosity; Setback, setback viscosity; PT, pasting temperature. Thermal characteristics: To, onset temperature; Tp, peak temperature; Tc, conclusion temperature; Tc - To, endothermic range; ΔH_R , retrogradation enthalpy. RC, relative crystallinity. Relaxation time T23, T22, T21. C_∞, experimental starch hydrolysis (%); K, kinetic constant; HI, hydrolysis index; eGI, estimated glycaemic index.

Chapter V Influence of time-temperature cycles on potato starch retrogradation *in tuber* and starch digestion *in vitro*

V.1 Introduction

Native starches are semi-crystalline polymers essentially composed of amylose and amylopectin and linked by α -D-glucan. The starch structure is influenced by thermomechanical history during cooking, cooling and storage. The on-going and non-equilibrium process of recrystallization of the cooked or gelatinised starch during cooling and storage is called retrogradation (Hoover, 1995; Jacobson et al., 1997). This phase transition is dependent on the relativity of starch temperature to the glass transition temperature of the starch-water system, T_g and to its melting temperature, T_m , due to variable levels of segmental motion within amorphous and crystalline domains. At temperatures below T_g molecular motion is restricted. As the temperature exceeds T_g but stays below T_m , it is in a rubber-like mobile state in which the molecular motion within the amorphous domain increases but some segments are still locked in crystallites. This rubber-like phase is stable until the melting temperature T_m is reached (Jenkins, 1972), above which the overall starch structure melts (Capron, Robert, Colonna, Brogly, & Planchot, 2007; Louise Slade & Levine, 1988). The rate of crystallinity development has been expressed as depending on the temperature difference between the storage temperature, T and specific glass transition temperature, T_g' , $\Delta T = (T - T_g')$ (Jouppila & Roos, 1997; Marsh & Blanshard, 1988). And a positive correlation between T_g' and stability at a constant storage T has been observed (Wang & Jane, 1994).

When storage temperature is between T_g and T_m , starch retrogradation involves three phases of crystallization often observed as three sequential steps (Slade & Levine, 1987; Wunderlich, 1980): (i) nucleation, (ii) propagation or growth of crystals, and (iii) maturation or crystal perfection. The overall crystallization rate depends mainly on the nucleation and propagation rate (Eerlingen et al., 1993). Nucleation has been observed to be faster at 4°C than at room temperature in potato starch (Nakazawa et al., 1985) and wheat grains (Jankowski & Rha, 1986). Similarly, propagation of crystallite development from nuclei was faster at higher temperatures (Silverio et al., 2000) but collapses into disorder at/above the starch melting temperature. Numbers of retrograded starch nuclei and chain length of retrograded amylose both increased at higher retrogradation temperatures (Lu, Jane, & Keeling, 1997) though the level of retrogradation was hindered, probably due to the increased kinetic motion of the molecules (Kalb & Sterling, 1961). The crystallization process occurs in the temperature range between the glass transition temperature and the melting temperature because nucleation and

propagation require orientation mobility of the amylose and amylopectin chains (Thompson & Fisher, 1997). The net rate of crystallization (nucleation and growth) has a maximum value at a temperature $T \sim 1/2(T_g + T_m)$ (Morris, 1990). The rate of crystal growth within the retrograded starch gel or paste could be increased by allowing nucleation to occur at a low temperature followed by storing closer to melting temperature (Slade & Levine, 1987).

A temperature cycling process is likely to induce stepwise nucleation and propagation which promotes the growth of crystalline regions and perfection of crystallites, resulting in a higher content of slowly digestible starch (SDS) in cereal starch pastes, potato starch pastes, and pea starch pastes (Silverio et al., 2000). Sievert & Pomeranz (1989) also showed that resistant starch (RS) of wheat and pea starch increased with increasing cycles of autoclaving and cooling. We extended the idea of the time-temperature cycle (TTC) processes to freeze/chill (TTC1) and chill/warm (TTC2) domains to investigate the effect of TTC on retrogradation rate of starch in cooked potato tuber. We expect the formation of ice crystals to concentrate gelatinised starch in neighbouring regions, accelerating reordering. We hypothesize that TTC cycles will cause the redistribution of water in a retrograded starchy matrix and thus affect structural characteristics such as crystalline/amorphous alignment, interaction of starchy matrix and water, starch digestibility and texture. In addition, TTC cycles between starch glass transition temperature and starch melting temperature might also enhance formation of retrograded starches *in tuber*. We studied the retrogradation of time-temperature cycle (TTC) processed potato tubers by blue value, differential scanning calorimetry (DSC) and LF NMR. And we investigated *in tuber* starch digestion using *in vitro* oral-gastro-small intestinal models.

V.2 Materials and methods

V.2.1 Materials and sample preparations

In season *cv.* Agria potato tubers (120g-150g) were purchased from a local supermarket. Same batch of tubers was used in all the experiments in this chapter. Whole uniform round or oval tubers were put singly into polythene bags and cooked in a water bath at 90°C for 25 minutes. Then the cooked potato tuber was stored in one of a number of 3-day time-temperature cycles (TTC) ranging between (i) -20°C and 4°C, TTC1 and (ii) 4°C and 65°C, TTC2 (Table V.1). The whole potato tubers were stored in -20°C freezer, or in 4°C fridge, or in 65°C water bath. The temperatures of TTC processes were chosen at the range that can potentially maximize the crystallization rate of starch retrogradation (Eerlingen et al., 1993). The temperature condition of 65°C was tested at 6, 24, and 30h durations to find the optimum according to the relaxation time. The test methods to characterise the starch crystalline structure are summarised in Table V.1.

Table V.1 Summary of all time-temperature cycle processes (left) and the test method that was performed (right).

Process	Code	Cook	Storage (temp °C/ duration hrs)	Blue value	Thermal properties	Relaxation time T ₂₂	<i>In vitro</i> digestion	Digesta thermal	Digesta PSD
	Raw	N	No storage	√	√	√	√	√	√
	FC	Y	No storage	√	√	√	√	√	√
TTC1	FCR3-t(-20/4/4)	Y	-20/24 4/24 4/24	√	√	√	√	√	√
TTC1	FCR3-t(4/-20/4)	Y	4/24 -20/24 4/24	√	√	√	√	-	√
TTC1	FCR3-t(4/4/-20)	Y	4/24 4/24 -20/24	-	-	√	-	-	-
	FCR3	Y	4/72	√	√	√	√	√	√
TTC2	FCR3-t(4/25/4)	Y	4/24 25/24 4/24	-	-	√	-	-	-
TTC2	FCR3-t(4/65_6hrs/4)	Y	4/30 65/6 4/36	-	-	√	-	-	-
TTC2	FCR3-t(4/65_24hrs/4)	Y	4/24 65/24 4/24	√	√	√	√	√	√
TTC2	FCR3-t(4/65_30hrs/4)	Y	4/24 65/30 4/18	-	-	√	-	-	-
TTC2	FCR3-t(4/4/65)	Y	4/24 4/24 65/24	√	√	√	√	-	√

*Ticks mark the tests that were carried out.

Samples were freeze-dried (Singh et al., 2014; Tamura et al., 2016) and powdered to measure the blue value, the total starch content and the amylose content, and thermal characteristics. Enzymes α -amylase (*Aspergillus oryzae*, 1.5 U/mg), pepsin (porcine gastric mucosa, 800–2500 units/mg protein), pancreatin (hog pancreas, 4 × USP), and invertase (Invertase, grade VII from baker’s yeast, 401 U/mg solid) were purchased from Sigma–Aldrich Ltd. (St Louis, USA). Amyloglucosidase (3260 U/ml) was purchased from Megazyme International Ireland Ltd. (Ireland).

V.2.2 Total starch content, amylose content, dry matter, and the blue value

Total starch content of the freeze-dried samples was determined by assay kit K-TSTA 07/11 (Megazyme International, Ireland) and the amylose content was estimated by lectin concanavalin A (Con A) solubility using Megazyme kit (K-AMYL 12/16, Megazyme International, Ireland). Dry matter content of tubers was determined by the AOAC 934.01 method (AOAC, 1990). To determine Blue Value, a freeze-dried potato sample (20mg) was dispersed in 10mL of 500mol/m³ KOH, transferred to a 100mL volumetric flask, and diluted with distilled water. An aliquot (2mL) of this test solution was pipetted into a 5mL test tube and 1mL of 100mol/m³ HCl was added followed by 100 μ L of iodine reagent. The volume was diluted to 5mL and absorbance measured at 625nm (Williams, Kuzina, & Hynka, 1970). A standard curve was plotted by mixtures of potato amylose and potato amylopectin purchased from Sigma–Aldrich Ltd. (St Louis, USA). Starch retrogradation was quantified by the loss of ability to form the blue complex with iodine (Jankowski, 1992) and presented as the blue value (Eq. 1) from the absorbance at 625nm (Gilbert & Spragg, 1964).

$$\text{Blue Value} = \frac{\text{Absorbance } 625\text{nm} \times 4}{\text{concentration } \left(\frac{\text{mg}}{\text{dl}}\right)} \quad \text{Eq. 1}$$

V.2.3 Thermal characteristics

Fresh potato tuber pieces were heated from 20°C to 95°C (10°C/min) to complete gelatinisation. Specific glass transition temperature T_g' of gelatinised potato tubers (Goff, 1994) was determined by scanning from -20°C to 20°C (5°C/min) with DSC (TA Q100, TA Instruments, Newcastle, DE).

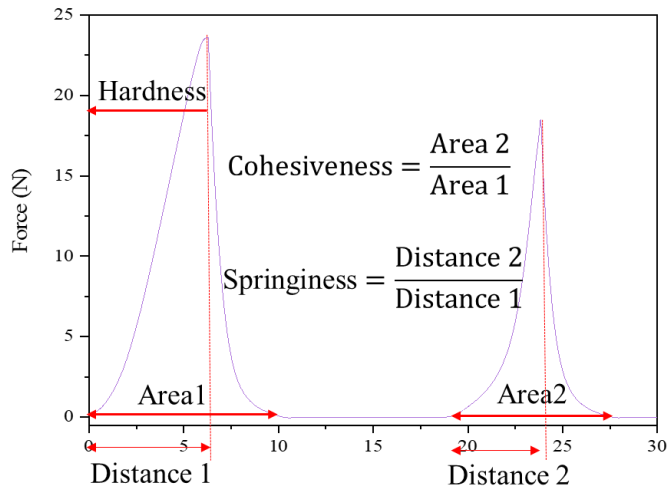
Freeze-dried samples including the TTC samples and the TTC +digested samples were mixed with distilled water at mass ratio 1 to 3 starch to water. Onset temperature T_o , peak temperature T_p , conclusion temperature T_c , and retrogradation enthalpy ΔH_R of the samples were measured by thermal scanning of the samples from 20°C to 95°C at a heating rate of 10°C per minute with an empty pan as reference (Wang & Jane, 1994). The pan was pierced with a hole and placed in an oven at 105°C for 24 hours to determine dry matter content. Thermal characteristics were determined by TA Universal Analysis 2000 software supplied with the TA Instruments (New Castle, USA).

V.2.4 Water mobility

Parenchyma tissue of *cv. Agria* potato tubers were sampled longitudinally by cork borer ($\varnothing 3.4 \times 80$ mm, approximately 0.5 g), and these samples inserted into glass tubes of 5 mm outside diameter (Wilma-LabGlass) and sealed to prevent moisture loss. Water mobility of TTC-processed samples was measured by a Spinsolve 1.5 LF-NMR spectrometer (Magritek Ltd.) with operating resonance frequency at 42.5 MHz. Before every measurement, samples were equilibrated at 25°C for 30 minutes. The transverse relaxation time T_2 was acquired by the Spinsolve®Carbon apparatus built-in program T_2 bulk function using the Carr-Purcell-Meiboom-Gill sequence (CPMG). The apparatus parameter setup was as previously reported (Chen, Singh, & Archer, 2018). Raw data were transformed to a continuous relaxation time distribution curve by inverse Laplace transformation. Then the Lawson and Hanson NNLS analysis method in Prospa®v3.1 (Magritek Ltd., NZ) was used to calculate relaxation time T_2 . All measurements were done in triplicate.

V.2.5 Texture analysis

Following the sampling method of V.2.4, the hardness of TTC-processed potato cylinders ($\varnothing 8 \times 10$ mm) were analysed by texture analyser (TAXT Plus, Stable Microsystems, Surrey, UK) (Kaur, Singh, Singh, et al., 2007). Each sample was compressed by a flat platen of 17 mm diameter using a 5kg load cell. The crosshead speed was 20 mm/min and the maximum extent of deformation 30% of the original height. The hardness of the samples is defined as the maximum force of the first peak (Figure V.1). While the cohesiveness is defined as the area of the second compression divided by the area of the first compression, and the springiness is defined as the distance of the detected height during the second compression divided by the original compression distance (Figure V.1). The chewiness is the factor of hardness, cohesiveness, and springiness (Figure V.1) (Friedman, Whitney, & Szczesniak, 1963). Texture profile analysis (TPA) was performed in triplicate.



$$\text{Chewiness} = \text{Hardness} \times \text{Cohesiveness} \times \text{Springiness}$$

- Cohesiveness: the resistance of deformation
- Springiness: the ratio of original product height
- Chewiness (solid food)

Figure V.1 Definitions of the parameters of texture profile analysis.

V.2.6 Starch digestion *in vitro*

Simulated salivary fluid (SSF) was prepared according to Kong, Oztop, Singh, & McCarthy (2011). Simulated gastric buffer (SGF) and simulated small intestine buffer (SIF) were prepared according to the US Pharmacopeia (Pharmacopeia U.S, 1995, 2000). SSF contained α -amylase, SGF contained pepsin, and SIF contained pancreatin, invertase, and amyloglucosidase (Bordoloi, Singh, et al., 2012).

TTC processed potato chips (40g, same thickness as previous study (Chen et al., 2018)) were mixed with pre-warmed SSF at mass ratio 1:1 using a mini food processor (The Mini Wizz Food Chopper, Breville®) for two minutes (Tamura, Kumagai, & Ogawa, 2013; Tamura, Okazaki, Kumagai, & Ogawa, 2017). The resulting potato bolus samples (80g) were topped up to 170g with distilled water and placed in a polyethylene mesh (Chen et al., 2018; Tamura et al., 2016). Starch digestibility was measured by the glucose released after a certain time of simulated oral digestion and simulated gastric-small intestinal digestion. Glucose released after two minutes of oral mastication (O_2), thirty minutes of gastric digestion (G_0 and G_{30}) and two hours of small intestinal digestion (I_0 , I_5 , I_{10} , I_{15} , I_{30} , I_{90} , and I_{120}) were analysed by GOPOD reagent (Format K-GLUK 07/11, Megazyme International Ireland Ltd, Ireland) and the results were expressed as starch hydrolysis (%) (Tamura et al., 2016). Hydrolysis index (HI) of the samples was calculated as the area under the curve during simulated small intestinal digestion, using white bread as a reference. The estimated glycaemic index (eGI) was calculated by the equation: $eGI = 39.71 + 0.549HI$, (Goñi et al., 1997). All measurements were done in triplicate.

V.2.6.1 The particle size distribution of the potato digesta

Particle size distribution of digesta of TTC-processed potato tubers samples at different digestion stages was determined using laser diffraction particle size analysis (Mastersizer 2000, Malvern Instruments Ltd., UK). The relative refractive index applied was 1.70.

V.2.6.2 Microstructure TTC-processed tubers

Freeze-dried TTC-processed tubers taken from different digestion times and stages were photographed using a scanning electron microscope (FEI Quanta 200 FEI Electron Optics, Eindhoven, The Netherlands) at different magnifications and representative images were chosen. An accelerating potential of 20 kV was used during micrography.

V.2.7 Statistical analysis

Results are expressed as means \pm one standard deviation. Subsequently, an analysis of variance (ANOVA) with Tukey's test was used to determine significant differences among the means at a significance level of $p < 0.05$. The data were subjected to correlation analysis and Pearson correlation coefficients were calculated by Minitab Statistical Software version 13 (Minitab Inc., State College, PA).

V.3 Results and discussion

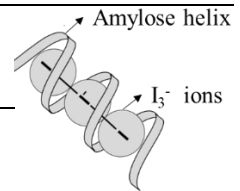
V.3.1 Total starch content, dry matter and blue value (BV)

Dry matter content of the potato tubers used was $23.5 \pm 3.1\%$, total starch content $70.8 \pm 1.2\%$ (d.b), and the amylose content $23.6 \pm 0.7\%$. BV was used qualitatively to reveal structural differences between samples. A deep-blue colour with maximum wavelengths (λ_{\max}) at 610 nm, and at 530–575 nm, indicate amylose-iodine complex (Rundle & French, 1943) and short amylopectin chain-iodine complexes (McGrance, Cornell, & Rix, 1998) respectively. The BV of raw potato sample was 1.3 (Table V.2) falling within the range reported for other native starches (Takeda, Hizukuri, Takeda, & Suzuki, 1987). Retrograded starch loses its ability to accommodate iodine to form blue complexes due to the formation of double-helical associations of 40-70 glucose units in retrograded amylose (Jane & Robyt, 1984). Moreover, the BV, reflecting the amount of soluble amylose in cooked potato, was found to decrease rapidly upon storage (Jankowski, 1992) as the aggregation of linear amylose became insoluble. Consistent with this, the BV of the 3-day retrograded sample (FCR3) was significantly lower than for freshly cooked samples (FC) ($p < 0.05$) (Table V.2). The BV of FCR3-t(4/-20/4) and FCR3-t(-20/4/4) were even lower than for FC (Table V.2). Freeze-chill cycles likely created starch-rich and starch-deplete regions, and hence impeded bonding of the starch-iodine complex. But there were no significant differences between the BV of FCR3, FCR3-t(4/-20/4), FCR3-t(-20/4/4), and FCR3-t(4/4/65). The lowest BV observed, for FCR3-t(4/65/4) (Table V.2) indicates the least formation of starch-iodine

complex. The TTC process of 4°C for a day may have allowed retrograding starch to form multiple nuclei; subsequent warming to 65°C then a further day at 4°C allowed these nuclei to grow further into larger aggregates. Therefore, the sporadic formation of nuclei in the retrograded starchy matrix led to its losing most of its ability to form starch-iodine complex (McIver et al., 1968).

Table V.2 Blue values of different time-temperature cycle processed potato samples.

	Raw	FC	FCR3	TTC1 FCR3- t(4/-20/4)	TTC1 FCR3- t(-20/4/4)	TTC2 FCR3- t(4/65/4)	TTC2 FCR3- t(4/4/65)
BV	1.3 ± 0.02 ^a	1.1± 0.1 ^b	0.9± 0.01 ^{cd}	0.8±0.02 ^{cd}	0.8±0.03 ^d	0.5 ±0.1 ^e	0.9±0.01 ^c



Different superscripts in the same row indicate significant differences ($p < 0.05$) ($n = 3$).

V.3.2 Thermal characteristics of TTC-processed potato tuber

The first peak temperature in the derivative curve of heat flow of gelatinised potato tuber starches was defined as the specific glass transition temperature (Sang, Alavi, & Shi, 2009; Wang & Jane, 1994) T_g' , -0.9°C, and the onset temperature of ice melting temperature T_m' was -2.5°C (

Figure V.2).

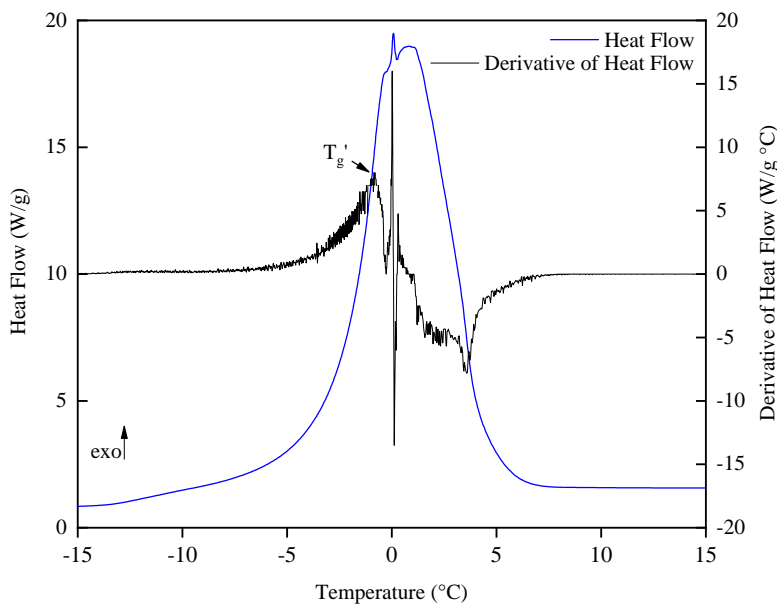


Figure V.2 Endotherm curve of potato tuber and its derivative curve.

When the storage temperature (T) of cooked potato tubers drops below the ice melting temperature, water in the starchy matrix progressively freezes to ice and the motion of gelatinised amylose and amylopectin is restricted (Yu, Ma, Zheng, Liu, & Sun, 2012). At this point, removal of water into ice crystal concentrates the solutes in the matrix. This results in alternating starch-deplete regions (ice) and starch-rich regions (Colwell, Axford, Chamberlain, & Elton, 1969). Later on during storage at 4°C, the starch-rich region might facilitate retrogradation (Kim, Muhrbeck, & Eliasson, 1993). Indeed, Table

V.3 shows the retrogradation enthalpy of the TTC1 samples to be significantly higher than for FCR3 ($p < 0.05$).

Retrogradation is likely to proceed as a crystallisation sequence of nucleation, propagation then maturation, each with temperature dependencies either thermodynamic or kinetic (Slade & Levine, 1987). We considered retrogradation likely to be accelerated if nucleation occurs at low temperature, and subsequent storage close to melting temperature is likely to enhance crystal growth rate (Slade & Levine, 1987). However, the retrogradation transition peak temperature T_p of FCR3 samples were higher than TTC2 samples. The retrogradation enthalpy ΔH_R of FCR3 samples and FCR3-t(4/65/4) and FCR3-t(4/4/65) samples showed no significant difference (Table V.3) where the signature of endothermal curves for TTC2 were not as obvious as for TTC1 samples (Figure V.3). It might be because there is also an optimum duration for nucleation and propagation to maximize retrogradation.

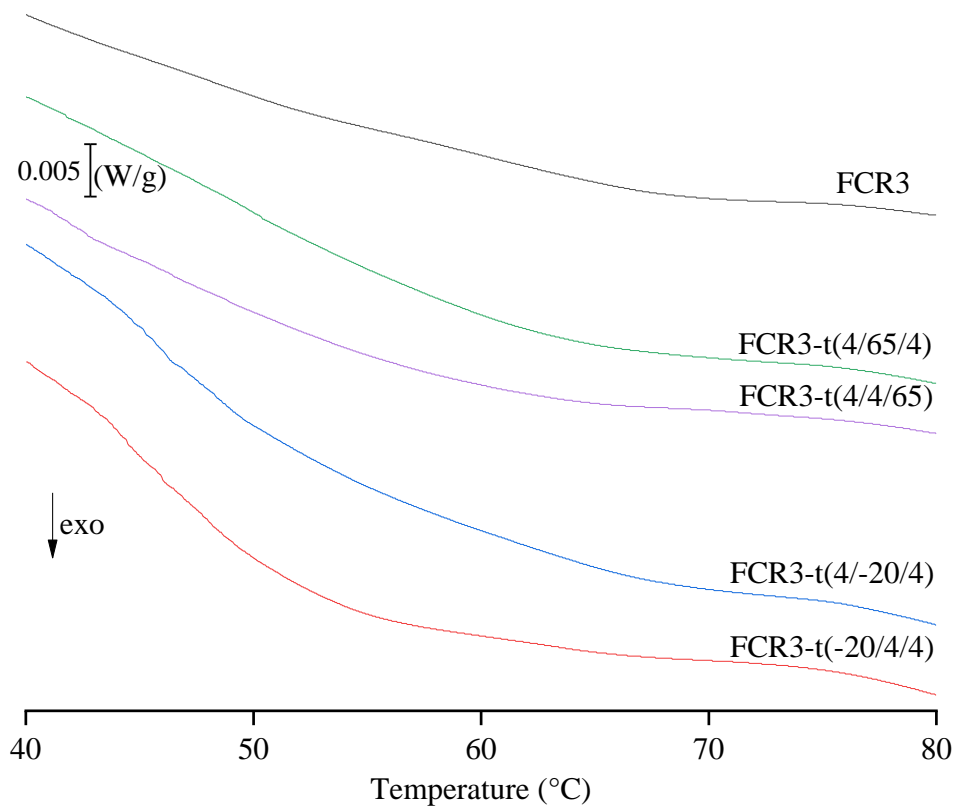


Figure V.3 Endothermal curves of 3-day retrograded tuber and TTC processed potato tubers.

Overall, retrogradation peak temperatures T_p of TTC1 chill-retrograded samples were significantly lower than for 3-day warm-retrograded TTC2 samples, which may imply the TTC1 retrograded starches were less compact than the sporadic nuclei of TTC2 retrograded starch. But the retrogradation enthalpies of FCR3-t(-20/4/4) samples were significantly higher than FCR3 and TTC2 samples which might show that, even though the structure were loose, there was overall more aggregation of retrograded starch. It might be that recrystallization of amorphous starch during chill storage was enhanced by prior freeze-concentration. Molecular mobility was enhanced by unfrozen water and

consequently, molecular rearrangements for nucleation could take place (Ronda & Roos, 2008) during the later stages of two-day storage at 4°C of FCR3-t(-20/4/4) samples.

Table V.3 Thermal characteristics of time-temperature cycle treated potato starch *in tuber*.

Process	Samples	T _o (°C)	T _p (°C)	T _c (°C)	T _c -T _o (°C)	ΔH _R (J/g d.b.)
	Raw	65.9 ±0.2 ^a	68.3±0.1 ^a	74.5 ±1.3 ^a	8.6 ±1.3 ^b	12.7 ±2.0 ^a
	FC	-	-	-	-	-
	FCR3	47.0 ±1.5 ^b	64.4 ±0.9 ^b	74.4 ±0.9 ^a	27.5 ±0.9 ^a	1.6 ±0.4 ^c
TTC1	FCR3-t(-20/4/4)	43.8 ±0.7 ^b	54.3 ±0.8 ^d	73.9 ±1.4 ^a	30.1 ±2.1 ^a	4.7 ±0.6 ^b
TTC1	FCR3-t(4/-20/4)	44.7 ±0.4 ^b	56.3 ±0.5 ^d	75.7 ±0.8 ^a	31.0 ±0.9 ^a	3.8 ±0.7 ^b
TTC2	FCR3-t(4/65/4)	46.5 ±2.2 ^b	60.7 ±2.0 ^c	75.6 ±0.9 ^a	29.1 ±3.0 ^a	2.3 ±0.9 ^{bc}
TTC2	FCR3-t(4/4/65)	46.8 ±0.3 ^b	60.4 ±2.2 ^c	74.0 ±3.4 ^a	27.1 ±3.3 ^a	2.2 ±0.8 ^{bc}

Different superscripts in the same column indicate significant differences (n=3, *p*< 0.05).

V.3.3 Water mobility of TTC processed potato tubers

There are four water pools in potato (i.e. water within the starch double helices of crystalline regions, in the amorphous region of amylose and amylopectin, loosely associated with the gelatinised starchy matrix, and within potato tuber cell cytoplasm). Different relaxation times T₂₀, T₂₁, T₂₂, and T₂₃ can be discerned in freshly cooked potatoes (FC) (Figure V.4a) (Chen et al., 2018).

The merging of water pools with relaxation time T₂₁ and T₂₂ was evident in TTC1-processed potatoes (Figure V.4b), which might be due to ice crystals damaging potato cells allowing extracellular and intracellular water to mix (Micklander et al., 2008). Simultaneously water congregates as ice at low temperatures creating zones within the tuber of frozen water fully dissociated from starch. The combined effects of the cellular structural changes and the changing concentration of starch within the matrix would have altered the water mobility of different water pools. As molecular movement at temperatures below the glass transition temperature were restricted, the crystallization of retrograded starch may not complete within a finite duration (Levine & Slade, 1988). Once the temperature was increased to 4°C during the freeze-chill cycle, starch retrogradation was impacted by water redistribution - nucleation may have been facilitated within the starch-rich, water-lean region leading to enhanced starch retrogradation overall. Tubers stored at -20°C for a day and then 4°C for two days, FCR3-t(-20/4/4) had the lowest relaxation time T₂₂ (Figure V.4b). This might point to a higher level of retrogradation because the relaxation time T₂₂ has been shown to correlate negatively with the enthalpy of retrogradation (Chen et al., 2018). A similar effect was observed in frozen bread as the level of starch retrogradation was higher when subjected to temperature fluctuation between -18°C and 4°C (Ronda et al., 2011).

The TTC2 cycle process was set to maximize both nucleation and propagation of starch retrogradation at temperatures between T_g' and T_m'. The relaxation time T₂₂ of FCR3-t(4/65°C 24hrs/4) was lower than for FCR3-t(4/65°C 30hrs/4) and FCR3-t(4/65°C 6hrs/4) (Figure V.4c) which might indicate that the 3-day storage condition of FCR3-t(4/65°C 24hrs/4) was nearest the optimum condition

for recrystallization. Lu et al. (1997) showed a smaller molecular subfraction of retrograded amylose entangled at 45°C than 25°C indicating starch propagation. Therefore, another three sets of TTC2 processes were performed with 3-day storage at (i) 4°C refrigeration (FCR3), at (ii) 4°C refrigeration then 25°C water bath (TTC-4/25), and at (iii) 4°C refrigeration then 65°C water bath (TTC-4/65) (Figure V.4d). The relaxation time T_{22} of FCR3-t(4/65/4) was lower than FCR3-t(4/25/4) (Figure V.4d) showing a higher level retrogradation. This might be due to a higher propagation temperature of TTC2 process giving enough molecular mobility to allow starch to rearrange its structure. The relaxation time T_{22} of FCR3-t(4/4/65) was the highest observed indicating that a relatively long nucleation period i.e. 4°C for two days and then propagation at 65°C for a day failed to promote substantial starch retrogradation (Figure V.4d).

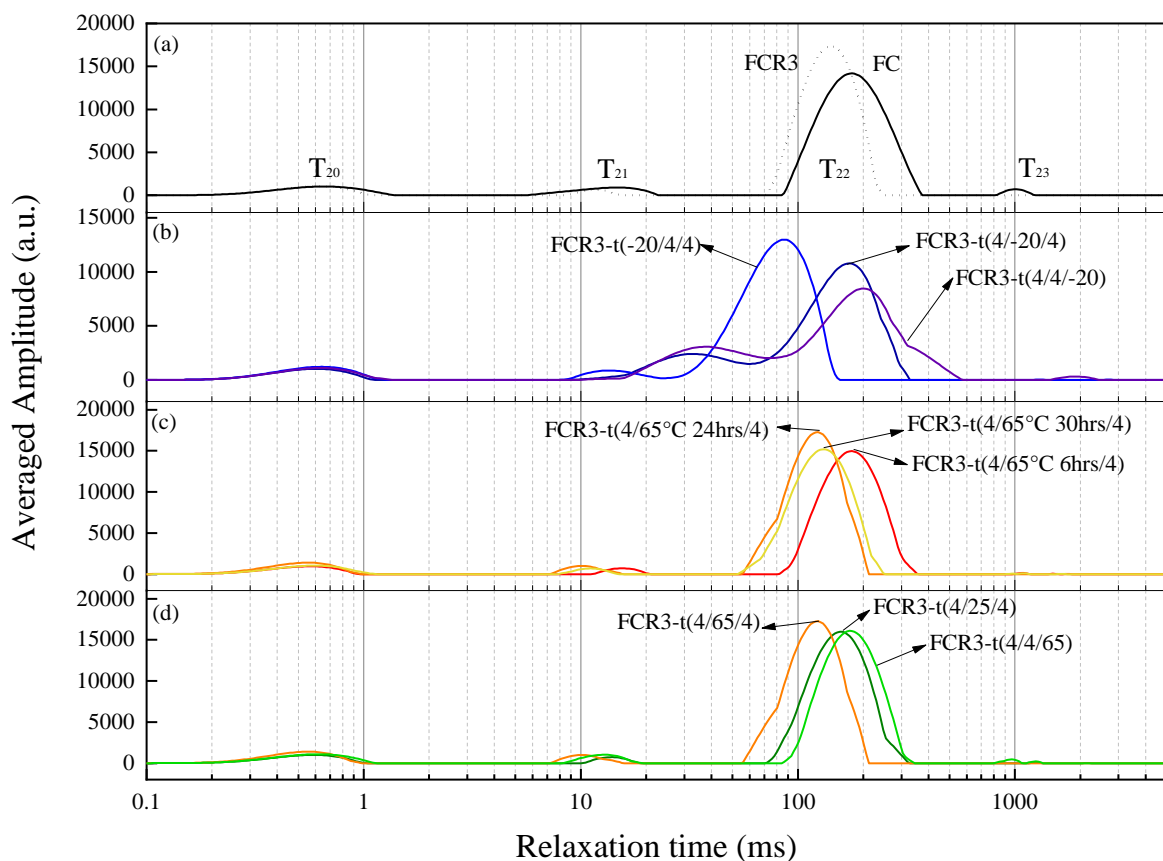


Figure V.4 Water pool profiles of (a) freshly cooked potato tubers, FC, and 3-day retrograded potato tubers, FCR3, and (b) TTC1-processed potato tubers, (c) TTC2-processed potato tubers, and (d) TTC-4/25 and 4/65 potato tubers.

V.3.4 Texture profile analysis

Texture profiles of TTC1 and TTC2-processed tubers revealed effects of the temperature fluctuations imposed during cooking and cold storage (Table V.4). The hardness and the cohesiveness of the raw tuber samples decreased after cooking (Table V.4). Cooking is known to soften the texture of potatoes because of starch gelatinisation and the rounding-off of cells by internal turgor pressure

(Shomer, 1995). Besides, thermal β -eliminative degradation of pectin in the middle lamella causes cell separation and permits cells to distend spontaneously (Matsuura-Endo, Ohara-Takada, Yamauchi, Mukasa, et al., 2002). Chill storage at 4°C of starchy food such as potato tubers was found to increase the hardness (Jankowski, 1992), however, the hardness of the freshly cooked samples was harder than FCR3 and the TTC1 samples (Table V.4). Freezing was shown to reduce the hardness of potatoes due to the loss of orderly cellular arrangement and deformation caused by intracellular and extracellular ice crystals (Sun & Li, 2003). Hence, the hardness of the TTC1-processed cylinders was significantly lower than for TTC2-processed cylinders ($n=3, p<0.05$) (Table V.4). However, the cohesiveness, i.e. the ability of the TTC1-processed cylinders to resist deformation between two compressions, was higher in TTC1 than for TTC2 samples, consistent with a coherent sponge-like structure. Springiness of all samples was similar. The high springiness recorded for FCR3 is an artefact of the potato cylinder adhering to the retracting probe in the second compression (Table V.4). The chewiness score (derived from hardness, cohesiveness, and springiness), was least in the FCR3 samples (Table V.4) indicating the temperature fluctuation of TTC probably changed the cellular structure.

Table V.4 Texture profile analysis of 3-days retrograded potato tubers under different time-temperature cycles process.

Process	Samples	Hardness (N)	Cohesiveness (%)	Springiness (%)	Chewiness (J)
	Raw	41.5 ± 0.7 ^a	49 ^b	69 ^b	14.0 ± 0.2 ^a
	FC	12.0 ± 0.3 ^b	23 ^d	66 ^b	1.8 ± 0.2 ^c
	FCR3	1.0 ± 0.1 ^d	16 ^d	120 ^a	0.2 ± 0.1 ^e
TTC1	FCR3-t(-20/4/4)	2.3 ± 0.3 ^d	59 ^a	76 ^{ab}	1.0 ± 0.1 ^d
TTC1	FCR3-t(4/-20/4)	2.0 ± 0.1 ^d	58 ^a	80 ^{ab}	0.9 ± 0.1 ^d
TTC2	FCR3-t(4/65/4)	10.8 ± 0.4 ^{bc}	32 ^c	76 ^{ab}	2.3 ± 0.2 ^b
TTC2	FCR3-t(4/4/65)	10.1 ± 0.7 ^c	36 ^c	87 ^{ab}	3.2 ± 0.6 ^b

Different superscripts in the same column indicate significant differences ($n=3, p<0.05$).

V.3.5 Starch hydrolysis (%) and estimated glycaemic index

The starch hydrolysis (%) curves of TTC-processed tubers are shown in Figure V.5. Measurement of the ease of starch digestion started with two minutes of simulated oral digestion where potato tubers were blended with SSF in mass ratio 1:1. α -Amylase is generally well integrated within the food bolus during this simulated oral processing and continues to release some glucose during gastric digestion (Rosenblum, Irwin, & Alpers, 1988; Tamura et al., 2017). However, starch hydrolysis (%) observed during the full digestion process ranged from 1-10% across the samples (Figure V.5) implying differences in ease of access to starch locally within the bolus. After 5 minutes of simulated small-intestinal digestion, starch hydrolysis of the FC tubers, at 76.3% was higher than for the TTC1-processed tubers (e.g. FCR3-t(-20/4/4), 37.7% and FCR3-t(4/-20/4), 39%) and for TTC2-processed tubers (e.g. FCR3-t(4/65/4), 40% and FCR3-t(4/4/65), 51.2%) (Figure V.5). This is consistent with rapidly digestible starch of FC (78.4%) being more abundant than in TTC-processed tubers (FCR3-t(-

20/4/4), 56.1%, FCR3-t(4/-20/4), 58.7%, FCR3-t(4/65/4), 51.6%, and FCR3-t(4/4/65), 58.9%) (Xie et al., 2014; Yadav, Sharma, & Yadav, 2009).

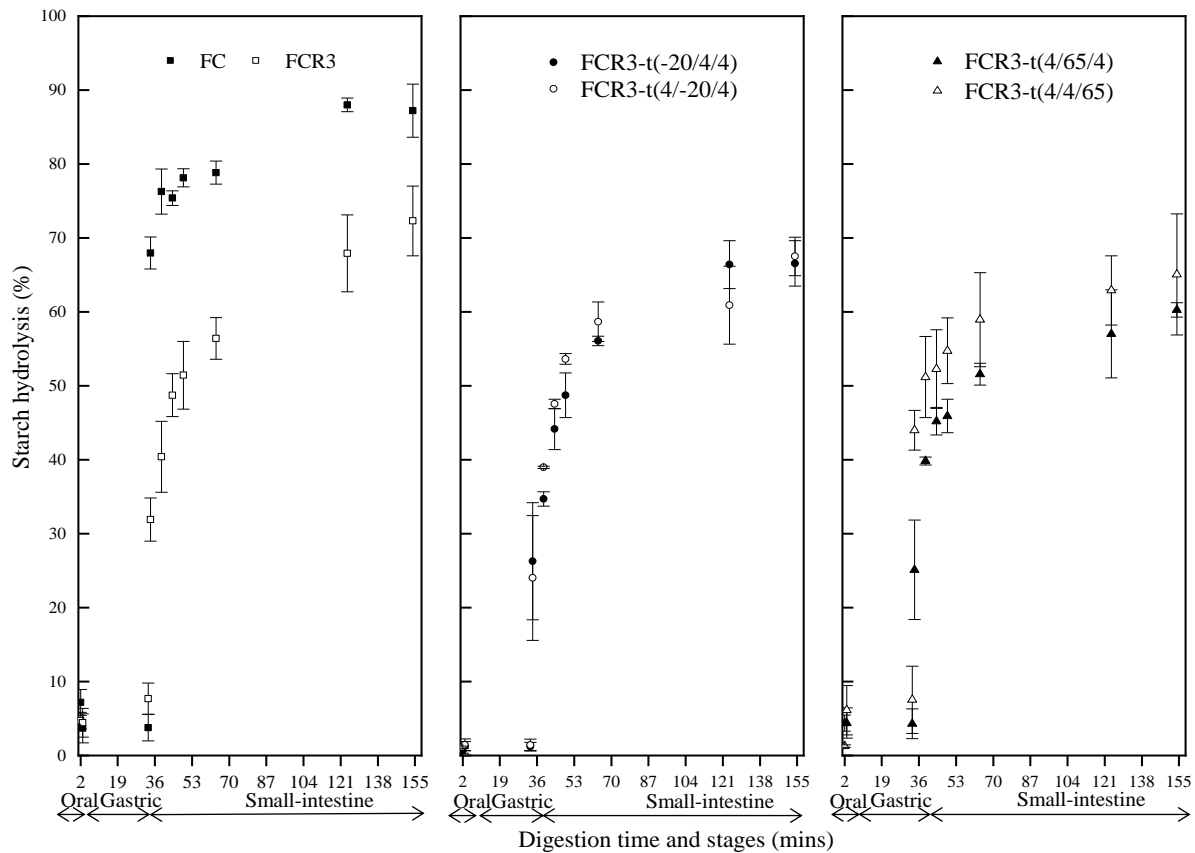


Figure V.5 Starch hydrolysis (%) of 3-day retrograded tubers, TTC1-processed tubers, and TTC2-processed tubers. Error bars represent standard deviation (n=3).

Starch hydrolysis (C_{∞} experimental), hydrolysis index (HI), and estimated glycaemic index (eGI) are shown in Table V.5. The HI of FC exceeded 100% as the white bread was used as reference (Chen et al., 2018; Goñi et al., 1997) and the AUC of bread was less than freshly cooked potato tuber. There were no significant differences between the experimental C_{∞} of 3-day retrograded samples, the TTC1-processed tubers, and the TTC2-processed potato tubers (Table V.5). This implies that the effect of TTC1 and TTC2 on cellular structure might make the processed starch equally vulnerable to enzymatic breakdown compared to 3-day retrograded samples even though TTC1-processed tubers showed a higher level of retrogradation (i.e. higher ΔH_R and lower T_{22}). Similarly, there were no significant difference of the HI and the eGI of the 3-day retrograded tubers, the TTC1 processed tubers, and the TTC2-processed tubers (Table V.5). There is potential for TTC1 to make big lumps recruiting more starch into retrograded structures, whereas TTC2 might make lots of small crystallites with much surface area for a small amount of retrograded starch - both time-temperature processes could result in similar starch hydrolysis behaviour as FCR3.

Table V.5 Starch hydrolysis (C_{∞} experimental), hydrolysis index (HI), and estimated glycaemic index (eGI) of TTC-processed potato tubers.

Process	Samples	C_{∞} experimental (%)	HI	eGI
	FC	87.2 ± 4.4^a	132.1 ± 0.7^a	112.3 ± 0.4^a
	FCR3	72.3 ± 5.8^{ab}	98.2 ± 6.0^b	93.6 ± 3.3^b
TTC1	FCR3-t(-20/4/4)	66.6 ± 4.3^b	92.7 ± 5.1^b	90.6 ± 2.8^b
TTC1	FCR3-t(4/-20/4)	63.1 ± 8.1^b	87.0 ± 9.8^b	87.5 ± 5.4^b
TTC2	FCR3-t(4/4/65)	65.1 ± 10.0^b	97.3 ± 9.2^b	93.1 ± 5.0^b
TTC2	FCR3-t(4/65/4)	60.3 ± 1.2^b	85.1 ± 5.4^b	86.5 ± 3.0^b

C_{∞} , experimental starch hydrolysis (%) after 2 hours of simulated small-intestinal digestion; HI, hydrolysis index; eGI , estimated glycaemic index. Different superscripts in same column indicate significant differences ($p < 0.05$) ($n=3$).

V.3.5.1 The particle size distribution of the potato digesta

The median diameter ($d_{0.5}$) of digesta particles of TTC-processed tubers, measured by laser light diffraction, ranged from 0.15mm to 0.2mm (Figure V.6). The bimodal peaks of the particle size distribution curves (Figure V.6a) are comparable to mastication results (Hoebler et al., 2000). The volume represented by large particles (12.7-15.9%) (Figure V.6c) was generally greater than the volume of small particles (0.5-1.5%) (Figure V.6b). For the freshly cooked samples, FCR3-t(4/-20/4) samples, FCR3-t(-20/4/4) samples, and FCR3-t(4/4/65) samples, the integrated volume of the small particle sizes increased and the volume of the large particle sizes decreased by the end of the simulated small-intestinal digestion (Figure V.6b & 3c) which is consistent with the increase in starch hydrolysis (%) during simulated gastric small-intestinal digestion. For FCR3, the integrated volume of both the large particles (Figure V.6b) and the small particles (Figure V.6c) decreased which might reflect the texture profiles such as the lower cohesiveness/chewiness and the higher springiness. For FCR3-t(4/65/4), the bimodal particle size distribution of the bolus of FCR3-t(4/65/4) changed to a unimodal particle distribution curve with a shoulder at 43 μ m at the end of the digestion (Figure V.6b & 3c). This might indicate competition between digestion of small, high surface area particles, and fission of larger particles into smaller ones.

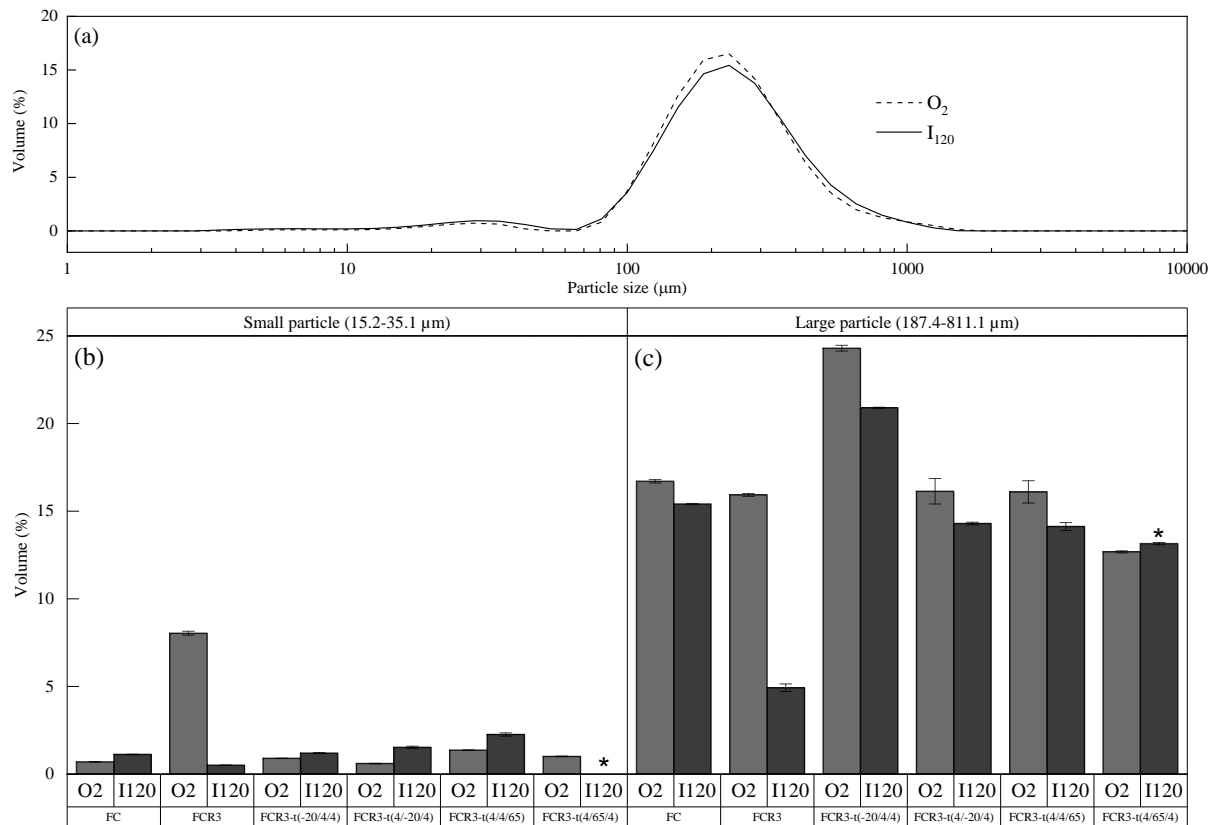
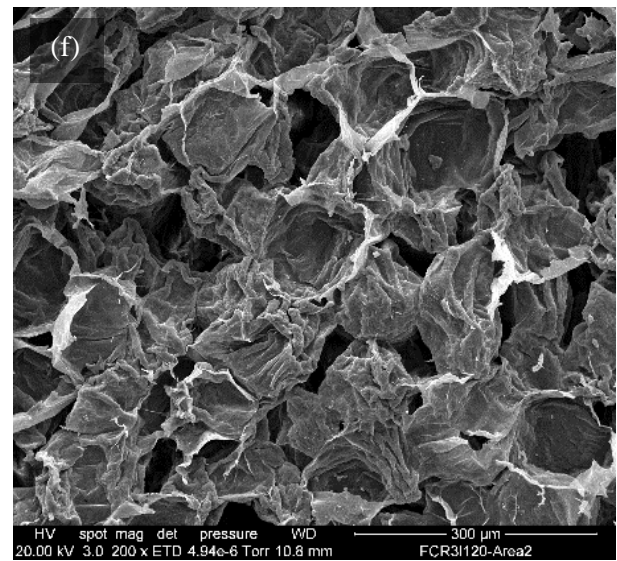
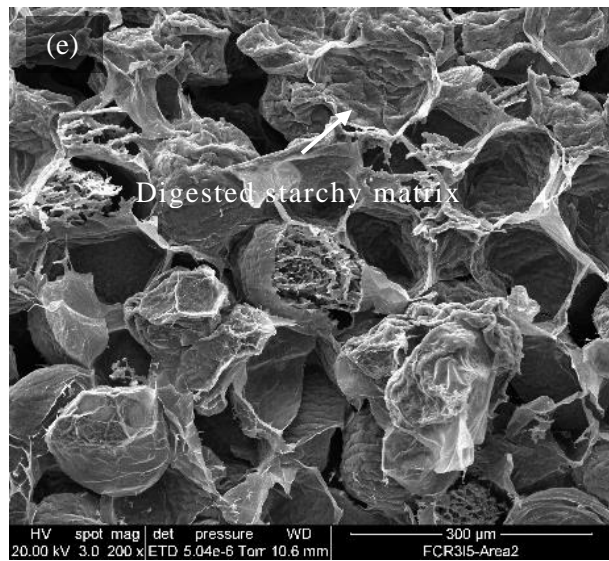
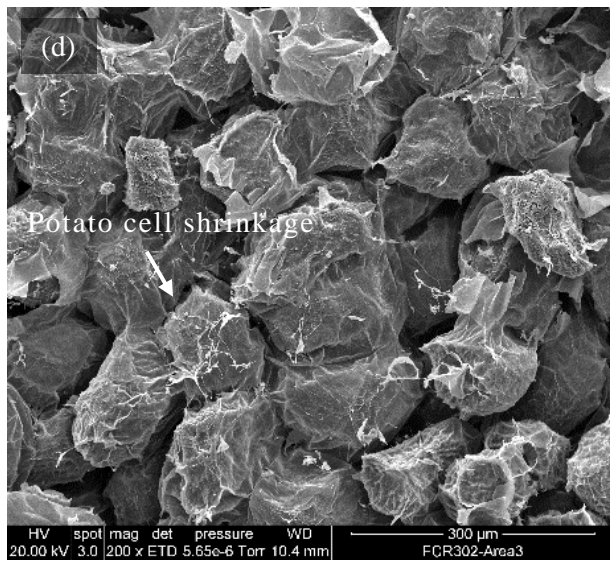
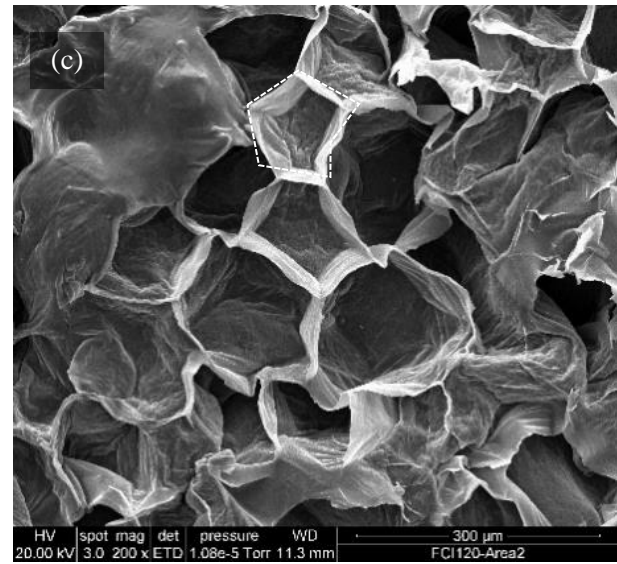
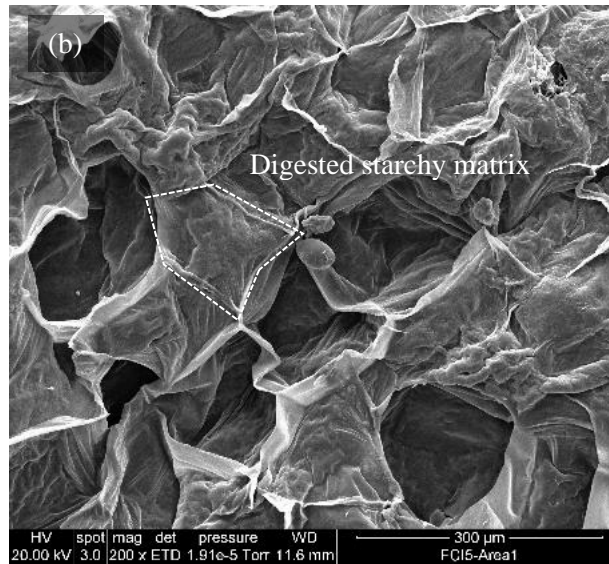
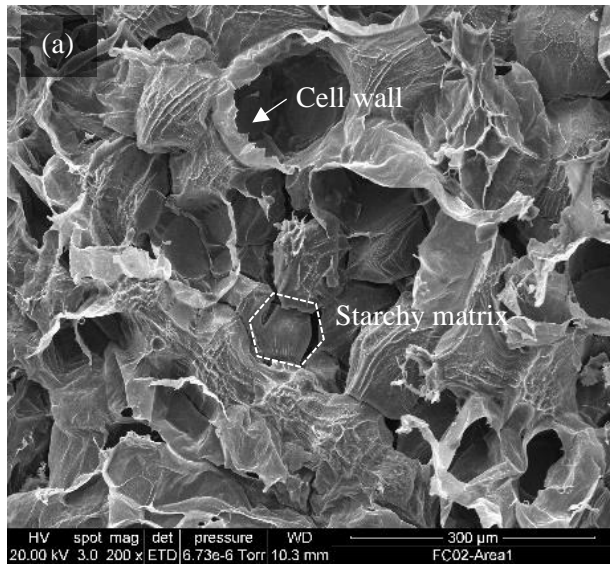


Figure V.6(a) Particle size distribution curves of bolus (O_2 , ---) and digesta (I_{120} , -) of freshly cooked potato tubers, and (b) the volume changes of small particles and (c) the large particles of different samples during and after digestion. *The particle size distribution of the digesta I_{120} of FCR3-t(4/65/4) was a unimodal curve with a shoulder at $43\mu\text{m}$. And error bars indicate the standard deviation of triplicate results.

Microstructural changes of FC (Figure V.7a,b,c), FCR3 (Figure V.7d,e,f), and TTC (Figure V.7g,h,i,j,k,l) processed tubers were revealed by SEM. From left to right, Figure V.7 shows SEM images of samples after 2 minutes of simulated oral digestion (O_2), and after 5 minutes (I_5) and 120 minutes (I_{120}) of simulated small-intestinal digestion. Increased cavities can be seen in the digested starchy matrix (Figure V.7b,e,h,k), especially for freshly cooked samples after simulated oral and gastric small-intestinal digestion. This might be due to *in vitro* digestion (Tamura et al., 2016) or removal of water during freeze-drying, causing shrinkage and wrinkles (Lopez-Rubio, Flanagan, Shrestha, Gidley, & Gilbert, 2008). In contrast to the cell shrinkage (Figure V.7d,j), the rounded-off potato cells of FCR3-t(-20/4/4) (Figure V.7g) might be due to the freezing right after cooking preventing moisture loss during storage (De Kock, Minnaar, Berry, & Taylor, 1995; Szymońska, Krok, & Tomasik, 2000). But ice crystal formation within the starchy matrix can weaken resistance to enzymatic breakdown yielding the uneven surface visible after digestion. TTC-processed samples appear to have more cell debris and starchy matrix remaining after digestion (Figure V.7i.l).



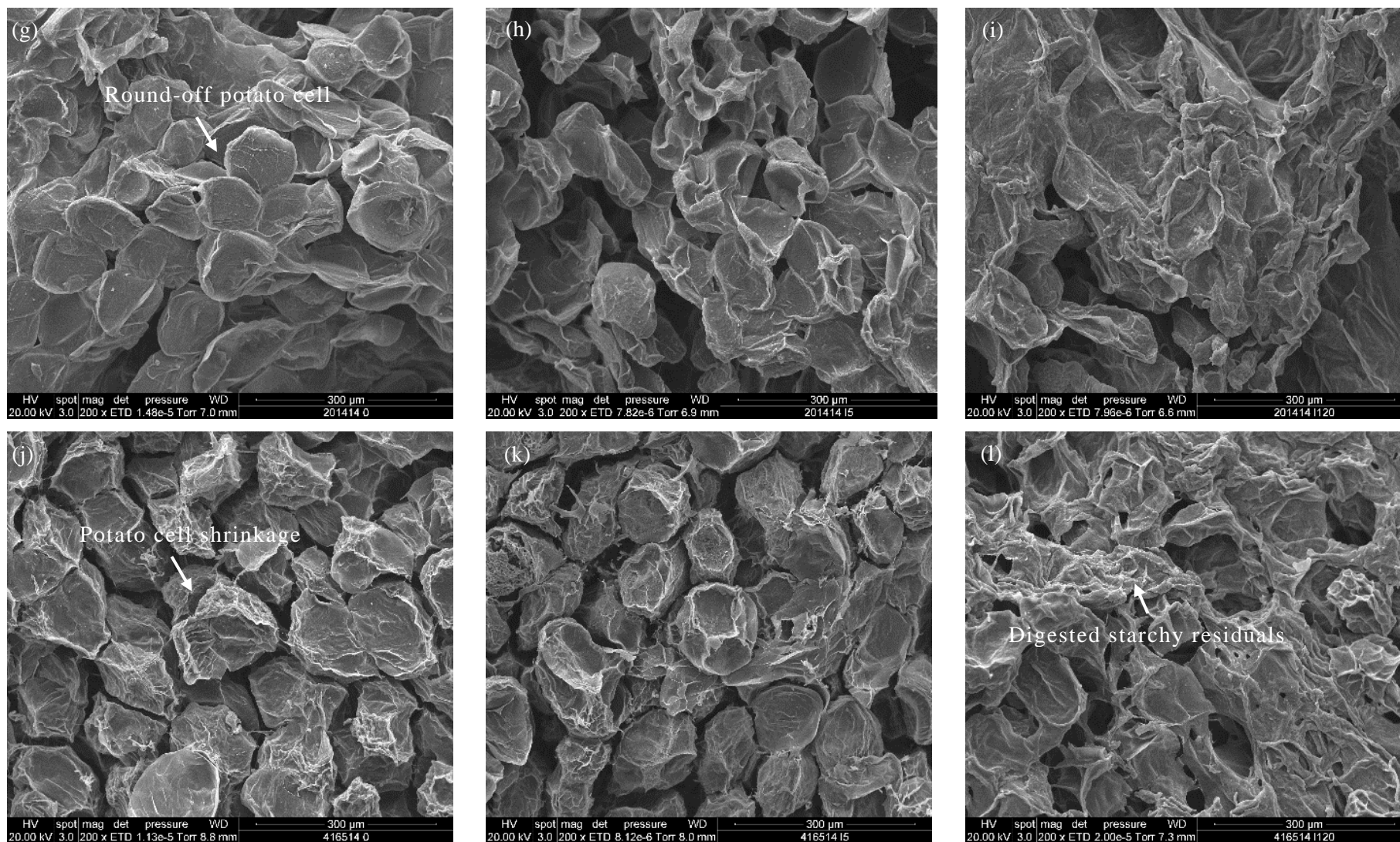


Figure V.7 SEM images of freshly cooked potato tubers digesta at O_2 (a), I_5 (b), and I_{120} (c); and 3-day retrograded tubers digesta at O_2 (d), I_5 (e), and I_{120} (f); and FCR3-t(-20/4/4) digesta at O_2 (g), I_5 (h), and I_{120} (i); and FCR3-t(4/65/4) digesta at O_2 (j), I_5 (k), and I_{120} (l).

V.3.5.2 Thermal characteristics of TTC digesta

Enthalpies of the remnants after the simulated oral-gastric-small intestinal digestion of raw tubers, freshly cooked tubers, 3-day retrograded tubers and TTC-processed tubers were measured by DSC (Table V.6). The retrogradation enthalpies of FCR3 and TTC digesta might reflect the abundance of starch crystallites remaining in the SDS, which would be a mix of amorphous and semi-crystalline material. The TTC process probably altered the distribution of starchy matrix in parenchyma cells resulting in SDS less prone to complete digestion (Guraya, James, & Champagne, 2001). A two-way ANOVA was run on 20 samples with replicates to examine the effect of TTC processes and digestion stages and time on retrogradation enthalpies. There was a significant interaction between the effects of TTC processes and of digestion stage on retrogradation enthalpies of the digesta, $F(12, 20) = 2.79$, $p = .021$. Simple main effects analysis showed that TTC processes affected retrogradation enthalpy of digesta more than did the digestion stage ($p < 0.05$). This might indicate that the formation of slowly digestible starch (SDS) through a TTC process unless disrupted in the oral cavity by salivary α -amylase, is not greatly prone to subsequent attack by gastric acid or other digestive mechanisms. Usually, SDS is mostly hydrolysed by enzymes secreted from the pancreas and is converted into small linear oligomers and α -limit dextrins in the small intestine (Lehmann & Robin, 2007b).

Table V.6 Retrogradation enthalpies of the TTC digesta samples (J/g d.b.) at different digestion time and stages.

		Undigested	Digestion time and stage			
			O ₂	G ₃₀	I ₅	I ₁₂₀
Raw		10.6 ±0.3	10.1 ±0.3	9.3 ±2.5	8.7 ±1.8	11.7 ±2.2
FC		1.1±0.0	1.3 ±0.3	2.2 ±0.5	1.8 ±0.9	0.2 ±0.1
FCR3		3.5±0.2	4.0 ±0.6	1.1 ±0.2	1.7 ±0.4	0.7 ±0.3
TTC1	FCR3-t(-20/4/4)	4.7±0.2	1.8 ±0.4	3.8 ±0.6	2.0 ±0.7	3.4 ±0.8
TTC2	FCR3-t(4/65/4)	3.4±0.1	4.2 ±0	2.5 ±1.3	0.9 ±0.4	1.9 ±1.0

V.4 Conclusion

A graphical precis of results obtained is in the Table V.7 where the relative starch crystalline structure were indicated by the numbers of the star- higher numbers of stars indicate more quantities of crystalline structure. Several, but not all, of the time-temperature cycle processes tested facilitated starch retrogradation *in tuber* more than did storage fixed at 4°C (FCR3) (Table V.7). The TTC1 process increased the retrogradation enthalpy and decreased water mobility, signifying that starch-rich and starch-depleted regions may have facilitated the formation of retrograded starch in starch-rich regions (Table V.7). TTC2-processed tubers held under chill and warm conditions showed the lowest blue value and starch digestibility *in vitro* (Table V.7). TTC processed tubers subsequently exposed to digestive enzyme *in vitro* showed, at 60-67%, lower extent of starch hydrolysis than either tubers retrograded for 3-days at 4°C (72%) or freshly cooked potato tubers (87%). These two sets of time-temperature

processes induced starch retrogradation *in tuber* differently though all such samples showed higher retrogradation enthalpies and lower starch digestibility where a negative correlation ($r=-0.65$, $p=0.005$) was obtained. The residual retrogradation enthalpies of digesta of TTC processed tubers suggest the formation of slowly digestible starch. Similar time-temperature cycle processes may be useful to the drive physicochemical changes of the potato product within the industrial cold chain.

Table V.7 Summary of all time-temperature cycle processes (left) and the relative level of starch crystalline structure implied by the test method was indicated by the number of stars (right).

Process	Code	Blue value	Thermal properties	Relaxation time T ₂₂	<i>In vitro</i> digestion	Digesta thermal	Digesta PSD
	Raw	*****	*****	*****	*****	*****	*****
	FC	**	*	**	**	**	**
TTC1	FCR3-t(-20/4/4)	****	****	*****	***	****	**
TTC1	FCR3-t(4/-20/4)	****	****	**	***	—	**
	FCR3	***	****	*****	***	**	***
TTC2	FCR3-t(4/65/4)	*****	***	***	***	***	***
TTC2	FCR3-t(4/4/65)	***	***	**	***	—	**

* The higher numbers of stars indicate more quantities of crystalline structure as indicated by each method. PSD, particle size distribution.

Chapter VI Starch retrogradation of *sous vide* processed potato tubers and oral-gastric-small intestinal starch digestion *in vitro*

VI.1 Introduction

Sous vide, known as *cuisine en papillote sous vide*, is a process where raw food is vacuum-sealed in a plastic pouch and cooked under controlled temperature. *Sous vide* cooked vegetables can give fresh-like taste and retain more nutrient than conventionally cooked vegetables (Iborra-Bernad, García-Segovia, & Martínez-Monzó, 2015; Kosewski et al., 2018). The development of *sous vide* product has great potential owing to the growing ready-meal (Euromonitor International, 2017b, 2017a). A *sous vide* catering system consists of *sous vide* cooking, rapid chilling, chilled storage, and reheating before serving (Sheard & Rodger, 1995; SVAC, 1991). The safety of *sous vide* products requires special attention due to the lower cooking temperatures than those used for conventional cooking. The recommended thermal process for *sous vide* cooked vegetables is 90°C for 10 minutes at the centre or its time-temperature equivalent to ensure a sufficient Pasteurization, such as a 6-log₁₀ reduction in psychrotrophic *Clostridium botulinum* and *Listeria monocytogenes*, or a 3-log₁₀ reduction in *Salmonella* species (Schellekens, 1996). The recommended chilled storage period is <5 days at <5°C owing to the potential temperature abuse in the chill chain, where botulinum spores could grow in the product and produce a potentially lethal toxin (New Zealand Food Safety, 2017).

Sous vide cooking is usually done at controlled temperatures for an extended period of time up to 72 hours with a shock heat burst before rapid chilling and chill /frozen storage to enhance shelf life. Optimising the time and temperature of a *sous vide* cooking process is the key to the desirable texture (Kadam, Tiwari, & O'Donnell, 2015). For traditionally cooked potato, cell wall separation and starch gelatinisation are two main changes in potato tissue contributing to the textural properties (Bartolome & Hoff, 1972b). *Sous vide* cooking softens vegetables by dissolving pectic material that cements the cells together but leaving the cell walls mostly intact. Composition of pectic material being abundant in the plant middle lamella is dependent on both enzymatic (Van Dijk, Fischer, Beekhuizen, Boeriu, & Stolle-Smits, 2002) and nonenzymatic reactions (Warren & Woodman, 1974). Pectin hydrolysis to demethylated pectin chains is catalysed by pectinases, such as polygalacturonases (PGs), pectin lyase (PL), and pectin methylesterases (PMEs) at low temperature (30-70°C) (Gummadi & Panda, 2003). The unesterified carboxyl groups can then link via calcium inter-chelation into egg box structures resulting in strengthening cell wall. The proton released may, on the other hand, stimulate the activity of cell wall hydrolases thus weakening the cell wall. Low-temperature blanching (LTB) from 50°C to

70°C is known to tailor the desired texture of potato product via selective denaturation of endogenous pectic hydrolases (Alessandrini, Romani, Rocculi, Sjöholm, & Rosa, 2011; García-Segovia, Andrés-Bello, & Martínez-Monzó, 2008). For instance, a stepwise LTB that increases the firmness of French fries is desirable (Kadam et al., 2015; Torres & Parreño, 2016) due to cross-linked pectate formation reducing sloughing and optimising oil uptake (Abu-Ghannam & Crowley, 2006; Yemenicioğlu, 2015; Yildiz & Wiley, 2017).

Annealing is a process whereby a partially crystalline material is held at a temperature below its melting temperature but above the glass transition temperature (Jayakody & Hoover, 2008). This permits a modest molecular reorganisation to occur and a more organized structure of lower free energy to form (Hoover & Vasanthan, 1993). The annealing temperature was often chosen as a function of the gelatinisation temperatures of the native starches, i.e., 3 to 4% below the gelatinisation peak temperature in Kelvin determined by DSC (Jacobs et al., 1995). When starch is gelatinised sufficiently (which will be associated with desirability to eat), the starch will be converted to glucose easily and have a correspondingly high glycaemic response. Hydrostatic pressure processed+retrograded potato starch has been shown to have greater resistance to digestive enzymes breakdown (Colussi, Kaur, et al., 2017). Two temperatures at below gelatinisation temperature (55°C) and at near to gelatinisation temperature (65°C) were, therefore set to study the effect of *sous vide* cooked starch *in tuber*.

The work reported below sought to use *sous vide* to achieve a process akin to annealing, resulting in potato pieces with good eating properties but significant resistance to digestive enzymes. Physicochemical properties of *sous vide* processed then refrigerated *cv. Agria* were studied to investigate the effect of *sous vide* on starch retrogradation *in tuber*. This included relative crystallinity measurements by XRD and thermal characteristics by DSC, as well as characterisation of structural changes of starch granules in potato cells by LF NMR. Potato *cv. Nadine*, a fairly firm and multi-purpose type, was *sous vide* processed and studied parallelly to investigate the influence of compositions and microstructure in different potato tubers. Wedges made from potato *cv. Agria* was vacuum-packed and cooked at low temperature (55°C and 65°C) for an extended period of time (10min to 48h) then refrigerated at 4°C and reheated at 60°C. The ease of starch digestibility of *sous vide* cooked potato was investigated by *in vitro* oral-gastric-small intestinal models.

VI.2 Materials and methods

VI.2.1 Materials and sample preparation

Both in-season *cv. Agria* (*Solanum tuberosum L.*, *cv. Agria*) and *cv. Nadine* (*Solanum tuberosum L.*, *cv. Nadine*) potatoes were purchased from the local market. Tubers of 120-150g were cut into 8 wedge-shaped potato pieces and vacuum-packed to prevent enzymatic browning by polyphenol oxidase (Rocha, Coulon, & Morais, 2003). Vacuum-packed *cv. Agria* potato wedges (A) and *cv. Nadine* potato wedges (N) were then individually immersed in a water bath at either 55°C (A55 and N55) or 65°C

(A65 and N65) for 48 hours. Treated samples were freeze-dried, milled, and sieved (by 500 µm mesh) prior to measuring the total starch content, amylose content, pasting properties, and relative crystallinity. Enzymes α -amylase (*Aspergillus oryzae*, 1.5 U/mg), pepsin (porcine gastric mucosa, 800–2500 units/mg protein), pancreatin (hog pancreas, 4 × USP), and invertase (Invertase, grade VII from baker's yeast, 401 U/mg solid) were purchased from Sigma–Aldrich Ltd. (St Louis, USA). Amyloglucosidase (3260 U/ml) was purchased from Megazyme International Ireland Ltd. (Ireland).

VI.2.2 Dry matter, total starch content, and amylose content

Dry matter content of fresh tubers was determined by the AOAC 934.01 method (AOAC, 1990). Total starch content of both freeze-dried *cv.* Agria and *cv.* Nadine was analysed by total starch assay kit K-TSTA 07/11 (Megazyme International, Ireland). Amylose content was estimated by lectin concanavalin A (Con A) solubility using Megazyme kit K-AMYL 12/16 (Megazyme International, Ireland).

VI.2.3 Potato microstructure

Thin slices of approximately 1 µm of perimedullary parenchyma of *sous vide* cooked wedges were viewed under a light microscope (LM) with differential interference contrast (DIC) optics (Zeiss, Germany). The same sections from the *sous vide* cooked wedges were freeze-dried and their fractured surface examined by scanning electron microscope (SEM) (FEI Quanta 200 FEI Electron Optics, Eindhoven, The Netherlands). Micrographs were taken at different magnifications and representative images were chosen. An accelerating potential of 20 kV was used during micrography.

Particle size distribution of powdered and milled (by 500 µm mesh) samples was determined by using laser diffraction particle size analysis (Mastersizer 2000, Malvern Instruments Ltd., UK). The relative refractive index applied was 1.70. All measurements were done in triplicate.

Cold-water solubility of *sous vide* cooked powdered and milled samples was measured (Eastman & Moore, 1984). One gram of sample was mixed with 100 mL of distilled water and stirred at low speed (120 rpm) for 20 min. The solution was centrifuged at room temperature (25°C) for 20 min at 1200g, then 25 ml of the supernatant was weighed after drying at 110 °C for 4 h. Cold-water solubility was calculated: $Solubility (\%) = \frac{Solid\ in\ 25ml\ supernatant\ (g) \times 4}{total\ sample\ (g)} \times 100$. All measurements were done in triplicate.

VI.2.4 Pasting properties

The pasting profiles of freeze-dried and powdered *sous vide* cooked wedges were obtained using a Rapid Visco-Analyzer (RVA, Newport Scientific, Sydney, Australia) with the 7.7 RVATM Potato Starch Method (2.0 g starch and 14% moisture basis) (AACCI Method 76-21.01, 1996). Parameters including peak viscosity (PV), viscosity at the end of hold time at 95 °C or hot-paste viscosity (HPV),

final viscosity (FV) at the end of cooling, breakdown (BD=PV-HPV), setback (SB=FV-HPV) and pasting temperature were recorded. All measurements were done in triplicate.

VI.2.5 X-ray diffraction

Sous vide cooked potato (freeze-dried and milled) was tightly packed in a 2 mm internal diameter polymer sleeve of a sample holder. Powder X-ray diffraction data were collected using a Rigaku Spider diffractometer equipped with a Micromax MM007 rotating anode generator with CuK α radiation (wavelength = 1.54180 Å), high flux Osmic multilayer mirror optics, and a curved image plate detector. Powder X-ray diffraction patterns measured with an exposure time of 180s, and with a rotation speed of 6° per second around the ϕ axis were processed into 1D diffractograms. Data were corrected by subtraction of the scattering measured from the empty polymer sleeve. The relative crystallinity, RC (%) was calculated by dividing the area of the peaks by the total area of the diffractogram from 4 to 40°.

VI.2.6 Thermal characteristics

A piece of fresh raw tuber of approximately 12.6 mg was sealed in a pan (Tzero Pan and Tzero Hermetic Lid, TA Instruments, USA). Then all samples were immersed in a water bath at 55°C or 65°C for 2 days. Thermal characteristics of *sous vide* cooked potatoes were obtained by TA Instruments Q100 Differential Scanning Calorimeter (DSC) (New Castle, Germany) scanning from 20°C to 95°C a rate of 10°C per minute. To determine dry matter content, the pan was pierced and placed in an oven at 105°C for 24 hours. The gelatinisation onset temperature (T_o , °C), gelatinisation peak temperature (T_p , °C), gelatinisation conclusion temperature (T_c , °C), and the enthalpy of starch gelatinisation (ΔH_G , expressed as J/g dry matter) were determined by TA Universal Analysis 2000 software (New Castle, Germany) supplied with the equipment. Then peak height index (PHI), the ratio of $\Delta H/(T_p-T_o)$, were calculated to provide numerical values descriptive of the relative shape of the endotherm (Krueger, Knutson, Inglett, & Walker, 1987). All measurements were done in triplicate.

VI.2.7 Water mobility by LF-NMR

Parenchyma tissue of both *cv.* Agria and *cv.* Nadine potato tubers were sampled longitudinally by cork borer ($\varnothing 3.4 \times 80$ mm, approximately 0.5 g), and these samples were inserted into glass tubes of 5 mm outside diameter (Wilmad-LabGlass) and sealed to prevent moisture loss. Then the water mobility of potato cylinders was measured after 1, 2, 20, 24, and 48 hours of *sous vide* cooking at 55°C or 65°C. Samples were placed in the 4°C refrigerator for three days, followed by reheating at 60°C for 5 minutes. Before every relaxation time measurement, all samples were equilibrated at 25°C for 30 minutes. LF-NMR proton relaxation time measurements were performed with a Spinsolve 1.5 LF-NMR spectrometer at an operating resonance frequency of 42.5 MHz (Magritek Ltd., NZ). The transverse relaxation time T_2 was acquired by the Spinsolve@Carbon apparatus built-in program T_2 bulk function

using the Carr-Purcell-Meiboom-Gill sequence (CPMG). The experimental setup of the measurements was the same as the previous study (Chen et al., 2018) and the relaxation times T_2 were analysed using Prospa©v3.1 (Magritek, 2016). All measurements were done in triplicate.

VI.2.8 Oral-gastric-small intestinal digestion *in vitro*

Simulated salivary fluid (SSF) was prepared according to Kong, Oztop, Singh, & McCarthy (2011). Simulated gastric buffer (SGF) and simulated small intestine buffer (SIF) were prepared according to the US Pharmacopeia (Pharmacopeia U.S, 1995, 2000). SSF contained α -amylase, SGF contained pepsin, and SIF contained pancreatin, invertase, and amyloglucosidase (Bordoloi, Singh, et al., 2012).

To simulate *sous vide* catering from cooking through chill storage to serving (Baldwin, 2012), both vacuum-packed *cv.* Agria, A and *cv.* Nadine, N wedges were firstly immersed in a water bath at either 55°C (A55 and N55) or 65°C (A65 and N65) for 48hours. Only *sous vide* cooked *cv.* Agria wedges were then stored in a 4°C refrigerator for three days (A65R3), followed by reheating at 60°C for 10 minutes (A65R3-r60). Due to the extensive exudate from A55 (Figure VI.1a), N55 (Figure VI.1b) and N65 (Figure VI.1c) tubers observed in preliminary experiments, *sous vide* cooked *cv.* Agria at 55°C and *cv.* Nadine at 55 & 65°C was not continued through chill storage and reheating. In addition, the raw-like texture these samples (A55, N55, and N65) might indicate that longer *sous vide* cooking time (>48hr) was needed (Bordoloi, Kaur, et al., 2012) to acquire a desirable texture.

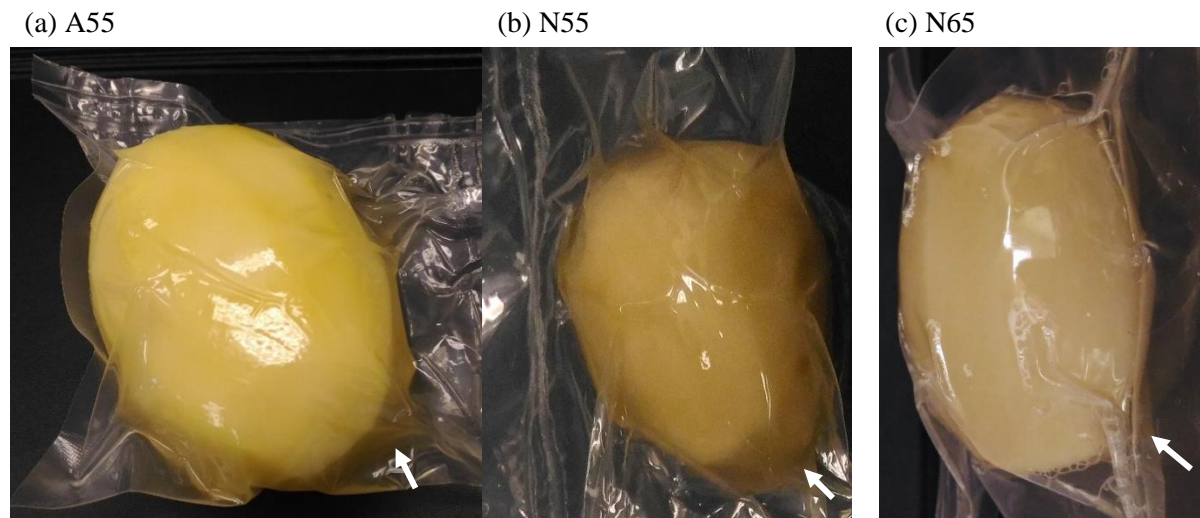


Figure VI.1 Appearance of *sous vide* cooked *cv.* Agria (a) at 55°C and *cv.* Nadine (b) at 55°C and (c) at 65°C.

Sous vide cooked wedges (40g) and pre-warmed SSF were weighed in a mass ratio of 1:1 and mixed by mini food processor for 2 minutes (The Mini Wizz Food Chopper, Breville®) (Tamura et al., 2013, 2017). The resulting bolus samples (80g) were topped up to 170g with distilled water and placed in a polyethylene mesh (Chen et al., 2018; Tamura et al., 2016). Starch digestibility was measured by the glucose released during simulated oral digestion and simulated gastric-small intestinal digestion. The

glucose content released after simulated oral mastication (O_2), thirty minutes of gastric digestion (G_0 and G_{30}) and two hours of small intestinal digestion (I_0 , I_5 , I_{10} , I_{15} , I_{30} , I_{90} , and I_{120}) were analysed by GOPOD reagent (Format K-GLUK 07/11, Megazyme International Ireland Ltd, Ireland) and the results were expressed as starch hydrolysis (%). Hydrolysis index (HI) of the samples was calculated as the area under the curves during simulated small intestinal digestion, using white bread as a reference. The estimated glycaemic index (eGI) was calculated by the following equation (Goñi et al., 1997): $eGI = 39.71 + 0.549HI$. All measurements were done in triplicate.

VI.2.9 Statistical analysis

Results are expressed as means \pm one standard deviation. Subsequently, an analysis of variance (ANOVA) with Tukey's test was used to determine significant differences among the means at a significance level of $p < 0.05$ by Minitab Statistical Software version 13 (Minitab, Inc., State College, PA).

VI.3 Results and discussion

VI.3.1 Dry matter, total starch content, amylose content

Dry matter of fresh tubers and total starch content and amylose content of freeze-dried powder of *cv. Agria* and *cv. Nadine* are shown in Table VI.1. Potato *cv. Agria* are commonly perceived as floury potatoes while *cv. Nadine* are known as waxy potatoes in culinary parlance. This perception could be related to the higher dry matter content and higher total starch content of *cv. Agria* than of *cv. Nadine* though the amylose content of starch from *cv. Agria* was lower than *cv. Nadine* (Van Dijk et al., 2002) (Table VI.1).

Table VI.1 Dry matter, total starch content and amylose content of potato *cv. Agria* and *cv. Nadine*.

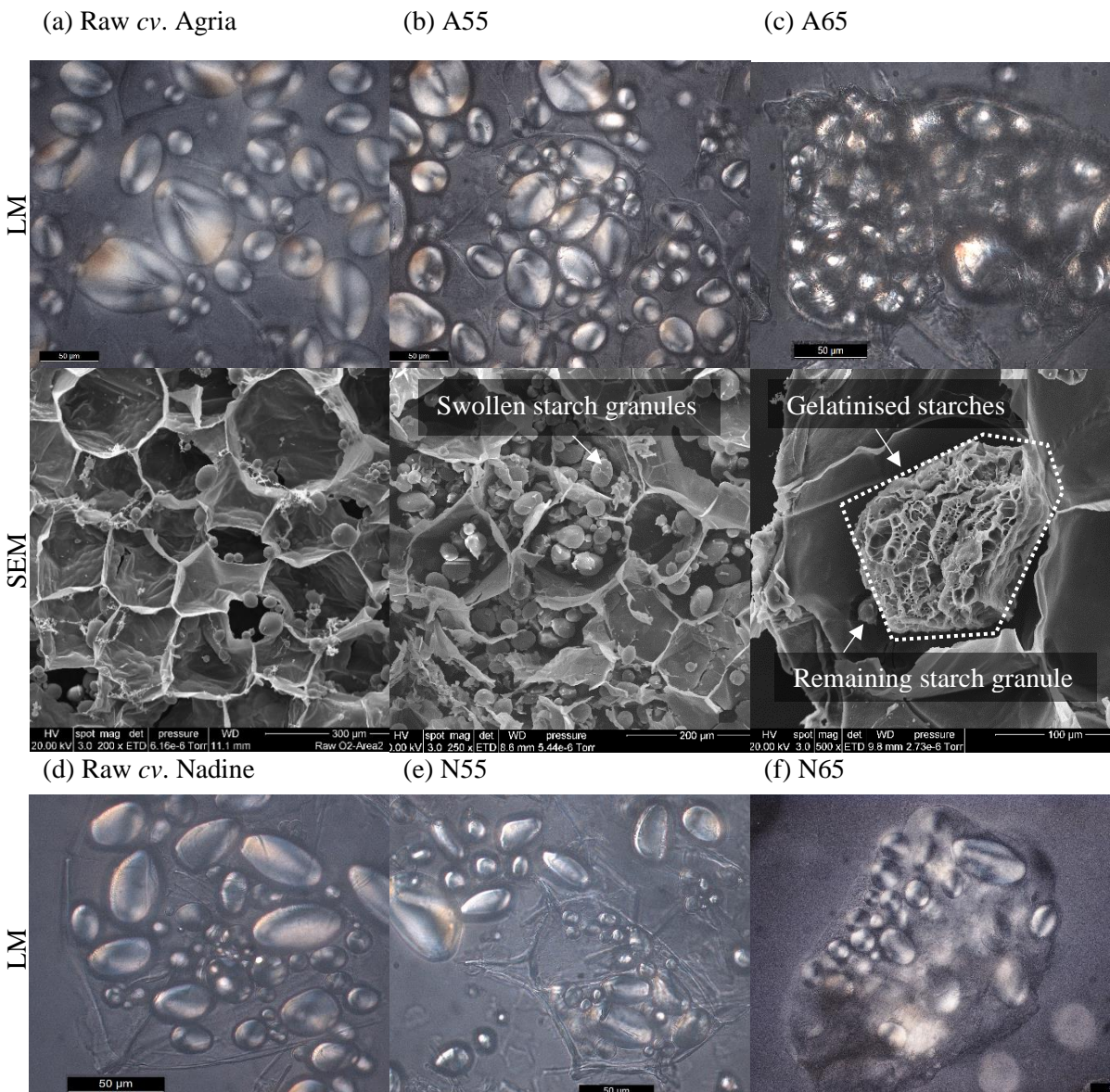
Cultivars	Dry matter (%)	Total starch content (% db)	Amylose content (%)	Amylose: Amylopectin*
<i>cv. Agria</i>	22.1 \pm 1.4 ^a	73.8 \pm 2.0 ^a	23.6 \pm 0.7 ^b	1:3.2 ^b
<i>cv. Nadine</i>	15.7 \pm 0.7 ^b	63.9 \pm 0.2 ^b	28.2 \pm 0.6 ^a	1:2.6 ^a

Different superscripts in the same column indicate significant differences ($p < 0.05$) ($n=3$). Amylose: Amylopectin ratio was calculated by the difference.

VI.3.2 Microstructure of *sous vide* cooked potatoes

Parenchyma tissue of raw potato *cv. Agria* and *cv. Nadine* tuber was composed of polyhedral cells with a diameter of approximately 200 μm and some intercellular spaces (Figure VI.3a&d). Globular to ellipsoid shapes of starch granules ranging from 5 to 100 μm in long dimension lay inside the potato cells (Figure VI.3a&d). LM and SEM micrographs of *sous vide* cooked potato tuber, A55, A65, N55 and N65 are shown in Figure VI.3b, c, e, &f. Swollen granules (Ratnayake & Jackson, 2007) can be

observed from the LM micrographs of both A55 and N55, but no granule surface changes (Rocha et al., 2011) are visible from the SEM micrographs (A55, Figure VI.3b and N55, Figure VI.3e). LM of A65 (Figure VI.3c) and N65 (Figure VI.3f) show remaining swollen starch granules embedded in a mixture of leached amylose and starchy matrix indicating the initiation of starch gelatinisation (García-Segovia et al., 2008). Both A65 (Figure VI.3c) and N65 (Figure VI.3f) show more debris on the surface of starch granules which could be either gelatinised starch or other cellular material. The SEM of A65 showed a sponge-like structure inside the potato cell indicating part of the granules were disrupted during *sous vide* cooking at 65°C. However, there were more intact starch granules in the potato cells of N65 observed by both LM and SEM than A65.



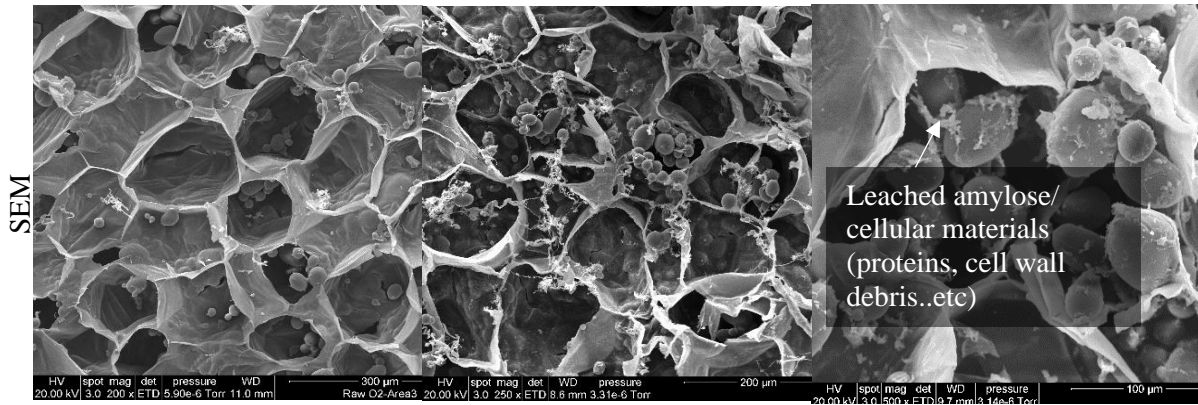


Figure VI.2 LM and SEM micrographs of (a) raw *cv. Agria*, *sous vide* cooked (b) at 55°C and (c) at 65°C *cv. Agria*; and for (d) raw *cv. Nadine*, and *sous vide* cooked at (e) 55°C and (f) 65°C *cv. Nadine*.

Particle size distribution of the powdered and sieved raw potato wedges and *sous vide* cooked potato wedges (at 55°C and 65°C) are shown (Figure VI.3a,b,c). Raw *cv. Agria* had a lower average particle diameter ($d_{3,2}$, $36.4 \pm 0.1 \mu\text{m}$) than raw *cv. Nadine* ($d_{3,2}$, $47.9 \pm 0.2 \mu\text{m}$) (Figure VI.3a). Raw potato *cv. Nadine* had a wider particle size distribution such that a bimodal peak showed the existence of large and small cells and other cell components. For *cv. Agria*, particle size distribution curves only showed a bimodal peak with $d_{3,2}$ at $47.8 \mu\text{m}$ after *sous vide* cooking at 55°C (Figure VI.3b). This could indicate the progression of cells and starch granules swelling over *sous vide* cooking (Gough & Pybus, 1971; Liu, Yu, Simon, Dean, & Chen, 2009). Inhomogeneous swelling may have contributed to starch granules of varied size fractions (Singh & Kaur, 2004) or the interaction of other cellular materials. Similarly, the particle size distribution curve of N55 continued to show a bimodal peak with a slightly increasing $d_{3,2}$ at $55.4 \mu\text{m}$ (Figure VI.3b). *Sous vide cv. Agria* at 55°C hydrated due to the ratio of surface area to weight, leading to the increase in particle size. The swollen particles ($d_{3,2}$, $94.8 \mu\text{m}$) and some possible granule disruption of A65 were shown by the particle size distribution curve with a main peak at $187 \mu\text{m}$ and a broad shoulder at $28 \mu\text{m}$ (Figure VI.3c). The $d_{3,2}$ of N65 ($53 \mu\text{m}$) increased only slightly though the volume proportion of small particles decreased (Figure VI.3c). This indicated potato *cv. Nadine* might be resistant to swelling upon heating at 65°C compared to *cv. Agria*. This might be due to the wider particles size distribution of *cv. Nadine* (Figure VI.3a). Nevertheless, other cell materials and molecular arrangements, such as amylose and amylopectin interaction and crystalline/amorphous lamella in starch granules might also affect the granules' deformation since higher amylose wheat starches have been shown to deform less than for lower amylose wheat starch (Kiseleva et al., 2005).

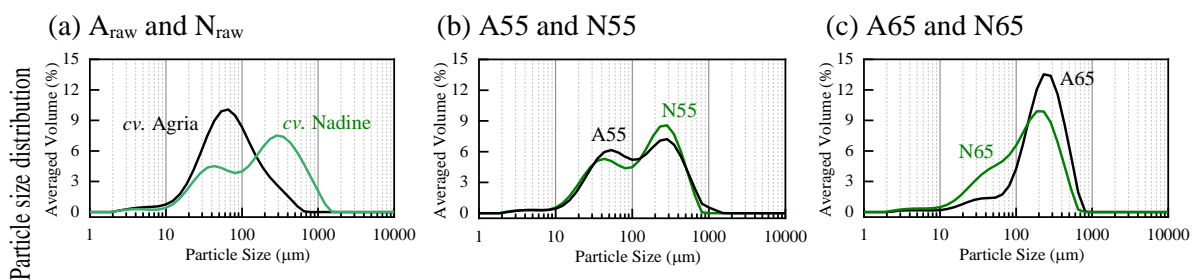


Figure VI.3 Particle size distribution of (a) A_{raw} and N_{raw} , for (b) A55 and N55, and for (c) A65 and N65.

Cold-water solubility of potato *cv.* Agria and *cv.* Nadine tend to decrease after *sous vide* cooking (Table VI.2). The reduced cold-water solubility of *sous vide* cooked potatoes (A55, A65, and N65) than raw tuber occurred due to limited swelling as observed by the micrographs. There was no significant difference between the cold-water solubility of two cultivars regardless in raw tubers or in *sous vide* cooked ones at 55°C or at 65°C (Table VI.2). Disruption of starch granular structure by superheating in aqueous ethanol solution are known to increase cold-water solubility (Chen & Jane, 1994; Jane, Craig, Seib, & Hosoney, 1986). This has been attributed to the disruption of granular structure where hydroxyl group of starch chains expose to water molecules, resulting in an increase in the solubility (Singh & Singh, 2003). Though N65 was partially gelatinised as observed by micrographs, cold-water solubility of N65 was the lowest among all the samples (Table VI.2), concurring with the lowest granule size of the residual starch. Crystalline perfect in residual starch of N65 may have contributed to less solubility.

Table VI.2 Cold-water solubility of *sous vide* cooked samples.

Samples	Cold-water solubility (%)
Raw <i>cv.</i> Agria	19.4 ±0.5 ^a
Raw <i>cv.</i> Nadine	18.7 ±0.5 ^a
A55	13.3 ±0.7 ^{bc}
N55	16.8 ±0.9 ^{ab}
A65	11.2 ±0.9 ^{cd}
N65	9 ±2.1 ^d

Different superscripts in same column indicate significant differences (n=3, $p < 0.05$).

VI.3.3 Pasting properties

Pasting profiles of raw freeze-dried and powdered potato *cv.* Agria (A_{raw}) and *cv.* Nadine (N_{raw}) are shown in Figure VI.4a. Initially, raw starch granules swelled, along with a pronounced increase in viscosity as the temperature was increased. Further granule swelling at 90°C led to a loss of granule integrity resulting in reduced viscosity. Entanglement of leached amylose during cooling likely led to the increased viscosity (Figure VI.4a). Pasting temperature of raw *cv.* Nadine ($70.4 \pm 1^\circ\text{C}$) was higher than for raw *cv.* Agria ($68.5 \pm 0^\circ\text{C}$) (n=3, $p < 0.05$) (Figure VI.4a). The higher pasting temperature of raw *cv.* Nadine might be due to a wider particle size distribution (Kim, Wiesenborn, Lorenzen, & Berglund, 1996; Wiesenborn, Orr, Casper, & Tacke, 1994). However, other pasting parameters, such as peak viscosity, breakdown viscosity, final viscosity, setback (%) of A_{raw} were higher than N_{raw} (Figure VI.4a). Pasting properties are influenced by the size, rigidity, amylose to amylopectin ratio and swelling power of raw starch granules (Kaur, Singh, McCarthy, & Singh, 2007).

Annealed potato starches have been shown to exhibit lower peak viscosity and improved shear stability due to reduced granular swelling and amylose leaching (Hoover & Vasanthan, 1994b; Tester, Debon, & Sommerville, 2000), and increased interaction between starch chains (Hoover & Vasanthan, 1994b). Consistently, the peak viscosity of *sous vide* cooked *cv.* Agria and *cv.* Nadine shifted toward a

higher temperature and a lower value (Figure VI.4b). *Sous vide* cooking below gelatinisation temperature allowed starch granules to swell reversibly leading to hydration of amorphous region and the increased mobility of glucan chains (Jayakody & Hoover, 2008). With the progression of *sous vide* cooking at 55°C, the order of the amorphous lamellae probably increased and, subsequently, the order of double helices of amylopectin was enhanced. The more ordered alignment of crystalline and amorphous lamellae in A55 and N55 than raw sample strengthened the interactions among molecular chains and restricted the hydrogen bonding forces between starch-water molecules, thus influencing pasting properties. The peak viscosity of A55 and N55 was lower than for A_{raw} and N_{raw} (Figure VI.4b). The lower breakdown viscosity of A55 and N55 than for A_{raw} and N_{raw} (Figure VI.4b) is attributed to the enhanced shear stability, which prevents the disruption of starch granules (Wang et al., 2017; Xu et al., 2018). Pasting viscosity of A65 and N65 increased gradually without displaying any obvious peak viscosity curve. *Sous vide* cooking at 65°C (only 1°C below gelatinisation onset temperature) induced more swollen granules which occupied the cellular space extensively and may have resulted in restricted water flow in potato cells. Aligned with the limited swelling of granules, pasting viscosity increased only gradually. The breakdown viscosities of A65 and N65 were lower than A55 and N55 indicated a better heat-shear pasting stability.

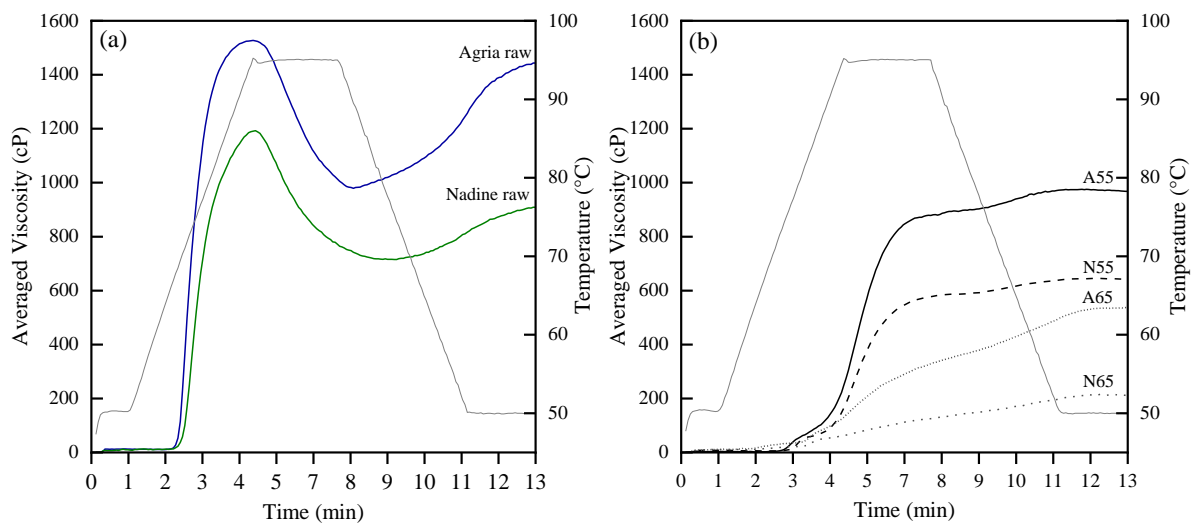


Figure VI.4 Pasting profile of freeze-dried and powdered (a) raw potato *cv.* Agria and *cv.* Nadine and (b) *sous vide* cooked (at 55°C and 65°C) potatoes.

VI.3.4 Relative crystallinity

X-ray diffraction patterns of both freeze-dried and powdered raw potatoes *cv.* Agria (A_{raw}) and *cv.* Nadine (N_{raw}), and *sous vide* cooked potatoes (at 55°C and 65°C) showed a B-type crystalline pattern with reflections at 5.6°, 15.0°, 17.2°, 22.4°, and 24.1° at 2 θ (Figure VI.5). After *sous vide* cooking the X-ray diffraction patterns of both potato cultivars remained the same (Figure VI.5) indicating the polymorphic patterns were unchanged (Vermeulen, Goderis, et al., 2006). The relative crystallinity, RC (%) of A_{raw} and N_{raw} were 27% and 23%, respectively (Figure VI.5). The RC of both *sous vide* cooked

potato *cv.* Agria, A55 and A65, and potato *cv.* Nadine, N55 and N65 increased when compared to A_{raw} and N_{raw} (Figure VI.5) though *sous vide* cooking at both 55°C or 65°C seemed to have altered the structure of starch granules. The increasing relative crystallinity could be due to the interplay of some factors such as the orientation of crystalline structure (Buléon, Gérard, et al., 1998), or the perfection of crystalline and amorphous regions (Gomand et al., 2012; Rocha et al., 2011), or the formation of amylose crystallite (Krueger, Knutson, et al., 1987; Krueger, Walker, Knutson, & Inglett, 1987). Potato *cv.* Nadine with low relative crystallinity (23%) increased greatly to 33% than potato *cv.* Agria did (from RC of 27% for A_{raw} to 32% for A55) after *sous vide* cooking at 55°C (Figure VI.5). This could be attributed to the higher amylose content of potato *cv.* Nadine in amorphous lamella, triggering the amorphous lamella to hydrate before other semi-crystalline regions. The extra water introduced to the amorphous lamella may have induced the transition of amorphous regions from a rigid glassy state to a mobile rubbery state, which in turn may have facilitated the hydration and dissociation of double helices in crystallites. Dissociation of crystallites occurs at the T_g of amorphous regions, but at 55°C ($<T_m$) limited dissociation of amylopectin double helices (most of which were in crystallites) was associated with limited swelling of granules (Tester & Debon, 2000). Thus, increased relative crystallinity of N55 was more pronounced (Figure VI.5). The phenomenon of raw potato with higher relative crystallinity exhibiting less change during *sous vide* cooking reinforced the findings in other research (Alvani, Qi, & Tester, 2012). However, when the temperature increased as in *sous vide* cooking at 65°C for 48 hours, the amorphous/crystalline lamella of A65 and N65 had gone through the early phase involving enhanced mobility of amorphous regions, but simultaneously with uncoiling of double helices and converting crystalline to amorphous material. The relative crystallinity of A65 and N65 was, therefore, lower than A55 and N55 with A65 very close A_{raw} and N_{raw} .

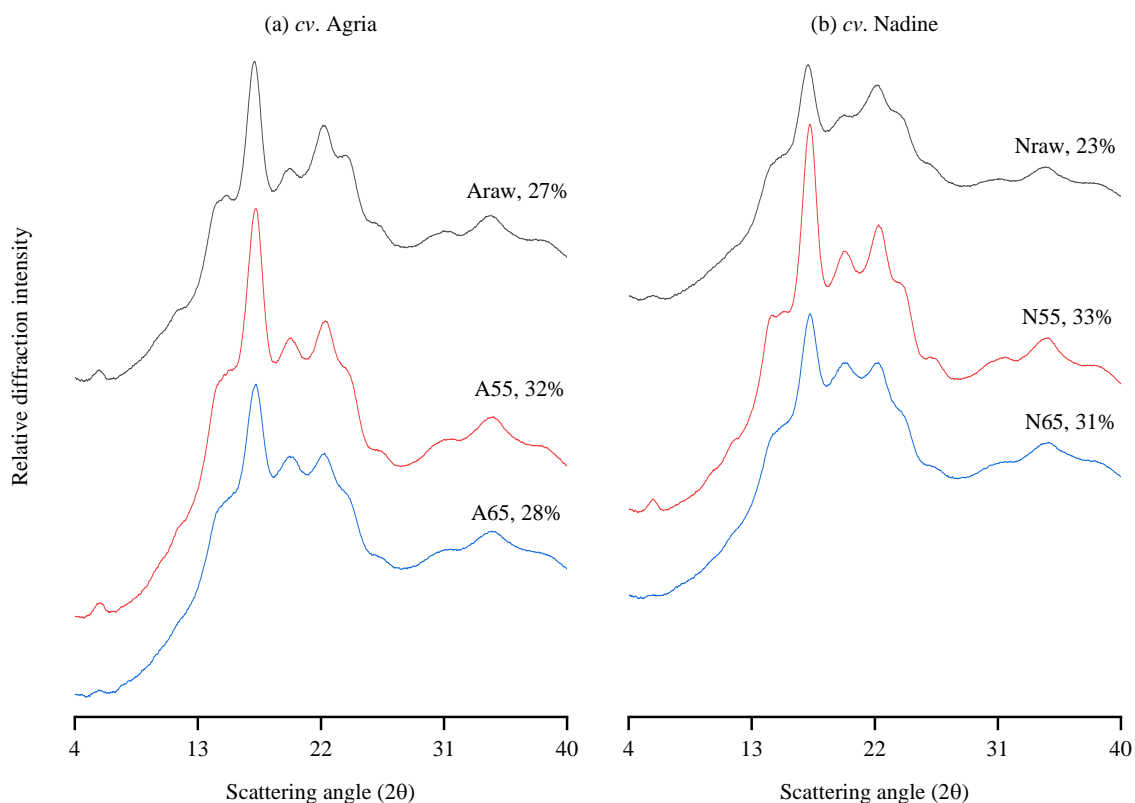


Figure VI.5 X-ray diffraction patterns and relative crystallinity of freeze-dried and powered raw and *sous vide* cooked (a) *cv. Agria* and (b) *cv. Nadine*.

*Relative crystallinity of the freeze-dried potato samples may vary by moisture content where the average moisture content of the samples were $7.6 \pm 0.1\%$. More experiments may be done for further confirmation.

VI.3.5 Thermal characteristics of *sous vide* cooked potato tubers

Endothermal curves and thermal characteristics (T_o , T_p , T_c , ΔH , and PHI) of raw, *sous vide* cooked, *sous vide* cooked-chill, and *sous vide* cooked-chill+reheated samples are shown in Figure VI.6 and Table VI.3. No significant difference between thermal characteristics of raw *cv. Agria*, a medium dry matter potato and raw *cv. Nadine*, a low dry matter potato (Karlsson & Eliasson, 2003a; Tester, Ansell, Snape, & Yusuph, 2005) were observed (Table VI.3a). *Sous vide* cooked (at 55°C) potato tubers showed similar effects to annealed potato starches (Kohyama & Sasaki, 2006) by increasing T_o and T_p , and the narrower transition temperature ($T_c - T_o$), unchanged gelatinisation enthalpies, and the higher PHI than raw tubers (Table VI.3a,b). The T_o and T_p of A55, N55, A55R3, N55R3, A55R3-r60, N55R3-r60 samples were all significantly higher than their raw potato tubers but not the T_c (Table VI.3a,b). Over 48 hours of *sous vide* cooking, the resulting higher T_o reflected that more energy was needed to initiate melting, indicating the possibility of weaker crystallites between crystalline/ amorphous lamella. The higher T_p concurred with the improvement of chain organization within the crystalline lamellae whereas other crystallites represented by T_c are less susceptible to chain movement on annealing (Larsson & Eliasson, 1991; Nakazawa & Wang, 2003; Wang, Powell, & Oates, 1997), and thus no significant

difference of T_c before and after *sous vide* cooking were shown (Table VI.3b). The significantly higher PHI of A55, N55, A55R3, N55R3, A55R3-r60, N55R3-r60 samples than raw *cv. Agria* and *cv. Nadine* was due to the significantly narrower transition temperature ($T_c - T_o$) (Table VI.3), which might indicate greater homogeneity and cooperative melting of crystallites (Kaur, Singh, Singh Sodhi, & Singh Gujral, 2002; Krueger, Walker, et al., 1987; Lawton & Wu, 1993). The starch crystalline perfection of A55, N55, A55R3, N55R3, A55R3-r60, N55R3-r60 samples were, however, not reflected by the significant difference in the enthalpies compared to their raw tubers (Table VI.3). *Sous vide* cooked potato tubers (A55 & N55) were so stable after storage (A55R3 & N55R3) and reheating (A55R3-r60 & N55R3-r60) that there was no significant difference in the thermal characteristics (Table VI.3a,b). This phenomenon could be attributed to the perfection of crystallites formed during *sous vide* cooking at 55°C.

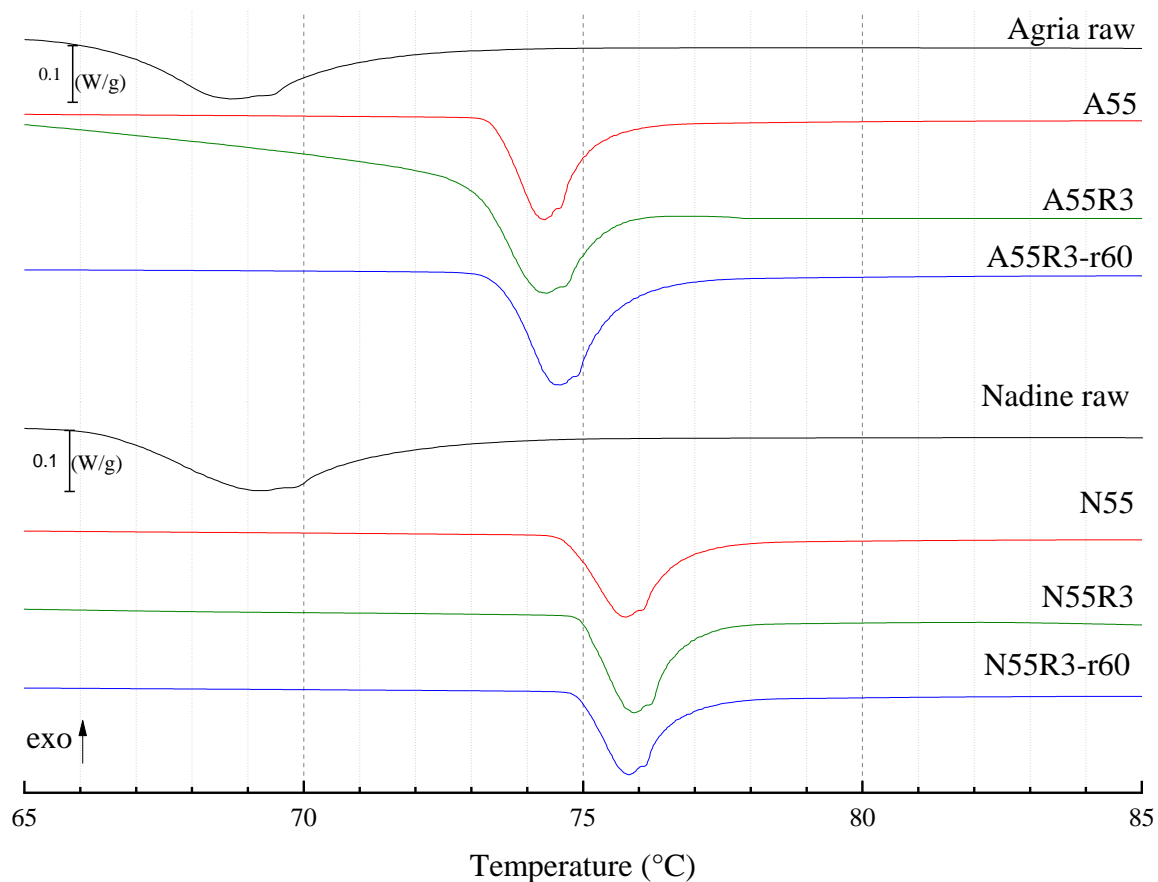


Figure VI.6 Endothermic curves of *sous vide* cooked-chill then reheated potato *cv. Agria* and *cv. Nadine*.

The DSC curve for *sous vide* cooked *cv. Agria* at 65°C did not reveal any obvious endothermic signature for A65 or A65R3-r60 (Figure VI.7). *Sous vide* cooking temperature (at 65°C) may cause partial gelatinisation (Siswoyo & Morita, 2010; Tsutsui et al., 2013). The A65R3 samples revealed a wider transition temperature ($T_c - T_o$) and smaller melting enthalpies (ΔH) than A55, exhibiting aggregation of disrupted starch granules during storage, similar to the effect of retrogradation (Chen et al., 2018) (Table VI.3c). However, the T_o , T_p , T_c of N65, N65R3, and N65R3-r60 significantly increased

(Table VI.3c) which might indicate some annealing on some of the starch granules. The ΔH , $T_c - T_o$, and PHI values of N65, N65R3, and N65R3-r60 were not significantly different from values for raw *cv.* Nadine tuber (Table VI.3c). Partially gelatinised starch with higher ΔH may have evened out gelatinised starches with lower ΔH . Differences in thermal characteristics between A65 and N65 occurred due to the different molecular arrangement in starch granules of each cultivar. This can be the interplay of amylose content, location of amylose and amylopectin within the starch granule interior, and amylopectin unit chain length distribution (Rocha et al., 2011; Waduge, Hoover, Vasanthan, Gao, & Li, 2006).

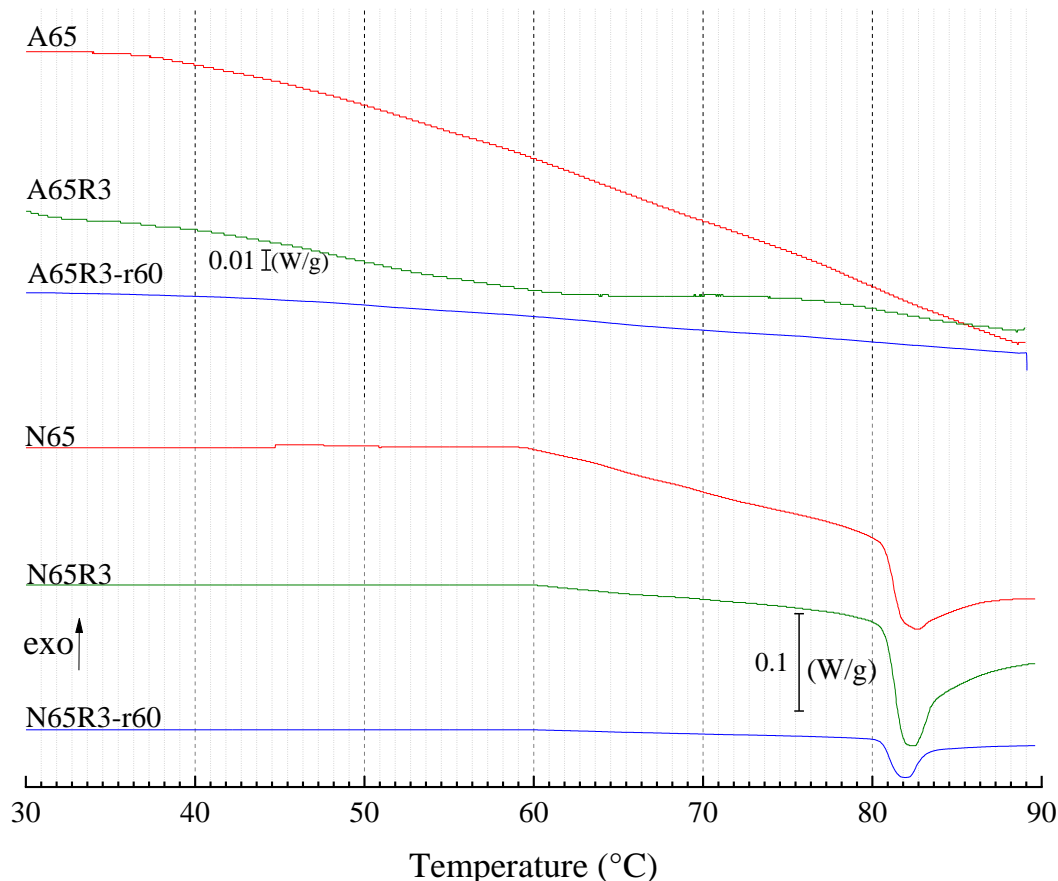


Figure VI.7 Endothermal curves of sous vide cooked-chill then reheated potato *cv.* Agria and *cv.* Nadine.

Table VI.3 Thermal characteristics of *sous vide* cooked potato tubers.

Samples	T_o (°C)	T_p (°C)	T_c (°C)	ΔH (J/g d.b.)	$T_c - T_o$ (°C)	PHI (J/g/°C)
(a) Raw tubers						
Agria Raw	66.0 ± 0.3 ^c	68.4 ± 0.3 ^c	74.2 ± 1.5 ^c	10.4 ± 0.3 ^{ab}	8.2 ± 1.5 ^b	4.3 ± 0.1 ^b
Nadine Raw	66.2 ± 0.4 ^c	68.5 ± 0.6 ^c	74.6 ± 0.5 ^c	13.1 ± 0.9 ^{ab}	8.4 ± 0.2 ^b	5.7 ± 1.0 ^b
(b) <i>Sous vide</i> cooking at 55°C, 48hrs → Chill storage at 4°C, 3days → Reheating at 60°C, 10mins						
A55	73.4 ± 1.2 ^b	74.3 ± 1.2 ^b	78.0 ± 2.5 ^c	13.5 ± 0.6 ^{ab}	3.9 ± 0.5 ^c	15.7 ± 2.0 ^a
A55R3	73.5 ± 1.4 ^b	74.4 ± 1.4 ^b	76.9 ± 1.0 ^c	12.8 ± 0.5 ^{ab}	3.3 ± 0.4 ^c	14.1 ± 0.6 ^a
A55R3-r60	73.5 ± 1.2 ^b	74.4 ± 1.3 ^b	78.3 ± 2.5 ^c	12.5 ± 2.0 ^{ab}	3.8 ± 0.3 ^c	14.7 ± 1.9 ^a
N55	74.5 ± 1.4 ^b	75.4 ± 1.4 ^b	78.4 ± 1.6 ^c	13.8 ± 3.5 ^{ab}	3.9 ± 0.3 ^c	15.8 ± 3.7 ^a
N55R3	74.6 ± 1.5 ^b	75.4 ± 1.5 ^b	78.7 ± 2.5 ^{bc}	14.3 ± 0.4 ^{ab}	3.3 ± 0.2 ^c	16.7 ± 1.4 ^a

N55R3-r60	74.3 ±1.4 ^b	75.1±1.4 ^b	77.8±1.9 ^c	14.9±1.6 ^a	3.5±0.5 ^c	18.7±2.8 ^a
(c) <i>Sous vide</i> cooking at 65°C, 48hrs→Chill storage at 4°C, 3days→Reheating at 60°C, 10mins						
A65	n.d.	n.d.	n.d.	n.d.	n.d.	n.d.
A65R3	51.2 ±4.8 ^d	61.5±4.1 ^d	72.7±3.9 ^c	1.1±0.6 ^c	21.5±5.0 ^a	-
A65R3-r60	n.d.	n.d.	n.d.	n.d.	n.d.	n.d.
N65	80.6±0.6 ^a	81.6±0.6 ^a	84.8±1.8 ^{ab}	7.9±5.4 ^{abc}	3.5±0.1 ^c	7.7±5.9 ^b
N65R3	80.8±0.5 ^a	81.9±0.5 ^a	85.8±1.8 ^a	8.0±4.3 ^{abc}	6.2±0.8 ^{bc}	7.6±5 ^b
N65R3-r60	80.0±1.3 ^a	81.3±1.1 ^a	85.0±2.0 ^{ab}	7.2±2.8 ^{bc}	4.9±0.8 ^c	5.4±1.6 ^b

T_o, onset temperature; T_p, peak temperature; T_c, conclusion temperature; and T_c-T_o transition temperature. ΔH, starch gelatinisation enthalpy, and *PHI*, peak height index = $\frac{\Delta H}{T_p - T_o}$. Different superscripts in the same column indicate significant differences ($p < 0.05$) (n=3).

VI.3.6 Water mobility of *sous vide* cooked potatoes

The average amplitude (M₀) of the initial signal of the relaxation time of *cv. Agria* (M₀=3.7*10⁵ a.u., n=3) was lower than for *cv. Nadine* (M₀=3.9*10⁵ a.u., n=3) indicating the higher dry matter of *cv. Agria* (22% relative to dm of 15% for *cv. Nadine*) (Hansen et al., 2010). Four water populations with relaxation times T₂₀, T₂₁, T₂₂, and T₂₃ can be discerned in both *cv. Agria* (Chen et al., 2018) and *cv. Nadine* (Figure VI.8a). Relaxation time T₂₀ represents the mobility of water in amylopectin double-helical structure of B-type crystallites (Figure VI.8a). The T₂₀ of raw *cv. Agria* was not significantly different from the T₂₀ of raw *cv. Nadine* as they are both B-type starch. Relaxation time T₂₁ may indicate the mobility of water in alternating amorphous and crystalline layers (Figure VI.8a). The T₂₁ of raw *cv. Nadine*, 8.6ms was significantly higher than the T₂₁ of raw *cv. Agria*, 6.1ms (n=3, $p < 0.05$) indicating the higher water mobility in the crystalline/ amorphous lamella. This may also reflect the higher water content of *cv. Nadine*. The relaxation time distribution curves of A55 showed a bimodal peak at relaxation time T₂₂ and T₂₃ like raw tubers resembling the diffusive exchange of water populations between the subcellular compartments (Figure VI.8a). This is consistent with a relatively undisrupted potato cell structure. The lower relaxation time T₂₂ and T₂₃ of A55 than for raw *cv. Agria* could indicate that the water in subcellular compartments was less mobile due to limited swelling (Figure VI.8a). Different to *sous vide* cooking at 55°C, the relaxation time distribution curve of A65 showed four separated peaks, which were similar to the cooked *cv. Agria* (Figure VI.8b). The peak separation at relaxation time T₂₂ and T₂₃ might indicate that leached amylose was able to hydrogen bond with part of the water distinct from the rest of the water existing freely in the cells (Figure VI.8b). The lower relaxation time T₂₂ and T₂₃ of A65 than A_{cooked} indicated less mobile water and a more compact structure of A65 than the starchy matrix in traditionally cooked potato (Figure VI.8b).

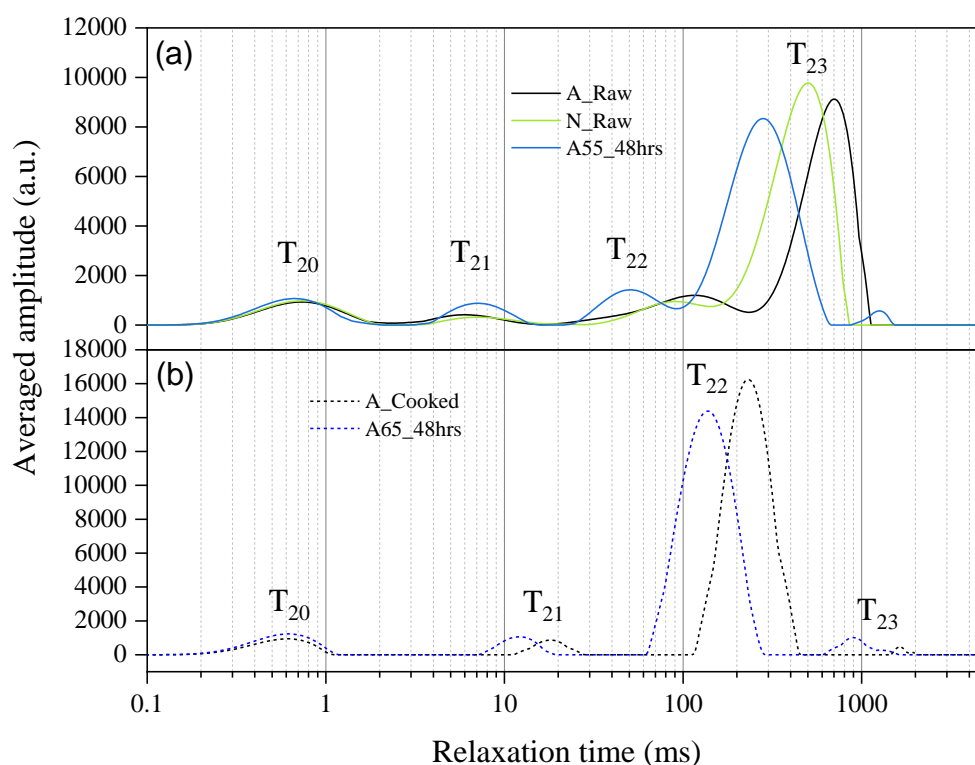


Figure VI.8 Relaxation time distribution curves of (a) raw *cv. Agria* and *cv. Nadine* and A55, and (b) cooked *cv. Agria* and A65.

Development of relaxation time of A55 and N55 reflected the granule structural changes during *sous vide* cooking at 55°C, chill storage, and reheating (Figure VI.9). There were no significant changes in T₂₀ over *sous vide* cooking, refrigeration, and reheating (Figure VI.9). Perry & Donald, (2000) reported that water in crystalline lamellae shows a lower density than water in amorphous lamellae, implying that crystalline lamellae are relatively impenetrable to bulk water at room temperature. Cooking above glass transition temperature but below gelatinisation temperature such as *sous vide* cooking at 55°C, allows starch granules to swell reversibly due to water flow between amorphous and crystalline lamellae (Ritota et al., 2008). Simultaneously, rising pressure from the movements of starch molecular chains in the crystalline regions (Vamadevan, Bertoft, Soldatov, & Seetharaman, 2013) and increasing glucan chain mobility in the amorphous regions (Genkina, Wasserman, & Yuryev, 2004) seem to have led to an increase in T₂₁ (Figure VI.9). The T₂₁ of A55 increased significantly after 2 hours of *sous vide* cooking but remained around 7-7.4 ms till the end of 48 hours of *sous vide* cooking, then chill storage and reheating at 60°C (Figure VI.9). During the initial swelling, the mobility of water diffusing between subcellular compartments decreased presumably due to increasing interaction between water molecules and starch granules (Micklander et al., 2008). Relaxation times T₂₂ and T₂₃ of A55 and N55 decreased significantly within 2 hours of *sous vide* cooking but remained stable at 50ms during the rest of the process (Figure VI.9). Cooke & Gidley, (1992) found that 40% of the helical units remain in the helical conformation when wheat, corn, potato starches were heated at gelatinisation onset temperature. This rearrangement occurred in a smaller scale than starch gelatinisation.

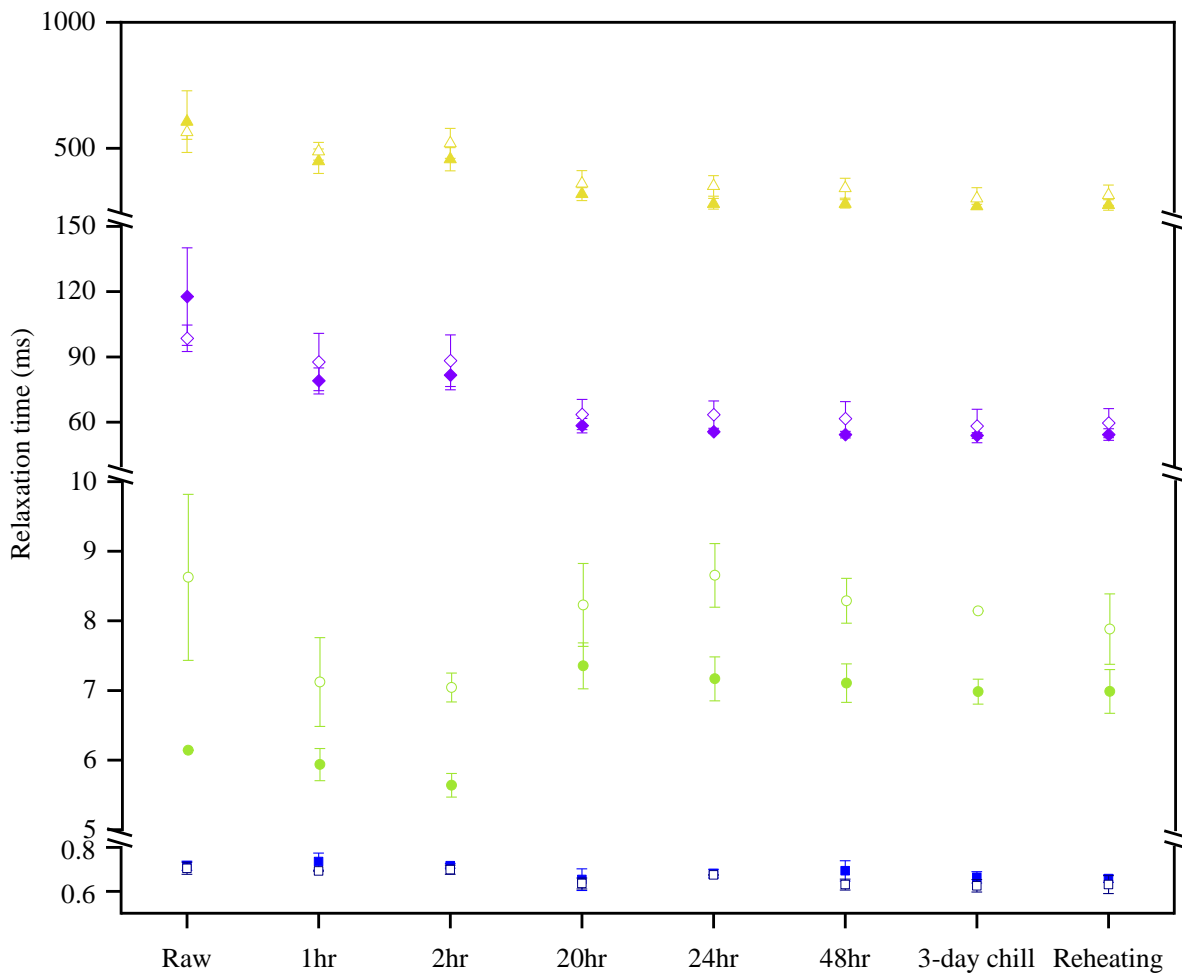


Figure VI.9 Development of relaxation time T_{20} (from 0.6 to 0.8ms, ■□), T_{21} (from 5 to 10ms, ●○), T_{22} (from 50 to 120ms, ◆◇), and T_{23} (from 250 to 1000ms, ▲△) during *sous vide* cooking at 55°C. Filled symbols represent *cv. Agria* and empty symbols represent *cv. Nadine* (mean \pm SD, $n=3$).

Substantial loss of helical order and hence unwinding of the double helices was observed as evidenced by a significant increase in the T_{21} of A65 and N65 (Figure VI.10). This small motion of the unwinding units was observed to be reversible and they were able to slip back into their original positions upon cooling (Donald, Lisa Kato, Perry, & Waigh, 2001). There were, therefore, no significant differences between the T_{21} of A65R3 and its raw counterparts (Figure VI.10). Amylose appeared to entangle with the unwinding amylopectin side chains in corn starches causing no reformation of the double helices upon cooling (Donald et al., 2001). Indeed, N65 with higher amount of amylose content seemed to form entanglements with chains from amylopectin double helices soon after 1 hour of *sous vide* cooking as no significant development of relaxation time T_{21} was observed for the rest of the process (Figure VI.10). The relaxation time T_{22} and T_{23} of A65 and N65 significantly increased after *sous vide* cooking probably due to the disruption of some starch granules (Figure VI.10). The leached amylose and gelatinised starch seemed to aggregate upon cooling so that the relaxation time of T_{22} and T_{23} decreased (Figure VI.10).

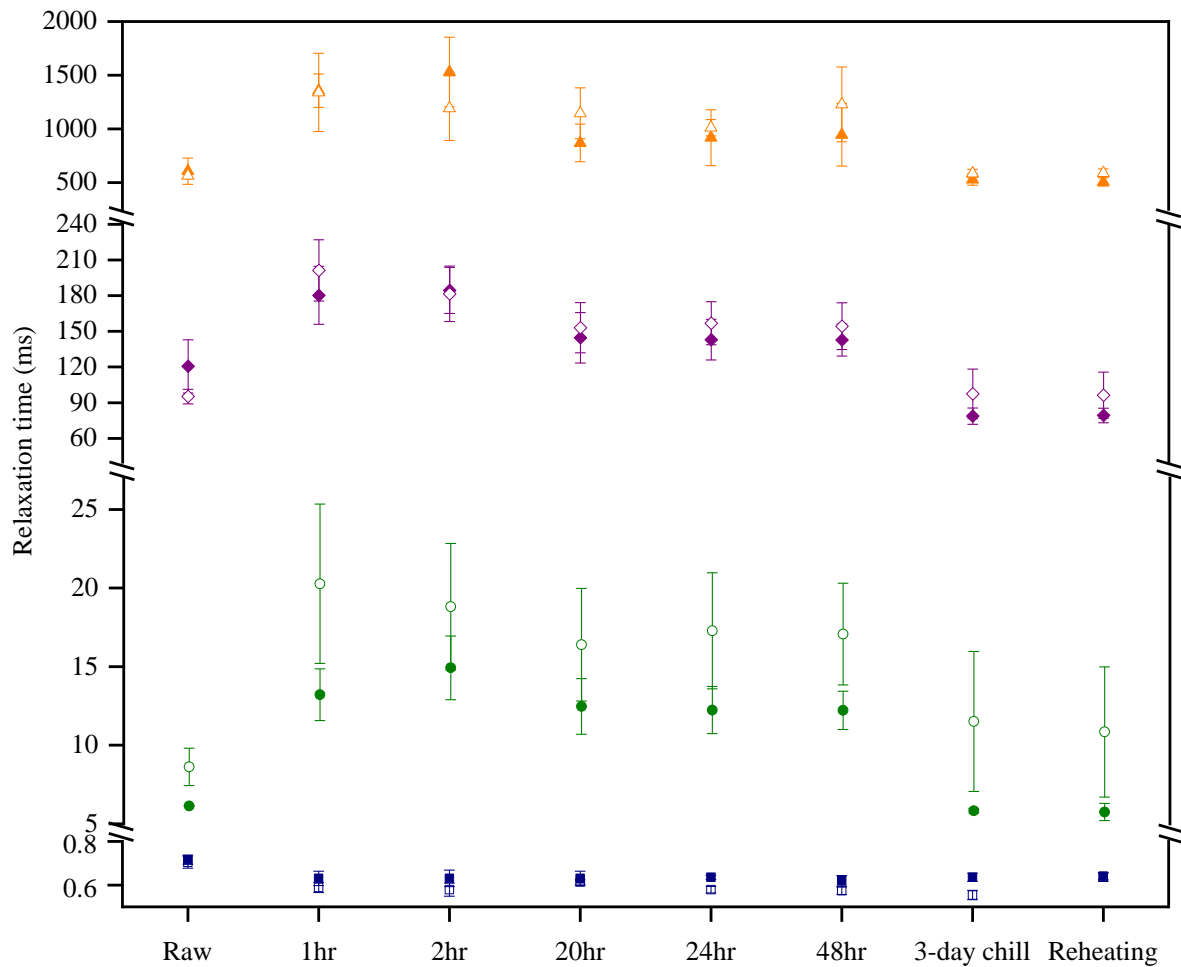


Figure VI.10 Development of relaxation time T_{20} (from 0.6 to 0.8ms, ■□), T_{21} (from 5 to 30ms, ●○), T_{22} (from 50 to 240ms, ◆◇), and T_{23} (from 250 to 2000ms, ▲△) during *sous vide* cooking at 65°C. Filled symbols represent *cv. Agria* and empty symbols represent *cv. Nadine* (mean \pm SD, n=3).

VI.3.7 Oral-gastric-small intestinal digestion *in vitro* of *sous vide* cooked potatoes

Starch hydrolysis (%) of *sous vide* cooked *cv. Agria* (A55, ranged from 0.2 to 1.4 %) and *sous vide* cooked *cv. Nadine* (N55, ranged from 4.9 to 11.7 %) maintained at low values, displaying the resistance toward enzymatic hydrolysis like raw tubers (Figure VI.11a). Different research reports have shown different trends for α -amylase hydrolysis of annealed starches owing to varied botanical sources, enzyme sources and concentration, and annealing conditions (Hoover & Vasanthan, 1993; Jacobs, Eerlingen, Spaepen, Grobet, & Delcour, 1997; O'Brien & Wang, 2008; Wang et al., 2017). Potato cell integrity depending on different cooking conditions has been shown to alter starch digestion more (Alvani et al., 2014) than its composition (Ek, Brand-Miller, & Copeland, 2012). This may be attributed to the particle size distribution of the bolus as well as the interaction between cellular components and the annealed starch *in tuber* (Figure VI.11a). There were no significant differences between A55 and N55 (Figure VI.11a) as the morphology of both *sous vide* cooked potato starch granules were swollen but intact. Starch hydrolysis (%) of *sous vide* cooked *cv. Agria*, A65 and *cv. Nadine*, N65 at 65°C

increased gradually reaching 60% and at 51% at the end of 2.5hr digestion (Figure VI.11a). The lower hydrolysis (%) levels of *sous vide* than freshly cooked potatoes may be attributed to starch structural perfection during *sous vide* cooking (Chung et al., 2010; Chung, Liu, et al., 2009). To simulate the cook-chill *sous vide* process, the *sous vide* cooked *cv.* Agria wedges at 65°C, A65 were stored in 4°C refrigerator for 3 days, A65R3 (Figure VI.11b) and then reheated at 60°C for 10 minutes, A65R3-r60 (Figure VI.11c). Starch hydrolysis (%) of A65R3 increased slowly during small-intestinal digestion due to the aggregation of leached amylose (Figure VI.11b). The lower starch hydrolysis of FCR3 than freshly cooked tubers may be attributed to the aggregation of disrupted amylose and amylopectin (Chen et al., 2018). However, the starch hydrolysis curve of A65R3-r60 overlapped with FCR3-r60 (Figure VI.11c). This showed that even though the structure of A65R3 has a mixture of starch granules with ordered crystalline/amorphous lamellae and leached amylose aggregated during chill storage, it was still sensitive to heat.

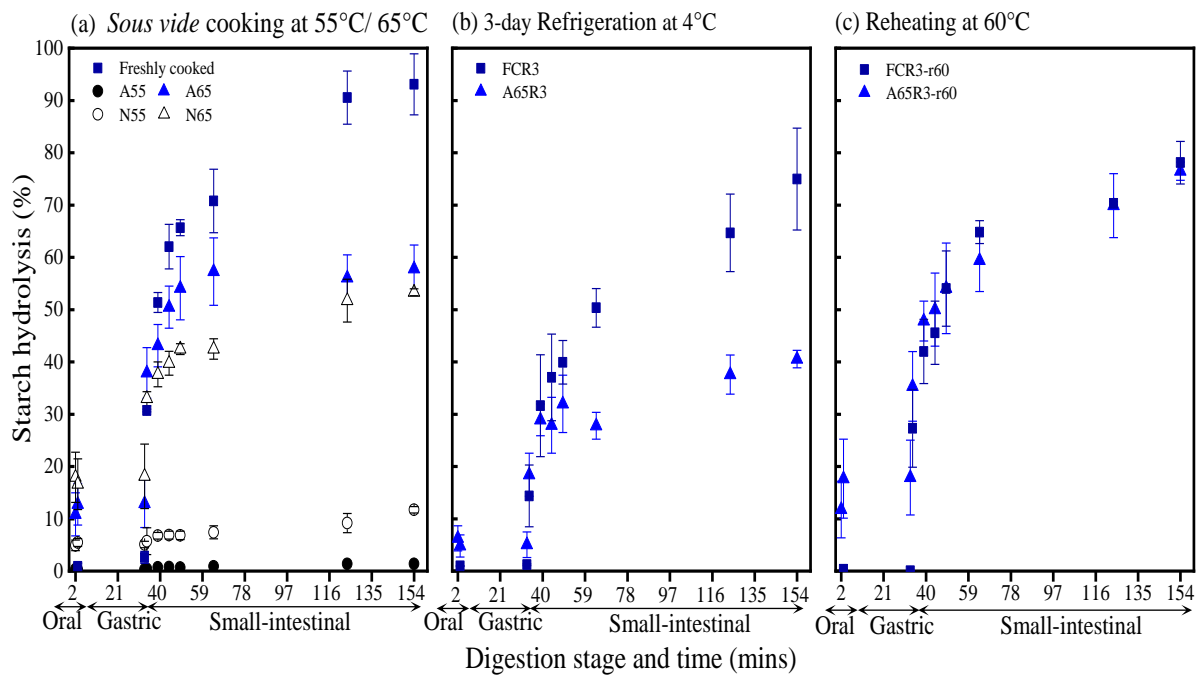


Figure VI.11 Starch hydrolysis (%) of (a) *sous vide* cooked potato wedges, (b) *sous vide* cooked-chill potato wedges, and (c) *sous vide* cooked-chill+reheated potato wedges. Error bars represent standard deviation (n=3).

Starch hydrolysis of *in vitro* digestion (C_{1120} experimental), hydrolysis index (HI), and estimated glycaemic index (*eGI*) are shown in Table VI.4. Hydrolysis index (HI) and estimated glycaemic index (*eGI*) of FC, A65 and N65 were significantly different from each other (Table VI.4). This implies that the extent of hydrolysis was proportional to the starch gelatinisation of samples (Chung, Lim, & Lim, 2006) as the extent of cooking or starch gelatinisation increases the glycaemic index. Hydrolysis index and estimated glycaemic index of A65 were significantly lower than traditionally cooked tubers (FC) but were not significantly different from A65R3-r60, FCR3 and FCR3-r60 (Table VI.4). Starch retrogradation during chill storage increased the starch melting temperatures of A65R3 (T_0 51.2 and T_c

72.2°C). Therefore, the HI and *eGI* of A65R3 were significantly lower than A65, A65R3-r60, FCR3 and FCR3-r60. The hydrolysis will be restricted (Alvani et al., 2014) unless the reheating temperature of cook-chill *sous vide* potato is higher than 51° C. Indeed, the cook-chill *sous vide* potato reheated at 60°C resulted in greatly hydrolysed starch.

Table VI.4 Starch hydrolysis (C_{∞} experimental), hydrolysis index (HI), and estimated glycaemic index (*eGI*) of *sous vide* cooked-chill then reheated potato wedges.

Samples	C_{∞} experimental (%)	HI	<i>eGI</i>
FC	93.1 ±5.8 ^a	82.8 ±0.04 ^a	85.2 ±0.02 ^a
<i>Sous vide</i> cooking at 55°C or 65°C for 48 hours			
A55	3.4 ±3.6 ^e	2.6 ±2.5 ^e	41.1 ±1.4 ^e
N55	11.7 ±0.8 ^e	8.5 ±1.6 ^e	44.4 ±0.9 ^e
A65	60.2 ±8.9 ^c	60.2 ±0.9 ^b	72.8 ±0.5 ^b
N65	50.9 ±0.9 ^{cd}	47.1 ±1.3 ^c	65.6 ±0.7 ^c
Chill storage at 4°C, 3days			
FCR3	74.7 ±1.8 ^b	61.3 ±2.2 ^b	73.4 ±1.2 ^b
A65R3	38.8 ±0.01 ^d	32.7 ±4.0 ^d	57.7 ±2.2 ^d
Reheating at 60°C, 10mins			
FCR3-r60	78.1±5.7 ^b	64.9±1.3 ^b	75.3 ±0.7 ^b
A65R3-r60	76.5 ±2.5 ^b	67.2±5.1 ^b	76.6±2.8 ^b

C_{∞} , experimental starch hydrolysis (%) after 2.5 hours of simulated gastric small-intestinal digestion; k, kinetic constant; HI, hydrolysis index; *eGI*, estimated glycaemic index. Different superscripts in same column indicate significant differences ($p < 0.05$) (n=3).

VI.4 Conclusion

Sous vide processing changes multiple properties of potato as summarised in Table VI.5. *Sous vide* cooking at both 55°C and 65°C improved pasting properties and increased relative crystallinity of both potato *cv.* Agria and *cv.* Nadine. Upon *sous vide* cooking at 55°C, both cultivars showed more homogenous crystalline structure indicated by higher PHI and lower starch hydrolysis than traditionally cooked wedges by 81-90%. *Sous vide* cooked potato *cv.* Agria and *cv.* Nadine at 55°C, except the raw-like appearance, displayed strengthened potato cell structure as evidenced by the micrographs, resulting in low starch hydrolysis (%). Relative crystallinity of raw *cv.* Agria increased from 27% to 32% after *sous vide* cooking. While potato *cv.* Nadine showed a larger increase in relative crystallinity from 23% to 33% after *sous vide* cooking. A *sous vide* processed potato tuber (at 65°C) contains an average amount of resistant starch of 11.4g/150g (where the average weight of a medium potato is 150g). The recommended intake of resistant starch is 15-20 grams per day for adults to regulate bowel health (<https://www.csiro.au/en/Research/Health/Nutrition-science/Nutrition-facts/Resistant-starch>). The intake of resistant starch in infants, however, shows a different picture. Resistant starch, particularly the lower molecular weight portions that escape digestion in the small intestine or after hydrolysis by the colonic microflora, can generate an excessive osmotic load in the large bowel, leading to diarrhoea.

The development of water mobility of two cultivars indicated the molecular rearrangement during *sous vide* cooking. This molecular rearrangement during *sous vide* cooking at 55°C occurred at a lower extend than that occurs during complete starch gelatinisation. The helical units was unchanged as evidenced by the relaxation time of T₂₁ ranged from 7-7.4ms over *sous vide* cooked-chill process. Substantial loss of helical order, unwinding of the double helices, was observed during *sous vide* cooking at 65°C as evidenced by a significant increase in the T₂₁ of A65 and N65. The leached amylose and gelatinised starch aggregated upon cooling as the relaxation time of T₂₂ and T₂₃ decreased. During *sous vide* cooking at 65°C, potato *cv. Agria* was partially gelatinised (ΔH , n.d.) in contrast to potato *cv. Nadine* which retained higher thermal characteristics (ΔH , 7.9 ±5.4 J/g d.b.). Despite *sous vide* cooking at 65°C initiating gelatinisation of some starch granules, part of the starch granules was still intact and thus A65 exhibited lower estimated glycaemic index (*eGI*) than traditionally cooked potato by 12.4. *Sous vide* cooked potato *cv. Agria* at 65°C was perceived more appealing with less exudate than from *sous vide* cooking at 55°C. *Sous vide* processing in both 55°C and 65°C combined with other hurdle techniques to control microbial growth and texture optimisation may be necessary for *sous vide* cooked potato.

Table VI.5 Observations and interpretations of *sous vide* cooked potatoes.

Observation	55°C	65°C
Microscopy	Limited swelling.	Partially gelatinised starches and leached amylose with cellular materials.
Pasting properties	↑	↑
Relative crystallinity	↑	↑
Thermal characteristics	↑	<i>cv. Agria</i> ↓; <i>cv. Nadine</i> ↑
Relaxation times	T ₂₀ X, T ₂₁ ↑, T ₂₂ ↓, T ₂₃ ↓	T ₂₀ X, T ₂₁ ↑, T ₂₂ ↑, T ₂₃ ↑
Starch hydrolysis (%)	A55, 3.4%; N55, 11.7%.	A65, 60.2%; N65, 50.9%.
Interpretation	<ul style="list-style-type: none"> • Starch granules close to raw. • Crystalline structures were highly ordered. • Starch digestibility closes to raw. 	<ul style="list-style-type: none"> • Starch partially gelatinised. • Residual crystalline structures were more ordered. • Digestibility intermediate raw-cooked.

Chapter VII Stability of retrograded starch *in tuber* during reheating

VII.1 Introduction

Starch is the main carbohydrate in human nutrition. It is hydrolysed to glucose as energy resource by digestive enzymes. A common measurement of the blood glucose response after consuming starchy food is the Glycaemic Index (GI). It is defined as the incremental area under the blood glucose response curve of a test food containing a standard amount of carbohydrates relative to a control food (glucose or white bread) during the first 2h after consumption (Foster-Powell et al., 2002; Ludwig, 2002). Predicting the glycaemic response of ingredients or complex foods by *in vitro* carbohydrate digestibility (Goñi et al., 1997) is a cost-effective way for product screening. Based on the rate of the glucose release during starch digestion *in vitro*, starch can be classified into rapidly digestible starch (RDS), slowly digestible starch (SDS) and resistant starch (RS) (Englyst et al., 1992). The digestibility and absorption of digested carbohydrates of native starches are dependent on physicochemical characteristics such as starch granule morphology, amylose to amylopectin ratio, molecular structure (Tester, Karkalas, & Qi, 2004), degree of branching in terms of steric hindrance and consequently mass transfer resistance (Colonna, Leloup, & Buléon, 1992). The diffusion of α -amylase into the substrate is considered as an important step of hydrolysis. For examples, the surface characteristics of native starches lead to an inside-out hydrolysis for corn and sorghum starch, or an exo-corrosion for potato starch (Benmoussa, Suhendra, Aboubacar, & Hamaker, 2006; Fannon et al., 1992). Additionally, interactions of starch with fibre, protein and other food components can also limit diffusion and adsorption of the enzyme (Colonna et al., 1992).

Starch is normally consumed after processing. Cooking/processing increases starch digestibility and palatability (Bordoloi, Kaur, et al., 2012; Tamura et al., 2016). The nutritional quality of starch depends on the processing and the state of the starch and its surrounding ingredients (Singh, Dartois, et al., 2010; Würsch, Del Vedovo, & Koellreutter, 1986). The excess of water and high temperature during processing causes starch gelatinisation and destroys its granular structure. Starch retrogradation decreases the starch digestibility due to the re-crystallisation of gelatinised starch (Dupuis et al., 2016; Gormley & Walshe, 1999; Mishra et al., 2008). The decrease in the digestibility of retrograded starch shows up as an increase in slowly digestible starch or resistant starch (Zhang & Hamaker, 2009). The rate of starch digestion is associated with physiological properties. Slowly digestible starch has a medium to low GI and thus reduces the glycaemic load of a food product compared to rapidly digestible starch with a high GI (Ells, Seal, Kettlitz, Bal, & Mathers, 2005). The physiological advantage of slowly digestible starch compared to rapidly digestible starch is the stabilizing effect on the blood glucose

level, resulting in distinct hormonal and metabolic profile. But the low thermal stability of the SDS structure limits the application in the food industry (Lehmann & Robin, 2007a).

Starch responds differently to the level of heating and cooling cycles (Hoover, 2001) as well as the water level during cooking (Slaughter, Ellis, & Butterworth, 2001). Hydrothermal treatments cause the swelling of granules, the loss of double-helical order within starch molecules, and amylose leaching and amylopectin unwinding. With subsequent cooling, the manner in which re-association of these disrupted starch molecules occurs during cooling and storage conditions to reform the starchy matrix (Chapter V) largely determines the resistance of the starch to enzymatic digestion (Shin et al., 2005). If starch is cooked at a temperature below gelatinisation temperature in excess water, the granule swelling is limited which is known as starch annealing. Annealing leads to the reorganisation of starch molecules e.g. amylopectin double helices and crystalline perfection (Jayakody & Hoover, 2008). This permits modest molecular reorganisation to occur and a more organized structure of lower free energy to form (Hoover & Vasanthan, 1993). Hence, *sous vide* cooked potatoes were shown to have higher retrogradation temperature, higher relative crystallinity and low digestibility (Chapter VI). The retrograded starchy matrix *in tuber* from TTC treatment and *sous vide* processing could exhibit in a different manner than from traditional cooked-chill potatoes during reheating. Experiments were carried out to characterise the structural changes of retrograded starch *in tuber* during reheating. Structural characteristics both of the time-temperature cycled treated potato and the *sous vide* cooked-chill potato during reheating were studied by LF-NMR, FTIR, and X-ray. And their structure-digestibility relations were investigated by a three-stage simulated oral-gastric-small intestinal digestion *in vitro*.

VII.2 Materials and methods

VII.2.1 Materials and sample preparations

In season *cv.* Agria and *cv.* Nadine potato tubers (120g-150g) were purchased from a local supermarket. Whole uniform-sized tubers were put singly into polythene bags and were either cooked conventionally in a water bath at 90°C for 25 minutes, refrigerated at 4°C for 3 days, then reheated at 90°C as control. The 3-day time-temperature cycles (TTC) processed potatoes as described in Chapter V were reheated at 90°C (Table VII.1).

Sous vide potatoes were cooked in a water bath at 65°C for 2 days (S) and then were stored in constant 4°C for 3 days as described in Chapter VI. The *sous vide* cooked potato tubers were reheated at 60°C for 10 minutes as the peak temperature of A65R3 by DSC was 61°C measured in Chapter VI (Table VII.1). The control (CL) for *sous vide* cooked-chill+reheated potatoes were traditionally cooked (90°C, 0.4h)-chill (4°C, 3days) + reheated at low temperature 60°C.

Table VII.1 Processing conditions of retrograded+reheated potato starch *in tuber* (left) and the structural stability refers to the parameters from the test methods (right).

Process	Code	Cooking (temp °C/ duration hr)	Storage (temp °C/ duration hr)	Reheating (temp °C/ duration min)	Potato cultivar
C	FCR3-r90	90 °C/ 0.4h	4°C/72h	90 °C/ 10min	<i>cv. Agria</i>
TTC1	FCR3-t(-20/4/4)-r90	90 °C/ 0.4h	-20°C/24h→ 4°C/24h	90 °C/ 10min	<i>cv. Agria</i>
TTC1	FCR3-t(4/-20/4)-r90	90 °C/ 0.4h	4°C/24h→ -20°C/24h→ 4°C/24h	90 °C/ 10min	<i>cv. Agria</i>
TTC2	FCR3-t(4/65/4)-r90	90 °C/ 0.4h	4°C/24h→ 65°C/24h→ 4°C/24h	90 °C/ 10min	<i>cv. Agria</i>
TTC2	FCR3-t(4/4/65)-r90	90 °C/ 0.4h	4°C/24h→ 4°C/24h→ 65°C/24h	90 °C/ 10min	<i>cv. Agria</i>
CL	FCR3-r60	90 °C/ 0.4h	4°C/72h	60 °C/ 10min	<i>cv. Agria</i> & <i>cv. Nadine</i>
S	A65R3-r60	65 °C/ 48h	4°C/72h	60 °C/ 10min	<i>cv. Agria</i> & <i>cv. Nadine</i>
S	N65R3-r60	65 °C/ 48h	4°C/72h	60 °C/ 10min	<i>cv. Agria</i> & <i>cv. Nadine</i>

VII.2.2 Water mobility

Parenchyma tissue of *cv. Agria* was sampled longitudinally by cork borer ($\varnothing 3.4 \times 80$ mm, approximately 0.5 g). These samples were inserted into glass tubes of 5 mm outside diameter (Wilmad-LabGlass) and sealed to prevent moisture loss. Water mobility of all TTC retrograded+reheated samples was measured by a Spinsolve 1.5 LF-NMR spectrometer (Magritek Ltd.) with operating resonance frequency at 42.5 MHz. Before every measurement, samples were equilibrated at 25°C for 30 minutes. The transverse relaxation time T_2 was acquired by the Spinsolve@Carbon apparatus built-in program T_2 bulk function using the Carr-Purcell-Meiboom-Gill sequence (CPMG). The apparatus parameter setup was as previously reported (Chen et al., 2018). Raw data were transformed to a continuous relaxation time distribution curve by inverse Laplace transformation. Then the Lawson and Hanson NNLS analysis method in Prospa©v3.1 (Magritek Ltd., NZ) was used to calculate relaxation time T_2 . All measurements were done in triplicate.

VII.2.3 ATR-FTIR measurement

FTIR spectra of the *sous vide* cooked-chill+reheated samples were obtained using a Nicolet 5700 spectrometer equipped with a Smart iTR™ Attenuated Total Reflectance (Thermo Electron Scientific Instruments Corp., Madison, WI USA). In ATR mode, an IR beam traverses a prism so it is internally reflected from the back of the prism where it is in contact with the sample. The depth of IR beam penetration is related to the wavelength (Harrick & Beckmann, 1974). The larger the wavelength, the greater the penetration of the wave. For starches, the absorbance of the wavenumber is between 1200 and 800 cm^{-1} in which the wavelength is between 8 and 12 μm , and so the average penetration depth is 2 μm . Because the average penetration depth is smaller than the average diameter of potato starch granules (43.0 μm), ATR-FTIR is often considered as a surface measurement (Sevenou et al., 2002a).

Samples were scanned from 4000 to 400 cm^{-1} with a spectral resolution of 4 cm^{-1} and 64 co-added scans were made per sample to acquire each spectrum. A background spectrum was used as a reference. Spectra were baseline-corrected over the wavenumber range between 1200 and 800 cm^{-1} and were self-

deconvoluted by Happ-Genzel apodization (Bretzlaff & Bahder, 1986; Cameron & Moffatt, 1984; Kauppinen et al., 1981) with a bandwidth of 38cm^{-1} and a resolution enhancement factor of 2.1 using Omnic software (Wang et al., 2017). IR absorbance values at 1047 and 1022 cm^{-1} were extracted from the spectra after baseline correction and deconvolution. The ratio of 1047 to 1022 cm^{-1} was used to express the amount of the ordered crystalline relative to the amorphous domains in starches (Capron et al., 2007; Van Soest et al., 1995).

VII.2.4 X-ray

Sous vide cooked potato flour was tightly packed in a 2 mm internal diameter polymer sleeves of a sample holder. Powder X-ray diffraction data were collected using a Rigaku Spider diffractometer equipped with a Micromax MM007 rotating anode generator with $\text{CuK}\alpha$ radiation (wavelength 1.5 \AA), high flux Osmic multilayer mirror optics, and a curved image plate detector. Powder X-ray diffraction patterns measured with an exposure time of 180s, with a rotation speed of 6° per second around the ϕ axis were processed into 1D diffractograms. Data were corrected by subtraction of the scattering measured from the empty polymer sleeve. The relative crystallinity, RC (%) was calculated by dividing the area of the peaks by the total area of the diffractogram from 4 to 40° .

VII.2.5 Starch digestion *in vitro*

Simulated salivary fluid (SSF) was prepared according to Kong, Oztop, Singh, & McCarthy (2011). Simulated gastric buffer (SGF) and simulated small intestine buffer (SIF) were prepared according to the US Pharmacopeia (Pharmacopeia U.S, 1995, 2000). SSF contained α -amylase, SGF contained pepsin, and SIF contained pancreatin, invertase, and amyloglucosidase (Bordoloi, Singh, et al., 2012).

Potato tubers were mixed with pre-warmed SSF at mass ratio 1:1 using a mini food processor (The Mini Wizz Food Chopper, Breville®) for two minutes (Tamura et al., 2017). The resulting potato bolus samples, approximately 80g, were topped up to 170g with distilled water and placed in a polyethylene mesh. Starch digestibility was measured by the glucose released after a certain time of simulated oral digestion and simulated gastric-small intestinal digestion. Glucose released after two minutes of oral mastication (O_2), thirty minutes of gastric digestion (G_0 and G_{30}) and two hours of small intestinal digestion (I_0 , I_5 , I_{10} , I_{15} , I_{30} , I_{90} , and I_{120}) were analysed by GOPOD reagent (Format K-GLUK 07/11, Megazyme International Ireland Ltd, Ireland) and the results were expressed as starch hydrolysis (%). Hydrolysis index (HI) of the samples was calculated as the area under the curve during simulated small intestinal digestion, using white bread as a reference. Estimated glycaemic index (*eGI*) was calculated by the equation: $eGI = 39.71 + 0.549HI$ (Goñi et al., 1997). All measurements were done in triplicate.

VII.2.6 Statistical analysis

Results are expressed as means \pm one standard deviation. Subsequently, an analysis of variance (ANOVA) with Tukey's test was used to determine significant differences among the means at a

significance level of $p < 0.05$. The data were subjected to correlation analysis and Pearson correlation coefficients were calculated by Minitab Statistical Software version 13 (Minitab, Inc., State College, PA).

VII.3 Results and discussion

VII.3.1 Structural stability of TTC-retrograded+reheated starch *in tuber* and its digestibility

Different water pools with relaxation time (T_{20} , T_{21} , T_{22} , and T_{23}) *in tuber* represent the existing water in various cell compartments (Chen et al., 2018). The relaxation time T_{22} was observed to be negatively correlated with retrogradation enthalpy ($p < 0.05$), so it can be an indicator for the extent of the starch retrogradation *in tuber* (Chen et al., 2018). For the T_{22} of TTC-retrograded tubers, FCR3-t(-20/4/4) had the lowest while FCR3-t(4/4/65) had the highest (Figure VII.1). This might indicate that FCR3-t(-20/4/4) had higher levels of retrograded starch and FCR3-t(4/4/65) had the least. As discussed in Chapter V several, but not all, TTC processes tested, facilitated starch retrogradation *in tuber* more than that noticed during storage at 4°C without TTC. There is potential for TTC1 to make few big aggregates, whereas TTC2 might make many small crystallites with much surface area. So the larger surface area of TTC2 retrograded tubers may require more heat than TTC1 retrograded tubers to melt the structure during reheating. Hence the relaxation times T_{22} of TTC2 retrograded+reheated tubers (FCR3-t(4/65/4)-r90 & FCR3-t(4/4/65)-r90) were lower than FCR3-r90 and FCR3-t(4/-20/4)-r90 (Figure VII.1). But the T_{22} of the FCR3-t(-20/4/4)-r90 was still the lowest (Figure VII.1).

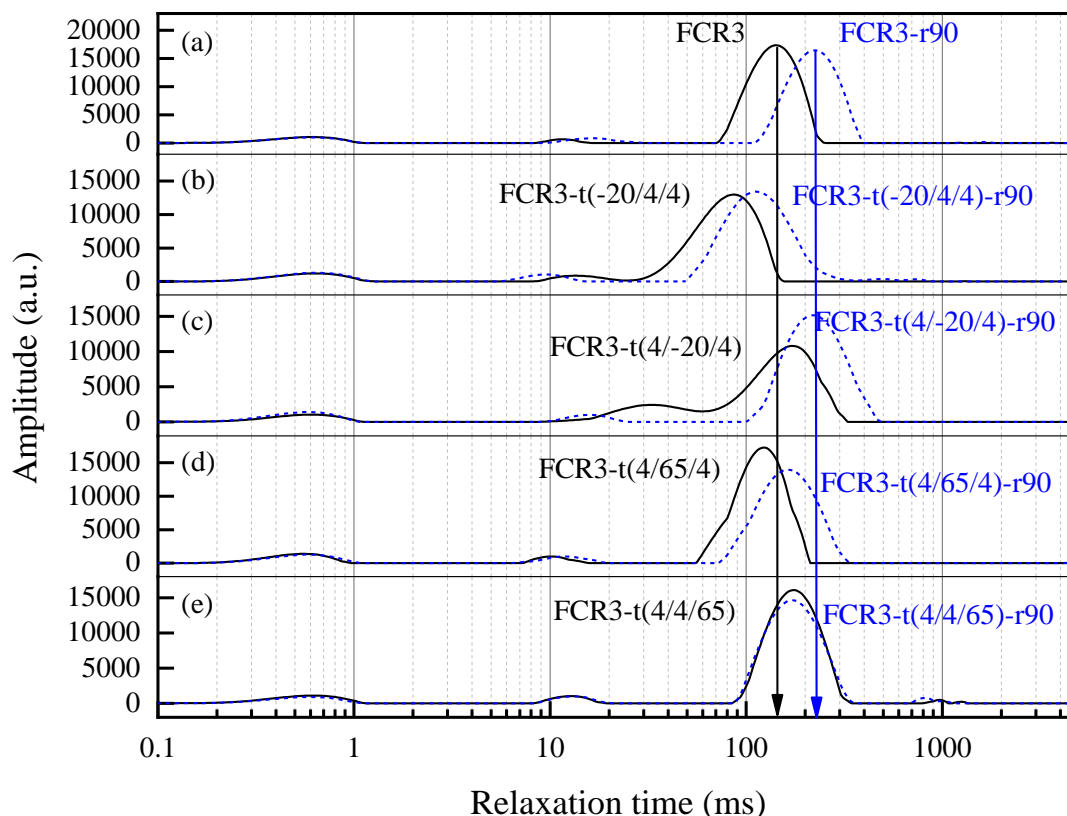


Figure VII.1 Relaxation time distribution curves of (a) traditionally cooked retrograded+reheated potato tubers and (b)-(e) TTC retrograded+reheated potato tubers.

The starch hydrolysis (%) curves of TTC-processed +reheated tubers are shown in Figure VII.2. Starch hydrolysis (%) observed during oral and gastric digestion *in vitro* ranged from 1-10% across the samples (Figure VII.2) reflecting differences in ease of access to starch locally within the bolus and stomach. After 5 minutes of simulated small-intestinal digestion, starch hydrolysis of the FC tubers, was calculated at 76.3%, higher than for TTC1-processed+reheated tubers (e.g. FCR3-t(-20/4/4)-r90, 65.2% and FCR3-t(4/-20/4)-r90, 68.5%) and TTC2-processed+reheated tubers (e.g. FCR3-t(4/65/4)-r90, 51.8% and FCR3-t(4/4/65), 58.6%) (Figure VII.2). The higher amount of slowly digestible starch in TTC-processed tubers (Xie et al., 2014; Yadav et al., 2009) may have contributed towards their improved heat stability and hence led to a lower starch hydrolysis (%).

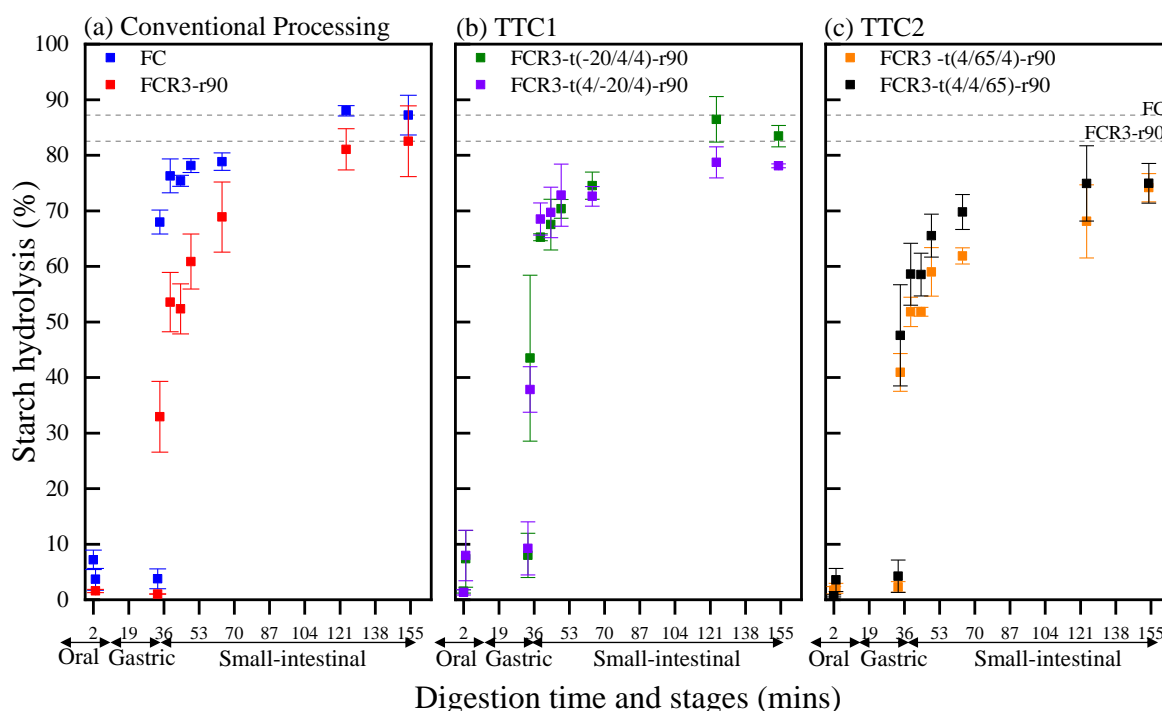


Figure VII.2 Starch hydrolysis (%) of (a) traditionally cooked retrograded+reheated, (b) the TTC1 retrograded+reheated, and (c) the TTC2 retrograded +reheated potato tubers.

Starch hydrolysis (C_{∞} experimental), hydrolysis index (HI), and estimated glycaemic index (eGI) are shown in Table VII.2. There were no significant differences between the experimental C_{∞} of 3-day retrograded+reheated samples, the TTC1-processed+reheated tubers, and the TTC2-processed+reheated potato tubers (Table VII.2). But the HI and eGI of FCR3-t(4/65/4)-r90 were significantly lower than FC and FCR3-t(-20/4/4)-r90 (Table VII.2).

Table VII.2 Starch hydrolysis (C_{∞} experimental), hydrolysis index (HI), and estimated glycaemic index (eGI) of TTC-retrograded+reheated potato tubers.

Samples	C_{∞} experimental (%)	HI	eGI
FC	87.2 ± 4.4 ^a	132.1 ± 0.7 ^a	112.3 ± 0.4 ^a
FCR3-r90	82.5 ± 7.8 ^{ab}	102.2 ± 6.0 ^{bc}	95.8 ± 3.3 ^{bc}
FCR3-t(-20/4/4)-r90	79.4 ± 7.3 ^{ab}	123.5 ± 11.7 ^{ab}	107.5 ± 6.4 ^{ab}
FCR3-t(4/-20/4)-r90	78.1 ± 0.4 ^{ab}	118.1 ± 8.3 ^{abc}	104.6 ± 4.5 ^{abc}
FCR3-t(4/4/65)-r90	74.9 ± 4.4 ^{ab}	114.6 ± 5.9 ^{abc}	102.6 ± 3.3 ^{abc}
FCR3-t(4/65/4)-r90	68.6 ± 9.9 ^{ab}	98.4 ± 10.0 ^c	93.8 ± 5.5 ^c

Different superscripts in same column indicate significant differences ($p < 0.05$) ($n=3$).

VII.3.2 Structural changes of *sous vide* cooked potato tubers during reheating

The short-range order i.e., the amount of double helix and the long-range order, the overall packing of double helices, of starch in *sous vide* cooked-chill+reheated potatoes were measured by ATR-FTIR and X-ray, respectively (Figure VII.3). Deconvoluted FTIR curves of the *sous vide* cooked-chill+reheated potatoes are shown in Figure VII.3a and the values represented the 1047/1022 of each sample. The absorbance at 1047 cm^{-1} and 1022 cm^{-1} were assigned to the ordered molecule domain and the

amorphous domain, respectively (Sevenou et al., 2002a). The ratio of the absorbance of 1047 cm^{-1} to 1022 cm^{-1} has been shown to be related to the amount of ordered starch to amorphous starch (Capron et al., 2007). The 1047/1022 of raw *cv. Agria* (0.79) were significantly lower than *cv. Nadine* (0.93) ($p < 0.05$) ($n=3$) though the RC of *cv. Agria* was observed to be higher than *cv. Nadine*. This may have occurred due to the higher levels of ordered starch molecules near the surface of the starch granule in *cv. Nadine*. The higher ratio of amylose (AM) to amylopectin (AP) in *cv. Nadine* (AM: AP= 1:2.55) than from *cv. Agria* (AM: AP= 1:3.24) may also be responsible for more ordered alignment of AP double helices in *cv. Nadine* ($r=0.909$, $p= 0.033$). There was no significant difference between the 1047/1022 of A_{raw} , A65, A65R3, and A65R3-r60 samples (Figure VII.3a) though their thermal characteristics were significantly different from each other (Chapter VI). This could be attributed to the alignment of amylose/amylopectin chains formed over the long *sous vide* cooking hours which were stable in subsequent cooling and reheating. For *sous vide* cooked *cv. Nadine*, the higher 1047/1022 of N65R3-r60 than for N65R3 (Figure VII.3a) occurred owing to the improved short-range order of N65R3 during low temperature reheating at 60°C. Comparing the 1047/1022 of all samples, the 1047/1022 of A65R3-r60 were significantly lower than N65R3-r60. This may be the molecular structure of *sous vide* cooked *cv. Nadine* is more thermally stable.

The ordered structures at a short-range level (Figure VII.3a) would be a prerequisite for the occurrence of long-range order (Figure VII.3b), but long-range order would not necessarily be presented when short-range order exists (Sevenou et al., 2002a). For potato *cv. Agria*, the RC of samples seemed to follow the same trend as the 1047/1022. The RC of A65 increased (28%) after *sous vide* cooking, and decreased after cooling (A65R3, 25%) and reheating (A65R3-r60, 24%) (Figure VII.3b). The RC of N65 increased (31%) after *sous vide* cooking, and further increased after cooling (N65R3, 34%), then slightly decreased after reheating (N65R3-r60, 31%) (Figure VII.3b). This happened due to the structural changes in *cv. Nadine* occurring deeper in the tuber during *sous vide* cooking than it could be detected by FTIR. The RC of all *cv. Nadine* followed the same trend as its thermal characteristics (Chapter VI) rather than its 1047/1022. This trend, the increase in both RC and T_o of N65, N65R3, and N65R3-r60, showed that structural change may have taken place in inter-block amylopectin chain (Vamadevan, Bertoft, & Seetharaman, 2013) instead of the alignment of crystalline and amorphous domain as 1047/1022 measured by FTIR.

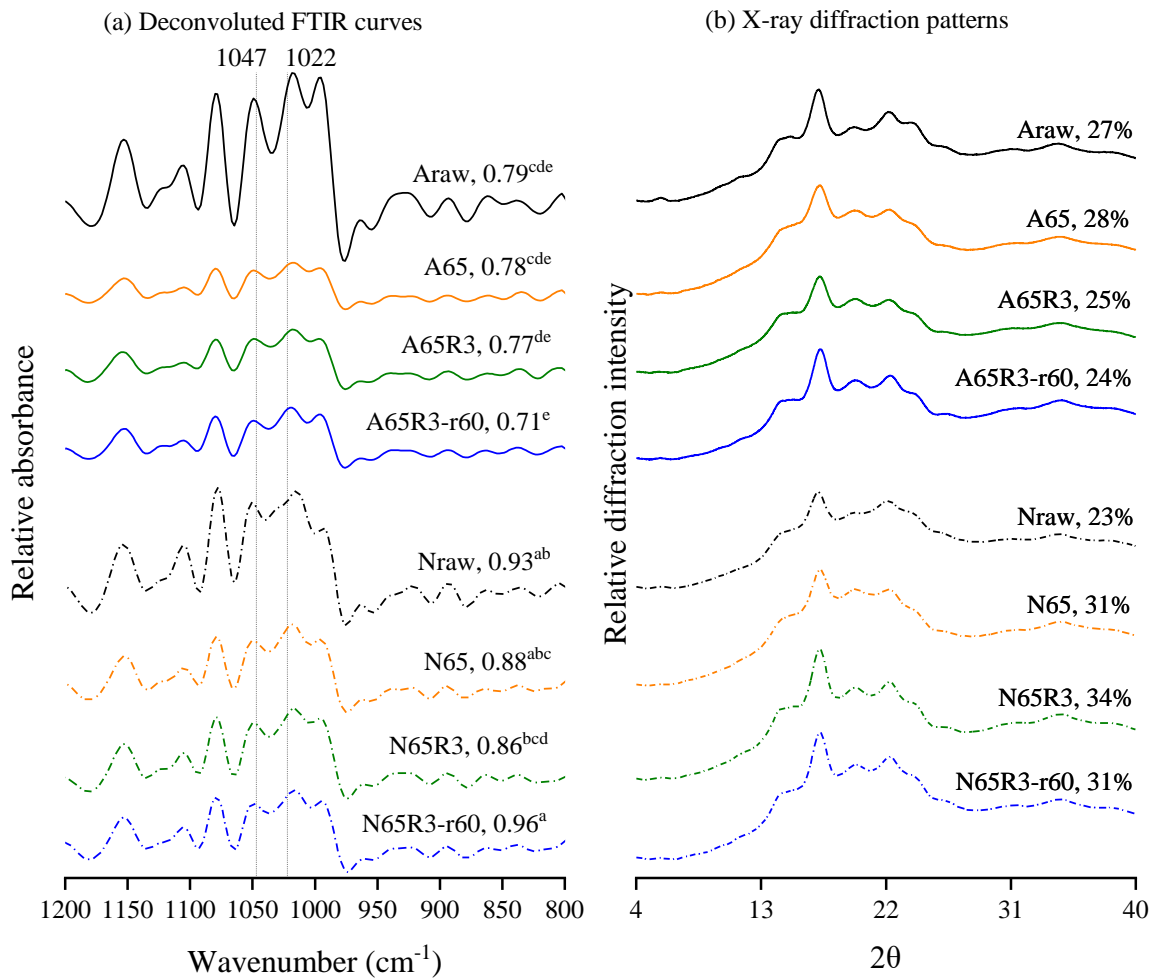


Figure VII.3(a) Deconvoluted FTIR curves of freeze-dried powder of *cv.* Agria, A and *cv.* Nadine, N. The values represented the 1047/1022 of each sample and different superscripts indicated significant differences ($p < 0.05$) ($n = 3$). (b) X-ray diffraction patterns and relative crystallinity of freeze-dried powder of *cv.* Agria and *cv.* Nadine. *Relative crystallinity of the freeze-dried potato samples may vary by moisture content where the average moisture content of the samples were $7.6 \pm 0.1\%$. More experiments may be done for further confirmation.

VII.3.3 Digestibility of *sous vide* cooked-chill+reheated potatoes

Starch hydrolysis (%) of *sous vide* cooked-chill+reheated *cv.* Agria (A65R3-r60) and *cv.* Nadine (N65R3-r60) are shown in Figure VII.4. Starch hydrolysis (%) of A65R3-r60 and N65R3-r60 ranged from 12-18% throughout oral and gastric digestion phases (Figure VII.4) implying differences in ease of access to starch locally within the bolus. Soon after 5 minutes of simulated small intestinal digestion, starch hydrolysis of the N65R3-r60 tubers (25%) was lower than for the A65R3-r60 (47%) and for the FCR3-r60 tubers (42%) (Figure VII.4). This is consistent with the results of the starch hydrolysis of *sous vide* cooked-chill tubers (Chapter VI) indicating potato *cv.* Nadine starch is more resistant to enzymatic breakdown after *sous vide* cooking. The starch hydrolysis (%) of N65R3-r60 gradually increased to a plateau value at 30% after small intestinal digestion (Figure VII.4). This might be attributed to perfection of crystalline domain leading to the increase in resistant starch (Chung et al., 2010). Starch hydrolysis curve of A65R3-r60, although overlapped with FCR3-r60 (Figure VII.4)

exhibited the same resistance toward enzymatic breakdown. Overall, *sous vide* cooked starch (at 65°C) in *cv.* Nadine was more resistant towards enzymatic digestion than in *cv.* Agria. Consistently, starch hydrolysis (C_{∞} experimental), hydrolysis index (HI) and estimated glycaemic index (*eGI*) of FCR3-r60 and A65R3-r60 were significantly higher than N65R3-r60 (Table VII.3). This shows the potential of potato *cv.* Nadine for developing the processed potato product with moderate *eGI*.

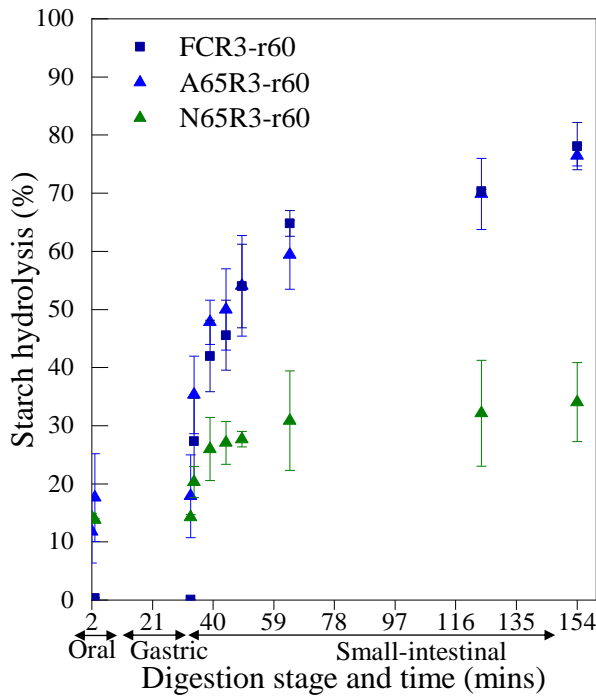


Figure VII.4 Starch hydrolysis (%) of retrograded +reheated *cv.* Agria potato tubers and *sous vide* cooked+reheated *cv.* Agria and *cv.* Nadine potato.

Table VII.3 Starch hydrolysis (C_{∞} experimental), hydrolysis index (HI), and estimated glycaemic index (*eGI*) of *sous vide* cooked potato tubers.

Samples	C_{∞} experimental (%)	HI	<i>eGI</i>
FCR3-r60	72.3 ± 7.4 ^a	64.9 ± 1.3 ^a	75.3 ± 0.7 ^a
A65R3-r60	74.0 ± 8.1 ^a	63.5 ± 7.4 ^a	74.6 ± 4.0 ^a
N65R3-r60	34.0 ± 9.6 ^b	31.3 ± 10.3 ^b	56.9 ± 5.7 ^b

Different superscripts in same column indicate significant differences ($p < 0.05$) (n=3).

VII.4 Conclusion

Time-temperature cycle treatments induced different extents of starch retrogradation *in tuber* (Table VII.4), but all TTC processed+reheated tubers had at least the same or lower relaxation time T_{22} than FCR3-r90. The TTC treated potato tubers were more stable than the 3-day retrograded tubers during reheating as shown by the relaxation time T_{22} (Table VII.4). TTC processed tubers, especially those stored at -20°C for a day and then at 4°C for 2days, had lower relaxation time T_{22} than 3-day retrograded tubers during reheating (Table VII.4). The resistance toward digestive enzymes hydrolysis, i.e. *eGI*

were, however, not significantly different in TTC processed+reheated tubers and 3-day retrograded+reheated tubers. Optimum TTC process may enhance the formation of retrograded starch *in tuber* (Chapter V), but the reheating stability in terms of starch hydrolysis was not as promising.

Sous vide cooking altered the structure of *cv. Agria* at the level of different depth into tuber molecular structure. Different trends in the short-range order (measured by FTIR) and long-range order (measured by XRD) of *sous vide* processed tubers were measured. No significant differences in the 1047/1022 of the samples after *sous vide* cooking at 65°C (0.78), chill storage (0.77) and reheating (0.71) were detected, neither for the relative crystallinity (RC) were measured in *cv. Agria*. The 1047/1022 of *sous vide* cooked-chill then reheated *cv. Nadine* (0.96) were significantly higher than for *sous vide* cooked-chill *cv. Nadine* (0.86), whereas the RC of *sous vide* cooked was higher than raw *cv. Nadine*. For potato *cv. Agria*, starch hydrolysis (%) of *sous vide* cooked wedges (at 65°C) were significantly lower than traditionally cooked wedges and they remained more resistant than 3-day retrograded wedges after refrigeration 4°C (Chapter VI). There was, however, no significant difference in the starch hydrolysis (%) between the 3-day retrograded+reheated (at 60°C) (72.3%) and *sous vide* cooked-chill+reheated (at 60°C) wedges upon reheating (74%) (Table VII.4). *Sous vide* cooked *cv. Nadine*, on the other hand, provided better nutritional functionality with moderate *eGI* (56.9) after chill storage and reheating, only the exudates appeared after 3-day refrigeration needed to be improved for possible commercial application.

Table VII.4 Structural stability refers to the parameters from the test methods.

Process	Code	Relaxation time T22	1047/ 1022	Relative crystallinity	Starch hydrolysis
C	FCR3-r90	*	-	-	*
TTC1	FCR3-t(-20/4/4)-r90	***	-	-	*
TTC1	FCR3-t(4/-20/4)-r90	*	-	-	**
TTC2	FCR3-t(4/65/4)-r90	**	-	-	***
TTC2	FCR3-t(4/4/65)-r90	**	-	-	***
CL	FCR3-r60	-	-	-	***
S	A65R3-r60	-	*	*	***
S	N65R3-r60	-	***	***	*****

* Number of stars indicate the stability of the structure- the more the stars, the more stable the structure.

Chapter VIII Industrial relevance

VIII.1 Introduction

Potato varieties have been developed to suit the purpose of processing. For instance, varieties with moderate to high dry matter (DM), low reducing sugar, and large, long, oval tubers are suitable for French fries (Figure VIII.1), while high DM, low reducing sugar, and moderate-sized oval tubers are preferred for crisps (Figure VIII.1). Moderate to low DM and small tubers are, on the other hand, the essential requirements for canned potatoes. The compositions of potato tubers (Agle & Woodbury, 1968) greatly determine the quality of processed potato products. Dry matter content is one of the most important factors of processing qualities over a range of uses due to the substantial effect on the texture, therefore, the suitability for processing. Potato *cv.* Agria, a multi-purpose and popular domestic use cultivar with medium-firm to slightly mealy potatoes, was chosen and used in the project.

During pre-harvest and post-harvest, agrotechnical practices (e.g. climatic factors and soil type) and technological conditions attribute to the quality and the composition of potato tubers (Mazza, Hung, & Dench, 1983) and hence the final product. Potatoes are normally washed after harvest to prevent surface contamination from soil, mud, and sand (Ahvenainen, 1996). Sometimes another washing after peeling and cutting/dicing is needed to remove microbes and tissue fluids before continuing on processing (Table VIII.1). Washing, combined with the air-bubble is preferable to dipping into water (Ohta & Sugawara, 1987). Blanching is a thermal treatment that commonly performed during the manufacture of potato products (Table VIII.1). Primary objective of blanching is to inactivate enzymes, which are responsible for alterations in sensory attributes (e.g. off-flavours and off-odours), but nutritional loss such as vitamins is inevitable. The blanched product is then either rapidly cooled or passed to the next process immediately. Vegetable tissue rupture during freezing is known to be due to the recrystallisation and sublimation of water. Quality of the frozen potato products deteriorates owing to temperature oscillation that ice crystals melt on the surface of smaller crystals and recrystallize on larger ones simultaneously during storage (Canet, 1989). Long periods of frozen storage are not harmful if a constant low temperature is maintained. For instance, a number of mechanical properties of blanched and frozen potatoes remained when storing at constant $-24\text{ }^{\circ}\text{C}$ (Canet, 1989; Steinka, Barone, Parisi, & Micali, 2017).

Table VIII.1 Processing flow charts of some common frozen potato products

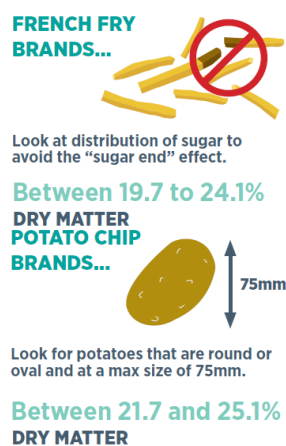


Figure VIII.1 Characteristics of different uses of potatoes (TOMRA Food, 2019).

Raw material	Unit processing				Potato products
Storage temperature (10-12.7°C) Reducing sugar (< 0.12% FW)		→Cutting	→Stepwise blanching	→Frying	French Fries
		→Whole tuber oven-baked	→Cooling		Roasted
	Washing, peeling	→Dicing	→Blanching	→Freezing and storage	Diced/Sliced Formed (Patties/ Hash Browns)
		→Blanching	→Shredding / Mixing	→Shaping	Mashed (frozen, made from fresh potatoes)
		→Cooking	→Mashing/ Mixing	→Cooling	

The following discussions are projections from the main three studies on the possible industrial applications with some foreseen issues that may need to be taken into consideration during upscaling and commercializing.

VIII.1.1 Retrograded+reheated potato tubers

Assertion: Consuming boiled potato after cooling or reheated at low temperature (50°C) after at least a day of refrigeration is recommended.

Rationale:

With the growing consumers' preference for convenient but healthy, natural, and high-quality food products, modulating starchy food to low glycaemic features through retrogradation has a great opportunity. Starch that escapes hydrolysis and absorption in the small intestine and enters the colon for fermentation is known as resistant starch (RS) (Englyst, Kingman, & Cummings, 1992). RS exhibits a low and slow digestibility which can be used as a vehicle for slow-release glucose in starchy food (Sajilata et al., 2006). Resistant starch, associated with a number of physiological effects has been proved to be beneficial for health (Nugent, 2005). During the fermentation of resistant starch by the colonic microflora, short-chain fatty acids (SCFA) such as acetic, propionic and butyric acids are formed. SCFA profiles derived from RS are lower in acetate and higher in butyrate than indigestible carbohydrates of those conventional dietary fibres. The SCFA such as butyrate are an energy source for colonic cells (Goñi et al., 1997) and may have a preventive role against development of colonic diseases, such as ulcerative colitis (Hoover & Zhou, 2003). Resistant starch content in a meal may modulate blood glucose by reducing peak postprandial blood glucose concentration (Hoebler, Karinithi, Chiron, Champ, & Barry, 1999; Jenkins et al., 1998).

Based on the food forms, in which the food is eaten, different measuring methods of RS were used leading to varied results (Åkerberg, Liljeberg, Granfeldt, Drews, & Björck, 1998; Haralampu, 2000). In our studies (Chapter IV, V, VI, and VII), the starch digestion *in vitro* simulates physiologic digestion, including the chewing process, followed by incubation of pepsin in simulated gastric condition (Goñi,

García-Diz, Mañas, & Saura-Calixto, 1996), and then in simulated small-intestinal condition with a mixture of digestive enzymes (pancreatin, amyloglucosidase and invertase) (Englyst et al., 1992). Starch nutritional fractions, i.e., rapidly digestible starch (RDS), slowly digestible starch (SDS), and resistant starch (RS) are defined by the glucose released after a certain time of simulated small-intestinal digestion (Figure VIII.2). *The amount of resistant starch measured would be different from the result of regulated methods in FSANZ.* The trend of RS content has been yet found to be similar among different methods- increasing resistant starch content with a longer period of starch retrogradation (Zhou, Chung, Kim, & Lim, 2013).

The significantly lower *eGI* of the 7-day retrograded tubers (FCR7, 71) than the freshly cooked tubers (FC, 101) and 7-day retrograded+reheated (at 90°C) tubers (FCR7-r90, 84) (Chen et al., 2018) can be attributed to the amount of resistant starch formed during 4°C refrigeration (Figure VIII.2). Our results concurred with the glycaemic responses of the 21 participants after consuming cooled (for 3 days) potato product (Tahvonon et al., 2006). Serving temperature has been reported to be more influential on the resistant starch content than variety (Raatz et al., 2016). The retrograded starch formed during cooling retained to some extent after reheating: the *eGI* and GI of retrograded+reheated (at 80 or 90 °C) potatoes were significantly lower than freshly cooked potatoes (Chen et al., 2018; Tahvonon et al., 2006). The resistant starch of the 1,3, and 7day-retrograded+reheated at 50°C tubers (FCR1-r50, FCR3-r50, and FCR7-r50) were significantly higher than freshly cooked and the 1-day retrograded+reheated at 90°C tubers potatoes by 25-32% (n=3, *p*<0.05) (Figure VIII.2). Resistant starch was observed to be heat sensitive where reheating at 70°C and 90°C decreased the resistant starch by 5-17% and 7-32%, respectively (Figure VIII.2).

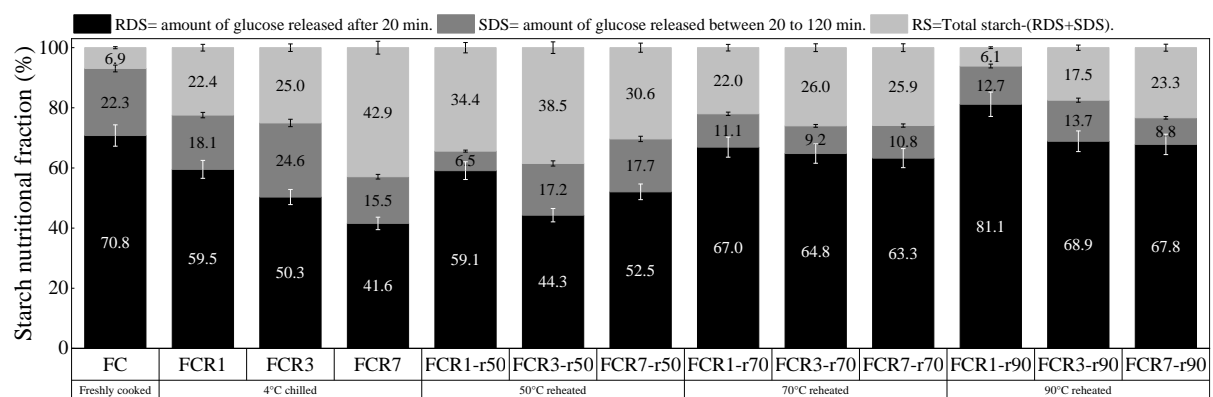


Figure VIII.2 Starch nutritional fractions (%) in boiled-chill+reheated potato tubers. Values on the bars indicate the relative amount of starch nutritional fractions (%). And error bars indicate the standard deviation of triplicate results.

VIII.1.2 Time-temperature cycles process

Assertion: A proper combination of the suitable cultivar with optimum time-temperature cycle process can obtain both healthy (i.e. high in resistant starch) and delicious (e.g. smooth and creamy mashed potato) processed potato product.

Rationale:

Starch retrogradation, the on-going and non-equilibrium process of recrystallisation of gelatinised starch during cooling and storage (Ratnajothi Hoover, 1995; Jacobson et al., 1997), involves three phases of crystallisation: (i) nucleation, (ii) propagation or growth of crystals, and (iii) maturation or crystal perfection (Slade & Levine, 1987; Wunderlich, 1980). The crystallisation is dependent on the relativity of starch temperature to the glass transition temperature of the starch-water system, T_g and to its melting temperature, T_m , due to variable levels of segmental motion within amorphous and crystalline domains.

A temperature cycling process is likely to induce stepwise nucleation and propagation which promotes the growth of crystalline regions and perfection of crystallites, resulting in a higher content of slowly digestible starch (SDS) and resistant starch (RS) in cereal, potato, and pea starches (Sievert & Pomeranz, 1989; Silverio et al., 2000). In an attempt to enhance the formation of the retrograded starch in cooked tubers, time-temperature cycle processes were studied. Several, but not all, of the time-temperature cycle processes tested facilitated starch retrogradation *in tuber* more than did storage fixed at 4°C (Chapter V).

Processed potato products commonly experience temperature fluctuation throughout storage and retail and foodservice (Nam, 2018). Product quality such as drip loss (syneresis) and textural changes are the main concerns for food manufactures despite the potential health benefit derived from the increase in the content of resistant starch by enhanced starch retrogradation in TTC processed potato tubers (Figure VIII.3).

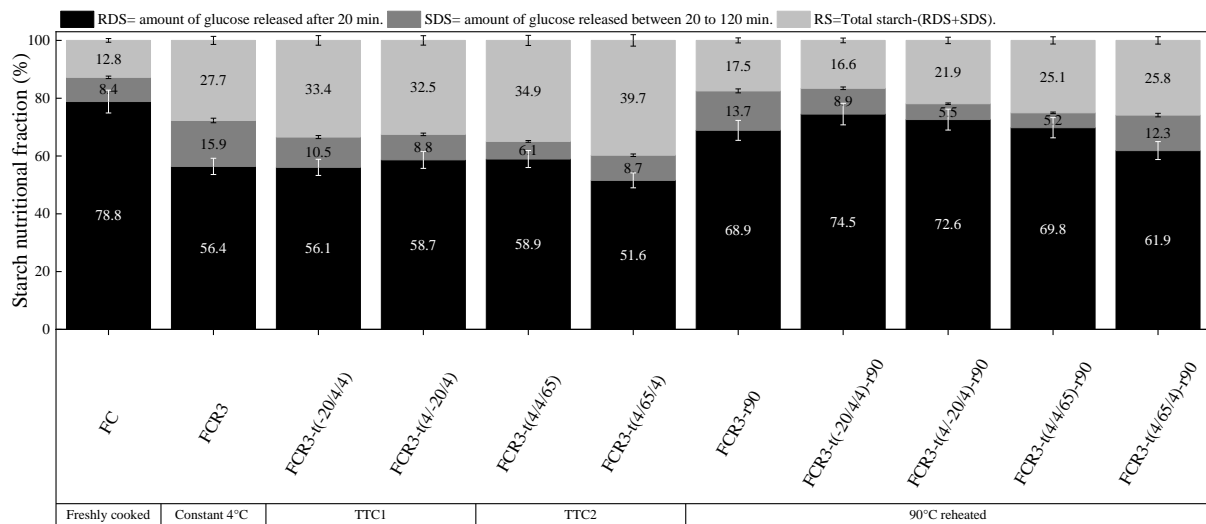


Figure VIII.3 Starch nutritional fractions (%) in TTC processed and TTC processed+reheated potato tubers. Values on the bars indicate the relative amount of starch nutritional fractions (%). And error bars indicate the standard deviation of triplicate results.

A project from The Pure Food Co. was carried out by Rina Nam to solve the undesirable sensory properties of the mashed potato mainly developed for the elderly. This foodservice supply chain involved two freeze-chill cycles (between -18°C and 4°C) before the reheating (at 75°C) and then serving (Nam, 2018). Some advantages of freeze-chill over chill storage in logistics include: (i) bulk production, (ii) microbiological control during storage, and (iii) controlled-release of frozen product into the chill chain during transportation (Redmond et al., 2004; Zanoni & Zavanella, 2012).

During cooking, starch granules imbibe water and swell as hydrogen bonding formed between water and hydroxyl groups on amylose or amylopectin. Gradually starch granules disintegrate owing to the disruption of crystalline structure. With subsequent cooling of the gelatinised starch in cooked potato, re-crystallisation of the starch chains occurs slowly expelling the excess of water. Freezing predisposes boiled potatoes to fragile cell structure as ice crystals freeze from the excess water introduced during cooking (Li, Zhu, & Sun, 2018). Freeze-chill, thus, causes the increase in syneresis, i.e. drip loss in the products than chill foods that had not been previously frozen. The time length of frozen storage had, however, no effect on syneresis, firmness/adhesiveness, vitamin C content, total viable count, or the sensory score as comparing the freeze-chill mashed potato with frozen mashed potato (Redmond, Gormley, & Butler, 2003).

Potato cultivars have a range of different characteristics in terms of appearance, size and shape as well as eating and cooking qualities. Two potato cultivars have been used to examine the effect of freeze-chill on the quality of mashed potato in her preliminary experiments (Nam, 2018). Potato dices of a 150g tuber have been cooked in boiling water till soft, then the water were drained. After one freeze-chill cycle at -18°C for one day then 4°C for a day, potato *cv.* Agria was observed to have less syneresis (%) at 2.1% than potato *cv.* Nadine did at a syneresis (%) of 27.9 % (Nam, 2018). This has

happened due to the dry matter content of two cultivars: the floury potato *cv. Agria* with a high dry matter of 23.1% compared to the waxy potato *cv. Nadine* with a low dry matter of 15.7%. Similarly, the mashed potato from *cv. Maris Piper*, a waxy and smooth textured potato has been observed to have the highest syneresis (%) followed by the mash from *cv. Rooster*, an all-round potato and *cv. Golden Wonder*, a very dry and floury potato (Redmond et al., 2003).

After reheating by microwave, the mashed potato from *cv. Agria* retained shape better than the mash of potato *cv. Nadine* (Nam, 2018). At the molecular level, amylose content, mainly located in the amorphous region, was higher in potato *cv. Nadine* (28.2%) than in *cv. Agria* (23.6%), triggering the amorphous lamella to hydrate excessively in potato *cv. Nadine* during cooking. Excess water was introduced to the amorphous lamella of potato *cv. Nadine* inducing the phase transition of amorphous regions followed by crystalline regions during cooking. The resulting disrupted amylose and amylopectin recrystallize during cooling where linear chains of amylose facilitate cross-linkages through hydrogen bonds, expelling the excess water from the retrograded potato *cv. Nadine*. Consequently, a more compact retrograded amylose in cook-chill then reheated *cv. Nadine* (than *cv. Agria*) were not able to imbibe the water again during reheating, resulting in less shaped mashed potato *cv. Nadine* than *cv. Agria*.

Additional water as well as other ingredients have been added to Rina Nam's recipe of the mashed potato to improve the sensory perception (Nam, 2018). These ingredients added (confidential) can either promote or delay starch retrogradation as discussed in Chapter II Review of literature though the physicochemical characteristics (NMR, X-ray, hydrolysis) haven't been examined in Rina's thesis. The logistic of the supply chain in Rina's report was very identical to the concept developed in Chapter V. The increase in retrograded starch in tuber induced by time-temperature cycle, i.e. -20C then 4C therefore, combined with other ingredients added to the mash can reduce GI potentially- confirmation of the physicochemical characteristics of the mashed potatoes are required.

VIII.1.3 *Sous vide* cooked-chill/cooked-frozen then reheated potato wedges

Microbial growth, the main concern of *sous vide* cooked product (Schellekens, 1996), could be control by blanching with a minimum heat penetration depth before *sous vide* cooking. Blanching involves heating vegetables and fruits rapidly to a predetermined temperature for a specified amount of time, typically 1 to less than 10 min. Blanching temperature and time are selected to inactivate oxidases, peroxidases, catalases, and lipoxygenases (Table VIII.2); meanwhile to retain as many nutrients as possible (Xiao et al., 2017).

Peroxidase (POD) is considered to be the most heat resistant enzyme in potato tuber (Anthon & Barrett, 2002); therefore, the activity of peroxidase has been widely used as an indicator for the level of blanching (Müftügil, 1985; Ramaswamy & Chen, 2011). POD, a heme-containing enzyme, is associated with wound-healing processes in plants. POD induces single-electron oxidation of phenolic compounds with the existence of hydrogen peroxide (H₂O₂). This reaction leads to the formation of

melanin and thus a browning effect. The assumption still needs to be further investigated due to the low hydrogen peroxide content in vegetable tissues (Veljovic-Jovanovic, Noctor, & Foyer, 2002). It could be the synergistic action between POD and polyphenol oxidase (PPO), where PPO oxidise some phenolics to generate hydrogen peroxide for POD (Jiang & Miles, 1993; Toivonen & Brummell, 2008).

Polyphenol oxidase activity is the greatest at the tuber exterior, including the skin and cortex tissue (where it is 1 to 2 mm beneath the skin) (Thygesen, Dry, & Robinson, 1995). PPO catalyses two continuous reactions: hydroxylation of monophenols to diphenols then oxidation of diphenols to quinones. Subsequent reactions of quinones, the highly reactive compounds lead to melanin accumulation, resulting in less attractive appearance (brown- or black-coloured products) and nutritional loss (Espín et al., 2000).

Pectin methyl esterase (PME) becomes active as potatoes are heated to the temperature between 50°C and 70°C (Canet, Alvarez, & Fernández, 2005). PME demethylates carboxymethyl groups of pectic polysaccharide chains and produces free carboxylic acid (Manmohit Kalia, 2015). Simultaneously, the increased permeability of cell walls allows the migration of solutes (e.g. Ca²⁺ or Mg²⁺ cations) from cytoplasm and vacuole to the membrane. Demethylated pectin chains can then link via calcium interchelation into egg box structures, which may lead to the strengthening of the cell wall (Grant, Morris, Rees, Smith, & Thom, 1973; Ross et al., 2011).

Table VIII.2 Enzyme activities of potato *cv.* Russet Burbank after a certain level of blanching.

Enzymes	Mechanism	Influences	T (°C) for D=5min
Peroxidase (POD)	POD may bond to endogenous hydrogen peroxide creating free radicals that react with a wide range of food constituents such as ascorbic acid, carotenoids and fatty acids.	Loss of colour and flavour, as well as nutrients degradation.	83.2
Polyphenol oxidase (PPO)	PPO catalyses the conversion of monophenols to o-diphenols and o-dihydroxyphenols, and then to o-quinones.	Melanin accumulation leads to brown- or black-coloured products.	66
Pectin methyl esterase (PME)	Demethylation of pectin materials by pectin methyl esterase (PME) leads to the cross-linking between demethoxylated pectin and calcium ions at low-temperature (50-70°C).	Low-temperature blanching firmness.	70

A stepwise blanching is often applied to the production of French fries to optimise the texture (Abu-Ghannam & Crowley, 2006; Canet et al., 2005) and to prevent both enzymatic and non-enzymatic browning (Kaymak & Kincal, 2007). Blanching at low temperature (50-70 °C) leads to a firmer texture, as a result of strengthened cell walls by pectin methyl esterase (Bartolome & Hoff, 1972a) and reduces disintegration of intercellular substances (Verlinden, Yuksel, Baheri, De Baerdemaeker, & Van Dijk, 2000). Blanching at high temperatures (80-100 °C) for long times (15 min), on the other hand, leads to

the loss of firmness (Andersson, Gekas, Lind, Oliveira, & Oste, 1994). Changes in both structural and physical properties of the constituents in the parenchyma, alter the texture of the resulting blanched fries (Ngobese, Workneh, & Siwela, 2017; Thygesen, Thybo, & Engelsen, 2001).

In the *sous vide* study (Chapter VI), wedges were vacuum packed immediately after peeling and cutting to prevent enzymatic browning by polyphenol oxidase (Rocha et al., 2003). Colour of the *sous vide* cooked potato wedges are yet to be quantified to ensure no undesirable effects occur (Figure VIII.4). Water exudates from *sous vide* cooked wedges (at 55°C) of potato *cv.* Agria and *cv.* Nadine were observed (Figure VIII.4a, b). This may have happened simultaneously with the crystalline perfection where excess water in amorphous and semi-crystalline regions of starch granules migrate to the space of inter/intra cell compartment, then appeared as exudates. No water/ less water was observed in *sous vide* cooked (at 65°C) wedges *cv.* Agria and *cv.* Nadine (Figure VIII.4c, d). Excess water, appearing as a result of crystalline perfection, may be stabilised by leached amylose from partially gelatinised starch, therefore no water (Figure VIII.4c) or fewer exudates (Figure VIII.4d). Lower dry matter and lower total starch content of potato *cv.* Nadine than *cv.* Agria may lead to more exudates in potato *cv.* Nadine.

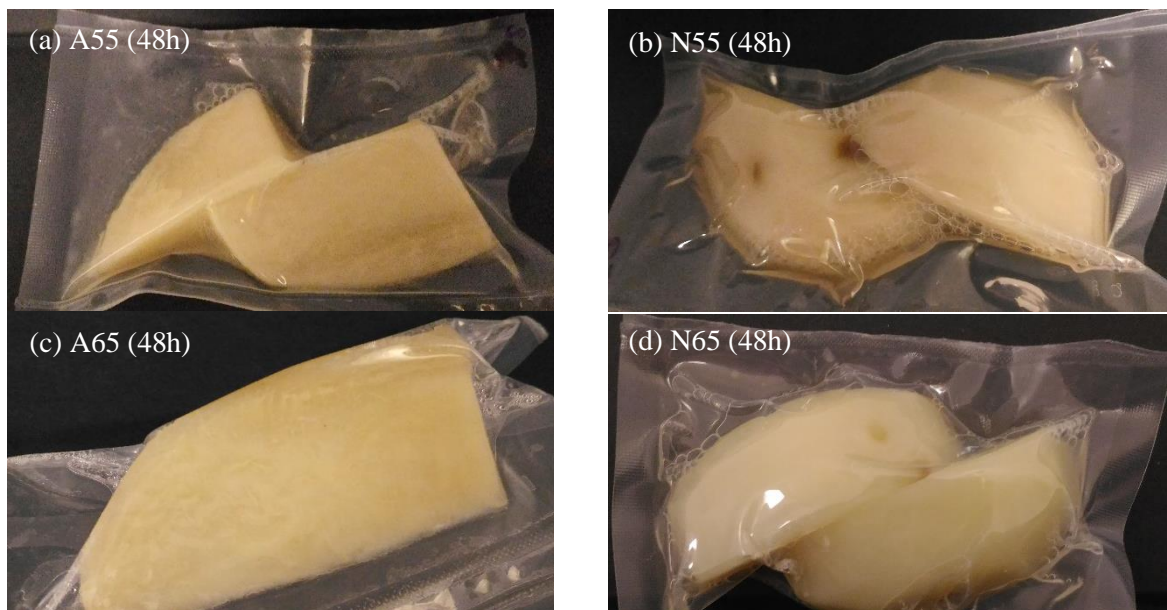


Figure VIII.4 Appearance of *sous vide* cooked wedges from *cv.* Agria (a) at 55°C and (c) at 65°C and from *cv.* Nadine (b) at 55°C and (d) at 65°C.

The study of starch microstructural changes in *sous vide* cooked potatoes and its starch digestion *in vitro* was carried out as mentioned in chapter VI. Discussions about the hardness, an important sensory perception for processed potato products, are given in the following context.

Assertion: For commercial application, *sous vide* cooking at 55°C for 2 hours could be chosen regardless of cultivars for further production and sensory optimisation.

Rationale:

Throughout *sous vide* cooking, refrigeration, and reheating, the processing temperature was kept below gelatinisation peak temperature. The texture of the *sous vide* cooked wedges thus could be attributed to both the swollen granules (Figure VIII.5a) or partially gelatinised starch (Figure VIII.5b) and the strengthening effect of the cell wall structure by PME. Significant decreases in hardness of *cv. Agria* occurred after 2 hours and 20 hours of *sous vide* cooking at 55°C but still significantly higher than traditionally cooked *cv. Agria* tuber (Figure VIII.5a). The texture of blanched potato strips at low temperatures (62.8 & 68.3°C) has been found to be independent on blanching time, whereas the texture of blanched strips at high temperatures (73.9, 79.4, 85 & 90.6°C) has been observed as a function of both temperature and time (Liu & Scanlon, 2007). For *cv. Nadine*, significant decreases in hardness happened soon after 10 minutes of *sous vide* cooking but remained at 22.5 ±3.5 N till the end of *sous vide* cooking, yet statistically similar to the traditionally cooked *cv. Nadine* (Figure VIII.5a). Changes in hardness by time concurred with the development of the relaxation time where relaxation times (T_{21} , T_{22} , and T_{23}) had significant changes after 2h of *sous vide* cooking at 55°C (Chapter VI).

Assertion: For commercial application, *sous vide* cooking at 65°C for 1 hour could be chosen regardless of cultivars for further production and sensory optimisation.

Rationale:

As for *sous vide* cooking at 65°C, a significant decrease in hardness of A65 took place after 1h (Figure VIII.5b). The hardness values of the *sous vide* cooked *cv. Agria* potatoes were similar to traditionally cooked *cv. Nadine* potatoes at 32h of *sous vide* cooking (Figure VIII.5b). For N65, the significant reduction in hardness happened within 10 min and remained at 21.8N to 24.7N till the end of *sous vide* cooking (Figure VIII.5b). It is, therefore, sensible to explore the possibility of *sous vide* cooking at 65°C for 1 hour on both cultivars.

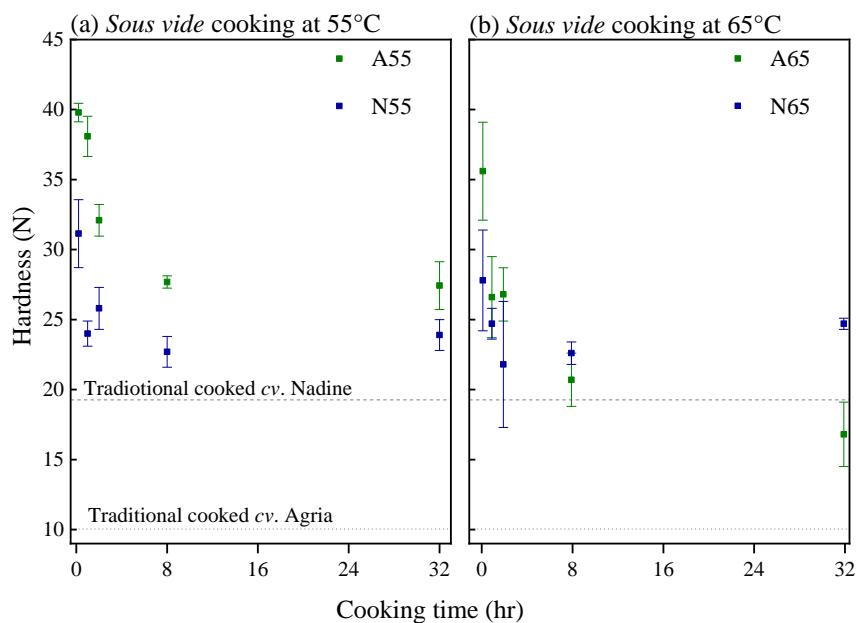


Figure VIII.5 Changes in hardness of potato *cv. Agria* and *cv. Nadine* during *sous vide* cooking at (a) 55°C and (b) 65°C.

The effect of *sous vide* cooking on the hardness might last even after reheating (Abu-Ghannam & Crowley, 2006). There was no significant difference between the hardness of A65 (for 48h) and traditionally cooked tubers (Figure VIII.6). After refrigeration then reheating at 60°C, the hardness of both FCR3 and FCR3-r60 were, however, significantly lower than for both A65R3 and A65R3-r60 (Figure VIII.6). This could also be the starch retrogradation came into play in terms of hardness.

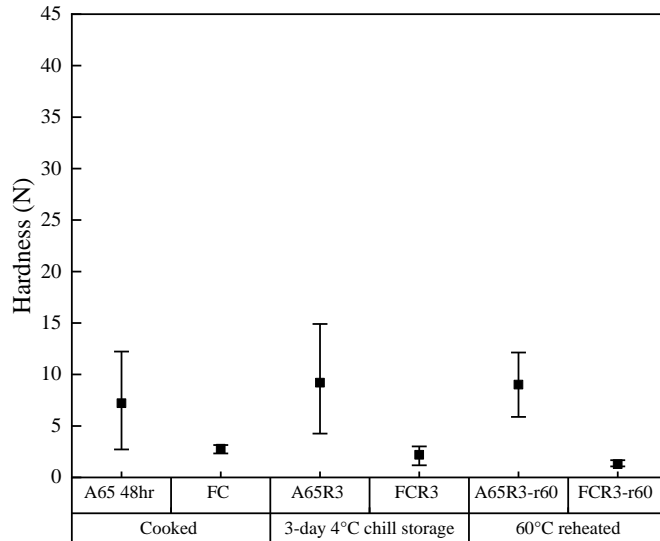
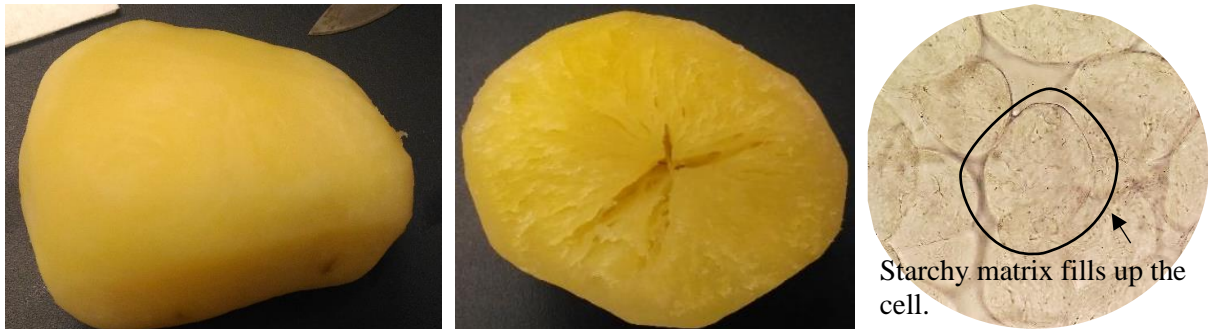


Figure VIII.6 Comparison of the hardness between the traditionally cooked-chill then reheated and the *sous vide* (at 65°C) cooked-chill then reheated potato *cv.* Agria.

Assertion: *Sous vide* cook-freeze process can be an alternative to *sous vide* cook-chill process for longer shelf life.

Rationale:

Sous vide cook-freeze then reheating process was carried out preliminarily to explore the alternative for longer shelf life. Appearance and microstructure (Figure VIII.7) and relaxation time distribution (Figure VIII.8) of *sous vide* cooked-frozen then reheated whole potato tuber were studied. *Sous vide* cooked-frozen *cv.* Agria were microwave reheated (1100W) for 5min, resulting in fully gelatinised starch with excess exudates *in tuber* (Figure VIII.7a). The other *sous vide* cooked-frozen *cv.* Agria was reheated in a water bath at 90°C, partially gelatinised potato *cv.* Agria, some swollen granules with ruptured ones, was obtained (Figure VIII.7b). For both reheating methods, cracks on the crosscut section seemed to align with pith (Figure VIII.7) where starch granules are found to be less compared to other sections, such as cortex, perimedullary zone and a vascular ring of the tuber (Rommens, Shakya, Heap, & Fessenden, 2010). It could be due to either the heat transfer or the inhomogeneous distribution of starch *in tuber*. Reheating in 90°C water bath (for 40min until the core temperature of the tuber reached 70°C) allowed frozen *sous vide* tuber to defrost progressively, resulting in more swollen but intact granules (Figure VIII.7b). This progressive reheating may allow hydroxyl group to interact with water molecules without disruption of granular structure, keeping more water within tuber than microwave reheated one.



(a) *Sous vide* cooked-frozen then microwave reheated *cv. Agria*.



(b) *Sous vide* cooked-frozen then water-bath reheated *cv. Agria*.

Figure VIII.7 Appearances and micrographs of *sous vide* cooked-frozen then reheated *cv. Agria* by (a) a microwave or (b) a water bath.

Freezing, a long-term preservation technique for foods offers a means to suppress microbial growth and to preserve taste and nutritional value. Formation of ice crystals or ice recrystallisation can, however, deteriorate the quality of foods in the cold chain. During freezing, ice nucleation initiates from extracellular space then propagate, compromising cell wall rigidity and cytoplasm intactness (Pearce, 2001). Ice crystals have a larger volume than water, so the cell walls and membranes are submitted to mechanical stresses leading to possible cell damage during freezing. As discussed in chapter VI, the relaxation time distribution of A65 was similar to freshly cooked tuber that four separated peaks were discerned (Figure VIII.8a). Relaxation time T_{22} , indicating the mobility of water associated with the starchy matrix, were lower in A65 than in freshly cooked tuber due to the crystalline perfection over *sous vide* process (Figure VIII.8a). The merging of water pools with relaxation time T_{21} and T_{22} was evident in both cooked-frozen and *sous vide* cooked-frozen tubers (Figure VIII.8b) where ice crystals may have damaged potato cells, allowing intercellular and intracellular water to mix (Micklender et al., 2008). The merged relaxation time of T_{21} and T_{22} was lower in cooked-frozen tuber than in *sous vide* cooked-frozen tuber (Figure VIII.8b). Freezing-concentrated effect may have been promoted in gelatinised starch of cooked-frozen tuber where amylose and amylopectin were more disrupted, compared to *sous vide* cooked-frozen tuber. During reheating, fully gelatinised starch in cooked-frozen+reheated tuber seemed to be able to form hydrogen bonds with water molecules again as evidenced by the lower relaxation time T_{23} (Figure VIII.8c). *Sous vide* cooked-frozen then reheated

tuber with higher relaxation time T_{23} (Figure VIII.8c), on the other hand, appeared to have more water freely flow between intracellular and intercellular spaces.

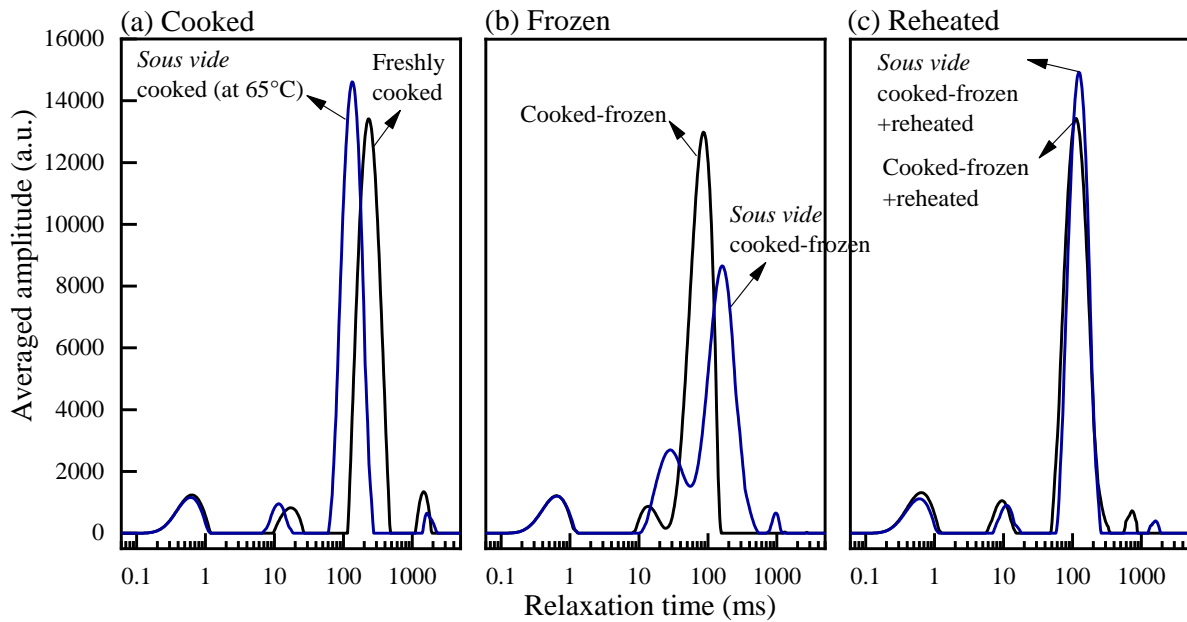


Figure VIII.8 Relaxation time of (a) freshly cooked and *sous vide* cooked (at 65°C) *cv.* Agria, and for (b) cooked-frozen and *sous vide* cooked-frozen *cv.* Agria, and for (c) cooked-frozen then reheated and *sous vide* cooked-frozen then reheated *cv.* Agria.

Bearing in mind the potential opportunity for commercialisation, the optimisation of the cooking duration can be further tested by full factorial design based on the change of hardness and the appearance/ colour by time. Sensory test should be conducted along the side. Understanding the critical control points (Table VIII.3), sufficient heat treatment combined other hurdle techniques (Table VIII.4) may be essential for the ‘haute cuisine’ of *sous vide* processed potato.

Table VIII.3 Processing steps and critical control points (CCPs) of *sous vide* cooked-chill/ cooked-frozen potato.

	Processes	Critical control points
Low risk area	Potato tuber receipt/ storage.	CCP1: Microbial growth (temp. abuse).
	Cutting, peeling, blanching.	
	Manual/automatic pump to the line.	
	Thermoforming <i>sous vide</i> pouches.	
	Manual/automatic product filling.	CCP2: Foreign body contamination.
High risk area	Vacuum sealing & cutting of <i>sous vide</i> pouches.	CCP3: Microbial contamination/ growth.
	<i>Sous vide</i> processing (65-95°C) by steam or water immersion, or water steaming in retort/cooker for a certain period of time and then cooling.	CCP4: Microbial growth.
	Blast-chilling (<5°C/90 min or blast freezing).	CCP5: Microbial growth (temp. abuse).
	Metal detection.	CCP6: Metal contamination.
	Labelling, boxing, palletising.	
	Chilled (<5°C) or frozen storage (<-18°C).	CCP7: Microbial growth (temp. abuse).
	Chilled or frozen distribution.	CCP8: Microbial growth (temp. abuse).
	Reheating and serving at home.	

Reprinted from “Handbook of Food Safety Engineering”, P468-496, Chapter 19 “Sous vide and cook-chill processing”, Gormley & Tansey, 2012, with permission from Elsevier.

Table VIII.4 Examples of hurdles.

Types	Techniques
Physical hurdles	Heat: blanching; pasteurisation; cooking.
	Cold: chilling; freezing; freeze-chilling.
	Packaging: ambient; vacuum; aseptic; MAP.
Physico-chemical hurdles	Salt; sugar; dehydration (a_w); spices.
	Acidity: acidulants; fermentation.
	Preservatives: sulphur dioxide; ethanol; smoke.
	Chlorine; ozone.
Microbial-derived hurdles	Competitive flora.
	Starter cultures.
	Bacteriocins.
Combined hurdles	

Reprinted from “Handbook of Food Safety Engineering”, P468-496, Chapter 19 “Sous vide and cook-chill processing”, Gormley & Tansey, 2012, with permission from Elsevier.

Chapter IX General discussion and conclusion

IX.1 Introduction

This thesis asked whether functional processed potato products with low glycaemic features could be made through starch retrogradation in whole tuber (*in tuber*). The underlying aim was to gain a better understanding of the mechanisms of starch retrogradation in tuber. This knowledge is expected to bring insights for optimising manufacturing condition and to formulate a scientific basis for new process designs. Challenges were to investigate starch retrogradation in tuber and to tailor a structure with low glycaemic features, and to retain resistance to digestive enzymes after reheating. In this chapter, the most important findings will be discussed and concluding remarks provided.

IX.2 Main findings and discussions

A literature review of mechanisms of starch retrogradation and its health implications is given in Chapter II, with a focus on existing and new technologies to create tailor-made structures displaying low glycaemic features. The research gap, lack of knowledge of the mechanism of starch retrogradation in tuber rather than starch-water systems, is identified in Chapter II, and thus methods to study starch retrogradation in potato tubers are developed and described in Chapter III.

Potato *cv.* Agria, the most popular cultivar to household use in New Zealand, was chosen in Chapter IV as a model to study starch retrogradation in a whole food. Potato tubers encompass different cell compartments (e.g. cell wall, vacuole, cytoplasm and intracellular spaces) where starch gelatinisation and starch retrogradation can occur, subject to local interactions with other cell components and subject to water availability. Starch retrogradation in tuber was investigated successfully by LF-NMR, a non-invasive technique. Water, the most abundant component in tuber appeared to exist in four states during starch retrogradation each with a relaxation time. Effects of processing, cooling and reheating on structures formed by gelatinised amylose and amylopectin, and the effects on water migration, were inferred from the vibration of hydrogen bonding as indicated by relaxation time. A cyclic pattern of the relaxation time T_{22} of freshly cooked, retrograded, and retrograded-then-reheated tubers was observed. The relaxation time of a water population indicates mobility- the water with low relaxation time is more mobile and less restricted. This could facilitate enzyme diffusion during digestion leading to greater starch hydrolysis (%): low relaxation time T_{22} was positively correlated to greater starch hydrolysis of the treated tubers ($p < 0.05$) in Chapter IV.

A 36% reduction of starch hydrolysis was observed with longer retrogradation times (for 7 days). Reheating of retrograded tuber restored 10% of the susceptibility to enzymatic hydrolysis and some

internal water mobility (measured by relaxation time T_{22}) in Chapter IV. Longer chill storage further improved the stability of retrograded tuber against reheating effects (Chen et al., 2018).

A temperature cycling process is likely to induce stepwise nucleation and propagation which promotes the growth of crystalline regions and perfection of crystallites, potentially resulting in a higher content of slowly digestible starch (SDS). We extended the idea of time-temperature cycle (TTC) processes to freeze/ chill (at $-20^{\circ}\text{C} / 4^{\circ}\text{C}$, TTC1) and chill/warm (at $4^{\circ}\text{C} / 65^{\circ}\text{C}$, TTC2) domains to investigate the effect of TTC on retrogradation rate of starch in cooked potato tuber in Chapter V. Time-temperature cycle processes tested gave different indications of starch retrogradation in tuber compared to storage fixed at 4°C . The TTC1 process increased the retrogradation enthalpy to 4.7 J/g d.b.(compared to the 1.6 J/g d.b. of the retrogradation enthalpy of 3-day retrograded tuber) and decreased water mobility to T_{22} , 86.5 ms signifying that starch-rich and starch-depleted regions facilitated the formation of retrograded starch in starch-rich regions. The TTC2-processed tubers held under chill and warm conditions showed the lowest blue value (at 0.5) and least starch digestibility *in vitro* (60.3%). These two sets of time-temperature processes induced starch retrogradation in tuber differently though all such samples ($n=6$) showed higher retrogradation enthalpies and lower starch digestibility between which a negative correlation ($r=-0.65$, $p=0.005$) was obtained. Similar time-temperature cycle processes can be useful to drive physico-chemical changes of the potato product within the industrial cold chain.

Annealing (heating starch at a temperature below gelatinisation temperature in excess water) permits a modest molecular reorganisation to occur and a more organised structure of lower free energy to form. In Chapter VI, a *sous vide* process akin to annealing was investigated, intending to create edible potato pieces with resistance to digestive enzymes. Extent of potato cell disruption and degree of the starch gelatinisation, resulting from a *sous vide* process, alter starch retrogradation. During cooling, the manner of re-association of *sous vide* cooked starch largely determines the resistance to digestive enzymes. *Sous vide* cooked (at 55°C) potato *cv.* Agria and *cv.* Nadine both retained intact potato cell structure as evidenced by limited swelling and the raw-like texture with the hardness of 24-27 N. During *sous vide* cooking at 65°C , potato *cv.* Agria was partially gelatinised, in contrast to potato *cv.* Nadine as seen from its endotherm curve. Although *sous vide* cooking at 65°C initiated gelatinisation in some starch granules, others were swollen but intact; *cv.* Agria treated at 65°C exhibited lower estimated glycaemic index (*eGI*) than traditionally cooked potato. For successful *sous vide* processing potato at either 55°C or 65°C , it needs to be combined with other hurdle techniques to control microbial growth and for texture optimisation.

Retrograded starch generated in TTC and *sous vide* processed tubers responded differently from traditionally cooked tuber during reheating. Reheating stability of processed then retrograded starch *in tuber* was investigated by LF-NMR, X-ray, FTIR and starch hydrolysis in Chapter VII. After reheating, one set of time-temperature cycle (TTC) processed potato tubers, stored at -20°C for a day then 4°C for 2 days, had a lower relaxation time T_{22} (at 88.7ms) than 3-day retrograded tubers (at 144.5ms) and the

rest of TTC processed+retrograded samples (at >120.7 ms). Starch hydrolysis (%) of TTC processed+retrograded then reheated samples were, however, not significantly different from the 3-day retrograded+reheated samples. Optimal TTC processing may enhance the formation of retrograded starch *in tuber* as observed in Chapter V, but the reheating stability in terms of starch hydrolysis was not as promising as in Chapter VII.

Trends of the value of 1047/1022 measured by ATR-FTIR were different from relative crystallinity measured by X-ray. This indicated that *sous vide* increased the overall crystallinity but decreased the regional alignment of crystalline to amorphous lamella. For potato *cv. Agria*, there was no significant difference between the starch hydrolysis of the 3-day retrograded then reheated (at 60°C) wedges (FCR3-r60) and for *sous vide* cooked-chill then reheated (at 60°C) wedges (A65-r60). Whereas *sous vide* cooked-chill then reheated *cv. Nadine* had moderate *eGI* at 56.9 (significantly lower than FCR3-r60 at 75.3 and A65R3-r60 at 74.6, $n=3$, $p < 0.05$), excess exudates appeared after refrigeration for 3 days.

Industrial relevance of Chapter IV, V, and VI, is discussed in Chapter VIII, with some issues foreseen for consideration during upscaling and commercialisation. Our results showed that boiled potatoes after at least a day of refrigeration then reheated at the low temperature (50°C) had higher resistant starch content (34.4%, d.b.) than did freshly cooked (6.9%, d.b.) or boiled-chill then reheated (at 90°C) tubers (6.1%, d.b.). Recommendation is, therefore, to consume boiled potato after cooling (where resistant starch content ranged 22.4- 42.9 %, d.b.), or reheated at low temperature (50°C) after at least a day of refrigeration. Product quality such as drip loss (syneresis), textural and nutritional changes are a concern for a food manufacturer. Combinations of suitable cultivars with appropriate time-temperature cycle processing can potentially produce potato products high in resistant starch with good organoleptic properties, but the problem remains a difficult one. *Sous vide* processing, a process akin to annealing, is industrially practicable to produce potato tuber with an intermediate GI (of 65.6-72.8). The desirable texture could be achieved by optimum cooking temperature and duration. For the 'haute cuisine' of *sous vide* processed potatoes, understanding the critical control points of the process is essential.

Resistant starch is regarded as dietary fibre in food regulations, e.g. USFDA or EU General Food law (EC) NO. 178/2002 around the world. In 2018, FSANZ (Food Standards Australia New Zealand) regulated a standard method to quantify resistant starch and can be labelled on nutrition information panel as a subgroup of dietary fibre. Assessment of dietary fibre needs is complex as the endpoints are ill defined. There is no biochemical marker that can be used to determine dietary fibre needs, so appearance or disappearance of clinical endpoints needs to be considered. In keeping with the concept of setting EARs (estimated average requirement) and RDIs (recommended dietary intake) or AIs (adequate intake) for prevention of deficiency states, the endpoints chosen in the estimation of requirements were adequate gastrointestinal function and adequate laxation rather than reduction of risk for chronic disease. Adequate intake of dietary fibre based on median intakes in populations of

Australia and New Zealand can be found in Nutrient Reference Values website (<https://www.nrv.gov.au/home>), no up to date limitation on RS intake was found.

IX.3 Concluding remarks

The current study brought to bear a wide variety of investigative tools in an attempt to discern whether an industrially practicable process could significantly reduce starch digestibility without making the potato unpleasant to eat.

Whole potato tuber is multi-component, more complex than is an isolated starch-water system, a difference to be considered when designing low glycaemic processed potato products. Starch, composed of amylose and amylopectin, in potato tubers can be structurally manipulated by controlled processing to modulate the starch digestion rate. Interactions of starch with other non-starch components *in tuber* also play a part in postprandial glycaemic response, influencing the assimilation of starch-derived glucose. Structural layout of a tuber (e.g. cell wall intactness, starch molecular architecture and water mobility) at each stage of food processing (i.e. degree of starch gelatinisation related to temperature and water content, degree of shear) and storage (such as cooling rate and time related to starch retrogradation) all influence its resistance to the hydrolysis of digestive enzymes. Understanding the mechanism of starch gelatinisation and retrogradation *in tuber* during processing is key to designing a tuber with low and slow glycaemic features. Other cell components *in tuber* e.g. protein, phosphorous, and cell wall may also impact relationships between starch structure and digestibility.

Potato *cv.* Agria was chosen as the main cultivar to study starch retrogradation *in tuber* due to its availability and popularity to New Zealand consumer. Sensory perception and culinary use of *cv.* Agria, (fairly firm and multi-purpose), are similar to *cv.* Russet Burbank, which is the cultivar used in Simplot's products. Potato *cv.* Nadine was occasionally tested in parallel for contrast.

Multiple techniques, e.g. microscopy (LM, and CLSM), DSC, and LF-NMR, were used in this thesis to study starch retrogradation *in tuber*. Details of the techniques developed are described in Chapter III. A full picture requires starch retrogradation to be studied from the macroscopic scale down to molecular level. Some of the techniques employed gave greater confidence than others. DSC showed endotherms which were long (spanning over 10K) and subtle, implying a slow evolution of structure rather than sudden transformation. Endotherms should be regarded as indicative and read in context with corroborating indicators. Among all, relaxation time T_{22} was positively correlated to greater starch hydrolysis (%) of the treated tubers ($r= 0.797$, $p= 0.032$) in this thesis. Relaxation time T_{22} represented the most abundant water population in the tubers, loosely interacting with starch by hydrogen bonding.

An oral-gastro-small intestinal digestion *in vitro* model was used to measure ease of starch hydrolysis expressed as an estimated glycaemia index. It is noted that when comparing and referencing across research papers, the parameters, such as pH, duration, enzyme concentration and activity, and composition of simulated digestive fluids of *in vitro* digestion, are needed to be considered.

Various approaches, including starch retrogradation *in tuber* described in Chapter IV, the time-temperature cycles process in Chapter V, and the *sous vide* cooked-chill process in Chapter VI, were thus carried out to produce potato tubers with lower *eGI* than the freshly cooked tuber. A significant reduction in *eGI* was observed with longer retrogradation times. Longer chill storage further improved the stability of retrograded tuber against reheating effects. Realignment of the gelatinised amylose and amylopectin is thought to have changed the distribution of crystalline and amorphous regions during refrigerated storage and subsequent reheating, resulting in starch digestibility varying with treatment combination. *Sous vide* processing combined with starch retrogradation *in tuber* resulted in potato tubers with intermediate *eGI* (40-72). After reheating at 60°C, the *eGI* of *sous vide* cooked-chill potatoes increased moderately (56-75).

Discoveries in this thesis can be helpful in refining existing process conditions (Chapter V) or as a basis for developing a new product with low estimated glycaemic index (Chapter VI). Utilization of existing or new technologies (e.g. HMT, UHP, or ultrasound as reviewed in Chapter II.3) to trigger starch molecular realignment during cooking and cooling, to create tailor-made structures displaying low glycaemic features seems to be possible: 1) When starch gelatinisation and retrogradation temperatures of certain potato cultivars are known, starch structure *in tuber* can be manipulated by controlled cooking and cooling regimes within existing or new technologies e.g. high hydrostatic pressure process and microwave. By different physico-chemical measurements, the relative amount of crystallites, contributed to slowly digestible starch, can then be examined in the processed potato tubers as a preliminary screening. 2) When the optimum processing parameters are determined, reheating temperature can be set to ensure the delivery of health benefits of resistant starch type 3 to consumer ends. We envision that the knowledge generated, along with other new techniques, will be helpful for the food industry to produce processed potato products with low glycaemic features.

However, the challenge is not trivial. Those processes shown in this thesis to be most effective at reducing *eGI* tended to be long and slow which is unattractive to a manufacturer. Reheating of treated tuber needed to be carefully controlled at temperatures such as 50-60°C which is difficult for a consumer. The potato reheated in this temperature range give a lukewarm sensation which may not be most appreciated by a consumer. Some of the emerging technologies are slow and expensive (UHP). For all this, structures can be influenced and *eGI* can be lowered and acceptable rewarmed products can be made. And there is a range of laboratory techniques able to be used to track a process during development. It may be possible yet to find a combination of industrially practicable techniques powerful enough to win a place in the potato process lines of the world.

Bibliography

- AACCI Method 76-21.01. (1996). General Pasting Method for Wheat or Rye Flour or Starch Using the Rapid Visco Analyser. AACC, AACCI Method 76-21.01. Retrieved from <http://methods.aaccnet.org/summaries/76-21-01.aspx>
- Abu-Ghannam, N., & Crowley, H. (2006). The effect of low temperature blanching on the texture of whole processed new potatoes. *Journal of Food Engineering*, 74(3), 335–344. <https://doi.org/10.1016/j.jfoodeng.2005.03.025>
- Adebowale, K. O., Afolabi, T. A., & Olu-Owolabi, B. I. (2005). Hydrothermal treatments of Finger millet (*Eleusine coracana*) starch. *Food Hydrocolloids*, 19(6), 974–983. <https://doi.org/10.1016/j.foodhyd.2004.12.007>
- Adebowale, K. O., & Lawal, O. S. (2003a). Functional properties and retrogradation behaviour of native and chemically modified starch of mucuna bean (*Mucuna pruriens*). *Journal of the Science of Food and Agriculture*, 83(15), 1541–1546. <https://doi.org/10.1002/jsfa.1569>
- Adebowale, K. O., & Lawal, O. S. (2003b). Microstructure, physicochemical properties and retrogradation behaviour of Mucuna bean (*Mucuna pruriens*) starch on heat moisture treatments. *Food Hydrocolloids*, 17(3), 265–272. [https://doi.org/10.1016/S0268-005X\(02\)00076-0](https://doi.org/10.1016/S0268-005X(02)00076-0)
- Adler, J., Baldwin, P. M., & Melia, C. D. (1995). Starch Damage Part 2: Types of Damage in Ball-milled Potato Starch, upon Hydration Observed by Confocal Microscopy. *Starch - Stärke*, 47(7), 252–256. <https://doi.org/10.1002/star.19950470703>
- Agle, W. M., & Woodbury, G. W. (1968). Specific gravity — dry matter relationship and reducing sugar changes affected by potato variety, production area and storage. *American Potato Journal*, 45(4), 119–131. <https://doi.org/10.1007/BF02863065>
- Agustiniano-Osornio, J. C., González-Soto, R. A., Flores-Huicochea, E., Manrique-Quevedo, N., Sánchez-Hernández, L., & Bello-Pérez, L. A. (2005). Resistant starch production from mango starch using a single-screw extruder. *Journal of the Science of Food and Agriculture*, 85(12), 2105–2110. <https://doi.org/10.1002/jsfa.2208>
- Ahmad, F. B., & Williams, P. A. (2001). Effect of Galactomannans on the Thermal and Rheological Properties of Sago Starch. *Journal of Agricultural and Food Chemistry*, 49(3), 1578–1586. <https://doi.org/10.1021/jf000744w>
- Ahvenainen, R. (1996). New approaches in improving the shelf life of minimally processed fruit and vegetables. *Trends in Food Science & Technology*, 7(6), 179–187. [https://doi.org/10.1016/0924-2244\(96\)10022-4](https://doi.org/10.1016/0924-2244(96)10022-4)
- Åkerberg, A. K. E., Liljeberg, H. G. M., Granfeldt, Y. E., Drews, A. W., & Björck, I. M. E. (1998). An In Vitro Method, Based on Chewing, To Predict Resistant Starch Content in Foods Allows Parallel Determination of Potentially Available Starch and Dietary Fiber. *The Journal of Nutrition*, 128(3), 651–660. <https://doi.org/10.1093/jn/128.3.651>

- Alessandrini, L., Romani, S., Rocculi, P., Sjöholm, I., & Rosa, M. D. (2011). Effect of steam cooking on the residual enzymatic activity of potatoes cv. Agria. *Journal of the Science of Food and Agriculture*, *91*(12), 2140–2145. <https://doi.org/10.1002/jsfa.4430>
- Alonso, R., Aguirre, A., & Marzo, F. (2000). Effects of extrusion and traditional processing methods on antinutrients and in vitro digestibility of protein and starch in faba and kidney beans. *Food Chemistry*, *68*(2), 159–165. [https://doi.org/10.1016/S0308-8146\(99\)00169-7](https://doi.org/10.1016/S0308-8146(99)00169-7)
- Alsaffar, A. A. (2010). Effect of thermal processing and storage on digestibility of starch in whole wheat grains. *Journal of Cereal Science*, *52*(3), 480–485. <https://doi.org/10.1016/j.jcs.2010.08.002>
- Alvani, K., Qi, X., & Tester, R. F. (2012). Gelatinisation properties of native and annealed potato starches. *Starch - Stärke*, *64*(4), 297–303. <https://doi.org/10.1002/star.201100130>
- Alvani, K., Tester, R. F., Lin, C. L., & Qi, X. (2014). Amylolysis of native and annealed potato starches following progressive gelatinisation. *Food Hydrocolloids*, *36*, 273–277. <https://doi.org/10.1016/j.foodhyd.2013.10.010>
- Ambigaipalan, P., Hoover, R., Donner, E., & Liu, Q. (2014). Starch chain interactions within the amorphous and crystalline domains of pulse starches during heat-moisture treatment at different temperatures and their impact on physicochemical properties. *Food Chemistry*, *143*, 175–184. <https://doi.org/10.1016/j.foodchem.2013.07.112>
- Anderson, A. K., & Guraya, H. S. (2006a). Effects of microwave heat-moisture treatment on properties of waxy and non-waxy rice starches. *Food Chemistry*, *97*(2), 318–323. <https://doi.org/10.1016/j.foodchem.2005.04.025>
- Anderson, A. K., & Guraya, H. S. (2006b). Effects of microwave heat-moisture treatment on properties of waxy and non-waxy rice starches. *Food Chemistry*, *97*(2), 318–323. <https://doi.org/10.1016/j.foodchem.2005.04.025>
- Anderson, A. K., Guraya, H. S., James, C., & Salvaggio, L. (2002). Digestibility and Pasting Properties of Rice Starch Heat-Moisture Treated at the Melting Temperature (T_m). *Starch - Stärke*, *54*(9), 401–409. [https://doi.org/10.1002/1521-379X\(200209\)54:9<401::AID-STAR401>3.0.CO;2-Z](https://doi.org/10.1002/1521-379X(200209)54:9<401::AID-STAR401>3.0.CO;2-Z)
- Andersson, A., Gekas, V., Lind, I., Oliveira, F., & Oste, R. (1994). Effect of preheating on potato texture. *Critical Reviews in Food Science and Nutrition*, *34*(3), 229–251. <https://doi.org/10.1080/10408399409527662>
- Anthon, G. E., & Barrett, D. M. (2002). Kinetic Parameters for the Thermal Inactivation of Quality-Related Enzymes in Carrots and Potatoes. *Journal of Agricultural and Food Chemistry*, *50*(14), 4119–4125. <https://doi.org/10.1021/jf011698i>
- AOAC. (1990). Official methods of analysis. *Airlington: Association of Official Analytical Chemistry*.
- Arapoglou, D., Varzakas, T., Vlyssides, A., & Israilides, C. (2010). Ethanol production from potato peel waste (PPW). *Waste Management*, *30*(10), 1898–1902. <https://doi.org/10.1016/j.wasman.2010.04.017>
- Arık Kibar, E. A., Gönenç, İ., & Us, F. (2011). Modeling of Retrogradation of Waxy and Normal Corn

- Starches. *International Journal of Food Properties*, 14(5), 954–967. <https://doi.org/10.1080/10942910903506202>
- Asp, N.-G., & Björck, I. (1989). Nutritional properties of extruded foods. In C. Mercier, P. Linko, & J. M. Harper (Eds.), *Extrusion Cooking* (pp. 399–434). American Association of Cereal Chemists.
- Asp, N.-G., van Amelsvoort, J. M. M., & Hautvast, J. G. A. J. (1996). Nutritional Implications Of Resistant Starch. *Nutrition Research Reviews*, 9(1), 1–31. <https://doi.org/10.1079/nrr19960004>
- Assifaoui, A., Champion, D., Chiotelli, E., & Verel, A. (2006). Characterization of water mobility in biscuit dough using a low-field 1H NMR technique. *Carbohydrate Polymers*, 64(2), 197–204. <https://doi.org/10.1016/j.carbpol.2005.11.020>
- Avrami, M. (1940). Kinetics of Phase Change. II Transformation-Time Relations for Random Distribution of Nuclei Kinetics of Phase Change. II Transformation-Time Relations for Random Distribution of Nuclei *. *The Journal of Chemical Physics III The Journal of Chemical Physics The Journal of Chemical Physics Kinetics of Heterogeneous Nucleation The Journal of Chemical Physics I. Interfacial Free Energy The Journal of Chemical Physics Journal of Chemical Physics*, 81(10), 212–198. <https://doi.org/10.1063/1.1750631>
- Baldwin, D. E. (2012). Sous vide cooking: A review. *International Journal of Gastronomy and Food Science*, 1(1), 15–30. <https://doi.org/10.1016/j.ijgfs.2011.11.002>
- Ballance, S., Knutsen, S. H., Fosvold, Ø. W., Wickham, M., Trenado, C. D.-T., & Monroe, J. (2018). Glycaemic and insulinaemic response to mashed potato alone, or with broccoli, broccoli fibre or cellulose in healthy adults. *European Journal of Nutrition*, 57(1), 199–207. <https://doi.org/10.1007/s00394-016-1309-7>
- Bartolome, L. G., & Hoff, J. E. (1972a). Firming of Potatoes: Biochemical Effects of Preheating. *Journal of Agricultural and Food Chemistry*, 20(2), 266–270. <https://doi.org/10.1021/jf60180a028>
- Bartolome, L. G., & Hoff, J. E. (1972b). Firming of potatoes. Biochemical effects of preheating. *Journal of Agricultural and Food Chemistry*, 20(2), 266–270. <https://doi.org/10.1021/jf60180a028>
- Beals, K. A. (2019). Potatoes, Nutrition and Health. *American Journal of Potato Research*, 96(2), 102–110. <https://doi.org/10.1007/s12230-018-09705-4>
- Becker, A., Hill, S. E., & Mitchell, J. R. (2001). Relevance of Amylose-Lipid Complexes to the Behaviour of Thermally Processed Starches. *Starch - Stärke*, 53(3–4), 121–130. [https://doi.org/10.1002/1521-379X\(200104\)53:3/4<121::AID-STAR121>3.0.CO;2-Q](https://doi.org/10.1002/1521-379X(200104)53:3/4<121::AID-STAR121>3.0.CO;2-Q)
- BeMiller, J. N., & Whistler, R. L. (2009). *Starch : chemistry and technology*. Elsevier Inc.
- Benmoussa, M., Suhendra, B., Aboubacar, A., & Hamaker, B. R. (2006). Distinctive Sorghum Starch Granule Morphologies Appear to Improve Raw Starch Digestibility. *Starch - Stärke*, 58(2), 92–99. <https://doi.org/10.1002/star.200400344>
- Berg, T., Singh, J., Hardacre, A., & Boland, M. J. (2012). The role of cotyledon cell structure during in vitro digestion of starch in navy beans. *Carbohydrate Polymers*, 87(2), 1678–1688.

<https://doi.org/10.1016/j.carbpol.2011.09.075>

- Bertoft, E. (2013). On the Building Block and Backbone Concepts of Amylopectin Structure. *Cereal Chemistry Journal*, 90(4), 294–311. <https://doi.org/10.1094/CCHEM-01-13-0004-FI>
- Bertoft, E. (2017). Understanding Starch Structure: Recent Progress. *Agronomy*, 7(3), 56. <https://doi.org/10.3390/agronomy7030056>
- Bhatnagar, S., & Hanna, M. A. (1994). Amylose-lipid complex formation during single-screw extrusion of various corn starches. *Cereal Chemistry*, 71(6), 582–587.
- Biliaderis, C. G. (1991). The structure and interactions of starch with food constituents. *Canadian Journal of Physiology and Pharmacology*, 69(1), 60–78. <https://doi.org/10.1139/y91-011>
- Biliaderis, C. G., & Galloway, G. (1989). Crystallization behavior of amylose-V complexes: Structure-property relationships. *Carbohydrate Research*, 189, 31–48. [https://doi.org/10.1016/0008-6215\(89\)84084-4](https://doi.org/10.1016/0008-6215(89)84084-4)
- Bird, A. R., Lopez-Rubio, A., Shrestha, A. K., & Gidley, M. J. (2009). Resistant Starch in Vitro and in Vivo. In *Modern Biopolymer Science* (pp. 449–510). Elsevier. <https://doi.org/10.1016/B978-0-12-374195-0.00014-8>
- Birt, D. F., Boylston, T., Hendrich, S., Jane, J.-L., Hollis, J., Li, L., ... Whitley, E. M. (2013). Resistant Starch: Promise for Improving Human Health. *Advances in Nutrition*, 4(6), 587–601. <https://doi.org/10.3945/an.113.004325>
- Björck, I., Asp, N.-G., Birkhed, D., & Lundquist, I. (1984). Effects of processing on availability of starch for digestion in vitro and in vivo; I Extrusion cooking of wheat flours and starch. *Journal of Cereal Science*, 2(2), 91–103. [https://doi.org/10.1016/S0733-5210\(84\)80022-3](https://doi.org/10.1016/S0733-5210(84)80022-3)
- Blanshard, J. M. V., & Farhat, I. A. (2000). Modeling the Kinetics of Starch Retrogradation. In *Bread Staling*. <https://doi.org/10.1201/9781420036671.ch9>
- Blazek, J., & Gilbert, E. P. (2011). Application of small-angle X-ray and neutron scattering techniques to the characterisation of starch structure: A review. *Carbohydrate Polymers*, 85(2), 281–293. <https://doi.org/10.1016/j.carbpol.2011.02.041>
- Boers, H. M., Seijen Ten Hoorn, J., & Mela, D. J. (2015). A systematic review of the influence of rice characteristics and processing methods on postprandial glycaemic and insulinaemic responses. *British Journal of Nutrition*, 114(7), 1035–1045. <https://doi.org/10.1017/S0007114515001841>
- Boltz, K. W., & Thompson, D. B. (1999). Initial Heating Temperature and Native Lipid Affects Ordering of Amylose During Cooling of High-Amylose Starches. *Cereal Chemistry Journal*, 76(2), 204–212. <https://doi.org/10.1094/CCHEM.1999.76.2.204>
- Borcak, B., Sikora, E., Sikora, M., Rosell, C. M., & Collar, C. (2012). Glycaemic response to frozen stored wheat rolls enriched with inulin and oat fibre. *Journal of Cereal Science*, 56(3), 576–580. <https://doi.org/10.1016/j.jcs.2012.07.008>
- Bordoloi, A., Kaur, L., & Singh, J. (2012). Parenchyma cell microstructure and textural characteristics of raw and cooked potatoes. *Food Chemistry*, 133(4), 1092–1100.

<https://doi.org/10.1016/j.foodchem.2011.11.044>

- Bordoloi, A., Singh, J., & Kaur, L. (2012). In vitro digestibility of starch in cooked potatoes as affected by guar gum: Microstructural and rheological characteristics. *Food Chemistry*, *133*(4), 1206–1213. <https://doi.org/10.1016/j.foodchem.2012.01.063>
- Bosmans, G. M., Lagrain, B., Deleu, L. J., Fierens, E., Hills, B. P., & Delcour, J. A. (2012). Assignments of Proton Populations in Dough and Bread Using NMR Relaxometry of Starch, Gluten, and Flour Model Systems. *Journal of Agricultural and Food Chemistry*, *60*(21), 5461–5470. <https://doi.org/10.1021/jf3008508>
- Botero-Uribe, M., Fitzgerald, M., Gilbert, R. G., & Midgley, J. (2017). Effect of pulsed electrical fields on the structural properties that affect french fry texture during processing. *Trends in Food Science & Technology*, *67*, 1–11. <https://doi.org/10.1016/j.tifs.2017.05.016>
- Botham, R. L., Ring, S. G., Noel, T. R., Morris, V. J., Englyst, H. N., & Cummings, J. H. (1994). A COMPARISON OF THE INVITRO AND INVIVO DIGESTIBILITIES OF RETROGRADED STARCH. (G. O. Phillips, P. A. Williams, & D. J. Wedlock, Eds.), *Gums and Stabilizers for the Food Industry* 7.
- Braşoveanu, M., & Nemţanu, M. R. (2014). Behaviour of starch exposed to microwave radiation treatment. *Starch - Stärke*, *66*(1–2), 3–14. <https://doi.org/10.1002/star.201200191>
- Bretzlaff, R. S., & Bahder, T. B. (1986). Apodization effects in Fourier transform infrared difference spectra. *Revue de Physique Appliquée*, *21*(12), 833–844. <https://doi.org/10.1051/rphysap:019860021012083300>
- Brodkorb, A., Egger, L., Alminger, M., Alvito, P., Assunção, R., Ballance, S., ... Recio, I. (2019). INFOGEST static in vitro simulation of gastrointestinal food digestion. *Nature Protocols*, *14*(4), 991–1014. <https://doi.org/10.1038/s41596-018-0119-1>
- Buléon, A., Colonna, P., Planchot, V., & Ball, S. (1998). Starch granules: structure and biosynthesis. *International Journal of Biological Macromolecules*, *23*(2), 85–112. [https://doi.org/10.1016/S0141-8130\(98\)00040-3](https://doi.org/10.1016/S0141-8130(98)00040-3)
- Buléon, A., Gérard, C., Riekkel, C., Vuong, R., & Chanzy, H. (1998). Details of the Crystalline Ultrastructure of C-Starch Granules Revealed by Synchrotron Microfocus Mapping. *Macromolecules*, *31*(19), 6605–6610. <https://doi.org/10.1021/ma980739h>
- Buléon, A., & Tran, V. (1990). Systematic conformational search for the branching point of amylopectin. *International Journal of Biological Macromolecules*, *12*(6), 345–352. [https://doi.org/10.1016/0141-8130\(90\)90041-8](https://doi.org/10.1016/0141-8130(90)90041-8)
- Buléon, A., Véronèse, G., & Putaux, J.-L. (2007). Self-Association and Crystallization of Amylose. *Australian Journal of Chemistry*, *60*(10), 706. <https://doi.org/10.1071/CH07168>
- Burton, P., & Lightowler, H. J. (2008). The impact of freezing and toasting on the glycaemic response of white bread. *European Journal of Clinical Nutrition*, *62*(5), 594–599. <https://doi.org/10.1038/sj.ejcn.1602746>

- Burton, Pat, & Lightowler, H. J. (2006). Influence of bread volume on glycaemic response and satiety. *British Journal of Nutrition*, 96(5), 877–882. <https://doi.org/10.1017/BJN20061900>
- Burton, W. G. (1978). The physics and physiology of storage. In *The Potato Crop* (pp. 545–606). Boston, MA: Springer US. https://doi.org/10.1007/978-1-4899-7210-1_15
- Burton, W. G., van Es, A., & Hartmans, K. J. (1992). The physics and physiology of storage. In *The Potato Crop* (pp. 608–727). Dordrecht: Springer Netherlands. https://doi.org/10.1007/978-94-011-2340-2_14
- Butterworth, P. J., Warren, F. J., Grassby, T., Patel, H., & Ellis, P. R. (2012). Analysis of starch amylolysis using plots for first-order kinetics. *Carbohydrate Polymers*, 87(3), 2189–2197. <https://doi.org/10.1016/j.carbpol.2011.10.048>
- Cael, S. J., Koenig, J. L., & Blackwell, J. (1973). Infrared and raman spectroscopy of carbohydrates. *Carbohydrate Research*, 29(1), 123–134. [https://doi.org/10.1016/S0008-6215\(00\)82075-3](https://doi.org/10.1016/S0008-6215(00)82075-3)
- Cai, L., Bai, Y., & Shi, Y.-C. (2012). Study on melting and crystallization of short-linear chains from debranched waxy starches by in situ synchrotron wide-angle X-ray diffraction. *Journal of Cereal Science*, 55(3), 373–379. <https://doi.org/10.1016/j.jcs.2012.01.013>
- Cameron, D., & Moffatt, D. (1984). Deconvolution, Derivation, and Smoothing of Spectra Using Fourier Transforms BT - Deconvolution, Derivation, and Smoothing of Spectra Using Fourier Transforms.
- Camire, M. E., Kubow, S., & Donnelly, D. J. (2009). Potatoes and Human Health. *Critical Reviews in Food Science and Nutrition*, 49(10), 823–840. <https://doi.org/10.1080/10408390903041996>
- Canet, W. (1989). Quality and stability of frozen vegetables. In S. Thorne (Ed.), *Developments in Food Preservation* (pp. 1–50).
- Canet, W., Alvarez, M. D., & Fernández, C. (2005). Optimization of low-temperature blanching for retention of potato firmness: Effect of previous storage time on compression properties. *European Food Research and Technology*, 221(3–4), 423–433. <https://doi.org/10.1007/s00217-005-1195-3>
- Capron, I., Robert, P., Colonna, P., Brogly, M., & Planchot, V. (2007). Starch in rubbery and glassy states by FTIR spectroscopy. *Carbohydrate Polymers*, 68(2), 249–259. <https://doi.org/10.1016/j.carbpol.2006.12.015>
- Carlstedt, J., Wojtasz, J., Fyhr, P., & Kocherbitov, V. (2015). Understanding starch gelatinization: The phase diagram approach. *Carbohydrate Polymers*, 129, 62–69. <https://doi.org/10.1016/j.carbpol.2015.04.045>
- Carr, H. Y., & Purcell, E. M. (1954). Effects of Diffusion on Free Precession in Nuclear Magnetic Resonance Experiments. *Physical Review*, 94(3), 630–638. Retrieved from <http://link.aps.org/doi/10.1103/PhysRev.94.630>
- Chang, S.-M., & Liu, L.-C. (1991). Retrogradation of Rice Starches Studied by Differential Scanning Calorimetry and Influence of Sugars, NaCl and Lipids. *Journal of Food Science*, 56(2), 564–566. <https://doi.org/10.1111/j.1365-2621.1991.tb05325.x>

- Charoenrein, S., Tatirat, O., Rengsutthi, K., & Thongngam, M. (2011). Effect of konjac glucomannan on syneresis, textural properties and the microstructure of frozen rice starch gels. *Carbohydrate Polymers*, 83(1), 291–296. <https://doi.org/10.1016/j.carbpol.2010.07.056>
- Chatakanonda, P., Chinachoti, P., Sriroth, K., Piyachomkwan, K., Chotineeranat, S., Tang, H. R., & Hills, B. P. (2003). The influence of time and conditions of harvest on the functional behaviour of cassava starch - A proton NMR relaxation study. *Carbohydrate Polymers*, 53(3), 233–240. [https://doi.org/10.1016/S0144-8617\(03\)00047-X](https://doi.org/10.1016/S0144-8617(03)00047-X)
- Chen, J., & Jane, J.-L. (1994). Properties of granular cold-water-soluble starches prepared by alcoholic-alkaline treatments. *Cereal Chemistry*, 71(6), 623–626.
- Chen, Jianshe, Khandelwal, N., Liu, Z., & Funami, T. (2013). Influences of food hardness on the particle size distribution of food boluses. *Archives of Oral Biology*, 58(3), 293–298. <https://doi.org/10.1016/j.archoralbio.2012.10.014>
- Chen, P., Wang, K., Kuang, Q., Zhou, S., Wang, D., & Liu, X. (2016). Understanding how the aggregation structure of starch affects its gastrointestinal digestion rate and extent. *International Journal of Biological Macromolecules*, 87, 28–33. <https://doi.org/10.1016/j.ijbiomac.2016.01.119>
- Chen, S.-H., & Teixeira, J. (1986). Structure and Fractal Dimension of Protein-Detergent Complexes. *Physical Review Letters*, 57(20), 2583–2586. <https://doi.org/10.1103/PhysRevLett.57.2583>
- Chen, Y.-F., Singh, J., & Archer, R. (2018). Potato starch retrogradation in tuber: Structural changes and gastro-small intestinal digestion in vitro. *Food Hydrocolloids*, 84, 552–560. <https://doi.org/10.1016/j.foodhyd.2018.05.044>
- Chen, Y.-F., Singh, J., Midgley, J., & Archer, R. (2019). Starch retrogradation of sous vide processed potato tubers and oral gastric small intestinal starch digestion in vitro. In *FSDH conference*.
- Chung, H.-J., Hoover, R., & Liu, Q. (2009). The impact of single and dual hydrothermal modifications on the molecular structure and physicochemical properties of normal corn starch. *International Journal of Biological Macromolecules*, 44(2), 203–210. <https://doi.org/10.1016/j.ijbiomac.2008.12.007>
- Chung, H.-J., Lim, H. S., & Lim, S.-T. (2006). Effect of partial gelatinization and retrogradation on the enzymatic digestion of waxy rice starch. *Journal of Cereal Science*, 43(3), 353–359. <https://doi.org/10.1016/j.jcs.2005.12.001>
- Chung, H.-J., Liu, Q., & Hoover, R. (2009). Impact of annealing and heat-moisture treatment on rapidly digestible, slowly digestible and resistant starch levels in native and gelatinized corn, pea and lentil starches. *Carbohydrate Polymers*, 75(3), 436–447. <https://doi.org/10.1016/j.carbpol.2008.08.006>
- Chung, H.-J., Liu, Q., & Hoover, R. (2010). Effect of single and dual hydrothermal treatments on the crystalline structure, thermal properties, and nutritional fractions of pea, lentil, and navy bean starches. *Food Research International*, 43(2), 501–508. <https://doi.org/10.1016/j.foodres.2009.07.030>

- Ciacco, C. F., & Fernandes, J. L. A. (1979). Effect of Various Ions on the Kinetics of Retrogradation of Concentrated Wheat Starch Gels. *Starch - Stärke*, 31(2), 51–53. <https://doi.org/10.1002/star.19790310205>
- Collier, G. R., Wolever, T. M. S., Wong, G. S., & Josse, R. G. (1986). Prediction of glycemic response to mixed meals in noninsulin-dependent diabetic subjects. *The American Journal of Clinical Nutrition*, 44(3), 349–352. <https://doi.org/10.1093/ajcn/44.3.349>
- Colonna, P., Leloup, V., & Buléon, A. (1992). Limiting factors of starch hydrolysis. *European Journal of Clinical Nutrition*, 46 Suppl 2, S17–32. Retrieved from <http://europepmc.org/abstract/MED/1330526>
- Colussi, R., Kaur, L., Zavareze, E. da R., Dias, A. R. G., Stewart, R. B., & Singh, J. (2017). High pressure processing and retrogradation of potato starch: Influence on functional properties and gastro-small intestinal digestion in vitro. *Food Hydrocolloids*, 75, 131–137. <https://doi.org/10.1016/j.foodhyd.2017.09.004>
- Colussi, R., Singh, J., Kaur, L., Zavareze, E. da R., Dias, A. R. G., Stewart, R. B., & Singh, H. (2017). Microstructural characteristics and gastro-small intestinal digestion in vitro of potato starch: Effects of refrigerated storage and reheating in microwave. *Food Chemistry*, 226, 171–178. <https://doi.org/10.1016/j.foodchem.2017.01.048>
- Colwell, K. H., Axford, D. W. E., Chamberlain, N., & Elton, G. A. H. (1969). Effect of storage temperature on the ageing of concentrated wheat starch gels. *Journal of the Science of Food and Agriculture*, 20(9), 550–555. <https://doi.org/10.1002/jsfa.2740200909>
- Conde-Petit, B., Handschin, S., Heinemann, C., & Escher, F. (2007). Chapter 8. Self-Assembly of Starch Spherulites as Induced by Inclusion Complexation with Small Ligands. In *Food Colloids* (pp. 117–126). Cambridge: Royal Society of Chemistry. <https://doi.org/10.1039/9781847557698-00117>
- Cooke, D., & Gidley, M. J. (1992). Loss of crystalline and molecular order during starch gelatinisation: origin of the enthalpic transition. *Carbohydrate Research*, 227, 103–112. [https://doi.org/10.1016/0008-6215\(92\)85063-6](https://doi.org/10.1016/0008-6215(92)85063-6)
- Czechowska-Biskup, R., Rokita, B., Lotfy, S., Ulanski, P., & Rosiak, J. M. (2005). Degradation of chitosan and starch by 360-kHz ultrasound. *Carbohydrate Polymers*, 60(2), 175–184. <https://doi.org/10.1016/j.carbpol.2004.12.001>
- D'Appolonia, B. L., & Morad, M. M. (1981). Bread Staling. *Cereal Chemistry*, 58(3), 186–190.
- da Rosa Zavareze, E., Mello El Halal, S. L., de los Santos, D. G., Helbig, E., Pereira, J. M., & Guerra Dias, A. R. (2012). Resistant starch and thermal, morphological and textural properties of heat-moisture treated rice starches with high-, medium- and low-amylose content. *Starch - Stärke*, 64(1), 45–54. <https://doi.org/10.1002/star.201100080>
- Dartois, A., Singh, J., Kaur, L., & Singh, H. (2010). Influence of guar gum on the in vitro starch digestibility-rheological and Microstructural characteristics. *Food Biophysics*, 5(3), 149–160.

<https://doi.org/10.1007/s11483-010-9155-2>

- Darwiche, G., Östman, E. M., Liljeberg, H. G., Kallinen, N., Björgell, O., Björck, I. M., & Almér, L.-O. (2001). Measurements of the gastric emptying rate by use of ultrasonography: studies in humans using bread with added sodium propionate. *The American Journal of Clinical Nutrition*, *74*(2), 254–258. <https://doi.org/10.1093/ajcn/74.2.254>
- Daussant, J., Mosse, J., & Vaughan, J. (Eds.). (1983). *Seed proteins* (Annual pro). London ; New York : Academic Press.
- Davies, T., Miller, D. C., & Procter, A. A. (1980). Inclusion Complexes of Free Fatty Acids with Amylose. *Starch - Stärke*, *32*(5), 149–158. <https://doi.org/10.1002/star.19800320503>
- De Kock, S., Minnaar, A., Berry, D., & Taylor, J. R. N. (1995). The effect of freezing rate on the quality of cellular and non-cellular par-cooked starchy convenience foods. *LWT - Food Science and Technology*, *28*(1), 87–95. [https://doi.org/10.1016/S0023-6438\(95\)80017-4](https://doi.org/10.1016/S0023-6438(95)80017-4)
- Deleu, L. J., Luyts, A., Wilderjans, E., Van Haesendonck, I., Brijs, K., & Delcour, J. A. (2019). Ohmic versus conventional heating for studying molecular changes during pound cake baking. *Journal of Cereal Science*, *89*, 102708. <https://doi.org/10.1016/j.jcs.2019.01.008>
- Demirkesen, I., Campanella, O. H., Sumnu, G., Sahin, S., & Hamaker, B. R. (2014). A Study on Staling Characteristics of Gluten-Free Breads Prepared with Chestnut and Rice Flours. *Food and Bioprocess Technology*, *7*(3), 806–820. <https://doi.org/10.1007/s11947-013-1099-3>
- Dhital, S., Bhattarai, R. R., Gorham, J., & Gidley, M. J. (2016). Intactness of cell wall structure controls the in vitro digestion of starch in legumes. *Food Funct.*, *7*(3), 1367–1379. <https://doi.org/10.1039/C5FO01104C>
- Diaz-Toledo, C., Kurilich, A. C., Re, R., Wickham, M. S. J., & Chambers, L. C. (2016). Satiety Impact of Different Potato Products Compared to Pasta Control. *Journal of the American College of Nutrition*, *35*(6), 537–543. <https://doi.org/10.1080/07315724.2015.1042560>
- Do, D. T., Singh, J., Oey, I., & Singh, H. (2018). Biomimetic plant foods: Structural design and functionality. *Trends in Food Science and Technology*, *82*(April), 46–59. <https://doi.org/10.1016/j.tifs.2018.09.010>
- Do, D. T., Singh, J., Oey, I., & Singh, H. (2019). Modulating effect of cotyledon cell microstructure on in vitro digestion of starch in legumes. *Food Hydrocolloids*, *96*, 112–122. <https://doi.org/10.1016/j.foodhyd.2019.04.063>
- Dona, A. C., Pages, G., Gilbert, R. G., Gaborieau, M., & Kuchel, P. W. (2009). Kinetics of In Vitro Digestion of Starches Monitored by Time-Resolved 1 H Nuclear Magnetic Resonance. *Biomacromolecules*, *10*(3), 638–644. <https://doi.org/10.1021/bm8014413>
- Donald, A. M., Lisa Kato, K., Perry, P. A., & Waigh, T. A. (2001). Scattering studies of the internal structure of starch granules. *Starch/Stärke*, *53*(10), 504–512. [https://doi.org/10.1002/1521-379X\(200110\)53:10<504::AID-STAR504>3.0.CO;2-5](https://doi.org/10.1002/1521-379X(200110)53:10<504::AID-STAR504>3.0.CO;2-5)
- Donovan, J. W. (1979). Phase transitions of the starch-water system. *Biopolymers*, *18*(2), 263–275.

<https://doi.org/10.1002/bip.1979.360180204>

- Doona, C. J., Feeherry, F. E., & Baik, M. Y. (2006). Water dynamics and retrogradation of ultrahigh pressurized wheat starch. *Journal of Agricultural and Food Chemistry*, *54*(18), 6719–6724. <https://doi.org/10.1021/jf061104h>
- Douzals, J. P., Perrier Cornet, J. M., Gervais, P., & Coquille, J. C. (1998). High-Pressure Gelatinization of Wheat Starch and Properties of Pressure-Induced Gels. *Journal of Agricultural and Food Chemistry*, *46*(12), 4824–4829. <https://doi.org/10.1021/jf971106p>
- Dupuis, J. H., Lu, Z. H., Yada, R. Y., & Liu, Q. (2016). The effect of thermal processing and storage on the physicochemical properties and in vitro digestibility of potatoes. *International Journal of Food Science and Technology*, *51*(10), 2233–2241. <https://doi.org/10.1111/ijfs.13184>
- Dürrenberger, M. B., Handschin, S., Conde-Petit, B., & Escher, F. (2001). Visualization of Food Structure by Confocal Laser Scanning Microscopy (CLSM). *LWT - Food Science and Technology*, *34*(1), 11–17. <https://doi.org/10.1006/fstl.2000.0739>
- Eastman, J., & Moore, C. O. (1984). COLD-WATER-SOLUBLE GRANULAR STARCH FOR GEL FOOD COMPOSTIONS.
- Edwards, C. H., Warren, F. J., Milligan, P. J., Butterworth, P. J., & Ellis, P. R. (2014). A novel method for classifying starch digestion by modelling the amylolysis of plant foods using first-order enzyme kinetic principles. *Food Funct.*, *5*(11), 2751–2758. <https://doi.org/10.1039/C4FO00115J>
- Eerlingen, R. C., Crombez, M., & Delcour, J. A. (1993). Enzyme-Resistant Starch. I. Quantitative and Qualitative Influence of Incubation Time and Temperature of Autoclaved Starch on Resistant Starch Formation. *Cereal Chem.*
- Eerlingen, R. C., & Delcour, J. A. (1995). Formation, Analysis, Structure and Properties of Type 3 Enzyme resistant Starch. *Journal of Cereal Science*, *22*, 129–138.
- Eerlingen, R. C., Jacobs, H., & Delcour, J. A. (1994). Enzyme-resistant starch. V. Effect of retrogradation of waxy maize starch on enzyme susceptibility. *Cereal Chem.*, *71*(4), 351–355.
- Ek, K. L., Brand-Miller, J., & Copeland, L. (2012). Glycemic effect of potatoes. *Food Chemistry*, *133*(4), 1230–1240. <https://doi.org/10.1016/j.foodchem.2011.09.004>
- Ek, K. L., Wang, S., Copeland, L., & Brand-Miller, J. C. (2014). Discovery of a low-glycaemic index potato and relationship with starch digestion in vitro. *The British Journal of Nutrition*, *111*(4), 699–705. <https://doi.org/10.1017/S0007114513003048>
- Elaissou, A.-C. (Ed.). (2006). *Carbohydrates in food*. CRC press Taylor & Francis (2 ed., Vol. 60). Retrieved from <http://linkinghub.elsevier.com/retrieve/pii/S030881469782715X>
- Elaissou, A.-C., & Ljunger, G. (1988). Interactions between amylopectin and lipid additives during retrogradation in a model system. *Journal of the Science of Food and Agriculture*, *44*(4), 353–361. <https://doi.org/10.1002/jsfa.2740440408>
- Elaissou, A.-C., & Wahlgren, M. (2004). Starch-lipid interactions and their relevance in food products. In *Starch in Food* (pp. 441–460). Elsevier. <https://doi.org/10.1533/9781855739093.3.441>

- Ells, L. J., Seal, C. J., Kettlitz, B., Bal, W., & Mathers, J. C. (2005). Postprandial glycaemic, lipaemic and haemostatic responses to ingestion of rapidly and slowly digested starches in healthy young women. *British Journal of Nutrition*, *94*(06), 948. <https://doi.org/10.1079/bjn20051554>
- Emami, S., Perera, A., Meda, V., & Tyler, R. T. (2012). Effect of Microwave Treatment on Starch Digestibility and Physico-chemical Properties of Three Barley Types. *Food and Bioprocess Technology*, *5*(6), 2266–2274. <https://doi.org/10.1007/s11947-011-0688-2>
- Englyst, H N, Kingman, S. M., & Cummings, J. H. (1992). Classification and measurement of nutritionally important starch fractions. *European Journal of Clinical Nutrition*, *46*, S33–S50.
- Englyst, Hans N., Kingman, S. M., & Cummings, J. H. (1992). Classification and measurement of nutritionally important starch fractions. *European Journal of Clinical Nutrition*, *46 Suppl 2*, S33-50. Retrieved from <http://www.ncbi.nlm.nih.gov/pubmed/1330528>
- Erdmann, J., Hebeisen, Y., Lippl, F., Wagenpfeil, S., & Schusdziarra, V. (2007). Food intake and plasma ghrelin response during potato-, rice- and pasta-rich test meals. *European Journal of Nutrition*, *46*(4), 196–203. <https://doi.org/10.1007/s00394-007-0649-8>
- Erlander, S. R., & Erlander, L. G. (1969). Explanation of Ionic Sequences in Various Phenomena X. Protein-Carbohydrate Interactions and the Mechanism for the Staling of Bread. *Starch - Stärke*, *21*(12), 305–315. <https://doi.org/10.1002/star.19690211202>
- Espín, J. C., Varón, R., Fenoll, L. G., Gilabert, M. A., García-Ruíz, P. A., Tudela, J., & García-Cánovas, F. (2000). Kinetic characterization of the substrate specificity and mechanism of mushroom tyrosinase. *European Journal of Biochemistry*, *267*(5), 1270–1279. <https://doi.org/10.1046/j.1432-1327.2000.01013.x>
- Euromonitor International. (2017a). *Ready meals in australia*.
- Euromonitor International. (2017b). *READY MEALS IN NEW ZEALAND*.
- Every, D., Gerrard, J. A., Gilpin, M. J., Ross, M., & Newberry, M. P. (1998). Staling in Starch Bread: the Effect of Gluten Additions on Specific Loaf Volume and Firming Rate. *Starch - Stärke*, *50*(10), 443–446. [https://doi.org/10.1002/\(SICI\)1521-379X\(199810\)50:10<443::AID-STAR443>3.0.CO;2-3](https://doi.org/10.1002/(SICI)1521-379X(199810)50:10<443::AID-STAR443>3.0.CO;2-3)
- Fan, D., Wang, L., Chen, W., Ma, S., Ma, W., Liu, X., ... Zhang, H. (2014). Effect of microwave on lamellar parameters of rice starch through small-angle X-ray scattering. *Food Hydrocolloids*, *35*, 620–626. <https://doi.org/10.1016/j.foodhyd.2013.08.003>
- Fannon, J. E., Hauber, R. J., & Bemiller, J. N. (1992). Surface pores of starch granules. *Cereal Chemistry*, *69*, 284–288.
- FAOSTAT. (2019). World potato production. Retrieved from <http://www.fao.org/faostat/en/#data/QC>
- Faraj, A., Vasanthan, T., & Hoover, R. (2004). The effect of extrusion cooking on resistant starch formation in waxy and regular barley flours. *Food Research International*, *37*(5), 517–525. <https://doi.org/10.1016/j.foodres.2003.09.015>
- Farhat, I. A. (2000). Advanced instrumental methods: the use of ¹H relaxation NMR to monitor starch

- retrogradation. In *The Stability and Shelf-Life of Food* (pp. 129–142). Elsevier. <https://doi.org/10.1533/9781855736580.1.127>
- Farhat, I. A., Belton, P. S., & Webb, G. A. (2007). *Magnetic resonance in food science : from molecules to man*. Cambridge, UK: RSC Pub., c2007. Retrieved from <http://ezproxy.massey.ac.nz/login?url=http://search.ebscohost.com/login.aspx?direct=true&db=c at00245a&AN=massey.b1976158&site=eds-live&scope=site>
- Farhat, I. A., Protzmann, J., Becker, A., Vallès-Pàmies, B., Neale, R., & Hill, S. E. (2001). Effect of the Extent of Conversion and Retrogradation on the Digestibility of Potato Starch. *Starch - Stärke*, 53(9), 431–436. [https://doi.org/10.1002/1521-379X\(200109\)53:9<431::AID-STAR431>3.0.CO;2-R](https://doi.org/10.1002/1521-379X(200109)53:9<431::AID-STAR431>3.0.CO;2-R)
- Fauster, T., Schlossnikl, D., Rath, F., Ostermeier, R., Teufel, F., Toepfl, S., & Jaeger, H. (2018). Impact of pulsed electric field (PEF) pretreatment on process performance of industrial French fries production. *Journal of Food Engineering*, 235, 16–22. <https://doi.org/10.1016/j.jfoodeng.2018.04.023>
- Fedec, P., Ooraikul, B., & Hadziyev, D. (1977). Microstructure of Raw and Granulated Potatoes. *Canadian Institute of Food Science and Technology Journal*, 10(4), 295–306. [https://doi.org/10.1016/S0315-5463\(77\)73551-5](https://doi.org/10.1016/S0315-5463(77)73551-5)
- Ferguson, L. R., Tasman-Jones, C., Englyst, H. N., & Harris, P. J. (2000). Comparative Effects of Three Resistant Starch Preparations on Transit Time and Short-Chain Fatty Acid Production in Rats. *Nutrition and Cancer*, 36(2), 170–176. <https://doi.org/10.1207/S15327914NC3602>
- Fernandes, G., Velangi, A., & Wolever, T. M. S. (2005). Glycemic index of potatoes commonly consumed in North America. *Journal of the American Dietetic Association*, 105(4), 557–562. <https://doi.org/10.1016/j.jada.2005.01.003>
- Ferrua, M. J., & Singh, R. P. (2015). Human Gastric Simulator (Riddet Model). In *The Impact of Food Bioactives on Health* (pp. 61–71). Cham: Springer International Publishing. https://doi.org/10.1007/978-3-319-16104-4_7
- Flores-Silva, P. C., Roldan-Cruz, C. A., Chavez-Esquivel, G., Vernon-Carter, E. J., Bello-Pérez, L. A., & Alvarez-Ramirez, J. (2017). In vitro digestibility of ultrasound-treated corn starch. *Starch/Stärke*, 69(9–10). <https://doi.org/10.1002/star.201700040>
- Food Standards Australia New Zealand. Approval report – Application A1142 Addition of a prescribed method of analysis for resistant starch Table of contents, 33 § (2018).
- Foster-Powell, K., Holt, S. H., & Brand-Miller, J. C. (2002). International table of glycemic index and glycemic load values: 2002. *Am J Clin Nutr*, 76(1), 5–56. Retrieved from <http://ajcn.nutrition.org/cgi/content/long/76/1/5>
- Foucault, M., Singh, J., Stewart, R. B., & Singh, H. (2016). Pilot scale production and in vitro gastro-small intestinal digestion of self-assembled recrystallised starch (SARS) structures. *Journal of Food Engineering*, 191, 95–104. <https://doi.org/http://dx.doi.org/10.1016/j.jfoodeng.2016.07.001>

- Frank, H. S., & Wen, W. Y. (1957). Ion-solvent interaction. Structural aspects of ion-solvent interaction in aqueous solutions: A suggested picture of water structure. *Discussions of the Faraday Society*, 24, 133–140. <https://doi.org/10.1039/DF9572400133>
- Fredriksson, H., Silverio, J., Andersson, R., Eliasson, A.-C., & Åman, P. (1998). The influence of amylose and amylopectin characteristics on gelatinization and retrogradation properties of different starches. *Carbohydrate Polymers*, 35(3–4), 119–134. [https://doi.org/10.1016/S0144-8617\(97\)00247-6](https://doi.org/10.1016/S0144-8617(97)00247-6)
- Friedman, H. H., Whitney, J. E., & Szczesniak, A. S. (1963). The Texturometer-A New Instrument for Objective Texture Measurement. *Journal of Food Science*, 28(4), 390–396. <https://doi.org/10.1111/j.1365-2621.1963.tb00216.x>
- Friedman, M., McDonald, G. M., & Filadelfi-Keszi, M. (1997). Potato Glycoalkaloids: Chemistry, Analysis, Safety, and Plant Physiology. *Critical Reviews in Plant Sciences*, 16(1), 55–132. <https://doi.org/10.1080/07352689709701946>
- Frost, K., Kaminski, D., Kirwan, G., Lascaris, E., & Shanks, R. (2009). Crystallinity and structure of starch using wide angle X-ray scattering. *Carbohydrate Polymers*, 78(3), 543–548. <https://doi.org/10.1016/j.carbpol.2009.05.018>
- Fu, Z., Wang, L., Li, D., Zhou, Y., & Adhikari, B. (2013). The effect of partial gelatinization of corn starch on its retrogradation. *Carbohydrate Polymers*, 97(2), 512–517. <https://doi.org/10.1016/j.carbpol.2013.04.089>
- Fuentes-Zaragoza, E., Riquelme-Navarrete, M. J., Sánchez-Zapata, E., & Pérez-Álvarez, J. a. (2010). Resistant starch as functional ingredient: A review. *Food Research International*, 43(4), 931–942. <https://doi.org/10.1016/j.foodres.2010.02.004>
- Funami, T., Kataoka, Y., Omoto, T., Goto, Y., Asai, I., & Nishinari, K. (2005a). Effects of non-ionic polysaccharides on the gelatinization and retrogradation behavior of wheat starch. *Food Hydrocolloids*, 19(1), 1–13. <https://doi.org/10.1016/j.foodhyd.2004.04.024>
- Funami, T., Kataoka, Y., Omoto, T., Goto, Y., Asai, I., & Nishinari, K. (2005b). Food hydrocolloids control the gelatinization and retrogradation behavior of starch. 2a. Functions of guar gums with different molecular weights on the gelatinization behavior of corn starch. *Food Hydrocolloids*, 19(1), 15–24. <https://doi.org/10.1016/j.foodhyd.2004.04.008>
- Furrer, A. N., Chegeni, M., & Ferruzzi, M. G. (2018). Impact of potato processing on nutrients, phytochemicals, and human health. *Critical Reviews in Food Science and Nutrition*, 58(1), 146–168. <https://doi.org/10.1080/10408398.2016.1139542>
- Gallant, D. J., Bouchet, B., Buléon, A., & Pérez, S. (1992). Physical characteristics of starch granules and susceptibility to enzymatic degradation. *European Journal of Clinical Nutrition*, 46 Suppl 2, S3-16. Retrieved from <http://www.ncbi.nlm.nih.gov/pubmed/1330527>
- Galvis, L., Bertinetto, C. G., Putaux, J.-L., Montesanti, N., & Vuorinen, T. (2016). Crystallite orientation maps in starch granules from polarized Raman spectroscopy (PRS) data. *Carbohydrate*

- Polymers*, 154, 70–76. <https://doi.org/10.1016/j.carbpol.2016.08.032>
- García-Alonso, A., & Goñi, I. (2000). Effect of processing on potato starch: In vitro availability and glycaemic index. *Nahrung/Food*, 44(1), 19–22. [https://doi.org/10.1002/\(SICI\)1521-3803\(20000101\)44:1<19::AID-FOOD19>3.0.CO;2-E](https://doi.org/10.1002/(SICI)1521-3803(20000101)44:1<19::AID-FOOD19>3.0.CO;2-E)
- García-Segovia, P., Andrés-Bello, A., & Martínez-Monzó, J. (2008). Textural properties of potatoes (*Solanum tuberosum* L., cv. Monalisa) as affected by different cooking processes. *Journal of Food Engineering*, 88(1), 28–35. <https://doi.org/10.1016/j.jfoodeng.2007.12.001>
- Gelders, G. G., Duyck, J. P., Goesaert, H., & Delcour, J. A. (2005). Enzyme and acid resistance of amylose-lipid complexes differing in amylose chain length, lipid and complexation temperature. *Carbohydrate Polymers*, 60(3), 379–389. <https://doi.org/10.1016/j.carbpol.2005.02.008>
- Genkina, N. K., Wasserman, L. A., & Yuryev, V. P. (2004). Annealing of starches from potato tubers grown at different environmental temperatures. Effect of heating duration. *Carbohydrate Polymers*, 56(3), 367–370. <https://doi.org/10.1016/j.carbpol.2003.12.009>
- Gidley, M. J. (1989). Molecular mechanisms underlying amylose aggregation and gelation. *Macromolecules*, 22(16), 351–358. <https://doi.org/10.1021/ma00191a064>
- Gidley, M. J., & Bulpin, P. V. (1987). Crystallisation of malto-oligosaccharides as models of the crystalline forms of starch: minimum chain-length requirement for the formation of double helices. *Carbohydrate Research*, 161(2), 291–300. [https://doi.org/10.1016/S0008-6215\(00\)90086-7](https://doi.org/10.1016/S0008-6215(00)90086-7)
- Gilbert, G., & Spragg, S. (1964). Iodimetric determination of amylose iodine sorption blue value. *Methods in Carbohydrate Chemistry*, 4, 168–169.
- Godefroidt, T., Ooms, N., Pareyt, B., Brijs, K., & Delcour, J. A. (2019). Ingredient Functionality During Foam-Type Cake Making: A Review. *Comprehensive Reviews in Food Science and Food Safety*, 1541-4337.12488. <https://doi.org/10.1111/1541-4337.12488>
- Goesaert, H., Brijs, K., Veraverbeke, W. S., Courtin, C. M., Gebruers, K., & Delcour, J. A. (2005a). Wheat flour constituents: how they impact bread quality, and how to impact their functionality. *Trends in Food Science & Technology*, 16(1–3), 12–30. <https://doi.org/10.1016/j.tifs.2004.02.011>
- Goesaert, H., Brijs, K., Veraverbeke, W. S., Courtin, C. M., Gebruers, K., & Delcour, J. A. (2005b). Wheat flour constituents: how they impact bread quality, and how to impact their functionality. *Trends in Food Science & Technology*, 16(1–3), 12–30. <https://doi.org/10.1016/j.tifs.2004.02.011>
- Gomand, S. V., Lamberts, L., Gommès, C. J., Visser, R. G. F., Delcour, J. A., & Goderis, B. (2012). Molecular and morphological aspects of annealing-induced stabilization of starch crystallites. *Biomacromolecules*, 13(5), 1361–1370. <https://doi.org/10.1021/bm3000748>
- Goñi, I., Garcia-Alonso, A., & Saura-Calixto, F. (1997). A starch hydrolysis procedure to estimate glycemic index. *Nutrition Research*, 17(3), 427–437. [https://doi.org/10.1016/S0271-5317\(97\)00010-9](https://doi.org/10.1016/S0271-5317(97)00010-9)
- Goñi, I., García-Diz, L., Mañas, E., & Saura-Calixto, F. (1996). Analysis of resistant starch: a method

- for foods and food products. *Food Chemistry*, 56(4), 445–449. [https://doi.org/10.1016/0308-8146\(95\)00222-7](https://doi.org/10.1016/0308-8146(95)00222-7)
- Goodfellow, B. J., & Wilson, R. H. (1990). A fourier transform IR study of the gelation of amylose and amylopectin. *Biopolymers*, 30(13–14), 1183–1189. <https://doi.org/10.1002/bip.360301304>
- Gormley, R., & Tansey, F. (2012). Sous Vide and Cook-Chill Processing. *Handbook of Food Safety Engineering*, 468–496. <https://doi.org/10.1002/9781444355321.ch19>
- Gormley, R., & Walshe, T. (1999). Effects of boiling, warm-holding, mashing and cooling on the levels of enzyme-resistant potato starch. *International Journal of Food Science and Technology*, 34(3), 281–286. <https://doi.org/10.1046/j.1365-2621.1999.00270.x>
- Gough, B. M., & Pybus, J. N. (1971). Effect on the Gelatinization Temperature of Wheat Starch Granules of Prolonged Treatment with Water at 50°C. *Starch - Stärke*, 23(6), 210–212. <https://doi.org/10.1002/star.19710230608>
- Gourineni, V., Stewart, M. L., Skorge, R., & Sekula, B. C. (2017). Slowly digestible carbohydrate for balanced energy: In vitro and in vivo evidence. *Nutrients*, 9(11), 1–10. <https://doi.org/10.3390/nu9111230>
- Granfeldt, Y., Bjorck, I., & Hagander, B. (1991). On the importance of processing conditions, product thickness and egg addition for the glycaemic and hormonal responses to pasta: A comparison with bread made from “pasta ingredients.” *European Journal of Clinical Nutrition*, 45(10), 489–499.
- Grant, G. T., Morris, E. R., Rees, D. A., Smith, P. J. C., & Thom, D. (1973). Biological interactions between polysaccharides and divalent cations: The egg-box model. *FEBS Letters*, 32(1), 195–198. [https://doi.org/10.1016/0014-5793\(73\)80770-7](https://doi.org/10.1016/0014-5793(73)80770-7)
- Gray, J. A., & BeMiller, J. N. (2003). Bread Staling: Molecular Basis and Control. *Comprehensive Reviews in Food Science and Food Safety*, 2(1), 1–21. <https://doi.org/10.1111/j.1541-4337.2003.tb00011.x>
- Gray, J. D., Kolesik, P., Hoj, P. B., And, ., & Coombe, B. G. (1999). Confocal measurement of the three-dimensional size and shape of plant parenchyma cells in a developing fruit tissue. *The Plant Journal*, 19(2), 229–236. <https://doi.org/10.1046/j.1365-313X.1999.00512.x>
- Gudmundsson, M. (1992). Effects of an added inclusion-amylose complex on the retrogradation of some starches and amylopectin. *Carbohydrate Polymers*, 17(4), 299–304. [https://doi.org/10.1016/0144-8617\(92\)90173-N](https://doi.org/10.1016/0144-8617(92)90173-N)
- Gudmundsson, M., & Eliasson, A.-C. (1990). Retrogradation of amylopectin and the effects of amylose and added surfactants/emulsifiers. *Carbohydrate Polymers*, 13, 295–315.
- Guerra, A., Etienne-Mesmin, L., Livrelli, V., Denis, S., Blanquet-Diot, S., & Alric, M. (2012). Relevance and challenges in modeling human gastric and small intestinal digestion. *Trends in Biotechnology*, 30(11), 591–600. <https://doi.org/10.1016/j.tibtech.2012.08.001>
- Guha, M., Ali, S. Z., & Bhattacharya, S. (1997). Twin-screw extrusion of rice flour without a die: Effect of barrel temperature and screw speed on extrusion and extrudate characteristics. *Journal of Food*

- Engineering*, 32(3), 251–267. [https://doi.org/10.1016/S0260-8774\(97\)00028-9](https://doi.org/10.1016/S0260-8774(97)00028-9)
- Guilbot, A., & Mercier, C. (1985). Starch. *Polysaccharide*, 3, 209.
- Gummadi, S. N., & Panda, T. (2003). Purification and biochemical properties of microbial pectinases— a review. *Process Biochemistry*, 38(7), 987–996. [https://doi.org/10.1016/S0032-9592\(02\)00203-0](https://doi.org/10.1016/S0032-9592(02)00203-0)
- Guo, J., Lian, X., Kang, H., Gao, K., & Li, L. (2016). Effects of glutenin in wheat gluten on retrogradation of wheat starch. *European Food Research and Technology*, 242(9), 1485–1494. <https://doi.org/10.1007/s00217-016-2649-5>
- Guraya, H. S., James, C., & Champagne, E. T. (2001). Effect of Cooling, and Freezing on the Digestibility of Debranched Rice Starch and Physical Properties of the Resulting Material. *Starch - Stärke*, 53(2), 64–74. [https://doi.org/10.1002/1521-379X\(200102\)53:2<64::AID-STAR64>3.0.CO;2-R](https://doi.org/10.1002/1521-379X(200102)53:2<64::AID-STAR64>3.0.CO;2-R)
- H.D.Goff. (1994). Measuring and interpreting the glass transition in frozen foods and model systems. *Food Research International*, 27, 187–189.
- H.R. Walter (Ed.). (1998). *Polysaccharide association structures in food*. Marcel Dekker, INC, New York.
- Hagenimana, A., Ding, X., & Fang, T. (2006). Evaluation of rice flour modified by extrusion cooking. *Journal of Cereal Science*, 43(1), 38–46. <https://doi.org/10.1016/j.jcs.2005.09.003>
- Hagiwara, S., Esaki, K., Nishiyama, K., Kitamura, S., & Kuge, T. (1986). Effect of micro-wave irradiation on potato starch granules. *Journal of the Japanese Society of Starch Science*, 33(1), 1–9. <https://doi.org/10.5458/jag1972.33.1>
- Hamaker, B. R., Zhang, G., & Venkatachalam, M. (2007). Modified carbohydrates with lower glycemic index. In *Novel Food Ingredients for Weight Control* (pp. 198–217). Elsevier. <https://doi.org/10.1533/9781845693114.2.198>
- Han, Z., Zeng, X. A., Yu, S. J., Zhang, B. S., & Chen, X. D. (2009). Effects of pulsed electric fields (PEF) treatment on physicochemical properties of potato starch. *Innovative Food Science & Emerging Technologies*, 10(4), 481–485. <https://doi.org/10.1016/j.ifset.2009.07.003>
- Han, Z., Zeng, X., Zhang, B., & Yu, S. (2009). Effects of pulsed electric fields (PEF) treatment on the properties of corn starch. *Journal of Food Engineering*, 93(3), 318–323. <https://doi.org/10.1016/j.jfoodeng.2009.01.040>
- Hanashiro, I., Abe, J., & Hizukuri, S. (1996). A periodic distribution of the chain length of amylopectin as revealed by high-performance anion-exchange chromatography. *Carbohydrate Research*, 283, 151–159. [https://doi.org/10.1016/0008-6215\(95\)00408-4](https://doi.org/10.1016/0008-6215(95)00408-4)
- Hansen, C. L., Thybo, A. K., Bertram, H. C., Viereck, N., Berg, F. Van Den, & Engelsens, S. B. (2010). Determination of dry matter content in potato tubers by low-field nuclear magnetic resonance (LF-NMR). *Journal of Agricultural and Food Chemistry*, 58(19), 10300–10304. <https://doi.org/10.1021/jf101319q>

- Haralampu, S. . (2000). Resistant starch—a review of the physical properties and biological impact of RS3. *Carbohydrate Polymers*, *41*(3), 285–292. [https://doi.org/10.1016/S0144-8617\(99\)00147-2](https://doi.org/10.1016/S0144-8617(99)00147-2)
- Harrick, N. J., & Beckmann, K. H. (1974). Internal Reflection Spectroscopy. In *Characterization of Solid Surfaces* (pp. 215–245). Boston, MA: Springer US. https://doi.org/10.1007/978-1-4613-4490-2_11
- Hätönen, K. A., Virtamo, J., Eriksson, J. G., Sinkko, H. K., Sundvall, J. E., & Valsta, L. M. (2011). Protein and fat modify the glycaemic and insulinaemic responses to a mashed potato-based meal. *British Journal of Nutrition*, *106*(02), 248–253. <https://doi.org/10.1017/S0007114511000080>
- Haugabrooks, E. (2013). *Evaluating the use of resistant starch as a beneficial dietary fiber and its effect on physiological response of glucose, insulin, and fermentation*. Iowa State University, Digital Repository, Ames. <https://doi.org/10.31274/etd-180810-2482>
- Haworth, W. N., Hirst, E. L., & Isherwood, F. A. (1937). Polysaccharides. XXIII Determination of Chain Length of Glycogen. *J. Chem. Soc.*, 577–581.
- Henry, C. J. K., Lightowler, H. J., Kendall, F. L., & Storey, M. (2006). The impact of the addition of toppings/fillings on the glycaemic response to commonly consumed carbohydrate foods. *European Journal of Clinical Nutrition*, *60*(6), 763–769. <https://doi.org/10.1038/sj.ejcn.1602380>
- Hesso, N., Le-Bail, A., Loisel, C., Chevallier, S., Pontoire, B., Queveau, D., & Le-Bail, P. (2015). Monitoring the crystallization of starch and lipid components of the cake crumb during staling. *Carbohydrate Polymers*, *133*, 533–538. <https://doi.org/10.1016/j.carbpol.2015.07.056>
- Hibi, Y., Kitamura, S., & Kuge, T. (1990). Effect of Lipids on the Retrogradation of Cooked Rice. *Cereal Chemistry*, *67*(1), 7–10.
- Hiele, F. J. H. (1959). Die Inhaltsstoffe der Kartoffel; Bildung, Verwertung, Erhaltung. *European Potato Journal*, *2*(4), 289–292. <https://doi.org/10.1007/BF02364591>
- Hills, B. P., & Le Floc’h, G. (1994). NMR studies of non-freezing water in cellular plant tissue. *Food Chemistry*, *51*(3), 331–336. [https://doi.org/10.1016/0308-8146\(94\)90035-3](https://doi.org/10.1016/0308-8146(94)90035-3)
- Hizukuri, S. (1985). Relationship between the distribution of the chain length of amylopectin and the crystalline structure of starch granules. *Carbohydrate Research*, *141*(2), 295–306. [https://doi.org/10.1016/S0008-6215\(00\)90461-0](https://doi.org/10.1016/S0008-6215(00)90461-0)
- Hizukuri, S. (1986). Polymodal distribution of the chain lengths of amylopectins, and its significance. *Carbohydrate Research*, *147*(2), 342–347. [https://doi.org/10.1016/S0008-6215\(00\)90643-8](https://doi.org/10.1016/S0008-6215(00)90643-8)
- Hoebler, C., Devaux, M. F., Karinthi, A., Belleville, C., & Barry, J. L. (2000). Particle size of solid food after human mastication and in vitro simulation of oral breakdown. *International Journal of Food Sciences and Nutrition*, *51*(5), 353–366. <https://doi.org/10.1080/096374800426948>
- Hoebler, C., Karinthi, A., Chiron, H., Champ, M., & Barry, J. L. (1999). Bioavailability of starch in bread rich in amylose: Metabolic responses in healthy subjects and starch structure. *European Journal of Clinical Nutrition*, *53*(5), 360–366. <https://doi.org/10.1038/sj.ejcn.1600718>
- Hoebler, C., Lecannu, G., Belleville, C., Devaux, M.-F., Popineau, Y., & Barry, J.-L. (2002).

- Development of an in vitro system simulating bucco-gastric digestion to assess the physical and chemical changes of food. *International Journal of Food Sciences and Nutrition*, 53(5), 389–402. <https://doi.org/10.1080/0963748021000044732>
- Hong, J., Chen, R., Zeng, X.-A., & Han, Z. (2016). Effect of pulsed electric fields assisted acetylation on morphological, structural and functional characteristics of potato starch. *Food Chemistry*, 192, 15–24. <https://doi.org/10.1016/j.foodchem.2015.06.058>
- Hoover, R., & Zhou, Y. (2003). In vitro and in vivo hydrolysis of legume starches by alpha amylase and resistant starch formation in legumes - a review. *Carbohydrate Polymers*, 54, 401–417.
- Hoover, Ratnajothi. (1995). Starch retrogradation. *Food Reviews International*, 11(2), 331–346. <https://doi.org/10.1080/87559129509541044>
- Hoover, Ratnajothi. (2001). Composition, molecular structure, and physicochemical properties of tuber and root starches: a review. *Carbohydrate Polymers*, 45(3), 253–267. [https://doi.org/10.1016/S0144-8617\(00\)00260-5](https://doi.org/10.1016/S0144-8617(00)00260-5)
- Hoover, Ratnajothi. (2010). The Impact of Heat-Moisture Treatment on Molecular Structures and Properties of Starches Isolated from Different Botanical Sources. *Critical Reviews in Food Science and Nutrition*, 50(9), 835–847. <https://doi.org/10.1080/10408390903001735>
- Hoover, Ratnajothi, & Senanayake, N. (1996). EFFECT OF SUGARS ON THE THERMAL AND RETROGRADATION PROPERTIES OF OAT STARCHES. *Journal of Food Biochemistry*, 20(6), 65–83. <https://doi.org/10.1111/j.1745-4514.1996.tb00585.x>
- Hoover, Ratnajothi, & Vasanthan, T. (1993). THE EFFECT OF ANNEALING ON THE PHYSICOCHEMICAL PROPERTIES OF WHEAT, OAT, POTATO AND LENTIL STARCHES. *Journal of Food Biochemistry*, 17(5), 303–325. <https://doi.org/10.1111/j.1745-4514.1993.tb00476.x>
- Hoover, Ratnajothi, & Vasanthan, T. (1994a). Effect of heat-moisture treatment on the structure and physicochemical properties of cereal, legume, and tuber starches. *Carbohydrate Research*, 252, 33–53. [https://doi.org/10.1016/0008-6215\(94\)90004-3](https://doi.org/10.1016/0008-6215(94)90004-3)
- Hoover, Ratnajothi, & Vasanthan, T. (1994b). THE FLOW PROPERTIES OF NATIVE, HEAT-MOISTURE TREATED, AND ANNEALED STARCHES FROM WHEAT, OAT, POTATO AND LENTIL. *Journal of Food Biochemistry*, 18(2), 67–82. <https://doi.org/10.1111/j.1745-4514.1994.tb00490.x>
- Horigane, A. K., Toyoshima, H., Hemmi, H., Engelaar, W. M. H. G., Okubo, A., & Nagata, T. (1999). Internal hollows in cooked rice grains (*Oryza sativa* cv. Koshihikari) observed by NMR micro imaging. *Journal of Food Science*, 64(1), 1–5. <https://doi.org/10.1111/j.1365-2621.1999.tb09849.x>
- Hsu, C.-L., & Heldman, D. R. (2005). INFLUENCE OF GLASS TRANSITION TEMPERATURE ON RATE OF RICE STARCH RETROGRADATION DURING LOW-TEMPERATURE STORAGE. *Journal of Food Process Engineering*, 28(5), 506–525.

<https://doi.org/10.1111/j.1745-4530.2005.00036.x>

- Hsu, R. J., Chen, H.-J., Lu, S., & Chiang, W. (2015). Effects of cooking, retrogradation and drying on starch digestibility in instant rice making. *Journal of Cereal Science*, *65*, 154–161. <https://doi.org/10.1016/j.jcs.2015.05.015>
- Hu, X.-P., Zhang, B., Jin, Z.-Y., Xu, X.-M., & Chen, H.-Q. (2017). Effect of high hydrostatic pressure and retrogradation treatments on structural and physicochemical properties of waxy wheat starch. *Food Chemistry*, *232*, 560–565. <https://doi.org/10.1016/j.foodchem.2017.04.040>
- Hu, X. P., Huang, T. T., Mei, J. Q., Jin, Z. Y., Xu, X. M., & Chen, H. Q. (2014). Effects of continuous and intermittent retrogradation treatments on in vitro digestibility and structural properties of waxy wheat starch. *Food Chemistry*, *174*, 31–36. <https://doi.org/10.1016/j.foodchem.2014.11.026>
- Hu, X. P., Xie, Y. Y., Jin, Z. Y., Xu, X. M., & Chen, H. Q. (2014). Effect of single-, dual-, and triple-retrogradation treatments on in vitro digestibility and structural characteristics of waxy wheat starch. *Food Chemistry*, *157*, 373–379. <https://doi.org/10.1016/j.foodchem.2014.02.065>
- Huang, H. K., Sheu, H. S., Chuang, W. T., Jeng, U. S., Su, A. C., Wu, W. R., ... Lai, H. M. (2014). Correlated changes in structure and viscosity during gelatinization and gelation of tapioca starch granules. *IUCrJ*, *1*, 418–428. <https://doi.org/10.1107/S2052252514019137>
- Huang, J. J., & White, P. J. (1993). Waxy corn starch: monoglyceride interaction in a model system. *Cereal Chemistry (USA)*, *70*(1), 42–47.
- Huang, S., & Moss, R. (1991). Light microscopy observations on the mechanism of dough development in Chinese steamed bread production. *Food Structure*, *10*(4), 289–293.
- Huang, Sidi, & Miskelly, D. (2019). Steamed bread-A review of manufacturing, flour quality requirements, and quality evaluation. *Cereal Chemistry*, *96*(1), 8–22. <https://doi.org/10.1002/cche.10096>
- Huen, J., Weikusat, C., Bayer-Giraldi, M., Weikusat, I., Ringer, L., & Lösche, K. (2014). Confocal Raman microscopy of frozen bread dough. *Journal of Cereal Science*, *60*(3), 555–560. <https://doi.org/10.1016/j.jcs.2014.07.012>
- Hug-Iten, S., Escher, F., & Conde-Petit, B. (2003). Staling of Bread: Role of Amylose and Amylopectin and Influence of Starch-Degrading Enzymes. *Cereal Chemistry Journal*, *80*(6), 654–661. <https://doi.org/10.1094/CCHEM.2003.80.6.654>
- Hug-Iten, S., Handschin, S., Conde-Petit, B., & Escher, F. (1999). Changes in Starch Microstructure on Baking and Staling of Wheat Bread. *Lebensmittel-Wissenschaft Und-Technologie*, *32*(5), 255–260. <https://doi.org/10.1006/fstl.1999.0544>
- Hultin, H. O., & Milner, M. (1978). *Postharvest biology and biotechnology*. Food & Nutrition Press. Retrieved from <http://ezproxy.massey.ac.nz/login?url=http://search.ebscohost.com/login.aspx?direct=true&db=c at00245a&AN=massey.b1025500&site=eds-live&scope=site>
- Huth, M., Dongowski, G., Gebhardt, E., & Flamme, W. (2000). Functional Properties of Dietary Fibre

- Enriched Extrudates from Barley. *Journal of Cereal Science*, 32(2), 115–128. <https://doi.org/10.1006/jcrs.2000.0330>
- I'Anson, K. J., Miles, M. J., Morris, V. J., Ring, S. G., & Nave, C. (1988). A study of amylose gelation using a synchrotron X-ray source. *Carbohydrate Polymers*, 8(1), 45–53. [https://doi.org/10.1016/0144-8617\(88\)90035-5](https://doi.org/10.1016/0144-8617(88)90035-5)
- Iborra-Bernad, C., García-Segovia, P., & Martínez-Monzó, J. (2015). Physico-Chemical and Structural Characteristics of Vegetables Cooked Under Sous-Vide, Cook-Vide, and Conventional Boiling. *Journal of Food Science*, 80(8), E1725–E1734. <https://doi.org/10.1111/1750-3841.12950>
- Iida, Y., Tuziuti, T., Yasui, K., Towata, A., & Kozuka, T. (2008). Control of viscosity in starch and polysaccharide solutions with ultrasound after gelatinization. *Innovative Food Science & Emerging Technologies*, 9(2), 140–146. <https://doi.org/10.1016/j.ifset.2007.03.029>
- Imberty, A., Buléon, A., Tran, V., & Pérez, S. (1991). Recent Advances in Knowledge of Starch Structure. *Starch - Stärke*, 43(10), 375–384. <https://doi.org/10.1002/star.19910431002>
- Imberty, A., Chanzy, H., & Perez, S. (1988). The Double-helical Nature of the Crystalline Part of A-starch. *Journal of Molecular Biology*, 201, 365–378.
- Imberty, A., & Pérez, S. (1988). Crystal structure and conformational features of α -panose. *Carbohydrate Research*, 181, 41–55. [https://doi.org/10.1016/0008-6215\(88\)84021-7](https://doi.org/10.1016/0008-6215(88)84021-7)
- Jacobasch, G., Dongowski, G., Schmiedl, D., & Müller-Schmehl, K. (2006). Hydrothermal treatment of Novelose 330 results in high yield of resistant starch type 3 with beneficial prebiotic properties and decreased secondary bile acid formation in rats. *British Journal of Nutrition*, 95(6), 1063–1074. <https://doi.org/10.1079/BJN20061713>
- Jacobs, H., Eerlingen, R. C., Clauwert, W., & Delcour, J. A. (1995). Influence of annealing on the pasting properties of starches from varying botanical sources. *Cereal Chemistry*, 72(5), 480–487. Retrieved from <http://cat.inist.fr/?aModele=afficheN&cpsid=3667454>
- Jacobs, H., Eerlingen, R. C., Spaepen, H., Grobet, P. J., & Delcour, J. A. (1997). Impact of annealing on the susceptibility of wheat, potato and pea starches to hydrolysis with pancreatin. *Carbohydrate Research*, 305(2), 193–207. [https://doi.org/10.1016/S0008-6215\(97\)10035-0](https://doi.org/10.1016/S0008-6215(97)10035-0)
- Jacobson, M. R., Obanni, M., & BeMiller, J. N. (1997). Retrogradation of starches from different botanical sources. *Cereal Chemistry*, 74(5), 511–518. <https://doi.org/10.1094/CCHEM.1997.74.5.511>
- Jalabert-Malbos, M. L., Mishellany-Dutour, A., Woda, A., & Peyron, M. A. (2007). Particle size distribution in the food bolus after mastication of natural foods. *Food Quality and Preference*, 18(5), 803–812. <https://doi.org/10.1016/j.foodqual.2007.01.010>
- Jane, J.-L. (1993). Mechanism of Starch Gelatinization in Neutral Salt Solutions. *Starch - Stärke*, 45(5), 161–166. <https://doi.org/10.1002/star.19930450502>
- Jane, J.-L., Chen, Y. Y., Lee, L. F., McPherson, A. E., Wong, K. S., Radosavljevic, M., & Kasemsuwan, T. (1999). Effects of amylopectin branch chain length and amylose content on the gelatinization

- and pasting properties of starch. *Cereal Chemistry*, 76(5), 629–637. <https://doi.org/10.1094/CCHEM.1999.76.5.629>
- Jane, J.-L., Craig, S. A. S., Seib, P. A., & Hosoney, R. C. (1986). Characterization of Granular Cold Water-Soluble Starch. *Starch - Stärke*, 38(8), 258–263. <https://doi.org/10.1002/star.19860380803>
- Jane, J.-L., Kasemsuwan, T., Leas, S., Zobel, H., & Robyt, J. F. (1994). Anthology of Starch Granule Morphology by Scanning Electron Microscopy. *Starch - Stärke*, 46(4), 121–129. <https://doi.org/10.1002/star.19940460402>
- Jane, J.-L., & Robyt, J. F. (1984). Structure studies of amylose-V complexes and retro-graded amylose by action of alpha amylases, and a new method for preparing amyloextrins. *Carbohydrate Research*, 132(1), 105–118. [https://doi.org/10.1016/0008-6215\(84\)85068-5](https://doi.org/10.1016/0008-6215(84)85068-5)
- Jane, J. (2006). Current Understanding on Starch Granule Structures. *Journal of Applied Glycoscience*, 53(3), 205–213. <https://doi.org/10.5458/jag.53.205>
- Jane, J., & Shen, J. J. (1993). Internal structure of the potato starch granule revealed by chemical gelatinization. *Carbohydrate Research*, 247, 279–290. [https://doi.org/10.1016/0008-6215\(93\)84260-D](https://doi.org/10.1016/0008-6215(93)84260-D)
- Jankowski, T. (1992). Influence of starch retrogradation on the texture of cooked potato tuber. *International Journal of Food Science & Technology*, 27(6), 637–642.
- Jankowski, T., & Rha, C. K. (1986). Retrogradation of Starch in Cooked Wheat. *Starch - Stärke*, 38(1), 6–9. <https://doi.org/10.1002/star.19860380103>
- Jayakody, L., & Hoover, R. (2008). Effect of annealing on the molecular structure and physicochemical properties of starches from different botanical origins - A review. *Carbohydrate Polymers*, 74(3), 691–703. <https://doi.org/10.1016/j.carbpol.2008.04.032>
- Jekle, M., Mühlberger, K., & Becker, T. (2016). Starch–gluten interactions during gelatinization and its functionality in dough like model systems. *Food Hydrocolloids*, 54, 196–201. <https://doi.org/10.1016/j.foodhyd.2015.10.005>
- Jenkins, A. D. (1972). *Polymer science : A materials science handbook*. Amsterdam : North-Holland Pub. Co.
- Jenkins, D. J. A., Kendall, C. W., Augustin, L. S., Franceschi, S., Hamidi, M., Marchie, A., ... Axelsen, M. (2002). Glycemic index: overview of implications in health and disease. *Am J Clin Nutr*, 76(1), 266S – 273. Retrieved from <http://ajcn.nutrition.org/cgi/content/short/76/1/266S>
- Jenkins, D. J. A., Vuksan, V., Kendall, C. W. C., Mehling, C. C., Vidgen, E., Augustin, L. S. A., ... Waring, S. (1998). Physiological Effects of Resistant Starches on Fecal Bulk, Short Chain Fatty Acids, Blood Lipids and Glycemic Index. *Journal of the American College of Nutrition*, 17(6), 609–616. <https://doi.org/10.1080/07315724.1998.10718810>
- Jenkins, D. J. A., Wolever, T. M. S., Jenkins, A. L., Giordano, C., Giudici, S., Thompson, L. U., ... Wong, G. S. (1986). Low glycemic response to traditionally processed wheat and rye products: bulgur and pumpernickel bread. *The American Journal of Clinical Nutrition*, 43(4), 516–520.

<https://doi.org/10.1093/ajcn/43.4.516>

- Jenkins, D. J. A., Wolever, T. M. S., & Taylor, R. H. (1981). Glycemic index of foods: A physiological basis for carbohydrate exchange. *American Journal of Clinical Nutrition*, *34*(3), 362–366.
- Jenkins, D. J. A., Wolever, T. M., Taylor, R. H., Barker, H., Fielden, H., Baldwin, J. M., ... Goff, D. V. (1981). Glycemic index of foods: a physiological basis for carbohydrate exchange. *The American Journal of Clinical Nutrition*, *34*(3), 362–366. <https://doi.org/10.1093/ajcn/34.3.362>
- Jenkins, P. J., & Donald, A. M. (1997). Breakdown of crystal structure in potato starch during gelatinisation. *Journal of Applied Polymer Science*, *66*, 225–232.
- Jiang, H., Zhang, Y., Hong, Y., Bi, Y., Gu, Z., Cheng, L., ... Li, C. (2015). Digestibility and changes to structural characteristics of green banana starch during in vitro digestion. *Food Hydrocolloids*, *49*, 192–199. <https://doi.org/10.1016/j.foodhyd.2015.03.023>
- Jiang, Y., & Miles, P. W. (1993). Generation of H₂O₂ during enzymic oxidation of catechin. *Phytochemistry*, *33*(1), 29–34. [https://doi.org/10.1016/0031-9422\(93\)85391-4](https://doi.org/10.1016/0031-9422(93)85391-4)
- Jiranuntakul, W., Puttanlek, C., Rungsardthong, V., Pancha-arnon, S., & Uttapap, D. (2011). Microstructural and physicochemical properties of heat-moisture treated waxy and normal starches. *Journal of Food Engineering*, *104*(2), 246–258. <https://doi.org/10.1016/j.jfoodeng.2010.12.016>
- Johnson, S. K., Thomas, S. J., & Hall, R. S. (2005). Palatability and glucose, insulin and satiety responses of chickpea flour and extruded chickpea flour bread eaten as part of a breakfast. *European Journal of Clinical Nutrition*, *59*(2), 169–176. <https://doi.org/10.1038/sj.ejcn.1602054>
- Jouppila, K., Kansikas, J., & Roos, Y. H. (1998). Factors affecting crystallization and crystallization kinetics in amorphous corn starch. *Carbohydrate Polymers*, *36*, 143–149. [https://doi.org/10.1016/S0144-8617\(98\)00024-1](https://doi.org/10.1016/S0144-8617(98)00024-1)
- Jouppila, K., & Roos, Y. H. (1997). The Physical State of Amorphous Corn Starch and Its Impact On Crystallization. *Carbohydrate Polymers*, *32*(2), 95–104.
- Jung, K., Lee, H., Lee, S. H., & Kim, J. C. (2016). Retrogradation of heat-gelatinized rice grain in sealed packaging: investigation of moisture relocation. *Food Science and Technology*, *37*(1), 97–102. <https://doi.org/10.1590/1678-457x.07816>
- Kadam, S. U., Tiwari, B. K., & O'Donnell, C. P. (2015). Improved thermal processing for food texture modification. *Modifying Food Texture*, *1*, 115–131. <https://doi.org/10.1016/B978-1-78242-333-1.00006-1>
- Kalb, A. J., & Sterling, C. (1961). Temperature and the Retrogradation of Starch. *Journal of Food Science*, *26*(6), 587–592. <https://doi.org/10.1111/j.1365-2621.1961.tb00800.x>
- Kalichevsky, M. T., Jaroszkiwicz, E. M., Ablett, S., Blanshard, J. M. V., & Lillford, P. J. (1992). The glass transition of amylopectin measured by DSC, DMTA and NMR. *Carbohydrate Polymers*, *18*(2), 77–88. [https://doi.org/10.1016/0144-8617\(92\)90129-E](https://doi.org/10.1016/0144-8617(92)90129-E)
- Karim, A. (2000). Methods for the study of starch retrogradation. *Food Chemistry*, *71*(1), 9–36.

[https://doi.org/10.1016/S0308-8146\(00\)00130-8](https://doi.org/10.1016/S0308-8146(00)00130-8)

- Karlsson, M. E., & Eliasson, A.-C. (2003a). Effects of time/temperature treatments on potato (*Solanum tuberosum*) starch: a comparison of isolated starch and starch in situ. *Journal of the Science of Food and Agriculture*, 83(15), 1587–1592. <https://doi.org/10.1002/jsfa.1583>
- Karlsson, M. E., & Eliasson, A.-C. (2003b). Gelatinization and retrogradation of potato (*Solanum tuberosum*) starch in situ as assessed by differential scanning calorimetry (DSC). *LWT - Food Science and Technology*, 36(8), 735–741. [https://doi.org/10.1016/S0023-6438\(03\)00093-8](https://doi.org/10.1016/S0023-6438(03)00093-8)
- Kauppinen, J. K., Moffatt, D. J., Mantsch, H. H., & Cameron, D. G. (1981). Fourier Self-Deconvolution: A Method for Resolving Intrinsically Overlapped Bands. *Applied Spectroscopy*, 35(3), 271–276. <https://doi.org/10.1366/0003702814732634>
- Kaur, K., & Singh, N. (2000). Amylose-lipid complex formation during cooking of rice flour. *Food Chemistry*, 71(4), 511–517. [https://doi.org/10.1016/S0308-8146\(00\)00202-8](https://doi.org/10.1016/S0308-8146(00)00202-8)
- Kaur, L., & Singh, J. (2016). Novel Applications of Potatoes. In *Advances in Potato Chemistry and Technology* (pp. 627–649). Elsevier. <https://doi.org/10.1016/B978-0-12-800002-1.00021-2>
- Kaur, L., Singh, J., McCarthy, O. J., & Singh, H. (2007). Physico-chemical, rheological and structural properties of fractionated potato starches. *Journal of Food Engineering*, 82(3), 383–394. <https://doi.org/10.1016/j.jfoodeng.2007.02.059>
- Kaur, L., Singh, J., Singh, N., & Ezekiel, R. (2007). Textural and pasting properties of potatoes (*Solanum tuberosum* L.) as affected by storage temperature. *Journal of the Science of Food and Agriculture*, 87(2), 520–526. <https://doi.org/10.1002/jsfa>
- Kaur, L., Singh, N., Singh Sodhi, N., & Singh Gujral, H. (2002). Some properties of potatoes and their starches I. Cooking, textural and rheological properties of potatoes. *Food Chemistry*, 79(2), 177–181. [https://doi.org/10.1016/S0308-8146\(02\)00129-2](https://doi.org/10.1016/S0308-8146(02)00129-2)
- Kawai, K., Fukami, K., & Yamamoto, K. (2007). State diagram of potato starch–water mixtures treated with high hydrostatic pressure. *Carbohydrate Polymers*, 67(4), 530–535. <https://doi.org/10.1016/j.carbpol.2006.06.026>
- Kaymak, F., & Kincal, N. S. (2007). Apparent diffusivities of reducing sugars in potato strips blanched in water. *International Journal of Food Science & Technology*, 29(1), 63–70. <https://doi.org/10.1111/j.1365-2621.1994.tb02047.x>
- Kim, C. S., & Walker, C. E. (1992a). Effects of Sugars and Emulsifiers on Starch Gelatinization Evaluated by Differential Scanning Calorimetry. *Cereal Chemistry*, 69(2), 212–217.
- Kim, C. S., & Walker, C. E. (1992b). Interactions between starches, sugars, and emulsifiers in high-ratio cake model systems. *Cereal Chemistry*, 69(2), 206–212.
- Kim, H.-S., Kim, B.-Y., & Baik, M.-Y. (2012). Application of Ultra High Pressure (UHP) in Starch Chemistry. *Critical Reviews in Food Science and Nutrition*, 52(2), 123–141. <https://doi.org/10.1080/10408398.2010.498065>
- Kim, H.-Y., Park, S. S., & Lim, S.-T. (2015). Preparation, characterization and utilization of starch

- nanoparticles. *Colloids and Surfaces B: Biointerfaces*, 126, 607–620. <https://doi.org/10.1016/j.colsurfb.2014.11.011>
- Kim, Ha Ram, Choi, S. J., Park, C.-S., & Moon, T. W. (2017). Kinetic studies of in vitro digestion of amylosucrase-modified waxy corn starches based on branch chain length distributions. *Food Hydrocolloids*, 65, 46–56. <https://doi.org/10.1016/j.foodhyd.2016.10.038>
- Kim, Hak Ryang, Muhrbeck, P., & Eliasson, A.-C. (1993). Changes in rheological properties of hydroxypropyl potato starch pastes during freeze-thaw treatments. III. Effect of cooking conditions and concentration of the starch paste. *Journal of the Science of Food and Agriculture*, 61(1), 109–116. <https://doi.org/10.1002/jsfa.2740610117>
- Kim, J.-Y., & Huber, K. C. (2013). Heat–moisture treatment under mildly acidic conditions alters potato starch physicochemical properties and digestibility. *Carbohydrate Polymers*, 98(2), 1245–1255. <https://doi.org/10.1016/j.carbpol.2013.07.013>
- Kim, J. H., Tanhehco, E. J., & Ng, P. K. W. (2006). Effect of extrusion conditions on resistant starch formation from pastry wheat flour. *Food Chemistry*, 99(4), 718–723. <https://doi.org/10.1016/j.foodchem.2005.08.054>
- Kim, Y., Wiesenborn, D., Lorenzen, J., & Berglund, P. (1996). Suitability of edible bean and potato starches for starch noodles. *Cereal Chemistry*.
- Kingman, S. M., & Englyst, H. N. (1994). The influence of food preparation methods on the in-vitro digestibility of starch in potatoes. *Food Chemistry*, 49(2), 181–186. [https://doi.org/10.1016/0308-8146\(94\)90156-2](https://doi.org/10.1016/0308-8146(94)90156-2)
- Kinnear, T. S., & Wolever, T. (2010). The effects of cooking, cooling and reheating on the Glycemic Index depends on potato variety. In *The FASEB Journal* (Vol. 24, pp. 553.2-553.2). Federation of American Societies for Experimental Biology. Retrieved from http://www.fasebj.org/content/24/1_Supplement/553.2
- Kirkpatrick, M. E., Heinze, P. H., Craft, C. C., Mountjoy, B. M., & Falatko., C. E. (1956). French-frying quality of potatoes as influenced by cooking methods, storage conditions, and specific gravity of tubers. *US Dept Agric Tech Bull* 1142.
- Kiseleva, V. I., Krivandin, A. V., Fornal, J., Błaszczak, W., Jeliński, T., & Yuryev, V. P. (2005). Annealing of normal and mutant wheat starches. LM, SEM, DSC, and SAXS studies. *Carbohydrate Research*, 340(1), 75–83. <https://doi.org/10.1016/j.carres.2004.10.012>
- Klucinec, J. D., & Thompson, D. B. (1999). Amylose and amylopectin interact in retrogradation of dispersed high amylose starches. *Cereal Chemistry*, 76(2), 282–291.
- Knorr, D., Heinz, V., & Buckow, R. (2006). High pressure application for food biopolymers. *Biochimica et Biophysica Acta (BBA) - Proteins and Proteomics*, 1764(3), 619–631. <https://doi.org/10.1016/j.bbapap.2006.01.017>
- Kohyama, K., & Sasaki, T. (2006). Differential scanning calorimetry and a model calculation of starches annealed at 20 and 50°C. *Carbohydrate Polymers*, 63(1), 82–88.

- <https://doi.org/10.1016/j.carbpol.2005.08.004>
- Kong, F., Oztop, M. H., Singh, R. P., & McCarthy, M. J. (2011). Physical Changes in White and Brown Rice during Simulated Gastric Digestion. *Journal of Food Science*, 76(6), E450–E457. <https://doi.org/10.1111/j.1750-3841.2011.02271.x>
- Kong, F., & Singh, R. P. (2010). A Human Gastric Simulator (HGS) to Study Food Digestion in Human Stomach. *Journal of Food Science*, 75(9), E627–E635. <https://doi.org/10.1111/j.1750-3841.2010.01856.x>
- Korus, J., Witczak, M., Ziobro, R., & Juszczak, L. (2009). The impact of resistant starch on characteristics of gluten-free dough and bread. *Food Hydrocolloids*, 23(3), 988–995. <https://doi.org/10.1016/j.foodhyd.2008.07.010>
- Kosewski, G., Górna, I., Bolesławska, I., Kowalówka, M., Więckowska, B., Główska, A. K., ... Przysławski, J. (2018). Comparison of antioxidative properties of raw vegetables and thermally processed ones using the conventional and sous-vide methods. *Food Chemistry*, 240(August 2017), 1092–1096. <https://doi.org/10.1016/j.foodchem.2017.08.048>
- Krezowski, P. A., Nuttall, F. Q., Gannon, M. C., Billington, C. J., & Parker, S. (1987). Insulin and glucose responses to various starch-containing foods in type II diabetic subjects. *Diabetes Care*, 10(2), 205–212. Retrieved from <http://www.ncbi.nlm.nih.gov/pubmed/3556106>
- Krueger, B. R., Knutson, C. A., Inglett, G. E., & Walker, C. E. (1987). A Differential Scanning Calorimetry Study on the Effect of Annealing on Gelatinization Behavior of Corn Starch. *Journal of Food Science*, 52(3), 715–718. <https://doi.org/10.1111/j.1365-2621.1987.tb06709.x>
- Krueger, B. R., Walker, C. A., Knutson, C. A., & Inglett, G. E. (1987). Differential Scanning Calorimetry of Raw and Annealed Starch Isolated from Normal and Mutant Maize Genotypes. *Cereal Chemistry*, 64(3), 187–190. Retrieved from <http://agris.fao.org/agris-search/search/display.do?f=1987/US/US87095.xml;US8737498>
- Kuang, Q., Xu, J., Liang, Y., Xie, F., Tian, F., Zhou, S., & Liu, X. (2017). Lamellar structure change of waxy corn starch during gelatinization by time-resolved synchrotron SAXS. *Food Hydrocolloids*, 62, 43–48. <https://doi.org/10.1016/j.foodhyd.2016.07.024>
- Kumar, V., Sinha, A. K., Makkar, H. P. S., de Boeck, G., & Becker, K. (2012). Dietary Roles of Non-Starch Polysachharides in Human Nutrition: A Review. *Critical Reviews in Food Science and Nutrition*, 52(10), 899–935. <https://doi.org/10.1080/10408398.2010.512671>
- Lamberti, M. (2003). *Structural properties of starch containing plant cell dispersions - investigation on instant mashed potatoes*. <https://doi.org/10.3929/ethz-a-004709980>
- Larsen, H., Rasmussen, O., Rasmussen, P., Alstrup, K., Biswas, S., Tetens, I., ... Hermansen, K. (2000). Glycaemic index of parboiled rice depends on the severity of processing: study in type 2 diabetic subjects. *European Journal of Clinical Nutrition*, 54(5), 380–385. <https://doi.org/10.1038/sj.ejcn.1600969>
- Larsson, I., & Eliasson, A.-C. (1991). Annealing of Starch at an Intermediate Water Content. *Starch -*

- Stärke*, 43(6), 227–231. <https://doi.org/10.1002/star.19910430606>
- Lau, E., Soong, Y. Y., Zhou, W., & Henry, J. (2015). Can bread processing conditions alter glycaemic response? *Food Chemistry*, 173, 250–256. <https://doi.org/10.1016/j.foodchem.2014.10.040>
- Laus, M. C., Klip, G., & Giuseppin, M. L. F. (2017). Improved Extraction and Sample Cleanup of Tri-glycoalkaloids α -Solanine and α -Chaconine in Non-denatured Potato Protein Isolates. *Food Analytical Methods*, 10(4), 845–853. <https://doi.org/10.1007/s12161-016-0631-2>
- Lawton, J. W., & Wu, Y. V. (1993). Thermal Behavior of Annealed Acetic Acid-Soluble Wheat Gluten, 70(4), 471–475.
- Lee, C. J., & Moon, T. W. (2015). Structural characteristics of slowly digestible starch and resistant starch isolated from heat–moisture treated waxy potato starch. *Carbohydrate Polymers*, 125, 200–205. <https://doi.org/10.1016/j.carbpol.2015.02.035>
- Lee, H. A., Kim, N. H., & Nishinari, K. (1998). DSC and rheological studies of the effects of sucrose on the gelatinization and retrogradation of acorn starch. *Thermochimica Acta*, 322(1), 39–46. [https://doi.org/10.1016/S0040-6031\(98\)00469-9](https://doi.org/10.1016/S0040-6031(98)00469-9)
- Leeman, M., Östman, E., & Björck, I. (2005). Vinegar dressing and cold storage of potatoes lowers postprandial glycaemic and insulinaemic responses in healthy subjects. *European Journal of Clinical Nutrition*, 59(11), 1266–1271. <https://doi.org/10.1038/sj.ejcn.1602238>
- Lehmann, U., & Robin, F. (2007a). Slowly digestible starch - its structure and health implications. *Trends in Food Science & Technology*, 18, 346–355.
- Lehmann, U., & Robin, F. (2007b). Slowly digestible starch – its structure and health implications: a review. *Trends in Food Science & Technology*, 18(7), 346–355. <https://doi.org/10.1016/j.tifs.2007.02.009>
- Levine, H., & Slade, L. (1988). *Water as a plasticizer : physico-chemical aspects of low-moisture polymeric systems. Water Science Reviews 3: Water Dynamics.* <https://doi.org/10.1017/CBO9780511552083.002>
- Li, D., Zhu, Z., & Sun, D. W. (2018). Effects of freezing on cell structure of fresh cellular food materials: A review. *Trends in Food Science and Technology*, 75(February), 46–55. <https://doi.org/10.1016/j.tifs.2018.02.019>
- Li, Q., Wu, Q. Y., Jiang, W., Qian, J. Y., Zhang, L., Wu, M., ... Wu, C. Sen. (2019). Effect of pulsed electric field on structural properties and digestibility of starches with different crystalline type in solid state. *Carbohydrate Polymers*, 207(November 2018), 362–370. <https://doi.org/10.1016/j.carbpol.2018.12.001>
- Li, W., Bai, Y., Mousaa, S. A. S., Zhang, Q., & Shen, Q. (2012). Effect of High Hydrostatic Pressure on Physicochemical and Structural Properties of Rice Starch. *Food and Bioprocess Technology*, 5(6), 2233–2241. <https://doi.org/10.1007/s11947-011-0542-6>
- Li, W., Tian, X., Wang, P., Saleh, A. S. M., Luo, Q., Zheng, J., ... Zhang, G. (2016). Recrystallization characteristics of high hydrostatic pressure gelatinized normal and waxy corn starch. *International*

- Journal of Biological Macromolecules*, 83, 171–177.
<https://doi.org/10.1016/j.ijbiomac.2015.11.057>
- Li, Z., Fredericks, P. M., Rintoul, L., & Ward, C. R. (2007). Application of attenuated total reflectance micro-Fourier transform infrared (ATR-FTIR) spectroscopy to the study of coal macerals: Examples from the Bowen Basin, Australia. *International Journal of Coal Geology*, 70(1–3), 87–94. <https://doi.org/10.1016/j.coal.2006.01.006>
- Lian, X., Cheng, K., Wang, D., Zhu, W., & Wang, X. (2018). Analysis of crystals of retrograded starch with sharp X-ray diffraction peaks made by recrystallization of amylose and amylopectin. *International Journal of Food Properties*, 00(00), 1–13. <https://doi.org/10.1080/10942912.2017.1362433>
- Lian, X., Guo, J., Wang, D., Li, L., & Zhu, J. (2014). Effects of Protein in Wheat Flour on Retrogradation of Wheat Starch. *Journal of Food Science*, 79(8), C1505–C1511. <https://doi.org/10.1111/1750-3841.12525>
- Lian, X., Zhu, W., Wen, Y., Li, L., & Zhao, X. (2013). Effects of soy protein hydrolysates on maize starch retrogradation studied by IR spectra and ESI-MS analysis. *International Journal of Biological Macromolecules*, 59, 143–150. <https://doi.org/10.1016/j.ijbiomac.2013.03.071>
- Lim, S.-T., Chang, E.-H., & Chung, H.-J. (2001). Thermal transition characteristics of heat–moisture treated corn and potato starches. *Carbohydrate Polymers*, 46(2), 107–115. [https://doi.org/10.1016/S0144-8617\(00\)00287-3](https://doi.org/10.1016/S0144-8617(00)00287-3)
- Lin Ek, K., Wang, S., Brand-Miller, J., & Copeland, L. (2014). Properties of starch from potatoes differing in glycemic index. *Food Funct.*, 5(10), 2509–2515. <https://doi.org/10.1039/C4FO00354C>
- Lin, J.-M., Lin, T.-L., Jeng, U.-S., Huang, Z.-H., & Huang, Y.-S. (2009). Aggregation structure of Alzheimer amyloid- β (1–40) peptide with sodium dodecyl sulfate as revealed by small-angle X-ray and neutron scattering. *Soft Matter*, 5(20), 3913. <https://doi.org/10.1039/b908203d>
- Lin, Y., Yeh, A.-I., & Lii, C. (2001). Correlation Between Starch Retrogradation and Water Mobility as Determined by Differential Scanning Calorimetry (DSC) and Nuclear Magnetic Resonance (NMR). *Cereal Chemistry*, 78(6), 647–653. <https://doi.org/10.1094/CCHEM.2001.78.6.647>
- Liu, E. Z., & Scanlon, M. G. (2007). Modeling the effect of blanching conditions on the texture of potato strips. *Journal of Food Engineering*, 81(2), 292–297. <https://doi.org/10.1016/j.jfoodeng.2006.08.002>
- Liu, Hang, Wang, L., Cao, R., Fan, H., & Wang, M. (2016). In vitro digestibility and changes in physicochemical and structural properties of common buckwheat starch affected by high hydrostatic pressure. *Carbohydrate Polymers*, 144, 1–8. <https://doi.org/10.1016/j.carbpol.2016.02.028>
- Liu, Hongsheng, Yu, L., Simon, G., Dean, K., & Chen, L. (2009). Effects of annealing on gelatinization and microstructures of corn starches with different amylose/amylopectin ratios. *Carbohydrate*

- Polymers*, 77(3), 662–669. <https://doi.org/10.1016/j.carbpol.2009.02.010>
- Liu, P.-L., Hu, X.-S., & Qun, S. (2010). Effect of high hydrostatic pressure on starches: A review. *Starch - Stärke*, 62(12), 615–628. <https://doi.org/10.1002/star.201000001>
- Liu, Y., Chen, J., Luo, S., Li, C., Ye, J., Liu, C., & Gilbert, R. G. (2017). Physicochemical and structural properties of pregelatinized starch prepared by improved extrusion cooking technology. *Carbohydrate Polymers*, 175, 265–272. <https://doi.org/10.1016/j.carbpol.2017.07.084>
- Lok, K. Y., Chan, R., Chan, D., Li, L., Leung, G., Woo, J., ... Henry, C. J. K. (2010). Glycaemic index and glycaemic load values of a selection of popular foods consumed in Hong Kong. *British Journal of Nutrition*, 103(4), 556–560. <https://doi.org/10.1017/S0007114509992042>
- Lopez-Rubio, A., Flanagan, B. M., Shrestha, A. K., Gidley, M. J., & Gilbert, E. P. (2008). Molecular rearrangement of starch during in vitro digestion: Toward a better understanding of enzyme resistant starch formation in processed starches. *Biomacromolecules*, 9(7), 1951–1958. <https://doi.org/10.1021/bm800213h>
- Lu, L. W., Venn, B., Lu, J., Monro, J., & Rush, E. (2017). Effect of cold storage and reheating of parboiled rice on postprandial glycaemic response, satiety, palatability and chewed particle size distribution. *Nutrients*, 9(5), 1–13. <https://doi.org/10.3390/nu9050475>
- Lu, T. J., Jane, J.-L., & Keeling, P. L. (1997). Temperature effect on retrogradation rate and crystalline structure of amylose. *Carbohydrate Polymers*, 33(1), 19–26. [https://doi.org/10.1016/S0144-8617\(97\)00038-6](https://doi.org/10.1016/S0144-8617(97)00038-6)
- Luallen, T. (2017). *Utilizing Starches in Product Development. Starch in Food: Structure, Function and Applications: Second Edition*. Elsevier Ltd. <https://doi.org/10.1016/B978-0-08-100868-3.00013-5>
- Luck, W. A. P. (1980). The Structure of Aqueous Systems and the Influence of Electrolytes. In *Water in Polymers* (pp. 43–71). ACS Symposium Series. <https://doi.org/10.1021/bk-1980-0127.ch003>
- Ludwig, D. S. (2002). The Glycemic Index. *JAMA*, 287(18), 2414. <https://doi.org/10.1001/jama.287.18.2414>
- Luo, Z., Fu, X., He, X., Luo, F., Gao, Q., & Yu, S. (2008). Effect of Ultrasonic Treatment on the Physicochemical Properties of Maize Starches Differing in Amylose Content. *Starch - Stärke*, 60(11), 646–653. <https://doi.org/10.1002/star.200800014>
- Lynch, D. R., Liu, Q., Tarn, T. R., Bizimungu, B., Chen, Q., Harris, P., ... Skjoldt, N. M. (2007). Glycemic index - A review and implications for the potato industry. *American Journal of Potato Research*. Retrieved from <http://www.scopus.com/inward/record.url?eid=2-s2.0-34447277632&partnerID=tZOtx3y1>
- Magritek. (2016). Prospa© v3.1. Retrieved from <http://www.magritek.com/prospa/>
- Mahasukhonthachat, K., Sopade, P. A., & Gidley, M. J. (2010). Kinetics of starch digestion and functional properties of twin-screw extruded sorghum. *Journal of Cereal Science*, 51(3), 392–401. <https://doi.org/10.1016/j.jcs.2010.02.008>

- Manful, J. T., Grimm, C. C., Gayin, J., & Coker, R. D. (2008). Effect of Variable Parboiling on Crystallinity of Rice Samples. *Cereal Chemistry Journal*, 85(1), 92–95. <https://doi.org/10.1094/CCHEM-85-1-0092>
- Manmohit Kalia, P. K. (2015). Pectin Methylsterases: A Review. *Journal of Bioprocessing & Biotechniques*, 05(05). <https://doi.org/10.4172/2155-9821.1000227>
- Marcone, M. F., Wang, S., Albabish, W., Nie, S., Somnarain, D., & Hill, A. (2013). Diverse food-based applications of nuclear magnetic resonance (NMR) technology. *Food Research International*, 51(2), 729–747. <https://doi.org/10.1016/j.foodres.2012.12.046>
- Marsh, R. D. L., & Blanshard, J. M. V. (1988). The application of polymer crystal growth theory to the kinetics of formation of the B-amylose polymorph in a 50% wheat-starch gel. *Carbohydrate Polymers*, 9(4), 301–317. [https://doi.org/10.1016/0144-8617\(88\)90048-3](https://doi.org/10.1016/0144-8617(88)90048-3)
- Marshall, W. E., & Chrastil, J. (1992). Interaction of Food Proteins with Starch. In *Biochemistry of Food Proteins* (pp. 75–97). Boston, MA: Springer US. https://doi.org/10.1007/978-1-4684-9895-0_3
- Matignon, A., & Tecante, A. (2017). Starch retrogradation: From starch components to cereal products. *Food Hydrocolloids*, 68, 43–52. <https://doi.org/10.1016/j.foodhyd.2016.10.032>
- Matsuura-Endo, C., Ohara-Takada, A., Yamauchi, H., Mori, M., & Fujikawa, S. (2002). Disintegration Differences in Cooked Potatoes from Three Japanese Cultivars: Comparison of Starch Distribution within One Tuber and Tissue Structure. *Food Science and Technology Research*, 8(3), 252–256. <https://doi.org/10.3136/fstr.8.323>
- Matsuura-Endo, C., Ohara-Takada, A., Yamauchi, H., Mukasa, Y., Mori, M., & Ishibashi, K. (2002). Disintegration Differences in Cooked Potatoes from Three Japanese Cultivars: Comparison of the Properties of Isolated Starch, Degree of Cell Separation with EDTA, and Contents of Calcium and Galacturonic Acid. *Food Science and Technology Research*, 8(4), 323–327. <https://doi.org/10.3136/fstr.8.323>
- Mazza, G., Hung, J., & Dench, M. J. (1983). Processing/Nutritional Quality Changes in Potato Tubers During Growth and Long Term Storage. *Canadian Institute of Food Science and Technology Journal*, 16(1), 39–44. [https://doi.org/10.1016/S0315-5463\(83\)72017-1](https://doi.org/10.1016/S0315-5463(83)72017-1)
- McCleary, B. V., & Monaghan, D. A. (2002). Measurement of resistant starch. *Journal of AOAC International*, 85(3), 665–675. Retrieved from <http://www.ncbi.nlm.nih.gov/pubmed/12083259>
- McCleary, B. V., & Rossiter, P. (2004). Measurement of novel dietary fibers. *Journal of AOAC International*, 87(3), 707–717. Retrieved from <http://www.ncbi.nlm.nih.gov/pubmed/15287670>
- McGill, C. R., Kurilich, A. C., & Davignon, J. (2013). The role of potatoes and potato components in cardiometabolic health: A review. *Annals of Medicine*, 45(7), 467–473. <https://doi.org/10.3109/07853890.2013.813633>
- McGrance, S. J., Cornell, H. J., & Rix, C. J. (1998). A Simple and Rapid Colorimetric Method for the Determination of Amylose in Starch Products. *Starch - Stärke*, 50(4), 158–163.

- [https://doi.org/10.1002/\(SICI\)1521-379X\(199804\)50:4<158::AID-STAR158>3.0.CO;2-7](https://doi.org/10.1002/(SICI)1521-379X(199804)50:4<158::AID-STAR158>3.0.CO;2-7)
- McIver, R. G., Axford, D. W. E., Colwell, K. H., & Elton, G. A. H. (1968). Kinetic study of the retrogradation of gelatinised starch. *Journal of the Science of Food and Agriculture*, *19*(10), 560–563. <https://doi.org/10.1002/jsfa.2740191003>
- McKenzie, M., & Corrigan, V. (2016). Potato Flavor. In *Advances in Potato Chemistry and Technology* (pp. 339–368). Elsevier. <https://doi.org/10.1016/B978-0-12-800002-1.00012-1>
- Meiboom, S., & Gill, D. (1958). Modified Spin-Echo Method for Measuring Nuclear Relaxation Times. *Review of Scientific Instruments*, *29*(8), 688–691. <https://doi.org/10.1063/1.1716296>
- Meyer, K. H., Gurtler, P., & Bernfeld, P. (1947). Structure of Amylopectin. *Nature*, *160*, 900. Retrieved from <http://dx.doi.org/10.1038/160900a0>
- Micklander, E., Peshlov, B., Purslow, P. P., & Engelsen, S. B. (2002). NMR-cooking: monitoring the changes in meat during cooking by low-field ¹H-NMR. *Trends in Food Science & Technology*, *13*(9–10), 341–346. [https://doi.org/10.1016/S0924-2244\(02\)00163-2](https://doi.org/10.1016/S0924-2244(02)00163-2)
- Micklander, E., Thybo, A. K., & van den Berg, F. (2008). Changes occurring in potatoes during cooking and reheating as affected by salting and cool or frozen storage – a LF-NMR study. *LWT - Food Science and Technology*, *41*(9), 1710–1719. <https://doi.org/10.1016/j.lwt.2007.10.015>
- Miles, M. J., Morris, V. J., Orford, P. D., & Ring, S. G. (1985). The roles of amylose and amylopectin in the gelation and retrogradation of starch. *Carbohydrate Research*, *135*(2), 271–281. [https://doi.org/10.1016/S0008-6215\(00\)90778-X](https://doi.org/10.1016/S0008-6215(00)90778-X)
- Miles, M. J., Morris, V. J., & Ring, S. G. (1984). Some recent observations on the retrogradation of amylose. *Carbohydrate Polymers*, *4*(1), 73–77. [https://doi.org/10.1016/0144-8617\(84\)90045-6](https://doi.org/10.1016/0144-8617(84)90045-6)
- Minekus, M., Alming, M., Alvito, P., Ballance, S., Bohn, T., Bourlieu, C., ... Brodkorb, A. (2014). A standardised static in vitro digestion method suitable for food – an international consensus. *Food Funct.*, *5*(6), 1113–1124. <https://doi.org/10.1039/C3FO60702J>
- Mishellany, A., Woda, A., Labas, R., & Peyron, M.-A. (2006). The Challenge of Mastication: Preparing a Bolus Suitable for Deglutition. *Dysphagia*, *21*(2), 87–94. <https://doi.org/10.1007/s00455-006-9014-y>
- Mishra, S., Monroe, J., & Hedderley, D. (2008). Effect of Processing on Slowly Digestible Starch and Resistant Starch in Potato. *Starch - Stärke*, *60*(9), 500–507. <https://doi.org/10.1002/star.200800209>
- Miyoshi, E. (2002). Effects of Heat-Moisture Treatment and Lipids on Gelatinization and Retrogradation of Maize and Potato Starches. *Cereal Chemistry Journal*, *79*(1), 72–77. <https://doi.org/10.1094/CCHEM.2002.79.1.72>
- Mohorič, A., Vergeldt, F., Gerkema, E., Dalen, G. van, Doel, L. R. van den, Vliet, L. J. van, ... Duynhoven, J. van. (2009). The effect of rice kernel microstructure on cooking behaviour: A combined μ -CT and MRI study. *Food Chemistry*, *115*(4), 1491–1499. <https://doi.org/10.1016/j.foodchem.2009.01.089>

- Mohr, W. P. (1972). Soggy-Centered French Fries. *Canadian Institute of Food Science and Technology Journal*, 5(4), 179–183. [https://doi.org/10.1016/S0315-5463\(72\)74124-3](https://doi.org/10.1016/S0315-5463(72)74124-3)
- Monro, J., Mishra, S., Blandford, E., Anderson, J., & Genet, R. (2009). Potato genotype differences in nutritionally distinct starch fractions after cooking, and cooking plus storing cool. *Journal of Food Composition and Analysis*, 22(6), 539–545. <https://doi.org/10.1016/j.jfca.2008.11.008>
- Morris, V. J. (1990). Starch gelation and retrogradation. *Trends in Food Science and Technology*, 1(C), 2–6. [https://doi.org/10.1016/0924-2244\(90\)90002-G](https://doi.org/10.1016/0924-2244(90)90002-G)
- Morris, W. L., Shepherd, T., Verrall, S. R., McNicol, J. W., & Taylor, M. A. (2010). Relationships between volatile and non-volatile metabolites and attributes of processed potato flavour. *Phytochemistry*, 71(14–15), 1765–1773. <https://doi.org/10.1016/j.phytochem.2010.07.003>
- Mortensen, M., Thybo, A. K., Bertram, H. C., Andersen, H. J., & Engelsen, S. B. (2005). Cooking Effects on Water Distribution in Potatoes Using Nuclear Magnetic Resonance Relaxation. *Journal of Agricultural and Food Chemistry*, 53(15), 5976–5981. <https://doi.org/10.1021/jf0479214>
- Moza, M. I., Mironescu, M., & Florea, A. (2012). INFLUENCE OF PHYSICAL TREATMENTS ON THE POTATO STARCH GRANULES MICRO- AND ULTRASTRUCTURE. *Bulletin UASVM Agriculture*, 69(2), 306–311. <https://doi.org/10.15835/buasvmcn-agr:8778>
- Mu, T.-H., Zhang, M., Raad, L., Sun, H.-N., & Wang, C. (2015). Effect of α -Amylase Degradation on Physicochemical Properties of Pre-High Hydrostatic Pressure-Treated Potato Starch. *PLOS ONE*, 10(12), e0143620. <https://doi.org/10.1371/journal.pone.0143620>
- Müftügil, N. (1985). The peroxidase enzyme activity of some vegetables and its resistance to heat. *Journal of the Science of Food and Agriculture*, 36(9), 877–880. <https://doi.org/10.1002/jsfa.2740360918>
- Müller, J. J., Gernat, C., Schulz, W., Müller, E.-C., Vorwerg, W., & Damaschun, G. (1995). Computer simulations of x-ray scattering curves: Gelation and crystallization process in amylose solutions. *Biopolymers*, 35(3), 271–288. <https://doi.org/10.1002/bip.360350303>
- Najjar, A. M., Parsons, P. M., Duncan, A. M., Robinson, L. E., Yada, R. Y., & Graham, T. E. (2008). The acute impact of ingestion of breads of varying composition on blood glucose, insulin and incretins following first and second meals. *British Journal of Nutrition*, 101(3), 391–398. <https://doi.org/10.1017/S0007114508003085>
- Nakazawa, F., Noguchi, S., Takahashi, J., & Takada, M. (1985). Retrogradation of gelatinized potato starch studied by differential scanning calorimetry. *Agricultural and Biological Chemistry*, 49(4), 953–957. <https://doi.org/10.1080/00021369.1985.10866856>
- Nakazawa, Y., & Wang, Y.-J. (2004). Effect of annealing on starch-palmitic acid interaction. *Carbohydrate Polymers*, 57(3), 327–335. <https://doi.org/10.1016/j.carbpol.2004.05.011>
- Nakazawa, Y., & Wang, Y. J. (2003). Acid hydrolysis of native and annealed starches and branch-structure of their Naegeli dextrins. *Carbohydrate Research*, 338(24), 2871–2882. <https://doi.org/10.1016/j.carres.2003.09.005>

- Nam, R. (2018). *Physicochemical and Sensory Modifications of Freeze-Thawed Mashed Potato*.
- Nayak, B., De J. Berrios, J., & Tang, J. (2014). Impact of food processing on the glycemic index (GI) of potato products. *Food Research International*, 56, 35–46. <https://doi.org/10.1016/j.foodres.2013.12.020>
- New Zealand Food Safety. (2017). *Food service and retail food control plan-Template -S39-00001 Specialist Food Service and Catering- Serve Safe*.
- Ngobese, N. Z., Workneh, T. S., & Siwela, M. (2017). Effect of low-temperature long-time and high-temperature short-time blanching and frying treatments on the French fry quality of six Irish potato cultivars. *Journal of Food Science and Technology*, 54(2), 507–517. <https://doi.org/10.1007/s13197-017-2495-x>
- Noda, T., Takigawa, S., Matsuura-Endo, C., Suzuki, T., Hashimoto, N., Kottarachchi, N. S., ... Zaidul, I. S. M. (2008). Factors affecting the digestibility of raw and gelatinized potato starches. *Food Chemistry*, 110(2), 465–470. <https://doi.org/10.1016/j.foodchem.2008.02.027>
- Novotni, D., Ćurić, D., Bituh, M., Colić Barić, I., Škevin, D., & Čukelj, N. (2011). Glycemic index and phenolics of partially-baked frozen bread with sourdough. *International Journal of Food Sciences and Nutrition*, 62(1), 26–33. <https://doi.org/10.3109/09637486.2010.506432>
- Nugent, A. P. (2005). Health properties of resistant starch. *Nutrition Bulletin*, 30(1), 27–54. <https://doi.org/10.1111/j.1467-3010.2005.00481.x>
- O'Brien, S., & Wang, Y. J. (2008). Susceptibility of annealed starches to hydrolysis by α -amylase and glucoamylase. *Carbohydrate Polymers*, 72(4), 597–607. <https://doi.org/10.1016/j.carbpol.2007.09.032>
- O'Sullivan, A. C., & Perez, S. (1999). The relationship between internal chain length of amylopectin and crystallinity in starch. *Biopolymers*, 50(4), 381–390. [https://doi.org/10.1002/\(SICI\)1097-0282\(19991005\)50:4<381::AID-BIP4>3.0.CO;2-W](https://doi.org/10.1002/(SICI)1097-0282(19991005)50:4<381::AID-BIP4>3.0.CO;2-W)
- Ogawa, Y., Glenn, G. M., Orts, W. J., & Wood, D. F. (2003). Histological Structures of Cooked Rice Grain. *Journal of Agricultural and Food Chemistry*, 51(24), 7019–7023. <https://doi.org/10.1021/jf034758o>
- Ohta, H., & Sugawara, W. (1987). Influence of processing and storage conditions on quality stability of shredded lettuce. *NIPPON SHOKUHIN KOGYO GAKKAISHI*, 34(7), 432–438. https://doi.org/10.3136/nskkk1962.34.7_432
- Östman, E. M., Nilsson, M., Liljeberg Elmståhl, H. G. M., Molin, G., & Björck, I. M. E. (2002). On the Effect of Lactic Acid on Blood Glucose and Insulin Responses to Cereal Products: Mechanistic Studies in Healthy Subjects and In Vitro. *Journal of Cereal Science*, 36(3), 339–346. <https://doi.org/10.1006/jcrs.2002.0469>
- Ottenhof, M. A., & Farhat, I. A. (2004). The effect of gluten on the retrogradation of wheat starch. *Journal of Cereal Science*, 40(3), 269–274. <https://doi.org/10.1016/j.jcs.2004.07.002>
- Palav, T., & Seetharaman, K. (2007). Impact of microwave heating on the physico-chemical properties

- of a starch–water model system. *Carbohydrate Polymers*, 67(4), 596–604. <https://doi.org/10.1016/j.carbpol.2006.07.006>
- Panlasigui, L. N., Thompson, L. U., Juliano, B. O., Perez, C. M., Jenkins, D. J. A., & Yiu, S. H. (1992). Extruded rice noodles: Starch digestibility and glycemic response of healthy and diabetic subjects with different habitual diets. *Nutrition Research*, 12(10), 1195–1204. [https://doi.org/10.1016/S0271-5317\(05\)80776-6](https://doi.org/10.1016/S0271-5317(05)80776-6)
- Park, E. Y., Baik, B.-K., & Lim, S.-T. (2009). Influences of temperature-cycled storage on retrogradation and in vitro digestibility of waxy maize starch gel. *Journal of Cereal Science*, 50(1), 43–48. <https://doi.org/10.1016/j.jcs.2009.02.004>
- Patterson, M. A., Fong, J. N., Maiya, M., Kung, S., Sarkissian, A., Nashef, N., & Wang, W. (2019). Chilled Potatoes Decrease Postprandial Glucose, Insulin, and Glucose-dependent Insulinotropic Peptide Compared to Boiled Potatoes in Females with Elevated Fasting Glucose and Insulin. *Nutrients*, 11(9), 2066. <https://doi.org/10.3390/nu11092066>
- Pearce, R. (2001). Plant Freezing and Damage. *Annals of Botany*, 87(4), 417–424. <https://doi.org/10.1006/anbo.2000.1352>
- Perdon, A. A., Marks, B. P., Siebenmorgen, T. J., & Reid, N. B. (1997). Effects of rough rice storage conditions on the amylograph and cooking properties of medium-grain rice cv. Bengal. *Cereal Chemistry*, 74(6), 864–867.
- Perdon, A. A., Siebenmorgen, T. J., Buescher, R. W., & Gbur, E. E. (1999). Starch retrogradation and texture of cooked milled rice during storage. *Journal of Food Science*, 64(5), 828–832. <https://doi.org/10.1111/j.1365-2621.1999.tb15921.x>
- Pérez, S., & Bertoft, E. (2010). The molecular structures of starch components and their contribution to the architecture of starch granules: A comprehensive review. *Starch/Staerke*, 62(8), 389–420. <https://doi.org/10.1002/star.201000013>
- Perry, P. A., & Donald, A. M. (2000a). SANS study of the distribution of water within starch granules. *Leaching Amylose. The Manner in Which Re-Association of These Starch Polymers Occurs during Cooling/Storage Conditions to Form a Gel Network Largely Determines the Subsequent Resistance of the Starch to E*, 28, 31–39.
- Perry, P. A., & Donald, A. M. (2000b). The effects of low temperatures on starch granule structure. *Polymer*, 41(16), 6361–6373. [https://doi.org/10.1016/S0032-3861\(99\)00813-7](https://doi.org/10.1016/S0032-3861(99)00813-7)
- Perry, P. A., & Donald, A. M. (2000c). The Role of Plasticization in Starch Granule Assembly. *Biomacromolecules*, 1(3), 424–432. <https://doi.org/10.1021/bm0055145>
- Peyron, M.-A., Mishellany, A., & Woda, A. (2004). Particle Size Distribution of Food Boluses after Mastication of Six Natural Foods. *Journal of Dental Research*, 83(7), 578–582. <https://doi.org/10.1177/154405910408300713>
- Pharmacopeia U.S. (1995). Simulated intestinal fluid. In *United States Pharmacopeial Convention* (Vol. 23, p. 2053). The National Formulary 9 (U.S. Pharmacopeia Board of Trustees).

- Pharmacopeia U.S. (2000). Simulated gastric fluid. In *United States Pharmacopeial Convention* (Vol. 24, p. 2235). The National Formulary 9 (U.S. Pharmacopeia Board of Trustees).
- Pinhero, R. G., Waduge, R. N., Liu, Q., Sullivan, J. A., Tsao, R., Bizimungu, B., & Yada, R. Y. (2016). Evaluation of nutritional profiles of starch and dry matter from early potato varieties and its estimated glycemic impact. *Food Chemistry*, 203, 356–366. <https://doi.org/10.1016/j.foodchem.2016.02.040>
- Pinhero, R. G., & Yada, R. Y. (2016). Postharvest Storage of Potatoes. In *Advances in Potato Chemistry and Technology* (pp. 283–314). Elsevier. <https://doi.org/10.1016/B978-0-12-800002-1.00010-8>
- Povlsen, V. T., Rinnan, Å., van den Berg, F., Andersen, H. J., & Thybo, A. K. (2003). Direct decomposition of NMR relaxation profiles and prediction of sensory attributes of potato samples. *LWT - Food Science and Technology*, 36(4), 423–432. [https://doi.org/10.1016/S0023-6438\(03\)00023-9](https://doi.org/10.1016/S0023-6438(03)00023-9)
- Pratiwi, M., Faridah, D. N., & Lioe, H. N. (2018). Structural changes to starch after acid hydrolysis, debranching, autoclaving-cooling cycles, and heat moisture treatment (HMT): A review. *Starch/Staerke*, 70(1–2), 1–13. <https://doi.org/10.1002/star.201700028>
- Putseys, J. A., Lamberts, L., & Delcour, J. A. (2010). Amylose-inclusion complexes: Formation, identity and physico-chemical properties. *Journal of Cereal Science*, 51(3), 238–247. <https://doi.org/10.1016/j.jcs.2010.01.011>
- Raatz, S. K., Idso, L., Johnson, L. K., Jackson, M. I., & Combs, G. F. (2016). Resistant starch analysis of commonly consumed potatoes: Content varies by cooking method and service temperature but not by variety. *Food Chemistry*, 208, 297–300. <https://doi.org/10.1016/j.foodchem.2016.03.120>
- Ramaswamy, H. S., & Chen, C. R. (2011). *Maximising the quality of thermally processed fruits and vegetables*. *Fruit and Vegetable Processing*. Woodhead Publishing Ltd. <https://doi.org/10.1533/9781855736641.2.188>
- Rasband, W. S. (1997). ImageJ. National Institutes of Health, Bethesda, Maryland, USA. Retrieved from <https://imagej.nih.gov/ij/>
- Ratnayake, W. S., & Jackson, D. S. (2007). A new insight into the gelatinization process of native starches. *Carbohydrate Polymers*, 67(4), 511–529. <https://doi.org/10.1016/j.carbpol.2006.06.025>
- Redmond, G. A., Gormley, T. R., & Butler, F. (2003). The effect of short- and long-term freeze-chilling on the quality of mashed potato. *Innovative Food Science and Emerging Technologies*, 4(1), 85–97. [https://doi.org/10.1016/S1466-8564\(02\)00082-6](https://doi.org/10.1016/S1466-8564(02)00082-6)
- Redmond, G., Ronan Gormley, T., Butler, F., Dempsey, A., Oxley, E., & Gerety, A. (2004). *Freeze-Chilling of Ready-to-eat Meal Components*. *Biosystems Engineering*.
- Reeve, R. M., Hautala, E., & Weaver, M. (1969). Anatomy and Compositional Variation within Potatoes I. Developmental Histology of the Tuber. *American Potato Journal*, 46, 361–373.
- Reeve, R. M., Hautala, E., & Weaver, M. L. (1970). Anatomy and compositional variations within potatoes III. Gross compositional gradients. *American Potato Journal*, 47(5), 148–162.

<https://doi.org/10.1007/BF02871192>

- Reeve, R. M., Weaver, M. L., & Timm, H. (1971). Anatomy and compositional variations within potatoes. IV. Total solids distribution in different cultivars. *American Potato Journal*, 48(8), 269–277. <https://doi.org/10.1007/BF02861727>
- Ribotta, P. D., Colombo, A., León, A. E., & Añón, M. C. (2007). Effects of Soy Protein on Physical and Rheological Properties of Wheat Starch. *Starch - Stärke*, 59(12), 614–623. <https://doi.org/10.1002/star.200700650>
- Ring, S. G., Colonna, P., I'Anson, K. J., Kalichevsky, M. T., Miles, M. J., Morris, V. J., & Orford, P. D. (1987). The gelation and crystallisation of amylopectin. *Carbohydrate Research*, 162(2), 277–293. [https://doi.org/10.1016/0008-6215\(87\)80223-9](https://doi.org/10.1016/0008-6215(87)80223-9)
- Ritota, M., Gianferri, R., Bucci, R., & Brosio, E. (2008). Proton NMR relaxation study of swelling and gelatinisation process in rice starch–water samples. *Food Chemistry*, 110(1), 14–22. <https://doi.org/10.1016/j.foodchem.2008.01.048>
- Riva, M., Fessas, D., & Schiraldi, A. (2000). Starch Retrogradation in Cooked Pasta and Rice. *Cereal Chemistry Journal*, 77(4), 433–438. <https://doi.org/10.1094/CCHEM.2000.77.4.433>
- Rocha, A. M. C. N., Coulon, E. C., & Morais, A. M. M. B. (2003). Effects of vacuum packaging on the physical quality of minimally processed potatoes. *Food Service Technology*, 3(2), 81–88. <https://doi.org/10.1046/j.1471-5740.2003.00068.x>
- Rocha, T. S., Cunha, V. A. G., Jane, J., & Franco, C. M. L. (2011). Structural characterization of peruvian carrot (*Arracacia xanthorrhiza*) starch and the effect of annealing on its semicrystalline structure. *Journal of Agricultural and Food Chemistry*, 59(8), 4208–4216. <https://doi.org/10.1021/jf104923m>
- Rojas, J. A., Rosell, C. M., & Benedito de Barber, C. (2001). Role of maltodextrins in the staling of starch gels. *European Food Research and Technology*, 212(3), 364–368. <https://doi.org/10.1007/s002170000218>
- Rommens, C. M., Shakya, R., Heap, M., & Fessenden, K. (2010). Tastier and healthier alternatives to french fries. *Journal of Food Science*, 75(4). <https://doi.org/10.1111/j.1750-3841.2010.01588.x>
- Ronda, F., Caballero, P. A., Quilez, J., & Roos, Y. H. (2011). Staling of frozen partly and fully baked breads. Study of the combined effect of amylopectin recrystallization and water content on bread firmness. *Journal of Cereal Science*, 53(1), 97–103. <https://doi.org/10.1016/j.jcs.2010.10.003>
- Ronda, F., & Roos, Y. H. (2008). Gelatinization and freeze-concentration effects on recrystallization in corn and potato starch gels. *Carbohydrate Research*, 343(5), 903–911. <https://doi.org/10.1016/j.carres.2008.01.026>
- Rondeau-Mouro, C., Cambert, M., Kovrljija, R., Musse, M., Lucas, T., & Mariette, F. (2015). Temperature-Associated Proton Dynamics in Wheat Starch-Based Model Systems and Wheat Flour Dough Evaluated by NMR. *Food and Bioprocess Technology*, 8(4), 777–790. <https://doi.org/10.1007/s11947-014-1445-0>

- Roos, Y. H., & Drusch, S. (2016). *Phase Transitions in Foods. Phase Transitions in Foods*. Elsevier. <https://doi.org/10.1016/B978-0-12-408086-7.00007-3>
- Rosenblum, J. L., Irwin, C. L., & Alpers, D. H. (1988). Starch and glucose oligosaccharides protect salivary-type amylase activity at acid pH. *The American Journal of Physiology*, 254(5 Pt 1), G775-80. <https://doi.org/10.1152/ajpgi.1988.254.5.G775>
- Ross, H. A., Wright, K. M., McDougall, G. J., Roberts, A. G., Chapman, S. N., Morris, W. L., ... Taylor, M. A. (2011). Potato tuber pectin structure is influenced by pectin methyl esterase activity and impacts on cooked potato texture. *Journal of Experimental Botany*, 62(1), 371–381. <https://doi.org/10.1093/jxb/erq280>
- Roulet, P., MacInnes, W. M., Wüsch, P., Sanchez, R. M., & Raemy, A. (1988). A comparative study of the retrogradation kinetics of gelatinized wheat starch in gel and powder form using X-rays, differential scanning calorimetry and dynamic mechanical analysis. *Food Hydrocolloids*, 2(5), 381–396. [https://doi.org/10.1016/S0268-005X\(88\)80003-1](https://doi.org/10.1016/S0268-005X(88)80003-1)
- Rueden, C. T., Schindelin, J., Hiner, M. C., DeZonia, B. E., Walter, A. E., Arena, E. T., & Eliceiri, K. W. (2017). ImageJ2: ImageJ for the next generation of scientific image data. *BMC Bioinformatics*, 18(1), 529. <https://doi.org/10.1186/s12859-017-1934-z>
- Rundle, R. E., & French, D. (1943). The Configuration of Starch in the Starch—Iodine Complex. III. X-Ray Diffraction Studies of the Starch—Iodine Complex 1. *Journal of the American Chemical Society*, 65(9), 1707–1710. <https://doi.org/10.1021/ja01249a016>
- Russell, P. L. (1987). The ageing of gels from starches of different amylose/amylopectin content studied by differential scanning calorimetry. *Journal of Cereal Science*, 6(2), 147–158. [https://doi.org/10.1016/S0733-5210\(87\)80051-6](https://doi.org/10.1016/S0733-5210(87)80051-6)
- Russell, P. L., & Oliver, G. (1989). The effect of pH and NaCl content on starch gel ageing. A study by differential scanning calorimetry and rheology. *Journal of Cereal Science*, 10(2), 123–138. [https://doi.org/10.1016/S0733-5210\(89\)80041-4](https://doi.org/10.1016/S0733-5210(89)80041-4)
- Sae-kang, V., & Suphantharika, M. (2006). Influence of pH and xanthan gum addition on freeze-thaw stability of tapioca starch pastes. *Carbohydrate Polymers*, 65(3), 371–380. <https://doi.org/10.1016/j.carbpol.2006.01.029>
- Sajilata, M. G., Singhal, R. S., & Kulkarni, P. R. (2006). Resistant starch - A review. *Comprehensive Reviews in Food Science and Food Safety*, 5(1), 1–17. <https://doi.org/10.1111/j.1541-4337.2006.tb00076.x>
- Salunkhe, D. K., Desai, B. B., & Chavan, J. K. (1989). Microscopic observations of starch grains in relation to maturity of potatoes. In *Quality and Preservation of Vegetables* (pp. 1–52). CRC Press Inc.
- Samant, S. K., Singhal, R. S., Kulkarni, P. R., & Rege, D. V. (2007). Protein-polysaccharide interactions: a new approach in food formulations. *International Journal of Food Science & Technology*, 28(6), 547–562. <https://doi.org/10.1111/j.1365-2621.1993.tb01306.x>

- Sang, Y., Alavi, S., & Shi, Y.-C. (2009). Subzero Glass Transition of Waxy Maize Starch Studied by Differential Scanning Calorimetry. *Starch - Stärke*, 61(12), 687–695. <https://doi.org/10.1002/star.200900164>
- Sanz, T., Salvador, A., Baixauli, R., & Fiszman, S. M. (2009). Evaluation of four types of resistant starch in muffins. II. Effects in texture, colour and consumer response. *European Food Research and Technology*, 229(2), 197–204. <https://doi.org/10.1007/s00217-009-1040-1>
- Sasaki, T., Yasui, T., & Matsuki, J. (2000). Effect of Amylose Content on Gelatinization, Retrogradation, and Pasting Properties of Starches from Waxy and Nonwaxy Wheat and Their F1 Seeds. *Cereal Chemistry*, 77(1), 58–63. <https://doi.org/http://dx.doi.org/10.1094/CCHEM.2000.77.1.58>
- Satrapai, S., & Suphantharika, M. (2007). Influence of spent brewer's yeast β -glucan on gelatinization and retrogradation of rice starch. *Carbohydrate Polymers*, 67(4), 500–510. <https://doi.org/10.1016/j.carbpol.2006.06.028>
- Schellekens, M. (1996). New research issues in sous-vide cooking. *Trends in Food Science and Technology*, 7(8), 256–262. [https://doi.org/10.1016/0924-2244\(96\)10027-3](https://doi.org/10.1016/0924-2244(96)10027-3)
- Schindelin, J., Arganda-Carreras, I., Frise, E., Kaynig, V., Longair, M., Pietzsch, T., ... Cardona, A. (2012). Fiji: an open-source platform for biological-image analysis. *Nature Methods*, 9(7), 676–682. <https://doi.org/10.1038/nmeth.2019>
- Schirmer, M., Jekle, M., & Becker, T. (2015). Starch gelatinization and its complexity for analysis. *Starch/Stärke*, 67(1–2), 30–41. <https://doi.org/10.1002/star.201400071>
- Schwanz Goebel, J. T., Kaur, L., Colussi, R., Elias, M. C., & Singh, J. (2019). Microstructure of indica and japonica rice influences their starch digestibility: A study using a human digestion simulator. *Food Hydrocolloids*, 94, 191–198. <https://doi.org/10.1016/j.foodhyd.2019.02.038>
- Selmi, B., Marion, D., Perrier Cornet, J. M., Douzals, J. P., & Gervais, P. (2000). Amyloglucosidase Hydrolysis of High-Pressure and Thermally Gelatinized Corn and Wheat Starches. *Journal of Agricultural and Food Chemistry*, 48(7), 2629–2633. <https://doi.org/10.1021/jf991332u>
- Sevenou, O., Hill, S. E., Farhat, I. A., & Mitchell, J. . (2002a). Organisation of the external region of the starch granule as determined by infrared spectroscopy. *International Journal of Biological Macromolecules*, 31(1–3), 79–85. [https://doi.org/10.1016/S0141-8130\(02\)00067-3](https://doi.org/10.1016/S0141-8130(02)00067-3)
- Sevenou, O., Hill, S. E., Farhat, I. A., & Mitchell, J. R. (2002b). Organisation of the external region of the starch granule as determined by infrared spectroscopy. *International Journal of Biological Macromolecules*, 31, 79–85.
- Sheard, M. A., & Rodger, C. (1995). Optimum heat treatments for “sous vide” cook-chill products. *Food Control*, 6(1), 53–56. [https://doi.org/10.1016/0956-7135\(95\)91454-S](https://doi.org/10.1016/0956-7135(95)91454-S)
- Shi, C. S., Guan, Q. Y., & Guo, T. W. (1990). Masticatory efficiency determined with direct measurement of food particles masticated by subjects with natural dentitions. *The Journal of Prosthetic Dentistry*, 64(6), 723–726. Retrieved from

<http://www.ncbi.nlm.nih.gov/pubmed/2079683>

- Shi, M., & Gao, Q. (2016). Recrystallization and in vitro digestibility of wrinkled pea starch gel by temperature cycling. *Food Hydrocolloids*, *61*, 712–719. <https://doi.org/10.1016/j.foodhyd.2016.06.033>
- Shi, Y.-C., & Seib, P. A. (1992). The structure of four waxy starches related to gelatinization and retrogradation. *Carbohydrate Research*, *227*, 131–145. [https://doi.org/10.1016/0008-6215\(92\)85066-9](https://doi.org/10.1016/0008-6215(92)85066-9)
- Shin, S. I., Kim, H. J., Ha, H. J., Lee, S. H., & Moon, T. W. (2005). Effect of Hydrothermal Treatment on Formation and Structural Characteristics of Slowly Digestible Non-pasted Granular Sweet Potato Starch. *Starch - Stärke*, *57*(9), 421–430. <https://doi.org/10.1002/star.200400377>
- Shogren, R. L. (1992). Effect of moisture content on the melting and subsequent physical aging of cornstarch. *Carbohydrate Polymers*, *19*(2), 83–90. [https://doi.org/10.1016/0144-8617\(92\)90117-9](https://doi.org/10.1016/0144-8617(92)90117-9)
- Shomer, I. (1995). Swelling behaviour of cell wall and starch in potato (*Solanum tuberosum* L.) tuber cells — I. Starch leakage and structure of single cells. *Carbohydrate Polymers*, *26*(1), 47–54. [https://doi.org/10.1016/0144-8617\(95\)98834-4](https://doi.org/10.1016/0144-8617(95)98834-4)
- Shrestha, A. K., Blazek, J., Flanagan, B. M., Dhital, S., Larroque, O., Morell, M. K., ... Gidley, M. J. (2015). Molecular, mesoscopic and microscopic structure evolution during amylase digestion of extruded maize and high amylose maize starches. *Carbohydrate Polymers*, *118*, 224–234. <https://doi.org/10.1016/j.carbpol.2014.11.025>
- Siddiqui, A. M., Provost, A., & Schwarz, W. H. (1991). Peristaltic pumping of a second-order fluid in a planar channel. *Rheologica Acta*, *30*(3), 249–262. <https://doi.org/10.1007/BF00366638>
- Sievert, D., & Pomeranz, Y. (1989). Enzyme-resistant starch. I. Characterization and evaluation by enzymatic, thermoanalytical, and microscopic methods. *Cereal Chem.* Retrieved from http://www.aaccnet.org/publications/cc/backissues/1989/Documents/66_342.pdf
- Sievert, D., & Pomeranz, Y. (1990). Enzyme-Resistant Starch. II. Differential Scanning Calorimetry Studies on Heat-Treated Starches and Enzyme-Resistant Starch Residues. *Cereal Chemistry*, *67*, 217–221.
- Sikora, M., Kowalski, S., & Tomasik, P. (2008). Binary hydrocolloids from starches and xanthan gum. *Food Hydrocolloids*, *22*(5), 943–952. <https://doi.org/10.1016/j.foodhyd.2007.05.007>
- Siljestrom, M., Bjork, I., Eliasson, A.-C., Lonner, C., Nyman, M., & Asp, N.-G. (1988). Effects on Polysaccharides During Baking and Storage- in vitro and in vivo studies. *Cereal Chemistry*, *65*(1), 1–13.
- Silverio, J., Fredriksson, H., Andersson, R., Eliasson, A.-C., & Åman, P. (2000). The effect of temperature cycling on the amylopectin retrogradation of starches with different amylopectin unit-chain length distribution. *Carbohydrate Polymers*, *42*(2), 175–184. [https://doi.org/10.1016/S0144-8617\(99\)00140-X](https://doi.org/10.1016/S0144-8617(99)00140-X)

- Silverio, J., Svensson, E., Eliasson, A.-C., & Olofsson, G. (1996). Isothermal microcalorimetric studies on starch retrogradation. *Journal of Thermal Analysis*, 47(5), 1179–1200. <https://doi.org/10.1007/BF01992822>
- Singh, H., Lin, J.-H., Huang, W.-H., & Chang, Y.-H. (2012). Influence of amylopectin structure on rheological and retrogradation properties of waxy rice starches. *Journal of Cereal Science*, 56(2), 367–373. <https://doi.org/10.1016/j.jcs.2012.04.007>
- Singh, J., Berg, T., Hardacre, A., & Boland, M. J. (2014). Cotyledon Cell Structure and In Vitro Starch Digestion in Navy Beans. In *Food Structures, Digestion and Health* (pp. 223–242). Elsevier. <https://doi.org/10.1016/B978-0-12-404610-8.00008-6>
- Singh, J., Dartois, A., & Kaur, L. (2010). Starch digestibility in food matrix: a review. *Trends in Food Science & Technology*, 21(4), 168–180. <https://doi.org/10.1016/j.tifs.2009.12.001>
- Singh, J., & Kaur, L. (Eds.). (2016a). *Advances in Potato Chemistry and Technology* (2nd ed.). Elsevier. <https://doi.org/10.1016/C2013-0-13578-7>
- Singh, J., & Kaur, L. (2016b). Chemistry, Processing, and Nutritional Attributes of Potatoes—An Introduction. In *Advances in Potato Chemistry and Technology* (Second Edi, pp. xxiii–xxvi). Elsevier. <https://doi.org/10.1016/B978-0-12-800002-1.02001-X>
- Singh, J., Kaur, L., McCarthy, O. J., Moughan, P. J., & Singh, H. (2008). RHEOLOGICAL AND TEXTURAL CHARACTERISTICS OF RAW AND PAR-COOKED TAEWA (MAORI POTATOES) OF NEW ZEALAND. *Journal of Texture Studies*, 39(3), 210–230. <https://doi.org/10.1111/j.1745-4603.2008.00139.x>
- Singh, J., Kaur, L., McCarthy, O. J., Moughan, P. J., & Singh, H. (2009). Development and characterization of extruded snacks from New Zealand Taewa (Maori potato) flours. *Food Research International*, 42(5–6), 666–673. <https://doi.org/10.1016/j.foodres.2009.02.012>
- Singh, J., Lelane, C., Stewart, R. B., & Singh, H. (2010). Formation of starch spherulites: Role of amylose content and thermal events. *Food Chemistry*, 121(4), 980–989. <https://doi.org/10.1016/j.foodchem.2010.01.032>
- Singh, J., McCarthy, O. J., & Singh, H. (2006). Physico-chemical and morphological characteristics of New Zealand Taewa (Maori potato) starches. *Carbohydrate Polymers*, 64(4), 569–581. <https://doi.org/10.1016/j.carbpol.2005.11.013>
- Singh, J., & Singh, N. (2001). Studies on the morphological, thermal and rheological properties of starch separated from some Indian potato cultivars. *Food Chemistry*, 75(1), 67–77. [https://doi.org/10.1016/S0308-8146\(01\)00189-3](https://doi.org/10.1016/S0308-8146(01)00189-3)
- Singh, J., & Singh, N. (2003). Studies on the morphological and rheological properties of granular cold water soluble corn and potato starches. *Food Hydrocolloids*, 17(1), 63–72. [https://doi.org/10.1016/S0268-005X\(02\)00036-X](https://doi.org/10.1016/S0268-005X(02)00036-X)
- Singh, N., & Kaur, L. (2004). Morphological, thermal, rheological and retrogradation properties of potato starch fractions varying in granule size. *Journal of the Science of Food and Agriculture*,

- 84(10), 1241–1252. <https://doi.org/10.1002/jsfa.1746>
- Singh, N., Singh, J., Kaur, L., Sodhi, N. S., & Gill, B. S. (2003). Morphological, thermal and rheological properties of starches from different botanical sources. *Food Chemistry*, 81(2), 219–231. [https://doi.org/10.1016/S0308-8146\(02\)00416-8](https://doi.org/10.1016/S0308-8146(02)00416-8)
- Siswoyo, T. A., & Morita, N. (2010). Influence of Annealing on Gelatinization Properties, Retrogradation and Susceptibility of Breadfruit Starch (*Artocarpus Communis*). *International Journal of Food Properties*, 13(3), 553–561. <https://doi.org/10.1080/10942910802713164>
- Sit, N., Misra, S., & Deka, S. C. (2014). Yield and Functional Properties of Taro Starch as Affected by Ultrasound. *Food and Bioprocess Technology*, 7(7), 1950–1958. <https://doi.org/10.1007/s11947-013-1192-7>
- Sjoo, M. E., Karin, A., & Eliasson, A. (2009). Comparison of Different Microscopic Methods for the Study of Starch and Other Components within Potato Cells. *Food Global Science Books*, 3(1), 39–44.
- Slade, L., & Levine, H. (1987). Recent Advances in Starch Retrogradation. *Industrial Polysaccharides*, (May), 387–430.
- Slaughter, S. L., Ellis, P. R., & Butterworth, P. J. (2001). An investigation of the action of porcine pancreatic α -amylase on native and gelatinised starches. *Biochimica et Biophysica Acta (BBA) - General Subjects*, 1525(1–2), 29–36. [https://doi.org/10.1016/S0304-4165\(00\)00162-8](https://doi.org/10.1016/S0304-4165(00)00162-8)
- Smits, A. L. M. (2001). *The Molecular Organisation in Starch Based Products: The Influence of Polyols used as Plasticisers*.
- Smits, A. L. M., Kruiskamp, P. ., Van Soest, J. J. G., & Vliegenthart, J. F. . (2003). The influence of various small plasticisers and malto-oligosaccharides on the retrogradation of (partly) gelatinised starch. *Carbohydrate Polymers*, 51(4), 417–424. [https://doi.org/10.1016/S0144-8617\(02\)00206-0](https://doi.org/10.1016/S0144-8617(02)00206-0)
- Sonia, S., Witjaksono, F., & Ridwan, R. (2015). Effect of cooling of cooked white rice on resistant starch content and glycemic response. *Asia Pacific Journal of Clinical Nutrition*, 24(4), 620–625. <https://doi.org/10.6133/apjcn.2015.24.4.13>
- Srichuwong, S., Fujiwara, M., Wang, X., Seyama, T., Shiroma, R., Arakane, M., ... Tokuyasu, K. (2009). Simultaneous saccharification and fermentation (SSF) of very high gravity (VHG) potato mash for the production of ethanol. *Biomass and Bioenergy*, 33(5), 890–898. <https://doi.org/10.1016/j.biombioe.2009.01.012>
- Srichuwong, S., & Jane, J. (2007). Physicochemical Properties of Starch Affected by Molecular Composition and Structures: A Review. *Food Science and Biotechnology*. Retrieved from <http://agris.fao.org/agris-search/search.do?recordID=KR2008000167#.WKkgPwRBuI0.mendeley>
- Srichuwong, S., Sunarti, T. C., Mishima, T., Isono, N., & Hisamatsu, M. (2005). Starches from different botanical sources I: Contribution of amylopectin fine structure to thermal properties and enzyme

- digestibility. *Carbohydrate Polymers*, 60(4), 529–538.
<https://doi.org/10.1016/j.carbpol.2005.03.004>
- Srikaeo, K., & Sangkhiaw, J. (2014). Effects of amylose and resistant starch on glycaemic index of rice noodles. *LWT - Food Science and Technology*, 59(2), 1129–1135.
<https://doi.org/10.1016/j.lwt.2014.06.012>
- Stamataki, N. S., Yanni, A. E., & Karathanos, V. T. (2017). Bread making technology influences postprandial glucose response: a review of the clinical evidence. *British Journal of Nutrition*, 117(7), 1001–1012. <https://doi.org/10.1017/S0007114517000770>
- Staudinger, H., & Husemann, E. (1937). Highly polymerized compounds. CL. The constitution of starch. 2. *Justus Liebigs Annalen Der Chemie*, 195–236.
- Steinka, I., Barone, C., Parisi, S., & Micali, M. (2017). *The Chemistry of Frozen Vegetables*. Cham: Springer International Publishing. <https://doi.org/10.1007/978-3-319-53932-4>
- Sterling, C., & Bettelheim, F. A. (1955). FACTORS ASSOCIATED WITH POTATO TEXTURE.. *Journal of Food Science*, 20(2), 130–137. <https://doi.org/10.1111/j.1365-2621.1955.tb16820.x>
- Stolt, M., Oinonen, S., & Autio, K. (2000). Effect of high pressure on the physical properties of barley starch. *Innovative Food Science & Emerging Technologies*, 1(3), 167–175.
[https://doi.org/10.1016/S1466-8564\(00\)00017-5](https://doi.org/10.1016/S1466-8564(00)00017-5)
- Straadt, I. K., Thybo, A. K., & Bertram, H. C. (2008). NaCl-induced changes in structure and water mobility in potato tissue as determined by CLSM and LF-NMR. *LWT - Food Science and Technology*, 41(8), 1493–1500. <https://doi.org/10.1016/j.lwt.2007.09.007>
- Sujka, M., & Jamroz, J. (2013). Ultrasound-treated starch: SEM and TEM imaging, and functional behaviour. *Food Hydrocolloids*, 31(2), 413–419. <https://doi.org/10.1016/j.foodhyd.2012.11.027>
- Sun, D. W., & Li, B. (2003). Microstructural change of potato tissues frozen by ultrasound-assisted immersion freezing. *Journal of Food Engineering*, 57(4), 337–345.
[https://doi.org/10.1016/S0260-8774\(02\)00354-0](https://doi.org/10.1016/S0260-8774(02)00354-0)
- Survase, S. A., Singh, J., & Singhal, R. S. (2016). The Role of Potatoes in Biomedical/Pharmaceutical and Fermentation Applications. In *Advances in Potato Chemistry and Technology* (pp. 603–625). Elsevier. <https://doi.org/10.1016/B978-0-12-800002-1.00020-0>
- Suzuki, A., & Hizukuri, S. (1979). Basic Studies on Cooking Potatoes II Effect of Potato Extract on the Interrelation of Gelatinization-Retrogradation of Potato Starch. *Cereal Chemistry*, 56, 257–260.
- Suzuki, T., Chiba, A., & Yarno, T. (2002). Interpretation of small angle x-ray scattering from starch on the basis of fractals. *Carbohydrate Polymers*, 34(4), 357–363. [https://doi.org/10.1016/s0144-8617\(97\)00170-7](https://doi.org/10.1016/s0144-8617(97)00170-7)
- SVAC. (1991). *Code of Pracrice for Sous Vide Catering Systems*. *Sous Vide Advisory Committee*.
- Szymońska, J., Krok, F., & Tomasik, P. (2000). Deep-freezing of potato starch. *International Journal of Biological Macromolecules*, 27(4), 307–314. [https://doi.org/10.1016/S0141-8130\(00\)00137-9](https://doi.org/10.1016/S0141-8130(00)00137-9)
- Tahvonon, R., Hietanen, R. M., Sihvonen, J., & Salminen, E. (2006). Influence of different processing

- methods on the glycemic index of potato (Nicola). *Journal of Food Composition and Analysis*, 19(4), 372–378. <https://doi.org/10.1016/j.jfca.2005.10.008>
- Takeda, Y., Hizukuri, S., Takeda, C., & Suzuki, A. (1987). Structures of branched molecules of amyloses of various origins, and molar fractions of branched and unbranched molecules. *Carbohydrate Research*, 165(1), 139–145. [https://doi.org/10.1016/0008-6215\(87\)80089-7](https://doi.org/10.1016/0008-6215(87)80089-7)
- Tamura, M., Kumagai, C., & Ogawa, Y. (2013). Relationships between histological tissue structure of cooked rice grain with various milling degrees and its digestibility during in vitro digestion. *Journal of the Japanese Society of Taste Technology*, 12(2), 30–36.
- Tamura, M., Okazaki, Y., Kumagai, C., & Ogawa, Y. (2017). The importance of an oral digestion step in evaluating simulated in vitro digestibility of starch from cooked rice grain. *Food Research International*, 94, 6–12. <https://doi.org/10.1016/j.foodres.2017.01.019>
- Tamura, M., Singh, J., Kaur, L., & Ogawa, Y. (2016). Impact of the degree of cooking on starch digestibility of rice – An in vitro study. *Food Chemistry*, 191, 98–104. <https://doi.org/10.1016/j.foodchem.2015.03.127>
- Tan, B., Tan, H. Z., Tian, X. H., Liu, M., & Shen, Q. (2011). Eight Underexploited Broad Beans From China: (II) Effects Of Steaming Methods On Their Quality And Microstructure. *Journal of Food Processing and Preservation*, 35(1), 20–45. <https://doi.org/10.1111/j.1745-4549.2009.00445.x>
- Tananuwong, K., & Reid, D. (2004). DSC and NMR relaxation studies of starch?water interactions during gelatinization. *Carbohydrate Polymers*, 58(3), 345–358. <https://doi.org/10.1016/j.carbpol.2004.08.003>
- Tang, H.-R., Godward, J., & Hills, B. P. (2000). The distribution of water in native starch granules—a multinuclear NMR study. *Carbohydrate Polymers*, 43(4), 375–387. [https://doi.org/10.1016/S0144-8617\(00\)00183-1](https://doi.org/10.1016/S0144-8617(00)00183-1)
- Teo, C. H., & Seow, C. C. (1992). A pulsed NMR method for the study of starch retrogradation. *Starch/Starke*, 44(8), 288–292.
- Tester, R. F., Ansell, R., Snape, C. E., & Yusuph, M. (2005). Effects of storage temperatures and annealing conditions on the structure and properties of potato (*Solanum tuberosum*) starch. *International Journal of Biological Macromolecules*, 36(1–2), 1–8. <https://doi.org/10.1016/j.ijbiomac.2005.02.008>
- Tester, R. F., & Debon, S. J. . (2000). Annealing of starch — a review. *International Journal of Biological Macromolecules*, 27(1), 1–12. [https://doi.org/10.1016/S0141-8130\(99\)00121-X](https://doi.org/10.1016/S0141-8130(99)00121-X)
- Tester, R. F., Debon, S. J. J., & Sommerville, M. D. (2000). Annealing of maize starch. *Carbohydrate Polymers*, 42, 287–299.
- Tester, R. F., Karkalas, J., & Qi, X. (2004). Starch - Composition, fine structure and architecture. *Journal of Cereal Science*, 39(2), 151–165. <https://doi.org/10.1016/j.jcs.2003.12.001>
- Tester, R. F., & Sommerville, M. . (2003). The effects of non-starch polysaccharides on the extent of gelatinisation, swelling and α -amylase hydrolysis of maize and wheat starches. *Food*

- Hydrocolloids*, 17(1), 41–54. [https://doi.org/10.1016/S0268-005X\(02\)00032-2](https://doi.org/10.1016/S0268-005X(02)00032-2)
- Thompson, D. B., & Fisher, D. K. (1997). Retrogradation of maize starch after thermal treatment within and above the gelatinization temperature range. *Cereal Chemistry*, 74(3), 344–351.
- Thybo, A. K., Andersen, H. J., Karlsson, A. ., Dønstrup, S., & Stødtkilde-Jørgensen, H. S. (2003). Low-field NMR relaxation and NMR-imaging as tools in differentiation between potato sample and determination of dry matter content in potatoes. *LWT - Food Science and Technology*, 36(3), 315–322. [https://doi.org/10.1016/S0023-6438\(02\)00210-4](https://doi.org/10.1016/S0023-6438(02)00210-4)
- Thybo, A. K., Bechmann, I. ., Martens, M., & Engelsen, S. . (2000). Prediction of Sensory Texture of Cooked Potatoes using Uniaxial Compression, Near Infrared Spectroscopy and Low Field¹H NMR Spectroscopy. *LWT - Food Science and Technology*, 33(2), 103–111. <https://doi.org/10.1006/fstl.1999.0623>
- Thygesen, L. G., Thybo, A. K., & Engelsen, S. B. (2001). Prediction of Sensory Texture Quality of Boiled Potatoes From Low-field¹H NMR of Raw Potatoes. The Role of Chemical Constituents. *LWT - Food Science and Technology*, 34(7), 469–477. <https://doi.org/10.1006/fstl.2001.0788>
- Thygesen, P. W., Dry, I. B., & Robinson, S. P. (1995). Polyphenol Oxidase in Potato (A Multigene Family That Exhibits Differential Expression Patterns). *Plant Physiology*, 109(2), 525–531. <https://doi.org/10.1104/pp.109.2.525>
- Tian, J., Chen, S., Wu, C., Chen, J., Du, X., Chen, J., ... Ye, X. (2016). Effects of preparation methods on potato microstructure and digestibility: An in vitro study. *Food Chemistry*, 211, 564–569. <https://doi.org/10.1016/j.foodchem.2016.05.112>
- Tian, J., Ogawa, Y., Shi, J., Chen, S., Zhang, H., Liu, D., & Ye, X. (2018). The microstructure of starchy food modulates its digestibility. *Critical Reviews in Food Science and Nutrition*, 1–12. <https://doi.org/10.1080/10408398.2018.1484341>
- Tian, Y., Li, D., Zhao, J., Xu, X., & Jin, Z. (2014). Effect of high hydrostatic pressure (HHP) on slowly digestible properties of rice starches. *Food Chemistry*, 152, 225–229. <https://doi.org/10.1016/j.foodchem.2013.11.162>
- Tian, Y., Zhang, L., Xu, X., Xie, Z., Zhao, J., & Jin, Z. (2012). Effect of temperature-cycled retrogradation on slow digestibility of waxy rice starch. *International Journal of Biological Macromolecules*, 51(5), 1024–1027. <https://doi.org/10.1016/j.ijbiomac.2012.08.024>
- Toivonen, P. M. A., & Brummell, D. A. (2008). Biochemical bases of appearance and texture changes in fresh-cut fruit and vegetables. *Postharvest Biology and Technology*, 48(1), 1–14. <https://doi.org/10.1016/j.postharvbio.2007.09.004>
- TOMRA Food. (2019). *Under the skin of the potato processing industry*.
- Torres, M. D. Á., & Parreño, W. C. (2016). *Thermal Processing of Potatoes. Advances in Potato Chemistry and Technology: Second Edition* (Second Edi). Elsevier Inc. <https://doi.org/10.1016/B978-0-12-800002-1.00014-5>
- Tsutsui, K., Katsuta, K., Matoba, T., Takemasa, M., Funami, T., Sato, E., & Nishinari, K. (2013).

- Effects of Time and Temperature of Annealing on Rheological and Thermal Properties of Rice Starch Suspensions during Gelatinization. *Journal of Texture Studies*, 44(1), 21–33. <https://doi.org/10.1111/j.1745-4603.2012.00361.x>
- Utrilla-Coello, R. G., Bello-Pérez, L. A., Vernon-Carter, E. J., Rodriguez, E., & Alvarez-Ramirez, J. (2013). Microstructure of retrograded starch: Quantification from lacunarity analysis of SEM micrographs. *Journal of Food Engineering*, 116(4), 775–781. <https://doi.org/10.1016/j.jfoodeng.2013.01.026>
- Vamadevan, V., & Bertoft, E. (2015). Structure-function relationships of starch components. *Starch - Stärke*, 67(1–2), 55–68. <https://doi.org/10.1002/star.201400188>
- Vamadevan, V., & Bertoft, E. (2018). Impact of different structural types of amylopectin on retrogradation. *Food Hydrocolloids*, 80, 88–96. <https://doi.org/10.1016/j.foodhyd.2018.01.029>
- Vamadevan, V., Bertoft, E., & Seetharaman, K. (2013). On the importance of organization of glucan chains on thermal properties of starch. *Carbohydrate Polymers*, 92(2), 1653–1659. <https://doi.org/10.1016/j.carbpol.2012.11.003>
- Vamadevan, V., Bertoft, E., Soldatov, D. V., & Seetharaman, K. (2013). Impact on molecular organization of amylopectin in starch granules upon annealing. *Carbohydrate Polymers*, 98(1), 1045–1055. <https://doi.org/10.1016/j.carbpol.2013.07.006>
- van de Velde, F., van Riel, J., & Tromp, R. H. (2002). Visualisation of starch granule morphologies using confocal scanning laser microscopy (CSLM). *Journal of the Science of Food and Agriculture*, 82(13), 1528–1536. <https://doi.org/10.1002/jsfa.1165>
- Van Dijk, C., Fischer, M., Beekhuizen, J. G., Boeriu, C., & Stolle-Smits, T. (2002). Texture of cooked potatoes (*Solanum tuberosum*). 3. Preheating and the consequences for the texture and cell wall chemistry. *Journal of Agricultural and Food Chemistry*, 50(18), 5098–5106. <https://doi.org/10.1021/jf011511n>
- Van Soest, J. J. G., de Wit, D., Tournois, H., & Vliegthart, J. F. G. (1994). Retrogradation of potato starch as studied by fourier transform infrared spectroscopy. *Starch/Stärke*, 46(12), 453–457.
- Van Soest, J. J. G., Tournois, H., de Wit, D., & Vliegthart, J. F. G. (1995). Short-range structure in (partially) crystalline potato starch determined with attenuated total reflectance Fourier-transform IR spectroscopy. *Carbohydrate Research*, 279(C), 201–214. [https://doi.org/10.1016/0008-6215\(95\)00270-7](https://doi.org/10.1016/0008-6215(95)00270-7)
- Vandeputte, G. E., Vermeylen, R., Geeroms, J., & Delcour, J. A. (2003). Rice starches. III. Structural aspects provide insight in amylopectin retrogradation properties and gel texture. *Journal of Cereal Science*, 38(1), 61–68. [https://doi.org/10.1016/S0733-5210\(02\)00142-X](https://doi.org/10.1016/S0733-5210(02)00142-X)
- Varatharajan, V., Hoover, R., Li, J., Vasanthan, T., Nantanga, K. K. M., Seetharaman, K., ... Chibbar, R. N. (2011). Impact of structural changes due to heat-moisture treatment at different temperatures on the susceptibility of normal and waxy potato starches towards hydrolysis by porcine pancreatic alpha amylase. *Food Research International*, 44(9), 2594–2606.

<https://doi.org/10.1016/j.foodres.2011.04.050>

- Veljovic-Jovanovic, S., Noctor, G., & Foyer, C. H. (2002). Are leaf hydrogen peroxide concentrations commonly overestimated? The potential influence of artefactual interference by tissue phenolics and ascorbate. *Plant Physiology and Biochemistry*, 40(6–8), 501–507. [https://doi.org/10.1016/S0981-9428\(02\)01417-1](https://doi.org/10.1016/S0981-9428(02)01417-1)
- Verbauwhede, A. E., Lambrecht, M. A., Jekle, M., Lucas, I., Fierens, E., Shegay, O., ... Delcour, J. A. (2019). Microscopic investigation of the formation of a thermoset wheat gluten network in a model system relevant for bread making. *International Journal of Food Science & Technology*, ijfs.14359. <https://doi.org/10.1111/ijfs.14359>
- Verlinden, B. E., Yuksel, D., Baheri, M., De Baerdemaeker, J., & Van Dijk, C. (2000). Low temperature blanching effect on the changes in mechanical properties during subsequent cooking of three potato cultivars. *International Journal of Food Science and Technology*, 35(3), 331–340. <https://doi.org/10.1046/j.1365-2621.2000.00391.x>
- Vermeulen, R., Derycke, V., Delcour, J. A., Goderis, B., Reynaers, H., & Koch, M. H. J. (2006). Gelatinization of Starch in Excess Water: Beyond the Melting of Lamellar Crystallites. A Combined Wide- and Small-Angle X-ray Scattering Study. *Biomacromolecules*, 7(9), 2624–2630. <https://doi.org/10.1021/bm060252d>
- Vermeulen, R., Goderis, B., & Delcour, J. A. (2006). An X-ray study of hydrothermally treated potato starch. *Carbohydrate Polymers*, 64(2), 364–375. <https://doi.org/10.1016/j.carbpol.2005.12.024>
- Waduge, R. N., Hoover, R., Vasanthan, T., Gao, J., & Li, J. (2006). Effect of annealing on the structure and physicochemical properties of barley starches of varying amylose content. *Food Research International*, 39(1), 59–77. <https://doi.org/10.1016/j.foodres.2005.05.008>
- Waigh, T A, Gidley, M. J., Komanshek, B. U., & Donald, A. M. (2000). The phase transformations in starch during gelatinization: a liquid crystalline approach. *Carbohydrate Research*, 328, 165–176.
- Waigh, Thomas A., Gidley, M. J., Komanshek, B. U., & Donald, A. M. (2000a). The phase transformations in starch during gelatinisation: a liquid crystalline approach. *Carbohydrate Research*, 328(2), 165–176. [https://doi.org/10.1016/S0008-6215\(00\)00098-7](https://doi.org/10.1016/S0008-6215(00)00098-7)
- Waigh, Thomas A., Gidley, M. J., Komanshek, B. U., & Donald, A. M. (2000b). The phase transformations in starch during gelatinisation: a liquid crystalline approach. *Carbohydrate Research*, 328(2), 165–176. [https://doi.org/10.1016/S0008-6215\(00\)00098-7](https://doi.org/10.1016/S0008-6215(00)00098-7)
- Waigh, Thomas A., Kato, K. L., Donald, A. M., Gidley, M. J., Clarke, C. J., & Riekell, C. (2000). Side-Chain Liquid-Crystalline Model for Starch. *Starch - Stärke*, 52(12), 450–460. [https://doi.org/10.1002/1521-379X\(200012\)52:12<450::AID-STAR450>3.0.CO;2-5](https://doi.org/10.1002/1521-379X(200012)52:12<450::AID-STAR450>3.0.CO;2-5)
- Wang, J., Rosell, C. M., & Benedito de Barber, C. (2002). Effect of the addition of different fibres on wheat dough performance and bread quality. *Food Chemistry*, 79(2), 221–226. [https://doi.org/10.1016/S0308-8146\(02\)00135-8](https://doi.org/10.1016/S0308-8146(02)00135-8)
- Wang, S., Li, C., Copeland, L., Niu, Q., & Wang, S. (2015). Starch Retrogradation: A Comprehensive

- Review. *Comprehensive Reviews in Food Science and Food Safety*, 14(5), 568–585. <https://doi.org/10.1111/1541-4337.12143>
- Wang, S., Wang, J., Wang, S., & Wang, S. (2017). Annealing improves paste viscosity and stability of starch. *Food Hydrocolloids*, 62, 203–211. <https://doi.org/10.1016/j.foodhyd.2016.08.006>
- Wang, W. J., Powell, A. D., & Oates, C. G. (1997). Effect of annealing on the hydrolysis of sago starch granules. *Carbohydrate Polymers*, 33(2–3), 195–202. [https://doi.org/10.1016/S0144-8617\(96\)00170-1](https://doi.org/10.1016/S0144-8617(96)00170-1)
- Wang, W., Zhou, H., Yang, H., Zhao, S., Liu, Y., & Liu, R. (2017). Effects of salts on the gelatinization and retrogradation properties of maize starch and waxy maize starch. *Food Chemistry*, 214, 319–327. <https://doi.org/10.1016/j.foodchem.2016.07.040>
- Wang, Y. J., & Jane, J.-L. (1994). Correlation between glass transition temperature and starch retrogradation in the presence of sugars and maltodextrins. *Cereal Chemistry*, 71(6), 527–531.
- Waramboi, J. G., Gidley, M. J., & Sopade, P. A. (2014). Influence of extrusion on expansion, functional and digestibility properties of whole sweetpotato flour. *LWT - Food Science and Technology*, 59(2), 1136–1145. <https://doi.org/10.1016/j.lwt.2014.06.016>
- Ward, R. (2011). *Development and Applications of a Low-Field Portable NMR System*.
- Warren, D. S., & Woodman, J. S. (1974). The texture of cooked potatoes: A review. *Journal of the Science of Food and Agriculture*, 25(2), 129–138. <https://doi.org/10.1002/jsfa.2740250204>
- Warren, F. J., Gidley, M. J., & Flanagan, B. M. (2016). Infrared spectroscopy as a tool to characterise starch ordered structure—a joint FTIR–ATR, NMR, XRD and DSC study. *Carbohydrate Polymers*, 139, 35–42. <https://doi.org/10.1016/j.carbpol.2015.11.066>
- Warren, F. J., Royall, P. G., Gaisford, S., Butterworth, P. J., & Ellis, P. R. (2011). Binding interactions of α -amylase with starch granules: The influence of supramolecular structure and surface area. *Carbohydrate Polymers*, 86(2), 1038–1047. <https://doi.org/10.1016/j.carbpol.2011.05.062>
- White, P. J., Abbas, I. R., & Johnson, L. A. (1989). Freeze-Thaw Stability and Refrigerated-Storage Retrogradation of Starches. *Starch - Stärke*, 41(5), 176–180. <https://doi.org/10.1002/star.19890410505>
- Wiesenborn, D. P., Orr, P. H., Casper, H. H., & Tacke, B. K. (1994). Potato starch paste behaviour as related to some physical/chemical properties. *Journal of Food Science*, 59(3), 644–648.
- Wilderjans, E., Luyts, A., Brijs, K., & Delcour, J. A. (2013). Ingredient functionality in batter type cake making. *Trends in Food Science & Technology*, 30(1), 6–15. <https://doi.org/10.1016/j.tifs.2013.01.001>
- Wilderjans, E., Luyts, A., Goesaert, H., Brijs, K., & Delcour, J. A. (2010). A model approach to starch and protein functionality in a pound cake system. *Food Chemistry*, 120(1), 44–51. <https://doi.org/10.1016/j.foodchem.2009.09.067>
- Willhoft, E. M. A. (1973). MECHANISM AND THEORY OF STALING OF BREAD AND BAKED GOODS, AND ASSOCIATED CHANGES IN TEXTURAL PROPERTIES. *Journal of Texture*

- Studies*, 4(3), 292–322. <https://doi.org/10.1111/j.1745-4603.1973.tb00844.x>
- Williams, P. C., Kuzina, F. D., & Hynka, I. (1970). A Rapid Colorimetric Procedure for Estimating the Amylose Content of Starches and Flours. *Cereal Chemistry*, 47(4), 411–420.
- Wilson, R. H., Goodfellow, B. J., Belton, P. S., Osborne, B. G., Oliver, G., & Russell, P. L. (1991). Comparison of fourier transform mid infrared spectroscopy and near infrared reflectance spectroscopy with differential scanning calorimetry for the study of the staling of bread. *Journal of the Science of Food and Agriculture*, 54(3), 471–483. <https://doi.org/10.1002/jsfa.2740540318>
- Witt, T., Douth, J., Gilbert, E. P., & Gilbert, R. G. (2012). Relations between molecular, crystalline, and lamellar structures of amylopectin. *Biomacromolecules*, 13(12), 4273–4282. <https://doi.org/10.1021/bm301586x>
- Woda, A., Mishellany, A., & Peyron, M.-A. (2006). The regulation of masticatory function and food bolus formation. *Journal of Oral Rehabilitation*, 33(11), 840–849. <https://doi.org/10.1111/j.1365-2842.2006.01626.x>
- Wolf, B. W., Bauer, L. L., & Fahey, G. C. (1999). Effects of chemical modification on in vitro rate and extent of food starch digestion: An attempt to discover a slowly digested starch. *Journal of Agricultural and Food Chemistry*, 47(10), 4178–4183. <https://doi.org/10.1021/jf9813900>
- Wu, C., Wu, Q.-Y., Wu, M., Jiang, W., Qian, J.-Y., Rao, S.-Q., ... Zhang, C. (2019). Effect of pulsed electric field on properties and multi-scale structure of japonica rice starch. *LWT*, 116, 108515. <https://doi.org/10.1016/j.lwt.2019.108515>
- Wu, W., Qiu, J., Wang, A., & Li, Z. (2019). Impact of whole cereals and processing on type 2 diabetes mellitus: a review. *Critical Reviews in Food Science and Nutrition*, 1–28. <https://doi.org/10.1080/10408398.2019.1574708>
- Wunderlich, B. (1980). *Macromolecular physics*. New York ; London [etc.] : Academic Press, 1980.
- Würsch, P., Del Vedovo, S., & Koellreutter, B. (1986). Cell structure and starch nature as key determinants of the digestion rate of starch in legume. *The American Journal of Clinical Nutrition*, 43(1), 25–29. <https://doi.org/10.1093/ajcn/43.1.25>
- Würsch, Pierre, & Gumy, D. (1994). Inhibition of amylopectin retrogradation by partial beta-amylolysis. *Carbohydrate Research*, 256(1), 129–137. [https://doi.org/10.1016/0008-6215\(94\)84232-9](https://doi.org/10.1016/0008-6215(94)84232-9)
- Wurzburg, O. B. (1972). Starches in the food industry. In E. Furia (Ed.), *Handbook of Food Additives* (2nd ed., pp. 361–395). CRC Press.
- Xiao, H. W., Pan, Z., Deng, L. Z., El-Mashad, H. M., Yang, X. H., Mujumdar, A. S., ... Zhang, Q. (2017). Recent developments and trends in thermal blanching – A comprehensive review. *Information Processing in Agriculture*, 4(2), 101–127. <https://doi.org/10.1016/j.inpa.2017.02.001>
- Xie, Y.-Y., Hu, X.-P., Jin, Z.-Y., Xu, X.-M., & Chen, H. Q. (2014). Effect of temperature-cycled retrogradation on in vitro digestibility and structural characteristics of waxy potato starch. *International Journal of Biological Macromolecules*, 67, 79–84.

<https://doi.org/10.1016/j.ijbiomac.2014.03.007>

- Xie, Y., Hu, X., Jin, Z., Xu, X., & Chen, H. (2014). International Journal of Biological Macromolecules Effect of temperature-cycled retrogradation on in vitro digestibility and structural characteristics of waxy potato starch, *67*, 79–84.
- Xie, Y. Y., Hu, X. P., Jin, Z. Y., Xu, X. M., & Chen, H. Q. (2014). Effect of repeated retrogradation on structural characteristics and in vitro digestibility of waxy potato starch. *Food Chemistry*, *163*, 219–225. <https://doi.org/10.1016/j.foodchem.2014.04.102>
- Xu, A., Chung, O. K., & Ponte, J. G. J. (1992). Bread crumb amylograph studies. 1. Effects of storage time, shortening, flour lipids, and surfactants. *Cereal Chemistry*, *69*, 495–501.
- Xu, M., Saleh, A. S. M., Gong, B., Li, B., Jing, L., Gou, M., ... Li, W. (2018). The effect of repeated versus continuous annealing on structural, physicochemical, and digestive properties of potato starch. *Food Research International*, *111*(January), 324–333. <https://doi.org/10.1016/j.foodres.2018.05.052>
- Yadav, B. S., Sharma, A., & Yadav, R. B. (2009). Studies on effect of multiple heating/cooling cycles on the resistant starch formation in cereals, legumes and tubers. *International Journal of Food Sciences and Nutrition*, *60*(sup4), 258–272. <https://doi.org/10.1080/09637480902970975>
- Yang, Q., Qi, L., Luo, Z., Kong, X., Xiao, Z., Wang, P., & Peng, X. (2017). Effect of microwave irradiation on internal molecular structure and physical properties of waxy maize starch. *Food Hydrocolloids*, *69*, 473–482. <https://doi.org/10.1016/j.foodhyd.2017.03.011>
- Yao, Y., Zhang, J., & Ding, X. (2002). Structure-retrogradation relationship of rice starch in purified starches and cooked rice grains: A statistical investigation. *Journal of Agricultural and Food Chemistry*, *50*(25), 7420–7425. <https://doi.org/10.1021/jf020643t>
- Yemenicioğlu, A. (2015). Strategies for Controlling Major Enzymatic Reaction in Fresh and Processed Vegetables. In *Handbook of Vegetable Preservation and Processing* (pp. 377–391). <https://doi.org/10.1201/b19252-18>
- Yildiz, F., & Wiley, R. C. (2017). *Minimally Processed Refrigerated Fruits and Vegetables*. (F. Yildiz & R. C. Wiley, Eds.). Boston, MA: Springer US. <https://doi.org/10.1007/978-1-4939-7018-6>
- Yoshimura, M., Takaya, T., & Nishinari, K. (1998). Rheological studies on mixtures of corn starch and konjac-glucomannan. *Carbohydrate Polymers*, *35*(1–2), 71–79. [https://doi.org/10.1016/S0144-8617\(97\)00232-4](https://doi.org/10.1016/S0144-8617(97)00232-4)
- You, Q., Zhang, X., Fang, X., Yin, X., Luo, C., & Wan, M. (2019). Ultrasonic-Assisted Preparation and Characterization of RS3 from Pea Starch. *Food and Bioprocess Technology*. <https://doi.org/10.1007/s11947-019-02277-z>
- Yu, K., Wang, Y., Xu, Y., Guo, L., & Du, X. (2016). Correlation between wheat starch annealing conditions and retrogradation during storage. *Czech Journal of Food Sciences*, *34*(No. 1), 79–86. <https://doi.org/10.17221/255/2015-CJFS>
- Yu, S., Jiang, L.-Z., & Kopparapu, N. K. (2015). Impact of Soybean Proteins Addition on Thermal and

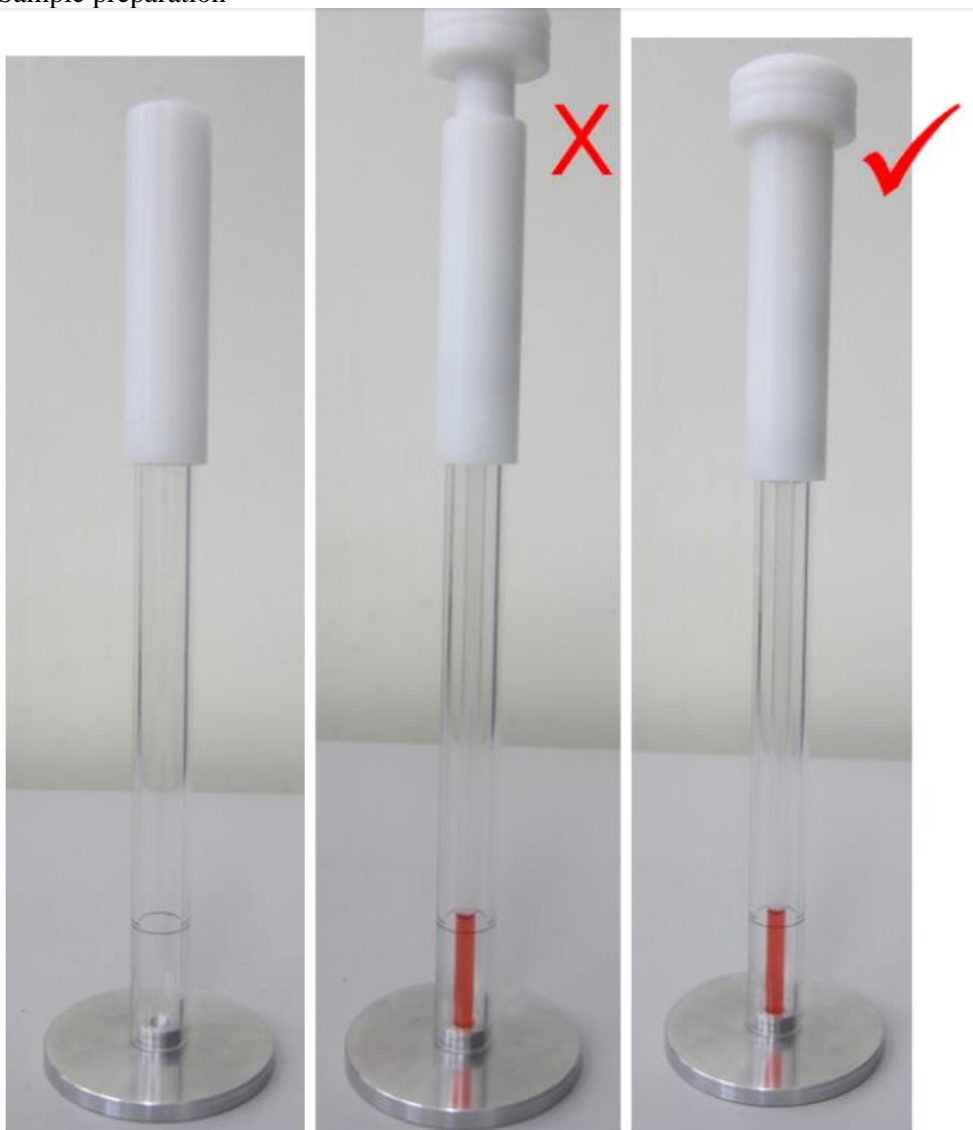
- Retrogradation Properties of Nonwaxy Corn Starch. *Journal of Food Processing and Preservation*, 39(6), 710–718. <https://doi.org/10.1111/jfpp.12280>
- Yu, S., Ma, Y., Zheng, X., Liu, X., & Sun, D. W. (2012). Impacts of Low and Ultra-Low Temperature Freezing on Retrogradation Properties of Rice Amylopectin During Storage. *Food and Bioprocess Technology*, 5(1), 391–400. <https://doi.org/10.1007/s11947-011-0526-6>
- Yu, S., Zhang, Y., Ge, Y., Zhang, Y., Sun, T., Jiao, Y., & Zheng, X. Q. (2013). Effects of ultrasound processing on the thermal and retrogradation properties of nonwaxy rice starch. *Journal of Food Process Engineering*, 36(6), 793–802. <https://doi.org/10.1111/jfpe.12048>
- Zaidul, I. S. M., Yamauchi, H., Kim, S.-J., Hashimoto, N., & Noda, T. (2007). RVA study of mixtures of wheat flour and potato starches with different phosphorus contents. *Food Chemistry*, 102(4), 1105–1111. <https://doi.org/10.1016/j.foodchem.2006.06.056>
- Zanoni, S., & Zavanella, L. (2012). Chilled or frozen Decision strategies for sustainable food supply chains. *International Journal of Production Economics*, 140(2), 731–736. <https://doi.org/10.1016/j.ijpe.2011.04.028>
- Zavareze, E. da R., & Dias, A. R. G. (2011). Impact of heat-moisture treatment and annealing in starches: A review. *Carbohydrate Polymers*, 83(2), 317–328. <https://doi.org/10.1016/j.carbpol.2010.08.064>
- Zeng, F., Gao, Q., Han, Z., Zeng, X., & Yu, S. (2016). Structural properties and digestibility of pulsed electric field treated waxy rice starch. *Food Chemistry*, 194, 1313–1319. <https://doi.org/10.1016/j.foodchem.2015.08.104>
- Zeng, S., Wu, X., Lin, S., Zeng, H., Lu, X., Zhang, Y., & Zheng, B. (2015). Structural characteristics and physicochemical properties of lotus seed resistant starch prepared by different methods. *Food Chemistry*, 186, 213–222. <https://doi.org/10.1016/j.foodchem.2015.03.143>
- Zhang, B., Dhital, S., Flanagan, B. M., Luckman, P., Halley, P. J., & Gidley, M. J. (2015). Extrusion induced low-order starch matrices: Enzymic hydrolysis and structure. *Carbohydrate Polymers*, 134, 485–496. <https://doi.org/10.1016/j.carbpol.2015.07.095>
- Zhang, B., Dhital, S., & Gidley, M. J. (2015). Densely packed matrices as rate determining features in starch hydrolysis. *Trends in Food Science & Technology*, 43(1), 18–31. <https://doi.org/10.1016/j.tifs.2015.01.004>
- Zhang, G., Ao, Z., & Hamaker, B. R. (2006). Slow digestion property of native cereal starches. *Biomacromolecules*, 7(11), 3252–3258. <https://doi.org/10.1021/bm060342i>
- Zhang, G., & Hamaker, B. R. (2009). Slowly digestible starch: concept, mechanism, and proposed extended glycemic index. *Critical Reviews in Food Science and Nutrition*, 49(10), 852–867. <https://doi.org/10.1080/10408390903372466>
- Zhang, J., Chen, F., Liu, F., & Wang, Z.-W. (2010). Study on structural changes of microwave heat-moisture treated resistant *Canna edulis* Ker starch during digestion in vitro. *Food Hydrocolloids*, 24(1), 27–34. <https://doi.org/10.1016/j.foodhyd.2009.07.005>

- Zhang, J., Wang, Z.-W., & Shi, X.-M. (2009). Effect of microwave heat/moisture treatment on physicochemical properties of *Canna edulis* Ker starch. *Journal of the Science of Food and Agriculture*, 89(4), 653–664. <https://doi.org/10.1002/jsfa.3497>
- Zhang, W., & Jackson, D. S. (1992). Retrogradation Behavior of Wheat Starch Gels with Differing Molecular Profiles. *Journal of Food Science*, 57(6), 1428–1432. <https://doi.org/10.1111/j.1365-2621.1992.tb06875.x>
- Zhang, X., Chen, Y., Zhang, R., Zhong, Y., Luo, Y., Xu, S., ... Guo, D. (2016). Effects of extrusion treatment on physicochemical properties and in vitro digestion of pregelatinized high amylose maize flour. *Journal of Cereal Science*, 68, 108–115. <https://doi.org/10.1016/j.jcs.2016.01.005>
- Zhang, Y., Liu, W., Liu, C., Luo, S., Li, T., Liu, Y., ... Zuo, Y. (2014). Retrogradation behaviour of high-amylose rice starch prepared by improved extrusion cooking technology. *Food Chemistry*, 158, 255–261. <https://doi.org/10.1016/j.foodchem.2014.02.072>
- Zheng, G. H., & Sosulski, F. w. (1998). Determination of Water Separation from Cooked Starch and Flour Pastes after Refrigeration and Freeze-thaw. *Journal of Food Science*, 63(1), 134–139. <https://doi.org/10.1111/j.1365-2621.1998.tb15693.x>
- Zhou, H., Wang, C., Shi, L., Chang, T., Yang, H., & Cui, M. (2014). Effects of salts on physicochemical, microstructural and thermal properties of potato starch. *Food Chemistry*, 156, 137–143. <https://doi.org/10.1016/j.foodchem.2014.02.015>
- Zhou, X., Baik, B.-K., Wang, R., & Lim, S.-T. (2010). Retrogradation of waxy and normal corn starch gels by temperature cycling. *Journal of Cereal Science*, 51(1), 57–65. <https://doi.org/10.1016/j.jcs.2009.09.005>
- Zhou, X., Chung, H.-J., Kim, J. Y., & Lim, S. T. (2013). In vitro analyses of resistant starch in retrograded waxy and normal corn starches. *International Journal of Biological Macromolecules*, 55, 113–117. <https://doi.org/10.1016/j.ijbiomac.2012.12.031>
- Zhou, X., & Lim, S.-T. (2012). Pasting viscosity and in vitro digestibility of retrograded waxy and normal corn starch powders. *Carbohydrate Polymers*, 87(1), 235–239. <https://doi.org/10.1016/j.carbpol.2011.07.045>
- Zhou, Z., Robards, K., Helliwell, S., & Blanchard, C. (2002). Ageing of Stored Rice: Changes in Chemical and Physical Attributes. *Journal of Cereal Science*, 35(1), 65–78. <https://doi.org/10.1006/jcrs.2001.0418>
- Zhu, F. (2015). Impact of ultrasound on structure, physicochemical properties, modifications, and applications of starch. *Trends in Food Science & Technology*, 43(1), 1–17. <https://doi.org/10.1016/j.tifs.2014.12.008>
- Zhu, F. (2017). NMR spectroscopy of starch systems. *Food Hydrocolloids*, 63, 611–624. <https://doi.org/10.1016/j.foodhyd.2016.10.015>
- Zobel, H. F. (1992). Starch granule structure. In *Developments in Carbohydrate Chemistry*.

Appendix A

- Tube specification
Wilmad NMR tubers 5mm 600MHZ frequency L7 in.

- Sample preparation

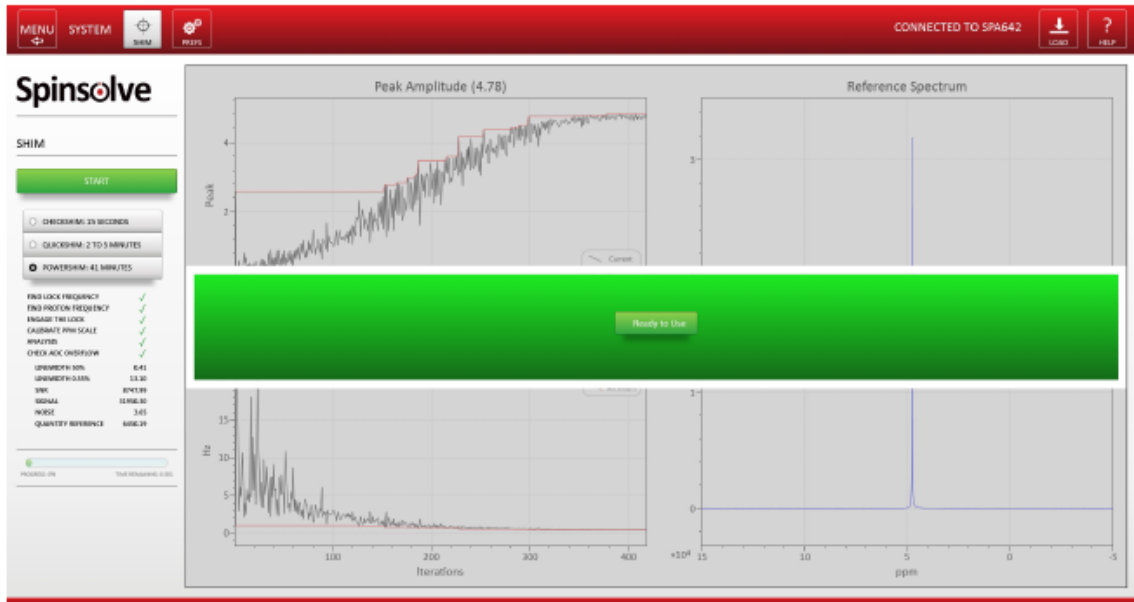


Left: empty sample depth gauge. Middle: holder too high in gauge. Right: sample holder correct.

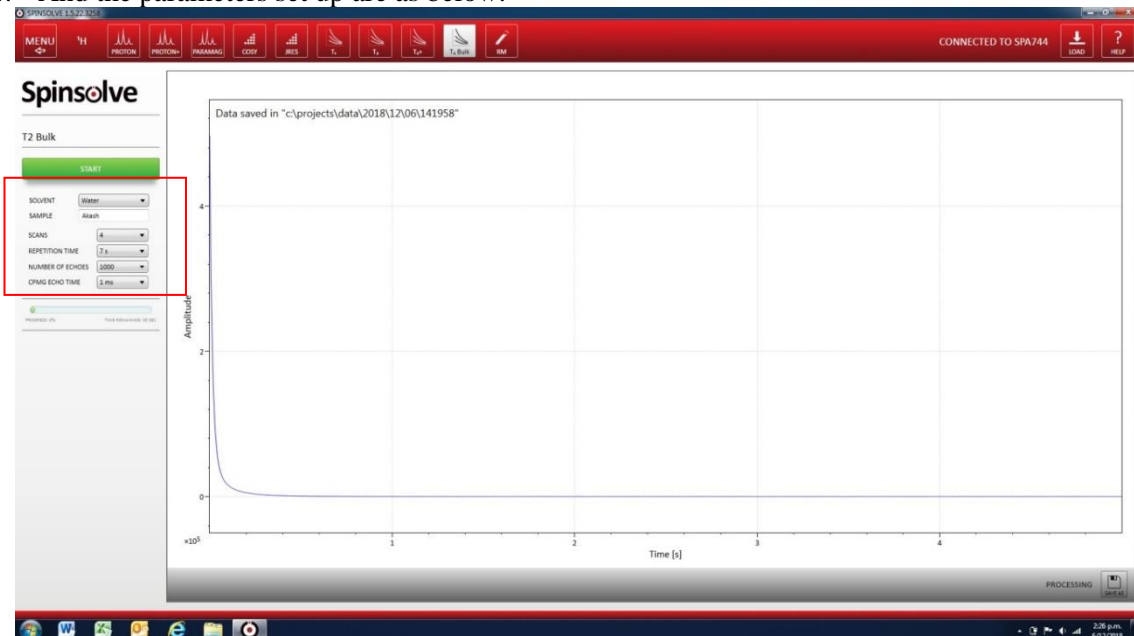
1. Press the sample holder down firmly to ensure it sits on top of the sample gauge (see image, right, above).
2. Put the bottom of the sample tube into the rounded base of the gauge.
3. Ensure the top of the sample liquid is above the black marker line on the gauge (see images below).

- Open SPINSOLVE app.
1. Under <system>, run <powershim> (41 min), using 10% water tube EVERY TIME before every use.

When the Powershim is completed successfully the Magritek Spinsolve is ready to use.

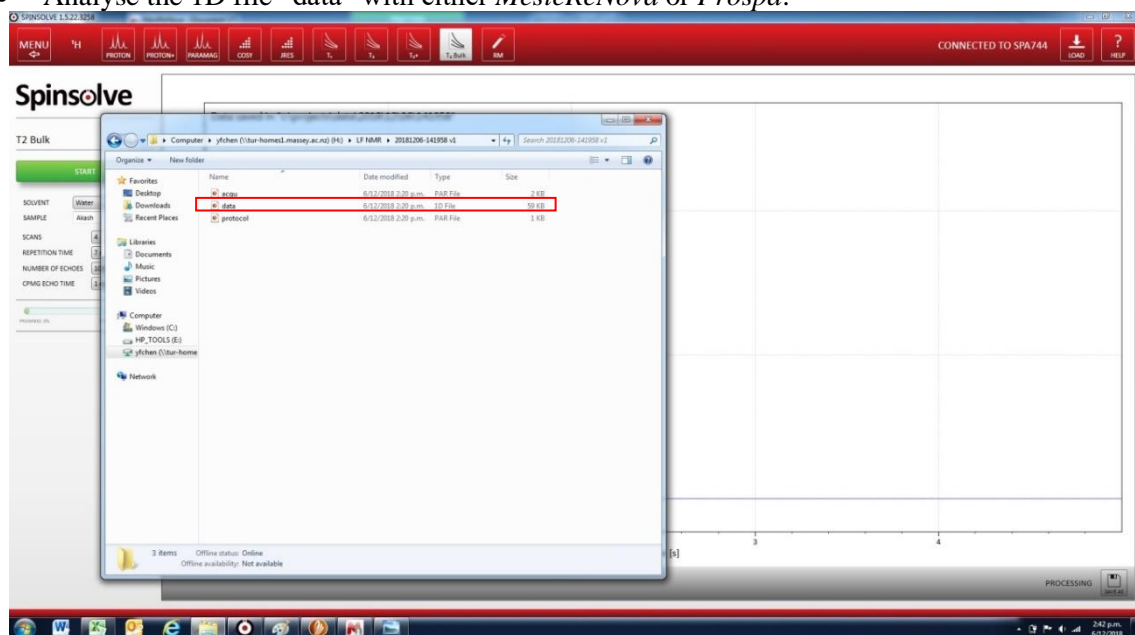


2. Back to <Menu>.
3. Under <¹H> find <T₂Bulk>.
4. And the parameters set up are as below.



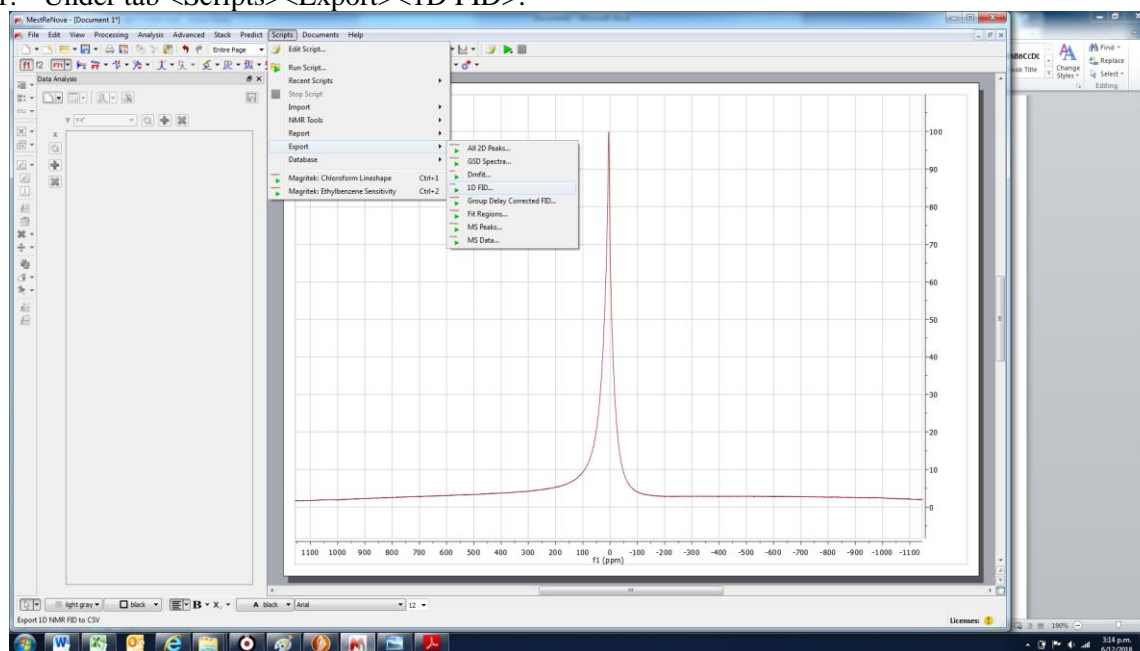
5. Save the data in H drive.

- Analyse the 1D file “data” with either *MesteReNova* or *Prospa*.



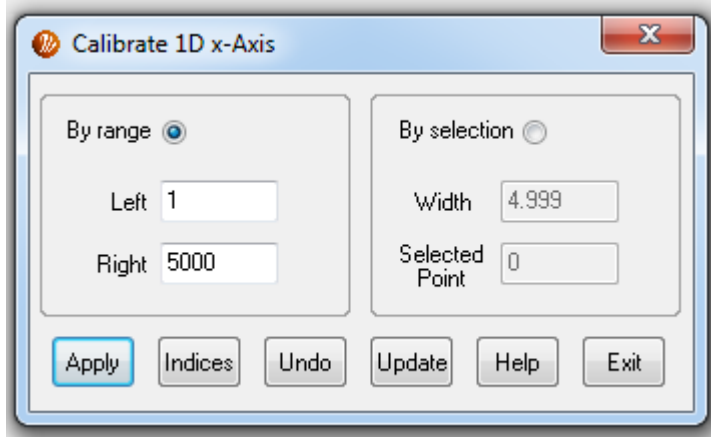
A. Export the 1D file to text by *MesteReNova*.

1. Under tab <Scripts><Export><1D FID>.

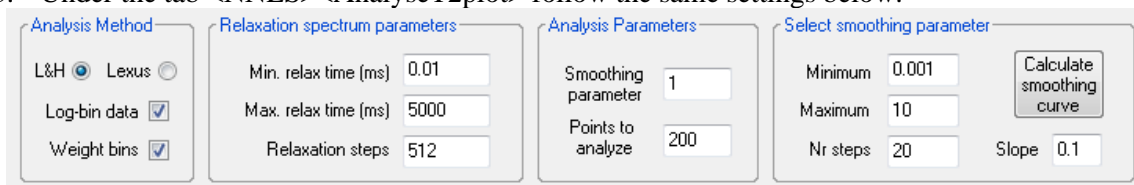


B. Analyse the T2 relaxation time distribution curve by *Prospa*.

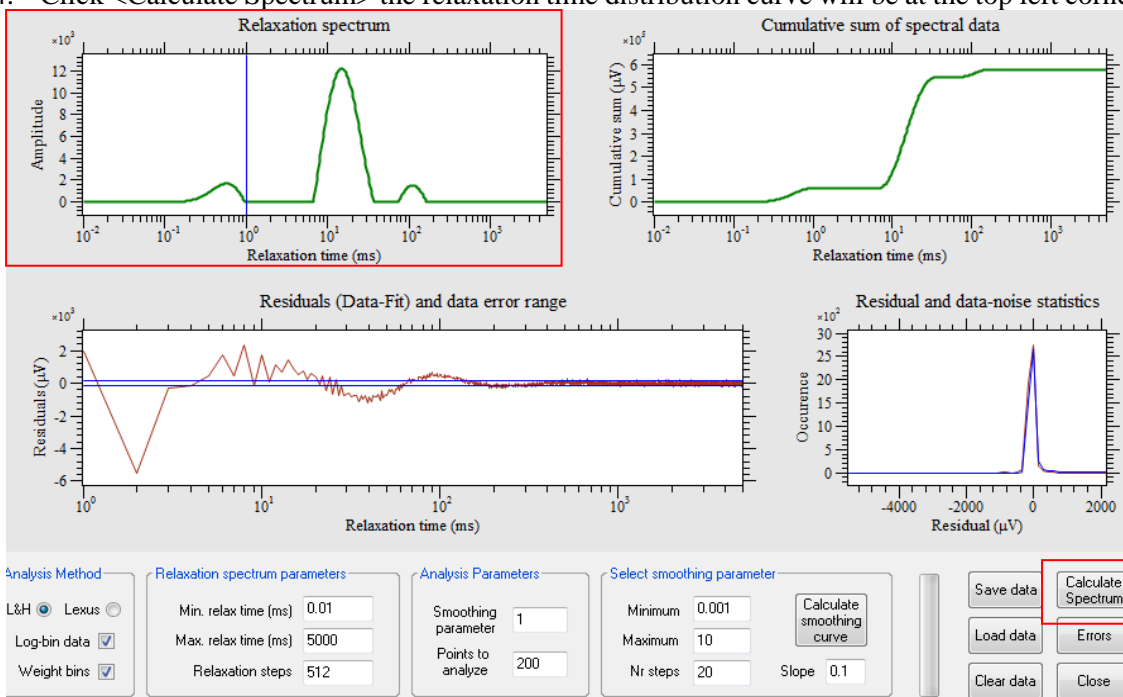
1. Open 1D file with Prospa.
2. Under tab <1D> <calibrate1d> change the <By range> to the settings below.













3. Under the tab <NNLS><AnalyseT2plot> follow the same settings below.



4. Click <Calculate Spectrum> the relaxation time distribution curve will be at the top left corner.



5. Click <Save data>, and under the same file in the H drive, all the data files after “L&H transformation” by Prospa will show up, the <spectrum> excel file is the raw data set of the above Relaxation spectrum in Prospa.

 cumulative_spectrum	6/12/2018 2:34 p.m.	Microsoft Excel C...	9 KB
 residuals	6/12/2018 2:34 p.m.	PT1 File	42 KB
 spectrum	6/12/2018 2:34 p.m.	1D File	5 KB
 spectrum	6/12/2018 2:34 p.m.	Microsoft Excel C...	8 KB
 spectrum	6/12/2018 2:34 p.m.	PT1 File	13 KB
 statistics	6/12/2018 2:34 p.m.	PT1 File	3 KB
 T2Analysis	6/12/2018 2:34 p.m.	PAR File	1 KB
 acqu	6/12/2018 2:20 p.m.	PAR File	2 KB
 data	6/12/2018 2:20 p.m.	1D File	59 KB
 protocol	6/12/2018 2:20 p.m.	PAR File	1 KB



MASSEY UNIVERSITY
GRADUATE RESEARCH SCHOOL

STATEMENT OF CONTRIBUTION DOCTORATE WITH PUBLICATIONS/MANUSCRIPTS

We, the candidate and the candidate's Primary Supervisor, certify that all co-authors have consented to their work being included in the thesis and they have accepted the candidate's contribution as indicated below in the *Statement of Originality*.

Name of candidate:	Yu-Fan Chen	
Name/title of Primary Supervisor:	Dr. Jaspreet Singh	
Name of Research Output and full reference:		
Starch retrogradation: An old tool to design new low glycaemic foods		
In which Chapter is the Manuscript /Published work:	Chapter 2	
Please indicate:		
<ul style="list-style-type: none"> The percentage of the manuscript/Published Work that was contributed by the candidate: 	80	
and		
<ul style="list-style-type: none"> Describe the contribution that the candidate has made to the Manuscript/Published Work: 	Yu-Fan reviewed relevant research articles from the literature, draft the manuscript and final editing.	
For manuscripts intended for publication please indicate target journal:		
Comprehensive Reviews in Food Science and Food Safety		
Candidate's Signature:		
Date:	1-11-19	
Primary Supervisor's Signature:		
Date:	1-11-19.	

(This form should appear at the end of each thesis chapter/section/appendix submitted as a manuscript/ publication or collected as an appendix at the end of the thesis)



MASSEY UNIVERSITY
GRADUATE RESEARCH SCHOOL

STATEMENT OF CONTRIBUTION DOCTORATE WITH PUBLICATIONS/MANUSCRIPTS

We, the candidate and the candidate's Primary Supervisor, certify that all co-authors have consented to their work being included in the thesis and they have accepted the candidate's contribution as indicated below in the *Statement of Originality*.

Name of candidate:	Yu-Fan Chen
Name/title of Primary Supervisor:	Dr. Jaspreet Singh
Name of Research Output and full reference:	
Potato starch retrogradation in tuber: Structural changes and gastro-small intestinal digestion in vitro	
In which Chapter is the Manuscript /Published work:	Chapter 4
Please indicate:	
<ul style="list-style-type: none"> The percentage of the manuscript/Published Work that was contributed by the candidate: 	80
and	
<ul style="list-style-type: none"> Describe the contribution that the candidate has made to the Manuscript/Published Work: 	
Yu-Fan standardized the protocol for LF-NMR, carried out the experiments, analyzed the results, and draft them to a full research article.	
For manuscripts intended for publication please indicate target journal:	
Food Hydrocolloids (Published)	
Candidate's Signature:	
Date:	1-11-19
Primary Supervisor's Signature:	
Date:	1-11-19.

(This form should appear at the end of each thesis chapter/section/appendix submitted as a manuscript/ publication or collected as an appendix at the end of the thesis)



MASSEY UNIVERSITY
GRADUATE RESEARCH SCHOOL

STATEMENT OF CONTRIBUTION DOCTORATE WITH PUBLICATIONS/MANUSCRIPTS

We, the candidate and the candidate's Primary Supervisor, certify that all co-authors have consented to their work being included in the thesis and they have accepted the candidate's contribution as indicated below in the *Statement of Originality*.

Name of candidate:	Yu-Fan Chen	
Name/title of Primary Supervisor:	Dr. Jaspreet Singh	
Name of Research Output and full reference:		
Influence of time-temperature cycles on potato starch retrogradation in tuber and starch digestion in vitro		
In which Chapter is the Manuscript /Published work:	Chapter 5	
Please indicate:		
• The percentage of the manuscript/Published Work that was contributed by the candidate:	85	
and		
• Describe the contribution that the candidate has made to the Manuscript/Published Work:	Yu-Fan developed the idea of TTC from literatures and carried out a series of experiments, analysed the results, then draft them to a full research article.	
For manuscripts intended for publication please indicate target journal:		
Food Hydrocolloids (Published)		
Candidate's Signature:		
Date:	1-11-19	
Primary Supervisor's Signature:		
Date:	1-11-19	

(This form should appear at the end of each thesis chapter/section/appendix submitted as a manuscript/ publication or collected as an appendix at the end of the thesis)



MASSEY UNIVERSITY
GRADUATE RESEARCH SCHOOL

STATEMENT OF CONTRIBUTION DOCTORATE WITH PUBLICATIONS/MANUSCRIPTS

We, the candidate and the candidate's Primary Supervisor, certify that all co-authors have consented to their work being included in the thesis and they have accepted the candidate's contribution as indicated below in the *Statement of Originality*.

Name of candidate:	Yu-Fan Chen	
Name/title of Primary Supervisor:	Dr. Jaspreet Singh	
Name of Research Output and full reference:		
Starch retrogradation of sous vide processed potato and oral-gastric-small intestinal starch digestion in vitro		
In which Chapter is the Manuscript /Published work:	Chapter 6	
Please indicate:		
<ul style="list-style-type: none"> The percentage of the manuscript/Published Work that was contributed by the candidate: 	80	
and		
<ul style="list-style-type: none"> Describe the contribution that the candidate has made to the Manuscript/Published Work: 	<p>Yu-Fan integrated ideas from meetings with the knowledge from literatures and designed the experiments. She analysed the results and draft them to a full research article.</p>	
For manuscripts intended for publication please indicate target journal:		
International Journal of Biological Macromolecules (Submitted)		
Candidate's Signature:		
Date:	1-11-19.	
Primary Supervisor's Signature:		
Date:	1-11-19.	

(This form should appear at the end of each thesis chapter/section/appendix submitted as a manuscript/ publication or collected as an appendix at the end of the thesis)



MASSEY UNIVERSITY
GRADUATE RESEARCH SCHOOL

STATEMENT OF CONTRIBUTION DOCTORATE WITH PUBLICATIONS/MANUSCRIPTS

We, the candidate and the candidate's Primary Supervisor, certify that all co-authors have consented to their work being included in the thesis and they have accepted the candidate's contribution as indicated below in the *Statement of Originality*.

Name of candidate:	Yu-Fan Chen	
Name/title of Primary Supervisor:	Dr. Jaspreet Singh	
Name of Research Output and full reference:		
Reheating stability of retrograded starch in processed potato tubers		
In which Chapter is the Manuscript /Published work:		Chapter 7
Please indicate:		
<ul style="list-style-type: none"> The percentage of the manuscript/Published Work that was contributed by the candidate: 		85
and		
<ul style="list-style-type: none"> Describe the contribution that the candidate has made to the Manuscript/Published Work: 		
Yu-Fan designed and conducted a series of experiments, analysed the results, then draft them to a full research article.		
For manuscripts intended for publication please indicate target journal:		
LWT		
Candidate's Signature:		
Date:	1-11-19	
Primary Supervisor's Signature:		
Date:	1-11-19	

(This form should appear at the end of each thesis chapter/section/appendix submitted as a manuscript/ publication or collected as an appendix at the end of the thesis)